DEPARTMENT OF CHEMISTRY, UNIVERSITY OF JYVÄSKYLÄ
RESEARCH REPORT No. 46

SYNTHESIS, STRUCTURE AND THERMAL BEHAVIOR OF SOLID COPPER(II) COMPLEXES OF 2-AMINO-2-HYDROXYMETHYL-1,3-PROPANEDIOL

BY

SIRPA KOTILA

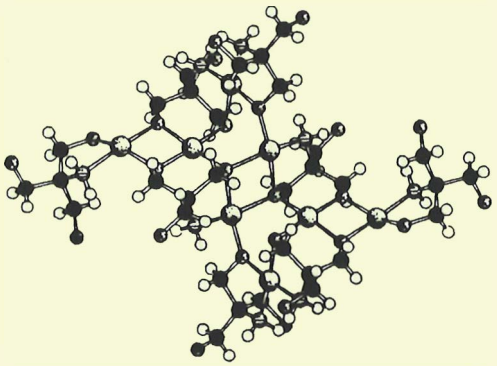

Academic Dissertation
for the Degree of
Doctor of Philosophy

Jyväskylä, Finland 1994
ISBN 951-34-0341-6
ISSN 0357-346X

DEPARTMENT OF CHEMISTRY, UNIVERSITY OF JYVÄSKYLÄ
RESEARCH REPORT No. 46

SYNTHESIS, STRUCTURE AND THERMAL BEHAVIOR OF SOLID COPPER(II) COMPLEXES OF 2-AMINO-2-HYDROXYMETHYL-1,3-PROPANEDIOL

BY

SIRPA KOTILA

Academic Dissertation
for the Degree of
Doctor of Philosophy

To be presented, by permission of the Faculty of Mathematics and Natural Sciences of the University of Jyväskylä, for public examination in Auditorium S-212, on September 9th, 1994, at 12 o'clock noon.

Jyväskylä, Finland
ISBN 951-34-0341-6
ISSN 0357-346X

URN:ISBN:978-952-86-0493-8
ISBN 978-952-86-0493-8 (PDF)
ISSN 0357-346X

University of Jyväskylä, 2025

List of original publications

This thesis is based on the following publications, which are referred to in the text by their Roman numerals:

I Kotila, S. and Valkonen, J., Copper(II) Complexes of 2-Amino-2-hydroxymethyl-1,3-propanediol. Part 1. Synthesis, Structure and Thermal Behavior of Three *trans*-Bis[2-amino-2-hydroxymethyl-1,3-propanediolato-(1-)-*O,N*]copper(II) Complexes, $[Cu(C_4H_{10}NO_3)_2]$, $[Cu(C_4H_{10}NO_3)_2(H_2O)]$ and $[Cu(C_4H_{10}NO_3)_2]\cdot 5H_2O$. *Acta Chem. Scand. 47* (1993) 950–956.
https://eurekamag.com/research/074/612/074612489.php

II Kotila, S. and Valkonen, J., Copper(II) Complexes of 2-Amino-2-hydroxymethyl-1,3-propanediol. Part 2. Synthesis, Structure and Thermal Behavior of *cis*-[2-Amino-2-hydroxymethyl-1,3-propanediol(1,3-)-*O,O',N*][2-amino-2-hydroxymethyl-1,3-propanediolato(1-)-*O,N*]nitratocopper(II), $[Cu(C_4H_{10}NO_3)(C_4H_{11}NO_3)(NO_3)]$, and *cis*-[2-Amino-2-hydroxymethyl-1,3-propanediol(1,3-)-*O,O',N*][2-amino-2-hydroxymethyl-1,3-propanediolato(1,3-)-*O,O',N*]copper(II) Sodium Bis(perchlorate), $[Cu(C_4H_{10}NO_3)(C_4H_{11}NO_3)]Na(ClO_4)_2$. *Acta Chem. Scand. 47* (1993) 957–964.
https://eurekamag.com/research/074/612/074612490.php

III Kotila, S. and Valkonen, J., Copper(II) Complexes of 2-Amino-2-hydroxymethyl-1,3-propanediol. Part 3. Synthesis, Structure and Thermal Behavior of Bis-*cis*-[2-amino-2-hydroxymethyl-1,3-propanediol-*O,N*][2-amino-2-hydroxymethyl-1,3-propanediolato-*O,N*]aquacopper(II) Sulfate and Chromate, $[Cu(C_4H_{10}NO_3)(C_4H_{11}NO_3)(H_2O)]_2X$, where $X = SO_4^{2-}$, CrO_4^{2-}.
Acta Chem. Scand. 48 (1994) 200–208.
https://eurekamag.com/research/074/612/074612491.php

IV Kotila, S. and Valkonen, J., Copper(II) Complexes of 2-Amino-2-hydroxymethyl-1,3-propanediol. Part 4. Synthesis, Structure and Thermal Behavior of *trans*-Bis[2-amino-2-hydroxymethyl-1,3-propanediolato-*O,N*]copper(II) Potassium Fluoride and Bromide, $[Cu(C_4H_{10}NO_3)_2]KF\cdot 3H_2O$ and $[Cu(C_4H_{10}NO_3)_2]KBr\cdot 2H_2O$. *Acta Chem. Scand. 48* (1994) 312–318.
https://eurekamag.com/research/082/717/082717838.php

V Kotila, S., Copper(II) Complexes of 2-Amino-2-hydroxymethyl-1,3-propanediol. Part 5. Synthesis, Structure and Thermal Behavior of *cis*-[2-Amino-2-hydroxymethyl-1,3-propanediol-*O,O',N*][2-amino-2-hydroxymethyl-1,3-propanediolato-*O,N*]aquacopper(II) Halide Monohydrate, $[Cu(C_4H_{10}NO_3)(C_4H_{11}NO_3)(H_2O)]X\cdot H_2O$, where $X = F^-$, Cl^-, Br^-, I^-. *Acta Chem. Scand.* (1994) *In press.*
https://eurekamag.com/research/082/717/082717839.php

PREFACE

This work was carried out in the Department of Chemistry at the University of Jyväskylä, from 1990–1994.

First of all, I want express my profound gratitude to my supervisor, Professor Jussi Valkonen, who gave me the opportunity to join his research group and introduced me to the fascinating world of *X*-ray crystallography. His guidance and constructive criticism throughout this study were extremely valuable.

I am especially grateful to lecturer Reijo Suontamo, Phil. Lic., who is the "father" of this thesis subject and also my very first tutor in the Inorganic and Analytical Chemistry Section, and to Dr. Ilkka Pitkänen for instructive discussions about thermal analysis. I owe a special debt of gratitude to my former colleague, Associate Professor Kari Rissanen (Department of Chemistry, University of Joensuu), whose advice concerning practical problems of structure solution was very much appreciated during the years he worked in our crystallography group.

Sincere thanks are also due to all my colleagues in the Department of Chemistry. In particular, I warmly thank Ms. Mirja Lahtiperä for running the mass spectra.

I am also indebted to sister Mary Edel–Lukko, O.C.D., for revising the language.

Last but not least, I wish to express my deepest gratitude to my family for their endless support and understanding during this work.

Financial support from the Leo and Regina Wainstein Foundation and the Ellen and Artturi Nyyssönen Foundation is gratefully acknowledged.

Jyväskylä, May 1994

Sirpa Kotila

I dedicate this work to my Parents.

ABSTRACT

Twenty solid copper(II) complexes with 2-amino-2-hydroxymethyl-1,3-propanediol (= tris, deprotonated form abbreviated $trisH_{-1}$) as the ligand were synthesized and their crystal structures were determined by single-crystal *X*-ray diffraction. The following thirteen compounds, explained in detail in five publications, form the basis of this thesis work: *trans*-$[Cu(trisH_{-1})_2]$ (**1**), *trans*-$[Cu(trisH_{-1})_2(H_2O)]$ (**2**), *trans*-$[Cu(trisH_{-1})_2]\cdot 5H_2O$ (**3**), *cis*-$[Cu(trisH_{-1})(tris)(NO_3)]$ (**4**), *cis*-$[Cu(trisH_{-1})(tris)]Na(ClO_4)_2$ (**5**), *cis*-$[Cu(trisH_{-1})(tris)(H_2O)]_2SO_4$ (**6**), *cis*-$[Cu(trisH_{-1})(tris)(H_2O)]_2CrO_4$ (**7**), *trans*-$[Cu(trisH_{-1})_2]KF\cdot 3H_2O$ (**8**), *trans*-$[Cu(trisH_{-1})_2]KBr\cdot 2H_2O$ (**9**), *cis*-$[Cu(trisH_{-1})(tris)(H_2O)]F\cdot H_2O$ (**10**), *cis*-$[Cu(trisH_{-1})(tris)(H_2O)]Cl\cdot H_2O$ (**11**), *cis*-$[Cu(trisH_{-1})(tris)(H_2O)]Br\cdot H_2O$ (**12**), and *cis*-$[Cu(trisH_{-1})(tris)(H_2O)]I\cdot H_2O$ (**13**). Compound **10** formed crystals of poor quality, which were not suitable for single-crystal determination, so the existence of the fluoride analogue is based on *X*-ray powder diffraction and thermal analysis. The other seven copper–tris complexes, as well as the structures published earlier, are also presented to illuminate the structural variety of the tris ligand. A literature survey concerning the solution studies of metal complexes of tris is also included.

Most of the compounds are mononuclear complexes with two tris ligands, and the coordination sphere around copper is square-planar, square-pyramidal or distorted octahedral in shape. The tris ligands are coordinated to copper via amino and one hydroxymethyl group resulting in a five-membered chelate structure; the longer apical bonds are formed with a water molecule, axial hydroxymethyl groups or anions (*e.g.* nitrate). In the basal coordination plane, *cis–trans* isomerism of the coordinated oxygen and nitrogen atoms is possible. Furthermore, the five-membered chelate rings can point out in two directions with respect to the coordination plane, giving rise to conformational *syn–anti* isomerism. In addition, all five- and six-coordinated species, which do not contain a center of symmetry, are optically active complexes, with two possible enantiomers, but because the syntheses are not stereoselective, the products are racemic mixtures. For some complex molecules, coordination isomerism as well as distortion isomerism of the coordination polyhedra was observed.

In addition to the mononuclear species, polynuclear complexes (tetra- and octanuclear) as well as chain structures (with a hydroxymethyl group or sulfate as a linking group) have also been observed for the tris ligand. In synthesis, a variety of factors, such as anion

type, solvent (water, ethanol), temperature, concentration, pH (alkaline addition), and metal–ligand–anion stoichiometry have been observed to affect the final product.

Crystal structures of these complexes are typically centrosymmetric, and hydrogen bonding plays a major role in crystal packing. All hydrogens in the OH, NH_2, H_2O groups participate in the three-dimensional hydrogen-bond network, where oxoanions and halides may also serve as acceptors for hydrogen bonds. Mononuclear *cis* complexes have the special characteristic of appearing as hydrogen-bonded dimers with short donor–acceptor contacts [O···O distances in the range 2.459(3)–2.565(4) Å], and in crystal structures these dimers exist in a stacked form.

The mass spectral fragmentation of tris has been analyzed, and the thermal behavior of the complexes has been determined by TG in air and nitrogen atmospheres.

CONTENTS

	PREFACE	3
	ABSTRACT	5
	CONTENTS	7
	ABBREVIATIONS	9
	NUMBERING SCHEME OF COMPLEXES	10
	COLOR CODE FOR ATOMS	11
1.	INTRODUCTION	13
1.1	General remarks about the ligand	13
1.2	Solution studies of metal–tris complexes	15
1.3	Solid state studies of metal–tris complexes	21
1.4	The aim of this study	22
2.	EXPERIMENTAL	24
2.1	Synthesis	24
2.2	*X*-Ray measurements	30
2.3	Mass spectrometry	31
2.4	Thermal analysis	31
3.	MOLECULAR STRUCTURES	32
3.1	General	32
3.2	Coordination sphere of copper	32
3.3	Isomerism of the complexes	34
	3.3.1 Conformational isomerism	34
	3.3.2 Stereo isomerism	37
	3.3.2 Isomerism of the coordination sphere of copper	38
3.4	Monomeric structure versus hydrogen-bonded dimers	38
3.5	Polynuclear complexes	40
3.6	Discussion	42
	FIGURE APPENDIX I	45

4.	CRYSTAL STRUCTURES	55
4.1	General	55
4.2	Crystal packing types	55
	FIGURE APPENDIX II	61
5.	MASS SPECTROMETRY	69
5.1	General	69
5.2	Results and discussion	69
6.	THERMOGRAVIMETRY	74
6.1	General	74
6.2	Decomposition of copper–tris compounds	75
6.3	Comparison of thermal stability of the organic ligand .	80
7.	CONCLUSIONS	84
8.	REFERENCES	87
	APPENDIX I	93
	APPENDIX II	94
	APPENDIX III	95
	APPENDIX IV	96
	APPENDIX V	97
	APPENDIX VI	98

ABBREVIATIONS

a	=	Axial hydroxymethyl group
B	=	Atomic temperature parameter [Å^2]
bipy	=	2,2'-Bipyridine
bistris	=	2-[Bis(2-(hydroxyethyl)amino]-2(hydroxymethyl)-1,3-propanediol
C_2	=	Two-fold axis of symmetry (Schönflies symbol)
d_{calc}	=	Calculated density [g cm^{-3}]
$d_{C\text{-}H}$	=	C—H distance
DTG	=	Derivative thermogravimetry
e	=	Equatorial hydroxymethyl group
E	=	Identity element of symmetry (Schönflies symbol)
EI	=	Electron-ionization technique (in mass spectrometry)
en	=	Ethylenediamine
ESR	=	Electron spin resonance
	=	Center of inversion (Schönflies symbol)
I	=	Ionic strength of a solution [mol dm^{-3}]
IR	=	Infrared spectroscopy
K	=	Equilibrium constant ($pK = -\log K$)
L	=	Ligand
M	=	General symbol for a metal ion
$M^{+\cdot}$	=	Molecular ion (in mass spectrometry)
MS	=	Mass spectrometry
phen	=	1,10-Phenantroline
R	=	General symbol for an organic side chain
R	=	Residual index, $R = \Sigma \mid \mid F_o \mid - \mid F_c \mid \mid / \Sigma \mid F_o \mid$
T	=	Temperature [°C]
TG	=	Thermogravimetry
tris	=	2-Amino-2-hydroxymethyl-1,3-propanediol
$trisH_{-1}$ ($trisH_{-2}$)	=	Deprotonated (twice deprotonated) form of tris
X	=	General symbol for halides in chemical formulas
XRD	=	*X*-Ray powder diffraction
Z	=	Number of formula units in a unit cell
Å	=	Ångström, 1×10^{-10} m

NUMBERING SCHEME OF COMPLEXES

For complex molecules, a three-number system is used, where the first number indicates the molecule, the second, the tris unit, and the third, the running number for each atom type.

Water molecules that are coordinated to the copper atom are named with three numbers (OW100, OW200) and lattice water with one number (OW1, OW2).

Atoms that belong to the anions are indicated by one number (*e.g.* N1, O1, O2, O3).

Disorder is shown in atom names by letter indexes. Normally, atoms that belong to the dominant complex molecule A do not have a letter index, but the other orientation is shown by letter B (*e.g.* O112B, O113B).

Axial hydroxymethyl groups: C113–O112, C123–O122, C213–O212, C223–O222
Equatorial hydroxymethyl groups: C114–O113, C124–O123, C214–O213, C224–O223

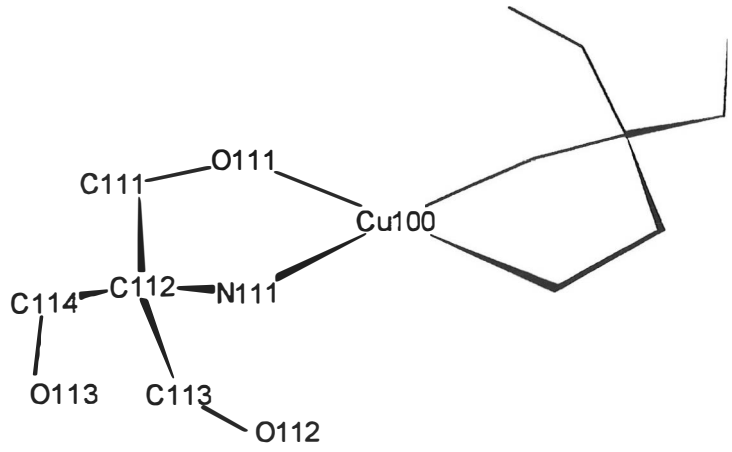

Numbering scheme for *trans* complexes
(the other half of the molecule is generated by inversion with respect to copper).

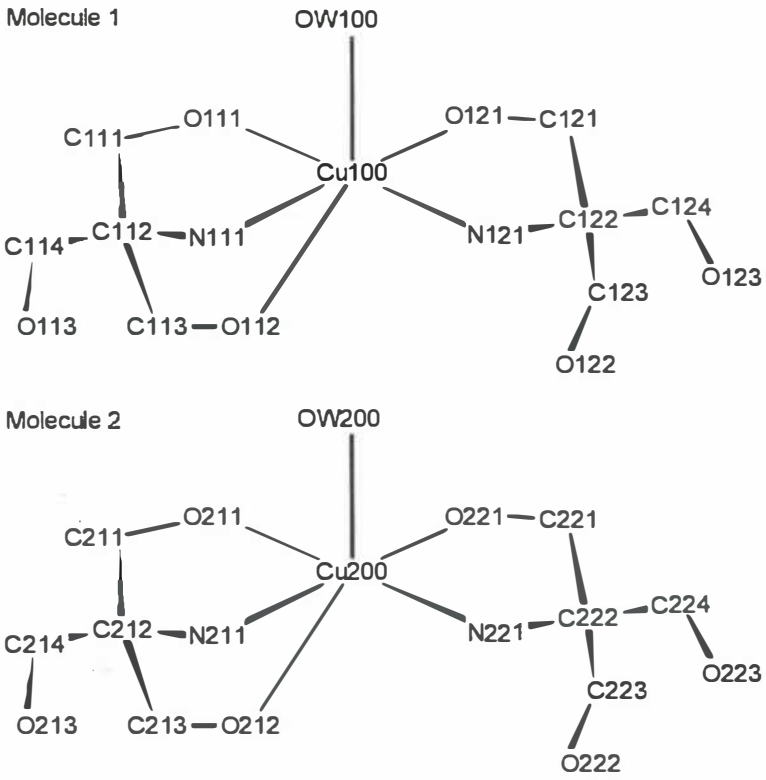

Numbering scheme for *cis* complexes.

COLOR CODE FOR ATOMS

Hydrogen (H)	= White
Carbon (C)	= Black
Nitrogen (N)	= Green
Oxygen (O)	= Red
Sulfur (S)	= Yellow
Chlorine (Cl)	= Blue–green
Potassium (K)	= Orange
Copper (Cu)	= Blue
Bromine (Br)	= Violet

1. INTRODUCTION

1.1 General remarks about the ligand

The organic ligand used in this study is 2-amino-2-hydroxymethyl-1,3-propanediol, and its structure is shown in Fig. 1.1. The ligand is also known by various other names, such as tris(hydroxymethyl)aminomethane, THAM, Trizma or less often used Tromethamine and Trometamol.[1] Hereafter the ligand is abbreviated tris.

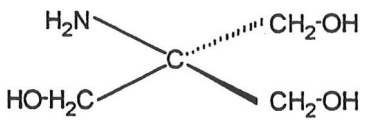

Fig. 1.1 Chemical formula of 2-amino-2-hydroxymethyl-1,3-propanediol (tris).

Tris is a commonly used buffering agent in biochemical[2] and seawater[3] studies, because its buffering region covers the physiological pH range 7–9. Like all buffers, tris contains a basic site, in this case an amino nitrogen, which can accept an extra proton. The acidity constant (pK_{AH}) of the protonated tris ($trisH^+$) in aqueous solutions varies in the range of 8.09–8.33,[4–7] depending on the temperature, the ionic strength of the solutions and the background electrolyte used. This pK_{AH} value means that tris is a slightly weaker base than ammonia [$pK_{AH}(NH_4^+)=9.2$],[7,8] what is expected on the basis of the structures. The presence of the hydroxy groups, two carbons distant from the basic nitrogen atom, leads to a systematic decrease in the basicity of the amino group;[6–9] each hydroxy group lowers the pK_{AH} value about 0.8 log units,[6,9] when compared with similar amines without hydroxy groups. This decrease in basicity is fairly independent of the type of amine (*i.e.* primary, secondary, tertiary). Fischer *et al.*[7] have also tried to determine the acidity constant for the deprotonation of one of the alcoholic hydroxy groups, but they did not observe any further deprotonation in the system up to a pH of 11, hence they concluded that the pK value for the hydroxy group must be ≥ 12.

Tris is a potential tetradentate ligand with its amino and three hydroxymethyl groups. Like all aminoalcohols, tris can form two distinctly different bond types with metal cations.

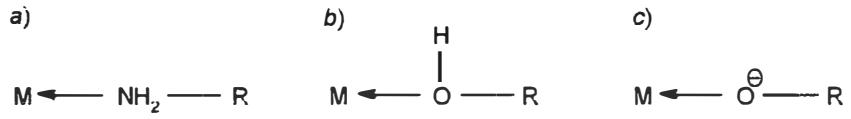

Fig. 1.2 Different coordination bond types of tris: *a*) a normal coordination bond of an amino nitrogen, *b*) a normal coordination bond of a hydroxy oxygen, and *c*) a covalent coordination bond of an alkoxy oxygen (deprotonated form abbreviated $trisH_{-1}$).[10]

One type of bonding involves a normal coordination bond between the metal and a lone-pair of nitrogen or oxygen atoms. The other type involves a classical covalent-coordination bond with an alkoxy oxygen.[10] These deprotonated species are abbreviated $trisH_{-n}$, where the negative subscript n indicates the number of protons removed from the ligand (normally $n=1$). The coordination types of tris are shown in Fig 1.2.

Commercially, tris is available in a number of compounds, such as a pure tris base and its different salts (the most important of them is the hydrochloride, $trisH^+.Cl^-$), not to mention various ready-made buffer solutions for special purposes. In addition to being a buffering agent, tris is also a useful secondary pH standard, since tris base and its hydrochloride salt can be blended to produce any desired pH between 7 and 9.[1,11] Tris is also used as a primary standard for HCl determinations (even though its molecular weight, 121.14, is rather low), because it is commercially available in a very pure form and is practically nonhygroscopic.[1] Tris was also suggested for a calorimetric standard in solution studies.[12]

Other uses of tris have also been noted in the literature. McFarland and Norris[13] reported that the use of tris greatly reduced the mortality of fish during transport. Since then, tris has been used as a water stabilizer and for reducing the CO_2 level in aquariums and in tropical fish transport.[1] Manfredi *et al.*[14] published the dramatic results they obtained when tris was injected intravenously into patients suffering from CO_2 retention. Nahas[15] used tris as a treatment for artificially-induced apnea in dogs. Tris is also a potential ligand for metal ions, and interference is known to occur when tris is used as a buffer in reactions, where metal ions are active sites. Catalytical activity of the coordinated metals may been enhanced or decreased, when compared with the system without the tris buffer. For example, the activity of pyruvate kinase (a Mg^{2+}-containing enzyme)[16] or horseradish peroxidase[17] were inhibited by tris, while the alkaline phosphatase (a Zn^{2+}-

containing enzyme)[18] was found to be activated by the tris buffer. The interfering mechanism most likely involves the metal binding capacity of tris, although its mild reducing nature may also be relevant.[19] Metal–tris complexes can also be used in titrations; Benesch and Benesch[20] have developed a method for the determination of sulfhydryl groups in proteins, in which a silver–tris complex was used as a titrant.

1.2 Solution studies of metal–tris complexes

Ever since the reactivity of tris towards metal ions was observed, the metal–tris interactions have been widely studied in various solvent systems. Potentiometric,[4,6,7,9,21–28] spectrophotometric,[4,7,9,10,21,22,29,31] polarographic[5,8,28] and electron spin resonance (ESR)[10,29,30] techniques were used in the solution studies. For example, the stability constants of the complexes of tris and the following metal ions have been determined manganese(II),[7] cobalt(II),[7,10,23] nickel(II),[4,7,9,22,24,25] copper(II),[4,5,7–10,21–24,28–30] zinc(II),[7,23,24] silver(I),[20,26,28] cadmium(II),[7,23,28] mercury(II),[23,27,31] and lead(II).[7,28] Furthermore, the stability of alkali[6] and alkaline earth[6,7] ion complexes were also measured in aqueous and mixed solvent systems. Comparisons between these studies are difficult to make, because the experiments were made in different conditions and with different methods. However, the orders of stability constants agree reasonably well, and the order is the same as generally observed for the Irving–Williams series,[32] extended to the alkali earth ions:[33] $Ba^{2+} < Sr^{2+} < Ca^{2+} < Mg^{2+} < Mn^{2+} < Fe^{2+} < Co^{2+} < Ni^{2+} < Cu^{2+} > Zn^{2+}$. Furthermore, when the complex formation abilities of tris were compared with various amines or aminoalcohols, tris proved to be one of the most favorable ligands for the copper(II) ion. In these comparisons, only 2-[bis(2-hydroxyethyl)amino]-2(hydroxymethyl)-1,3-propanediol (= bistris, Fig. 1.3) was able to form binary metal complexes, which were clearly more stable than those of tris.[6,9]

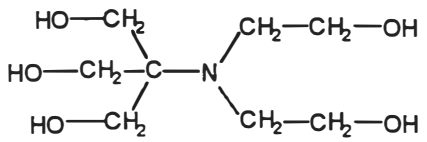

Fig. 1.3 Chemical formula of 2-[bis(2-hydroxyethyl)amino]-2(hydroxymethyl)-1,3-propanediol (bistris).

The results of the comprehensive stability constant studies by Sigel *et al.*[6] and Fischer *et al.*[7] are given in Tables 1.1 and 1.2. The logarithms of the stability constants determined for the binary $M(tris)^{2+}$ complexes are summarized in Table 1.1 (for comparison, the corresponding data for ammonia complexes, $M(NH_3)^{2+}$, are also given). To obtain some general estimation of the concentrations of binary tris complexes in different conditions, the percentage values are given in Table 1.2. These figures show that a strongly coordinating metal ion like Cu^{2+} exists in the physiological pH range (even in low concentrations) mainly in its complex form; in other metal cation systems, there are also considerable amounts of the complex present, especially with the metal ions of the second half of the 3d transition series, or with Cd^{2+} and Pb^{2+}. These calculations refer to a complex system with a metal–ligand ratio of 1:1, and an increase in the ligand concentration over that of the metal ion will drastically increase the percentage of the metal complex.

Table 1.1 Logarithms of stability constants of some binary $M(tris)^{2+}$ and $M(NH_3)^{2+}$ complexes.[7]

M^{2+}	log $K^{M}_{M(tris)}$ at 25°C and at		log $K^{M}_{M(NH_3)}$ *(I, T)*
	I=0.1 mol dm^{-3}	I=1.0 mol dm^{-3}	
Mg^{2+}	≤ 0.7	≤ 1.0	0.23 (2.0 mol dm^{-3}, 23°C)
Ca^{2+}	≤ 0.7	–	–0.2 (2.0 mol dm^{-3}, 23°C)
Ba^{2+}	≤ 0.7	≤ 1.2	–
Mn^{2+}	≤ 0.9	≤ 1.0	0.8 (0.5–5 mol dm^{-3}, 20–30°C)
			1.00 (2.0 mol dm^{-3}, 20°C)
Co^{2+}	1.73 ± 0.02	–	1.99 (0 mol dm^{-3}, 20°C)
Ni^{2+}	2.74 ± 0.02	2.67 ± 0.06	2.72 (0 mol dm^{-3}, 25°C)
Cu^{2+}	4.05 ± 0.02	4.24 ± 0.29	4.04 ± 0.03 (0 mol dm^{-3}, 25°C)
Zn^{2+}	1.94 ± 0.02	–	2.21 (0 mol dm^{-3}, 25°C)
Cd^{2+}	1.94 ± 0.02	1.88 ± 0.06	2.55 (0 mol dm^{-3}, 25°C)
Pb^{2+}	≤ 2.7	–	–

Table 1.2. Effect of tris concentration and pH on the concentration of the binary $M(tris)^{2+}$ complex in aqueous solutions of several metal–tris mixtures.[6,7]

M^{n+}	Percentage of $M(tris)^{n+}$ present											
	$[tris]_{total}$ = 0.01 mol dm^{-3} at pH						$[tris]_{total}$ = 0.1 mol dm^{-3} at pH					
	6	6.5	7	7.5	8	9	6	6.5	7	7.5	8	9
Li^+		0.01		0.08				0.09		0.8		
Na^+		~0		0.03				0.03		0.3		
K^+		–		–				≤0.02		≤0.2		
Rb^+		–		–				≤0.02		≤0.2		
Mg^{2+}		0.03		0.3				0.3		2.5		
Ca^{2+}		0.03		0.2				0.3		2.3		
Sr^{2+}		0.02		0.2				0.2		1.7		
Ba^{2+}		0.02		0.1				0.2		1.4		
Co^{2+}	0.4	–	3.5	–	16	26	3.8	–	27	–	68	81
Ni^{2+}	3.7	–	23	–	53	64	28	–	78	–	95	98
Cu^{2+}	35	54	70	81	87	90	88	–	99	–	100	100
Zn^{2+}/Cd^{2+}	0.6	–	5.4	–	22	34	6.0	–	37	–	77	87

$[M]_{total}$ = 0.01 mol dm^{-3} = the total concentration of the metal ion.

$[tris]_{total}$ = the total concentration of the tris ligand.

An increase in ligand concentration will also introduce new complex species with different metal–ligand ratios. Complex-formation equilibria between tris and metal cations in aqueous solutions have been studied by Bai and Martell (Cu, Ni),[4] Hall *et al.* (Cu, Ni),[22] Bologni *et al.* (Cu, Ni, Zn),[24] Forsling (Ni),[25] as well as Granberg *et al.* (Ag).[26] For example, the following complex equilibria were found to take place in the aqueous reaction of copper(II) with tris (0.10 mol dm^{-3} KNO_3, 25°C) according to Bai and Martell:[4]

$$ML_{n-1}^{2+} + L \rightleftharpoons ML_n^{2+} \quad (n = 1,2,3,4) \qquad K_n \qquad (1.1)$$

$$ML^{2+} \rightleftharpoons M(LH_{-1})^{+} + H^{+} \qquad K_{1a} \qquad (1.2)$$

$$2\ M(LH_{-1})^{+} \rightleftharpoons [M(LH_{-1})]_2^{2+} \qquad K_{ad} \qquad (1.3)$$

$$ML_2^{2+} \rightleftharpoons ML(LH_{-1})^{+} + H^{+} \qquad K_{2a} \qquad (1.4)$$

$$ML(LH_{-1})^{+} \rightleftharpoons M(LH_{-1})_2 + H^{+} \qquad K_{2b} \qquad (1.5)$$

The copper–tris reaction was fast and equilibrium rapidly achieved. Titrations were made in various molar ratios, and when the copper–tris mole ratio was greater than 1:1, copper(II) remained in the solution over a wide pH range (approximately 4–12). "Ordinary" complexes with neutral ligands were formed first, which undergo further dissociation as the pH increased. The most basic product in all the solutions was $Cu(LH_{-1})_2$.[4] The equilibrium constants (K) of the complex formation reactions 1.1–1.5 are given in Table 1.3.

Table 1.3 Equilibrium constants for the complexes of Cu^{2+} with tris in water solution at 25°C (ionic strength 0.10 mol dm^{-3} KNO_3).[4,29]

Complex	Equilibrium constant	log K		Maximum concentration [%]
ML^{2+}	K_1	3.95	5.4	31
ML_2^{2+}	K_2	3.68	5.8	22
ML_3^{2+}	K_3	3.47	6.4	29
ML_4^{2+}	K_4	3.0	7.6	75
$M(LH_{-1})^{+}$	K_{1a}	−6.0	5.9	13
$[M(LH_{-1})]_2^{2+}$	K_{ad}	2.2	6.5	16
$ML(LH_{-1})^{+}$	K_{2a}	−6.32	6.0	2
$M(LH_{-1})_2$	K_{2b}	−7.90	>9	>60

The potentiometric study of Bologni *et al.*[24] for copper–tris equilibria under different ionic strength (0.15 mol dm^{-3} NaCl, 25°C) also showed a fairly complicated model consisting of seven complex species: ML^{2+}, $M(LH_{-1})^{+}$, $ML(LH_{-1})^{+}$, $M(LH_{-1})_2$, ML_3^{2+}, $M_2(LH_{-1})_2^{2+}$, and $M_2(LH_{-2})(LH_{-1})^{+}$.

When nickel was used in the equilibrium studies, the reactions between Ni^{2+} and tris were extremely slow and polynuclear complexes (up to tetranuclear species) were obtained even in the presence of excess ligand.[24,25] With zinc(II)[24] and silver(I)[26] as a metal ion, only mononuclear complexes, such as ZnL^{2+}, AgL^{+}, and AgL_2^{+}, were observed.

In metal complexes, the primary binding site of tris is the basic amino group. The role of hydroxy groups has been more under discussion. When the stability constants of metal–tris complexes were compared with those of ammonia (Table 1.1 and refs. 7, 9 and 20), the values for a given metal proved to be about the same, even though the basicity of tris is one pH unit smaller than that of ammonia. If the basicity of the amino group was the only factor determining the stability of tris complexes, their stability would be considerably lower than the stability of ammonia complexes. This gave a clear indication that at least one hydroxy group of tris is involved in coordination, and chelates are formed as a result. The stabilizing effect of five-membered chelate rings is stated by Bai and Martell,[4] Hall *et al.*,[5] Sigel *et al.*,[6] Fischer *et al.*,[7] Scheller *et al.*,[9] and Allen *et al.*[19] However, the metal/tris-hydroxy bonds are relatively weak allowing tris to act as a simple monodentate ligand[7] when forming higher complex species, like $Cu(tris)_4^{2+}$, or with certain metal ions (silver).[20]

Structure proposals based on solution studies are presented for copper–tris complexes in the following articles. Bai and Martell[4] have given the most likely arrangements for species $Cu(LH_{-1})^{+}$, its hydrated dimer $[Cu(LH_{-1})(H_2O)]_2^{2+}$, $CuL(LH_{-1})^{+}$, and $Cu(LH_{-1})_2$, which are shown in Fig 1.3. For copper, Dotson[10] has presented a dimeric structure along with two mononuclear structures similar to *c*) in Fig 1.3 (the other monomer proposal involves solvent interaction, where two ethanol molecules are axially attached to the copper complex). Further, the structure proposal of Hall and Swisher[21] is identical with *d*) in Fig. 1.3. However, the structures given by Boyd *et al.*[30] differ markedly from the others, and they are shown in Fig. 1.4. In their ESR studies, they

observed that the copper(II)–copper(II) separation in the dimer complex is about 4.7 Å, which will rule out the proposal given by Bai and Martell [structure *b*) in Fig 1.3]. On the other hand, in the solutions of tris and copper(II) chloride with the molar ratio of 1:1, they observed species with an extremely close copper separation of about 3 Å. The models they have given refer to these copper–copper separations and coordination geometries observed by ESR.

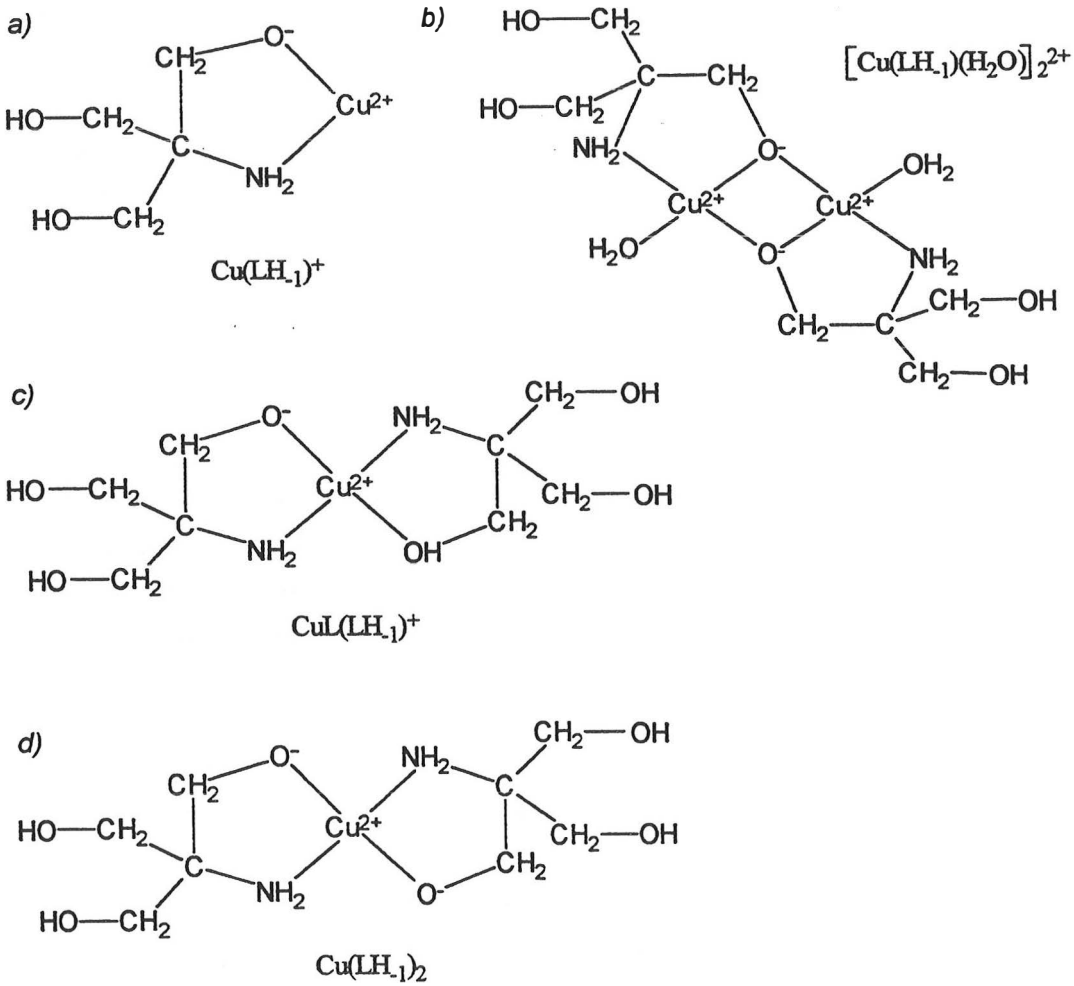

Fig. 1.3 Structure proposals for copper–tris complexes based on potentiometric titrations by Bai and Martell.[4]

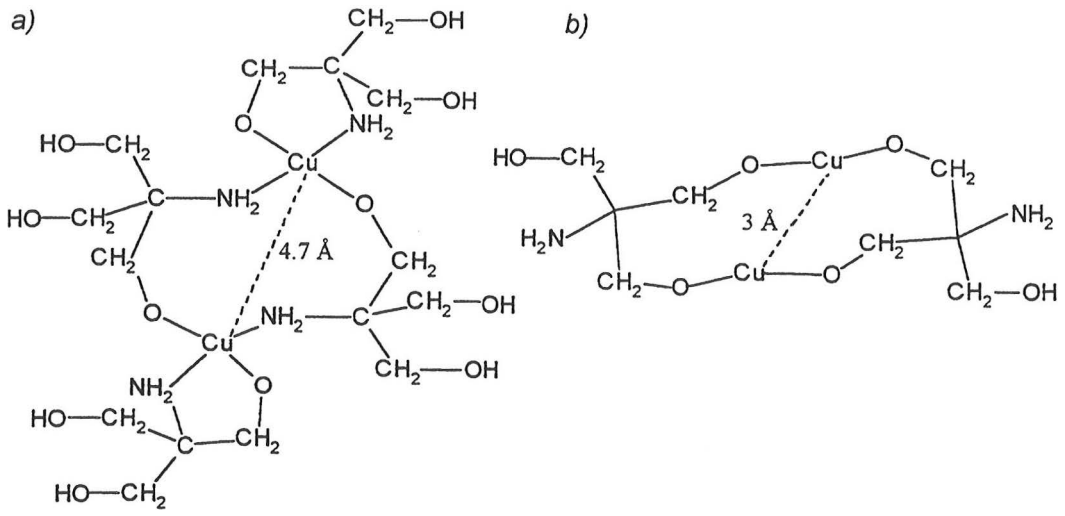

Fig. 1.4 Structure proposals for copper–tris complexes based on ESR studies by Boyd *et al.*[30]

1.3. Solid state studies of metal–tris complexes

The solid state chemistry of tris and its compounds is less well known. In spite of the biological importance of tris, its crystal structure was not determined until 1980 by Eilerman and Rudman.[34] Tris, like many compounds with approximately spherical molecules, undergoes a solid–solid phase transition just below the melting point. As a part of their studies on polymorphism, Eilerman and Rudman determined the crystal structures of tris at six different temperatures (–129.2–149.9°C) by single-crystal *X*-ray techniques. Between -268.2°C and its melting point (172.9°C), tris exhibits one solid–solid phase transition at 134.2°C, forming an orientationally disordered phase I. The ordered form, phase II (-268.2–134.2°C) is orthorhombic ($Pn2_1a$, a=8.844(1), b=7.794(1), c=8.795(1) Å at 21.9°C, Z=4, d_{calc}=1.327 g cm^{-3}), and the crystal structure can be described as a layer structure with strong intralayer hydrogen bonding. The disordered phase I (134.2–172.9°C) is a body-centered-cubic structure ($Im3m$, a=6.876(6) Å at 149.9°C, Z=2, d_{calc}=1.237 g cm^{-3}). The effect of increasing thermal motion on the crystal and molecular parameters was investigated, and a mechanism for the phase transition was suggested.

Rudman *et al.*[35] have also published a report on the crystal structures of tris hydrogen-halides, trisH$^+$.X^-, where X = F, Cl, Br, I. The first three analogues (X = F, Cl, Br) were isostructural with a rhombohedral space group, $R\bar{3}(H)$, but trisH$^+$.I$^-$ crystallized in a cubic space group, $I2_13$, which is rarely found for an organic compound. All trisH$^+$.X^- compounds were extensively hydrogen bonded, but no solid–solid phase transitions were observed for them.

Even though solid metal–tris compounds have been indicated in several papers, only a few single-crystal X-ray structures have been published. For example, Dotson[36] has prepared a series of crystalline complexes with the first row bi- and trivalent transition metals from manganese to zinc, and the compounds were characterized by elemental analysis, IR, magnetic susceptibility measurements and X-ray powder diffraction. Hall and Swisher[21] have prepared two solid compounds, Cu(trisH$_{-1}$)$_2$·H$_2$O and Cu(tris)$_2$SO$_4$, which were identified by elemental analysis. Solid platinum(IV)[37] and ruthenium(III)[38] compounds containing tris have also been reported earlier. However, crystal structures were not determined in these studies, probably because of the poor crystallinity of the samples, or perhaps because no single-crystal X-ray diffractometer was available. Altogether, crystal structures of seven metal–tris compounds were determined in the 1980s by single-crystal X-ray techniques, and they are gathered in Table 1.4. The last three articles came to our knowledge after this project was already started. These structures will be discussed in more detail in Chapters 3 and 4 along with the structures determined in this work.

1.4. The aim of this study

Solution studies have given quite a lot of information about the stoichiometry of the metal–tris complexes, deprotonation level of the ligands and equilibria between different species in solution. However, many of these conclusions and structural suggestions are based on indirect observations. For example, the polarographic method can not distinguish between a coordinated hydroxide ion and a coordinated alkoxy group of the ligand, so the chelate formation is deduced from the high stability coefficients observed for the complexes. The number of hydroxymethyl groups, coordinated to the metal ions, is also under discussion. Furthermore, many different complementary methods are needed in solution studies to obtain reliable information.

Table 1.4 Single-crystal structures of compounds containing tris.

Compound	Author	Year	Ref.
tris	Eilerman and Rudman	1980	34
$trisH^+.X^-$ (X = F, Cl, Br, I)	Rudman *et al.*	1983	35
$[Ni(tris)_2](ClO_4)_2$	Ivarsson	1982	39
$[Cu(trisH_{-1})_2]NaClO_4 \cdot H_2O$	Ivarsson	1984	40
$[Cu(trisH_{-1})(tris)]_2Br_2$	Masi *et al.*	1984	41
$[Cu(trisH_{-1})Cl]_4$	Masi *et al.*	1984	41
$[Cu(trisH_{-1})(tris)(H_2O)]Cl \cdot H_2O$	Mazus *et al.*	1986	42
$[Cu(trisH_{-1})_2(H_2O)]$	Colombo *et al.*	1987	29
$[Cu(trisH_{-1})_2] \cdot 5H_2O$	Mazus *et al.*	1987	43

Because of this lack of structural information concerning metal–tris complexes, we decided to start an investigation on solid metal–tris compounds. Copper(II) was chosen for the metal cation, because of its excellent complex-formation properties. The aim of this study was to reveal the structural variety of copper–tris compounds, and to obtain information about the coordination sphere of copper, as well as the role of hydroxymethyl groups in chelate formation. Different conditions and anions were used in the synthesis, the structures of the solid products were determined by single-crystal *X*-ray diffraction and the compounds were characterized with the methods available at our Department of Chemistry (thermogravimetry, infrared spectroscopy, mass spectrometry, and *X*-ray powder diffraction).

2. EXPERIMENTAL

2.1 Synthesis

The syntheses in this work can be divided into two subgroups according to the solvent used in the reactions, namely water and ethanol, and their general procedures are given in Schemes 2.1 and 2.2. The solid copper–tris complexes prepared in this work are gathered in Table 2.1 along with the structures published by Colombo,[29] Ivarsson,[40] Masi *et al.*,[41] and Mazus *et al.*[42,43] Table 2.1 also contains the synthetic conditions for the reactions, and presents the numbering system for the compounds, used from here on.

Water is a good solvent for tris and its copper complexes, therefore in water synthesis the crystallization of the products requires quite concentrated solutions. On the other hand, ethanol (and methanol) as a solvent is quite different, because it dissolves tris well when hot, but the solubility decreases drastically when the solution cools down to room temperature. For instance, the effect of the solvent can be seen in the shape of the crystalline products. In water synthesis, where the crystallization is a slow process lasting for several days or weeks, the crystals grow evenly in all directions yielding products with a prismatic, rod- or plate-shaped habit, where all crystal dimensions are comparable. In ethanol, the products normally crystallize overnight producing needle-shaped crystals, because the crystallization is faster in one of the morphologic directions. Often, the crystal quality is also poor, but it may be improved by adding a few drops of water to the final mother liquor to slow down the crystallization process. Correspondingly, ethanol or methanol additions can be used in the final stage of the water synthesis to precipitate the product. Water and ethanol syntheses differ also in this respect, that water synthesis yields normally only one product, whereas in ethanol the product is very often a mixture of compounds. The most common side product is the monohydrate complex (**2**).

Slightly alkaline conditions are required for the amino group to form coordination bonds with metals. In some literature references,[29,40] the pH of the solution was adjusted to 9.5–10.0 with NaOH or KOH, but the addition of hydroxides is not mandatory, because the protolysis reaction of the amino group yields hydroxides in water solutions and alkoxides in alcoholic solutions (Reactions 2.1 and 2.2). Autoprotolysis of tris is also possible.

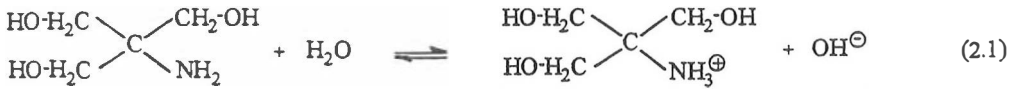

(2.1)

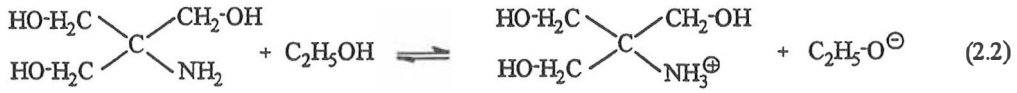

(2.2)

For example, the metal–ligand molar ratio of 1:4 has proved to be a good choice for preparing mononuclear complexes, because half of the ligand is participating in the complex-formation reaction, while the other half is balancing the protolytic equilibrium. An excess of the ligand also prevents the formation of polynuclear species.[4,30]

The basic *trans* complexes, $[Cu(trisH_{-1})_2]$ (**1–3**), with varying amounts of crystalline water, can be obtained from a number of syntheses containing different copper(II) or copper(I) salts as a starting material. The metal–ligand stoichiometric ratio of 1:4 is recommended and the concentration should be quite low. The degree of crystalline water depends on the solvent, reaction temperature, crystallization temperature and time. The anhydrous complex, $[Cu(trisH_{-1})_2]$ (**1**), crystallizes from dilute alcoholic solutions but is often accompanied by the monohydrate form, $[Cu(trisH_{-1})_2(H_2O)]$ (**2**), especially if the reaction is heated for a long period of time. Tris is so reactive towards copper, that even metallic copper powder forms these complexes with tris in ethanol within a few days. In water syntheses, both monohydrate (**2**) and pentahydrate (**3**) forms can be obtained as a product. The coordination of water to the copper ion is promoted by heat, thus producing the monohydrate complex. Long crystallization times (lasting for weeks) also favor the formation of the monohydrate species. According to experimental observations, the monohydrate complex is the most stable form of this complex family, and the most common side product in both solvents. The choice of the anion affects the formation of the pentahydrate compound, $[Cu(trisH_{-1})_2]\cdot 5H_2O$ (**3**). It readily crystallizes from water solutions of copper(II) sulfate or acetate, because these anions participate in the protolytic reactions, making the solution more alkaline. The concentration has to be high enough so that the product will crystallize within a day or two. Otherwise, the monohydrate form results. Storing the solutions below room temperature (~15°C) also favors the formation of the pentahydrate compound. Alkaline addition is also useful when preparing these

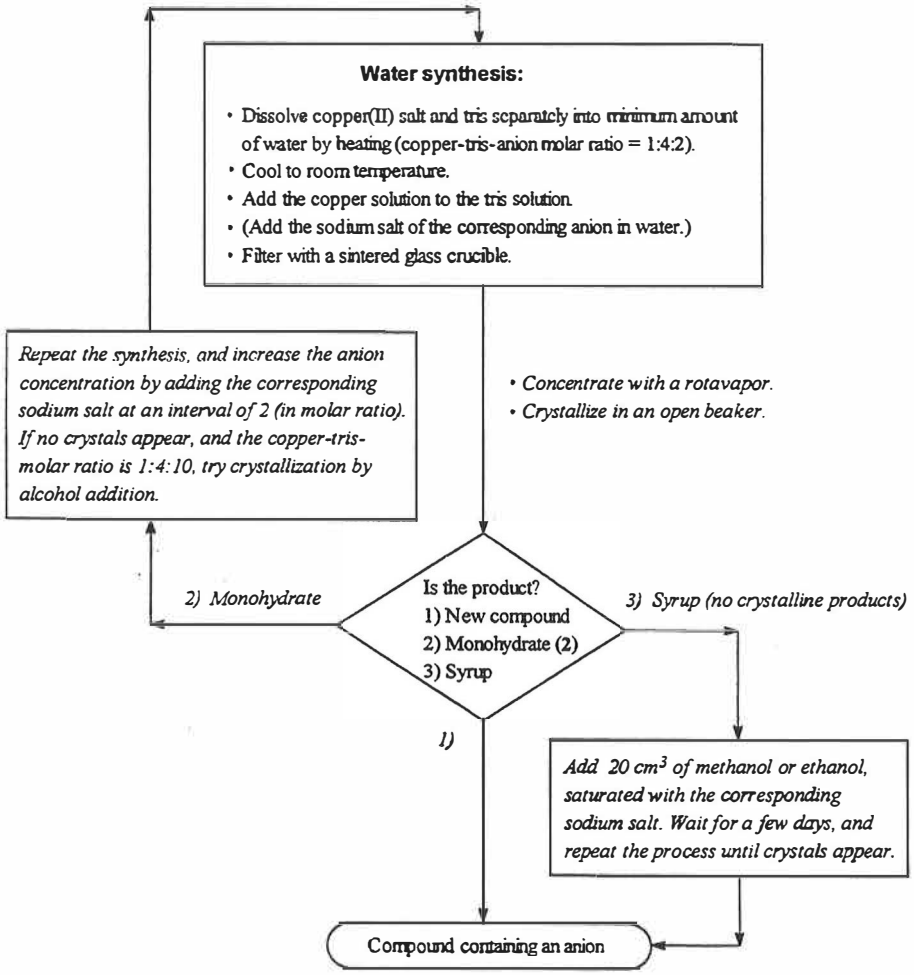

Scheme 2.1 General procedure for concentrated water synthesis.

Ethanol synthesis:

1. Dissolve 0.015 mol of tris in 40 cm^3 of ethanol in a round-bottomed flask with a refluxing condenser.
2. Dissolve 0.0075 or 0.015 mol of copper(II) salt separately in a minimum amount of ethanol by heating.
3. Add warm copper solution to the warm tris solution.
4. (Reflux for 5-30 min.)
5. Cool.
6. (Add 0.015 mol of KOH or NaOH in a minimum amount of ethanol.)
7. Decant or filter with a sintered glass crucible.
8. Crystallize at room temperature overnight.

Scheme 2.2 General procedure for ethanol synthesis.

deprotonated species **1**–**3**. Polyakov *et al.*[45] have also made similar observations when preparing the pentahydrate form (**3**).

The preparation of copper–tris complexes containing anions requires concentrated water solutions to force the anion into the crystal structure. Many of the compounds readily crystallize from a water solution with a metal–ligand–anion molar ratio of 1:4:2, which is concentrated with a rotavapor into a syrupy solution. However, if the monohydrate complex is obtained as a product after this concentration, the synthesis is repeated increasing the anion content gradually (by adding the corresponding sodium salt) until the desired product is produced. A molar ratio of 1:4:8 was successful with the nitrate (**4**) and perchlorate (**5**) compounds. Sometimes, if no crystals appear, the crystallization may be achieved by addition of methanol or ethanol to the concentrated solution (compounds **5**, **10** and **13**). Heating up the solution works in some cases (*e.g.* for compounds **4** and **17**, it promotes the coordination of nitrate to copper), but on the other hand, it may lead to unwanted products, such as the monohydrate in the perchlorate (**5**) and chromate (**7**) syntheses. The corresponding sulfate synthesis (**6**) has a different molar ratio, because it was prepared by a modified method of Brannon *et al.*[46] In addition, both sulfate compounds were crystallized from a water–methanol (1:1 v/v) solution.

Concentrated water synthesis with a metal–ligand–anion molar ratio of 1:4:2 (or higher) was also tried with a number of other anions, such as phosphate, borate, acetate, vanadate(V), molybdate(VI), wolframate(VI), selenate(VI), perbromate, periodate, cyanide, and thiocyanate. Even though these experiments failed to produce new compounds, they showed that the blue copper–tris complex is quite stable, because phosphate was the only anion that was able to precipitate copper out of the complex. On the other hand, cyanide and thiocyanate were able to displace tris from the complex by forming more stable complexes with copper themselves. The main problem in many of these experiments was that corresponding copper(II) salts were not available, and copper(II) chloride and alkali metal salts of the anion in question were used instead, whereupon a more complex mixture of ions resulted.

Polynuclear compounds were obtained from ethanolic syntheses with a metal–ligand stoichiometric ratio of 1:2 or 1:1. In earlier studies, it was stated that polynuclearity is achieved by alkaline addition,[4] but according to my experiments, the polynuclearity is caused by ethanol as a solvent and a low metal–ligand molar ratio. For example,

syntheses of compounds **9** and **19** demonstrates that the alkaline addition breaks down the octanuclear complex. The syntheses are otherwise similar, but for compound **9**, potassium hydroxide is added at the end of the reaction, and a new salt containing deprotonated mononuclear complexes, potassium and bromide results. The synthesis is sensitive to temperature, where hydroxide is added, and to the alkali metal used (*e.g.* sodium does not produce corresponding compounds). The same syntheses were also tried with fluoride and chloride as an anion with different results. In the case of chloride, the tetranuclear complex published by Masi *et al.*,[41] $[Cu(trisH_{-1})Cl]_4$, is formed. The complex is very stable and does not break down in alkaline conditions, because it is already in a deprotonated form. Fluoride is exceptional in all respects, because the same stoichiometry (1:2:2) in ethanol yields a *trans* complex with a chain structure (**14**), and after KOH addition, a similar potassium compound (**8**) is observed as with bromide above, but it contains one extra water molecule. In the corresponding water synthesis (**16**), hexafluorosilicate is formed, where the silicon atom is taken from the glassware. In addition to the octanuclear compounds given in Table 2.1 (**19** and **20**), there is also evidence that in the presence of nitrate, polynuclear complexes are also formed, and the mononuclear *trans* nitrate-complex, $[Cu(tris)_2(NO_3)_2]$ (**17**), is a byproduct of this polynuclear nitrate synthesis.

Summary of the synthetic work:

- Mononuclear *trans* complexes are formed in dilute water or ethanol solutions with a metal–ligand molar ratio of 1:4.
- Mononuclear *cis* complexes containing anions are formed in concentrated water solutions with a metal–ligand–anion molar ratio of 1:4:2 (or higher anion concentration).
- Polynuclear complexes are formed in ethanol solutions with a metal–ligand molar ratio of 1:2 or 1:1 (but heating or an excessively high dilution leads to mononuclear complexes).
- Coordination of water to copper is favored and can be improved by heating.
- Addition of alkali hydroxides leads to formation of fully deprotonated species, normally to mononuclear *trans* complexes.
- In ethanolic solutions, there is more flexibility regarding the deprotonation level of tris.

Table 2.1 Synthetic conditions for copper–tris compounds.

Compound	Color	Solvent	Metal–tris–anion stoichiometry	Alkaline addition	Heating	Authors	Ref.
1 *trans*-[Cu(trisH$_{-1}$)$_2$]	Violet	EtOH	1:2(or 4)	(Yes)	No	Kotila & Valkonen	I
2 *trans*-[Cu(trisH$_{-1}$)$_2$(H_2O)]	Blue	H_2O or EtOH	1:4	(Yes)	(Yes)	Kotila & Valkonen	I
– " –	Blue	H_2O	1:10	No	No	Colombo *et al.*	29
3 *trans*-[Cu(trisH$_{-1}$)$_2$]·5H_2O	Violet	H_2O	1:4	(Yes)	No	Kotila & Valkonen	I
– " –	Violet	H_2O	1:2	Yes	No	Mazus *et al.*	43
4 *cis*-[Cu(trisH$_{-1}$)(tris)(NO_3)]	Blue	H_2O	1:4:8	No	Yes	Kotila & Valkonen	II
5 *cis*-[Cu(trisH$_{-1}$)(tris)]Na(ClO_4)$_2$	Blue	H_2O	1:4:8	No	No	Kotila & Valkonen	II
6 *cis*-[Cu(trisH$_{-1}$)(tris)(H_2O)]$_2$$SO_4$	Blue	H_2O	1:3:1	No	Yes	Kotila & Valkonen	III
7 *cis*-[Cu(trisH$_{-1}$)(tris)(H_2O)]$_2$$CrO_4$	Green	H_2O	1:4:2	No	No	Kotila & Valkonen	III
8 *trans*-[Cu(trisH$_{-1}$)$_2$]KF·3H_2O	Light brown	EtOH	1:2:2	Yes	No	Kotila & Valkonen	IV
9 *trans*-[Cu(trisH$_{-1}$)$_2$]KBr·2H_2O	Brown	EtOH	1:2:2	Yes	No	Kotila & Valkonen	IV
10 *cis*-[Cu(trisH$_{-1}$)(tris)(H_2O)]F·H_2O	Light blue	H_2O	1:4:2	No	No	Kotila	V
11 *cis*-[Cu(trisH$_{-1}$)(tris)(H_2O)]Cl·H_2O	Blue	H_2O	1:4:2	No	No	Kotila	V
– " –	Blue	H_2O	1:3.5:2	No	No	Mazus *et al.*	42
12 *cis*-[Cu(trisH$_{-1}$)(tris)(H_2O)]Br·H_2O	Blue	H_2O	1:4:2	No	No	Kotila	V
13 *cis*-[Cu(trisH$_{-1}$)(tris)(H_2O)]I·H_2O	Blue	H_2O or EtOH	1:4:2	No	No	Kotila	V
14 *trans*-{[Cu(tris)$_2$]F_2}$_n$	Colorless	EtOH	1:2:2	No	No	Kotila	44
15 *cis*-[Cu(trisH$_{-1}$)(tris)]F	Blue	H_2O	1:4:2	No	No	Kotila	44
16 *cis*-[Cu(trisH$_{-1}$)(tris)(H_2O)]$_2${SiF_6}	Blue	H_2O	1:2:2	No	Yes	Kotila	44
17 *trans*-[Cu(tris)$_2$(NO_3)$_2$]	Blue	EtOH	1:2:2	No	Yes	Kotila	44
18 *cis*-[Cu(tris)$_2$(SO_4)]$_n$	Turquoise	H_2O+MeOH(1:1)	1:2:1	No	No	Kotila	44
19 [Cu$_8$(trisH$_{-2}$)$_4$(trisH$_{-1}$)$_2$(tris)$_2$]Br_6·6H_2O·EtOH	Green	EtOH	1:2:2	No	No	Kotila	44
20 [Cu$_8$(trisH$_{-2}$)$_4$(trisH$_{-1}$)$_2$(tris)$_2$](ClO_4)$_6$·6H_2O·EtOH	Green	EtOH	1:2:2	No	No	Kotila	44
21 *trans*-[Cu(trisH$_{-1}$)$_2$]$NaClO_4$·H_2O	Violet	H_2O	1:2:12	Yes	No	Ivarsson	40
22 *cis*-{[Cu(trisH$_{-1}$)(tris)]Br}$_n$	Blue	EtOH	1:2:2	No	No	Masi *et al.*	41
23 [Cu(trisH$_{-1}$)Cl]$_4$	Green	EtOH	1:1:2	No	No	Masi *et al.*	41

2.2 *X*-Ray measurements

X-Ray diffraction measurements were performed on an automatic Enraf–Nonius CAD-4 diffractometer with graphite-monochromated MoK_α radiation (λ = 0.71073 Å). Crystals were mounted on a glass fiber and measured in an air atmosphere. The only exceptions were compounds, which contained volatile crystalline water or ethanol (compound **8** and all octanuclear species), and they were measured in a glass capillary containing a drop of mother liquor. All unit-cell parameters were obtained by a least-squares analysis of 25 centered reflections. Intensities were collected by the $\omega/2\theta$ scan technique and corrected for Lorentz and polarization effects. During the data collection, two or three standard reflections were monitored every 60 minutes as an intensity check and crystal orientation was confirmed after every 400–500 reflections. Absorption corrections were done by the DIFABS[47] program for all compounds except compound **13** (an empirical Ψ-scan was necessary for this iodide compound to obtain the right solution from the direct methods).

The positions of the heavy atoms (Cu, I, Br, Cr, Cl, and Na) were solved by direct methods using the SHELXS-86 program.[48] The other non-hydrogen atoms were located by successive Fourier synthesis and refined by full-matrix least-squares methods with anisotropic thermal parameters. The hydrogens attached to carbons and nitrogens were included in their calculated positions after the isotropic refinement ($d_{\text{C-H,N-H}}$ = 0.95 Å), and the hydrogens in hydroxy groups and water molecules were located by Fourier difference synthesis after the anisotropic refinement of the non-hydrogen atoms. All hydrogens were refined as riding atoms with a fixed isotropic temperature parameter, B = 5.00 Å^2.

The calculations were carried out on a MicroVAX 3100 computer, using the MolEN[49] structure determination package supplied by Enraf–Nonius. The atomic scattering factors and real and imaginary dispersion corrections for scattering factors were taken from the *International Tables*.[50] The figures were drawn with the SCHAKAL-87 and SCHAKAL-92 programs.[51,52]

In the structures of compounds **6**, **7**, and **13**, disorder in the orientation of the terminal hydroxymethyl groups is observed, and structures **6**, **7**, **8**, and **17** contain disordered anions. The multiplicities of these hydroxymethyl groups were found by presuming that

the isotropic thermal parameters of both orientations would be equal in magnitude. A detailed description of how the disorder was handled is given in the corresponding article.

2.3 Mass spectrometry

Mass spectra of the solid samples were obtained on a Finnigan-MAT 212 mass spectrometer using electron ionization (EI) techniques. Direct introduction of the solid sample was used, and the sample chamber was heated from 25 to 300°C. Other operational parameters were: ion source 250°C, acceleration potential of electrons 3 kV, energy of the electron beam 70 eV. The mass-to-charge ratio (*m/z*) was verified using perfluorokerosene, C_nF_{2n+2}, as a mass-unit standard.

Deuterated samples were prepared by dissolving tris into deuterated water (Merck, for spectroscopy, 99.75%) followed by shaking and heating. The dissolving and recrystallization procedures were repeated three times, and each dissolution was done with a fresh volume of deuterated water.

2.4 Thermal analysis

Thermal studies were carried out on a Perkin—Elmer thermogravimetric analyzer TGA7. The thermogravimetric (TG) and derivative (DTG) curves were obtained at a heating rate of 2°C min^{-1} in dynamic air and nitrogen atmospheres with a gas flow of 50 cm^3 min^{-1}. In general, the samples were analyzed in a temperature range of 25—900°C. However, some samples were measured up to 970°C, if the decomposition of the anion required high temperatures. The sample size was 7.00 ± 0.50 mg, even though some exceptions were made with needle-shaped crystals, which were so light that even a sample of 3—4 mg filled the platinum crucible (compounds **7**, **8**, and **9**). The 3-mg sample size was also used for the perchlorate compound (**5**), because of the possible risk of explosion. When a nitrogen atmosphere was used, the equipment was flushed for 30—45 minutes with nitrogen before the temperature program was initiated to remove oxygen from the oven. The temperature scale was calibrated magnetically using the following ferromagnetic standards and magnetic transition temperatures (°C): alumel (163), nickel (354), Perkalloy (596), and iron (780).

3. MOLECULAR STRUCTURES

3.1 General

Structurally, copper–tris complexes are mainly mononuclear. The figures of known mononuclear complexes along with some other structural examples are presented in Figure Appendix I at the end of this chapter, and the bond lengths and angles characterizing these molecules are given in the corresponding publications or will be published later.

The mononuclear species contain two tris ligands, which are coordinated to the copper atom via one amino and one hydroxymethyl group, forming a five-membered chelate ring. In addition to these basal coordination bonds, which are in the range 1.901(3)–2.032(1) Å, the apical positions can be occupied by a water molecule, terminal hydroxymethyl group (tris acting as a tridentate ligand) or an anion (nitrate). These apical bonds are longer due to the Jahn–Teller effect [2.200(2)–2.778(1) Å]. Hence, the coordination sphere of copper varies from square-planar to square-pyramidal or distorted octahedral in shape. The complex molecules can be either neutral or cationic, depending on the deprotonation level of the ligands and other coordinated groups. The deprotonation level of the ligands in mononuclear species varies from zero (tris) to one ($trisH_{-1}$), and all combinations are observed. However, the deprotonated hydroxymethyl groups are always located in the basal coordination plane, and their coordination bonds are normally the shortest. Similar copper(II) complexes with five-membered chelate rings are also formed with 2-amino-2-methyl-1-propanol[53] and ethylenediamine[54,55] as ligands.

3.2 Coordination sphere of copper

The most distinctive differences in bond lengths and angles are observed in the coordination sphere of copper, and these dimensions are given in Appendix I and II. Basal and apical coordination bonds are shown in Appendix I, and selected angles characterizing the distortion of the coordination sphere are collected in Appendix II. The illustration defining the angles given in Appendix II is presented in Fig. 3.1. Otherwise, the bond lengths and angles obtained for the ligand are close to the typical values of C–C [1.541(3) Å], C–O [1.43(1) Å], and C–N [1.472(5) Å] single bonds of organic compounds.[56]

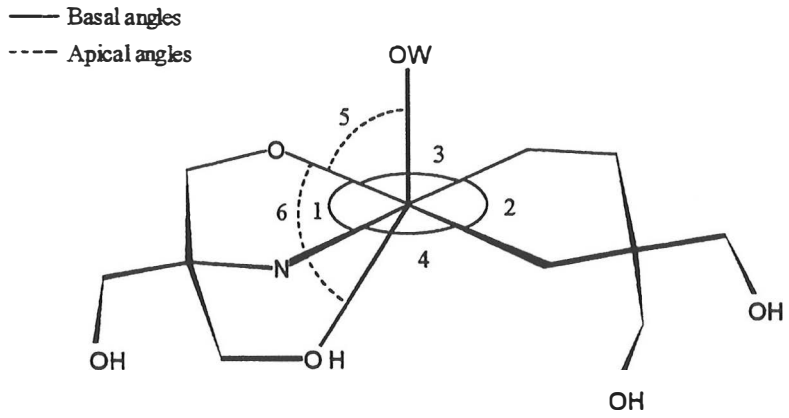

Fig. 3.1 Angles used to define the coordination sphere of copper (see Appendix II).

The basic dilemma, when talking about coordination spheres, centers on how long a coordination bond can be and still be regarded as a coordination bond. This question is valid especially for the longer apical bonds. In the earlier copper–tris structure by Masi *et al.*,[41] copper–oxygen separations of 2.551 and 2.778 Å (compound **22**) were not considered as apical coordination bonds, and the structure was treated as a square-planar coordination sphere. On the other hand, in the comprehensive review article by Gazo *et al.*,[57] which is discussing the plasticity of the coordination sphere of copper(II) complexes, distances up to 3.5 Å were considered as apical coordination bonds, even though most of them were in the range 2.4–2.8 Å.

On the basis of a few individual structures, it is very difficult to say whether the terminal hydroxymethyl group is actually coordinated to copper, or the structure is just a conformation. But when the whole set of copper–tris complexes is examined together, some trends are found, which support the existence of the third coordination bond between copper and the ligand. First, a very short apical bond to hydroxymethyl group is found in compound **15**, [Cu(trisH$_{-1}$)(tris)]F, where the Cu–O distance is 2.386(3) Å, which can be considered as a coordination bond. Then, according to structural analogy, the corresponding longer apical bonds can be treated as coordination bonds, where the bond strength decreases with increasing Cu–O bond distance. Second, the lone-pairs of hydroxy oxygens are oriented towards copper, which can be deduced from the orientation of the OH hydrogen (found from a difference Fourier map). Third, the coordination plane of complexes containing this tridentate ligand is flatter than in the five-coordinated species (see Appendix III). The most distorted square pyramid is observed for

trans-[Cu(trisH$_{-1}$)$_2$(H$_2$O)] (**2**), where the copper atom is located 0.2256(3) Å from the square plane defined by oxygens and nitrogens towards the apex of the pyramid. In compounds **6**, **7** and **16**, where the complex molecules are clearly five-coordinated, the copper is displaced 0.1898(4)–0.1694(5) Å from the square plane. In the remaining structures, with assumed six-coordination, the distance of copper from the least-squares plane of O111, N111, O121, and N121 (or the corresponding set) is much smaller [0.0613(5)–0.0032(3) Å], suggesting that the coordination sphere is approaching octahedral geometry. Fourth, in the structures containing only one tridentate ligand, the tridentate behavior is systematically related to the non-protonated ligand, and they are all *syn* conformers. Furthermore, the apical coordination angles with respect to the basal oxygen atom of the same ligand are in the range 71.96(8)–84.0(1)°, which is not exceptional, because apical angles as low as 54.4(2)° have been reported for extremely distorted octahedral complexes.[58] In the molecular structures in Figure Appendix I, bond lengths smaller than 2.80 Å are considered as coordination bonds.

3.3 Isomerism of the complexes

Mononuclear copper–tris complexes possess a lot of conformational as well as stereo isomerism, and Table 3.1 summarizes the information given in the following paragraphs.

3.3.1 Conformational isomerism

Since the sigma bonds of the organic group are not rigid, the terminal hydroxymethyl groups can rotate around the carbon–carbon bond, forming an infinite number of arrangements. However, these rotational conformations are not of equal stability, but normally, the staggered conformation shown in Fig. 3.2 is the most stable. Furthermore, the staggered conformation can be divided into *anti* and *gauche* conformations depending on the relative positions of substituents (Fig. 3.3), where the *anti* conformation would be energetically the most favorable, if all other substituents would be hydrogens. Nevertheless, in the tris ligand, there are four non-hydrogen atoms attached to carbon C112 (or the corresponding carbon), and as a result, the conformations can generally be classified as just staggered. The torsion angles of the terminal hydroxymethyl groups calculated with respect to carbon atoms in the chelate ring are given in Appendix IV. The values obtained are close to ±60° or ±180°, corresponding to staggered conformations.

Table 3.1 Symmetry and isomerism of the complexes.

Compound (and *cis–trans* isomerism)	Molecular symmetry (Schönflies)	*syn–anti* Isomerism (monomer)	Coord. number of copper	Molecule optically active	Molecular structure	Symmetry of the dimer	
						Schönflies	*syn–anti*
1 *trans*-[Cu(trisH$_{-1}$)$_2$]	*i*	*anti*	4		Monomer		
2 *trans*-[Cu(trisH$_{-1}$)$_2$(H_2O)]	C_2	*syn*	5	Yes	Monomer		
3 *trans*-[Cu(trisH$_{-1}$)$_2$]·5H_2O	*i*	*anti*	4		Monomer		
4 *cis*-[Cu(trisH$_{-1}$)(tris)(NO_3)]	*E*	*syn*	6	Yes	Dimer	*i*	*syn*
5 *cis*-[Cu(trisH$_{-1}$)(tris)]Na(ClO_4)$_2$	*E*	*anti*	6	Yes	Dimer	*i*	#
6 *cis*-[Cu(trisH$_{-1}$)(tris)(H_2O)]$_2SO_4$	*E*	*anti*	5	Yes	Dimer	*i*	*anti*
7 *cis*-[Cu(trisH$_{-1}$)(tris)(H_2O)]$_2CrO_4$	*E*	*anti*	5	Yes	Dimer	*i*	*anti*
8 *trans*-[Cu(trisH$_{-1}$)$_2$]KF·3H_2O	*i*	*anti*	4		Monomer		
9 *trans*-[Cu(trisH$_{-1}$)$_2$]KBr·2H_2O	*i*	*anti*	4		Monomer		
11 *cis*-[Cu(trisH$_{-1}$)(tris)(H_2O)]Cl·H_2O	*E*	*syn*	6	Yes	Dimer	*E*	*syn*
12 *cis*-[Cu(trisH$_{-1}$)(tris)(H_2O)]Br·H_2O	*E*	*syn*	6	Yes	Dimer	*E*	*syn*
13 *cis*-[Cu(trisH$_{-1}$)(tris)(H_2O)]I·H_2O	*E*	*syn*	6	Yes	Dimer	*i*	*syn*
14 *trans*-{[Cu(tris)$_2$]F_2}$_n$	*i*	*anti*	6		Chain		
15 *cis*-[Cu(trisH$_{-1}$)(tris)]F	*E*	*syn*	5	Yes	Dimer	*i*	#
16 *cis*-[Cu(trisH$_{-1}$)(tris)(H_2O)]$_2${SiF_6}	*E*	*anti*	5	Yes	Dimer	*i*	*anti*
17 *trans*-[Cu(tris)$_2$(NO_3)$_2$]	*i*	*anti*	6		Monomer		
18 *cis*-[Cu(tris)$_2$(SO_4)]$_n$	*E*	*anti*	6	Yes	Double chain		
19 [Cu_8(trisH$_{-2}$)$_4$(trisH$_{-1}$)$_2$(tris)$_2$]Br_6·6H_2O·EtOH	*i*	–	5–6*		Octanuclear		
20 [Cu_8(trisH$_{-2}$)$_4$(trisH$_{-1}$)$_2$(tris)$_2$](ClO_4)$_6$·6H_2O·EtOH	*i*	–	5–6*		Octanuclear		
21 *trans*-[Cu(trisH$_{-1}$)$_2$]$NaClO_4$·H_2O (Ivarsson)[40]	*i*	*anti*	4		Monomer		
22 *cis*-{[Cu(trisH$_{-1}$)(tris)]Br}$_n$ (Masi *et al.*)[41]	*E*	*syn*	6	Yes	Dimeric chain	*i*	#
23 [Cu(trisH$_{-1}$)Cl]$_4$ (Masi *et al.*)[41]	*i*	–	4–5		Tetranuclear		

* Weak apical coordination bonds with anions and crystalline water are taken into account. # Undefined.
Schönflies symbols: C_2 = two-fold axis of symmetry, *i* = center of inversion, and *E* = identity element of symmetry.

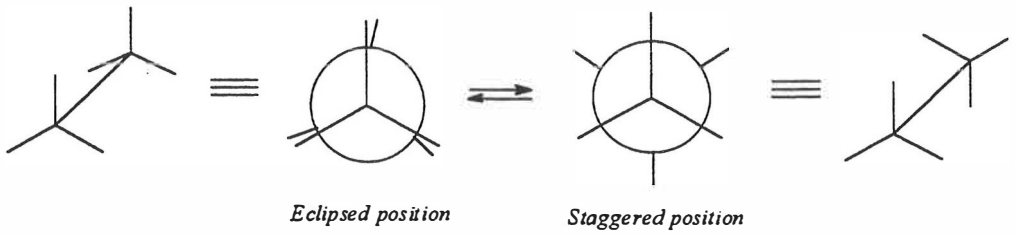

Fig. 3.2 The two extreme rotational positions of a sigma-bonded carbon chain.

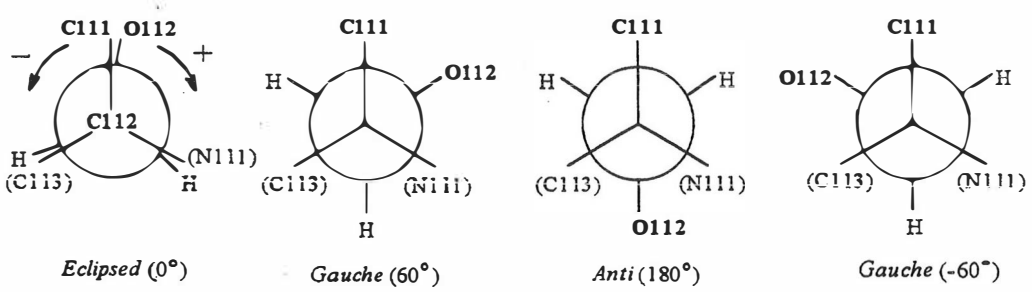

Fig. 3.3 Conformations of terminal hydroxymethyl groups with respect to ring carbons. Example above shows the torsion angles of the C111–C112–C113–O112 chain (torsion angles of copper–tris complexes are given in Appendix IV).

The potential energy differences between different conformations are not very significant, because all conformations are represented in Appendix IV. Hence, the preference of one conformation over the others is more likely chosen on the basis of hydrogen bonding.

The conformation of the chelate rings is not fixed. The five-membered chelate rings are in an *envelope* conformation, where Cu100, O111, N111, and C111 (or the corresponding set) are the atoms defining the plane, and C112 (or C122, C212, C222) is the atom, bent out of the plane. These chelate rings can point in the same direction (*syn*) or in opposite directions (*anti*) with respect to the coordination plane, leading to *syn–anti* isomerism (Fig. 3.4). *Syn/anti* descriptions in Table 3.1 refer to this type of isomerism. Furthermore, terminal hydroxymethyl groups are in an axial or equatorial position in relation to this plane, where the axial groups have the possibility to coordinate to the copper ion of the same mononuclear unit if the conformation is right.

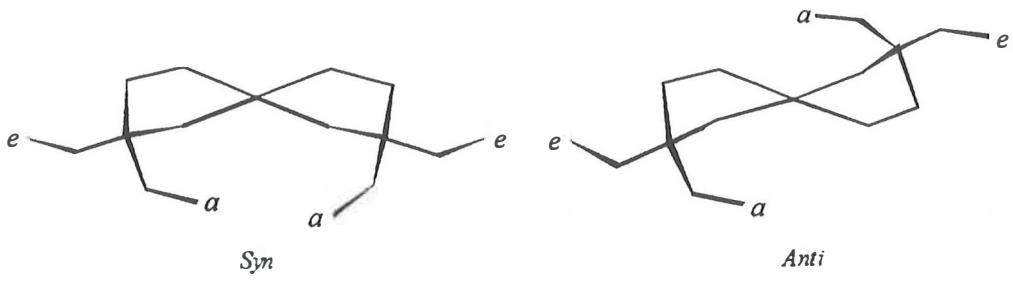

Fig. 3.4 ***Syn–anti*** isomerism of the mononuclear copper–tris complexes, and the positions of axial (*a*) and equatorial (*e*) hydroxymethyl groups.

3.3.2 Stereo isomerism

The most obvious type of structural isomerism is *cis–trans* isomerism of the oxygen and nitrogen atoms in the basal coordination plane, and both types are encountered among mononuclear copper–tris complexes. *Cis* isomers are closely related to the formation of hydrogen-bonded dimers, which is explained in Chapter 3.4.

All five- and six-coordinated complexes (which do not contain an inversion center) are also optically active complexes with two possible enantiomers, which are mirror images of each other (Fig. 3.5). The enantiomers are identical in all other respects, except that they rotate plane-polarized light in opposite directions. However, because the syntheses are not stereoselective, the product is a racemic mixture containing both enantiomers in equal amounts.

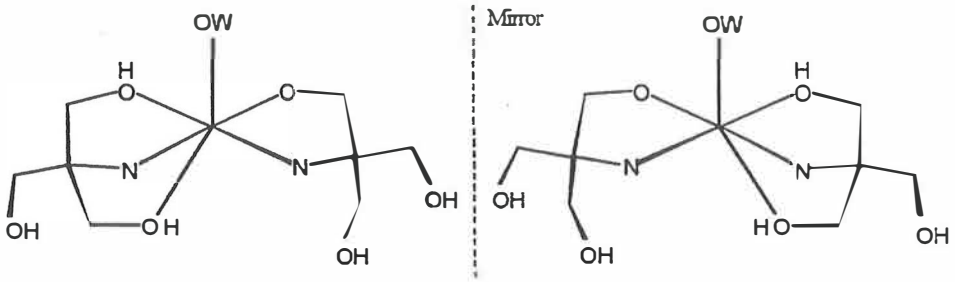

Fig. 3.5 Optical isomers of an octahedral copper–tris complex.

3.3.3 Isomerism of the coordination sphere of copper

The coordination sphere of copper exhibits two types of isomerism for complex species with the same stoichiometric composition, namely coordination isomerism and distortion isomerism.[57,59]

In this context coordination isomerism means complexes with identical ligands, but different coordination numbers. For example, cationic complexes $[Cu(trisH_{-1})(tris)]^+$ and $[Cu(trisH_{-1})(tris)(H_2O)]^+$ form five- and six-coordinated species depending on which anion is used in the synthesis (see Figure Appendix I, Fig. 3.8).

As a consequence of the marked plasticity of the coordination sphere of copper(II), copper complexes can form several stable arrangements, which differ in the lengths of their coordination bonds, as well as the degree of distortion of the coordination polyhedra.[57] In copper–tris complexes, distortion isomerism has been observed for the monohydrate halide compounds, $[Cu(trisH_{-1})(tris)(H_2O)]X{\cdot}H_2O$, X = Cl, Br (**11** and **12**),[V] which consist of two different complex molecules that are distortion isomers of each other. Molecule 1 has a more distorted octahedron with one short and one long apical bond [2.355(3) and 2.752(3) Å in **11**], whereas in molecule 2 the structure is more regular [apical bonds 2.486(3) and 2.638(3) Å in **11**]. Furthermore, the disordered *trans* nitrate compound, $[Cu(tris)_2(NO_3)_2]$ (**17**),[44] contains two molecules, which differ only with respect to the coordination angles of nitrates. The difference between the two orientations of nitrates is 6.4(1)°. In addition, the $[Cu(trisH_{-1})(tris)]^+$ molecules in the anhydrous fluoride[44] (**15**) and bromide[41] (**22**) compounds show marked differences in the apical bond lengths and angles.

3.4 Monomeric structure versus hydrogen-bonded dimers

Cis–trans isomerism is very closely related to whether the complexes appear as monomers or hydrogen-bonded dimers. All mononuclear *trans* complexes are monomeric units containing some intramolecular symmetry. Generally, the internal symmetry element is an inversion center (*i*), and the molecule is an *anti* conformer, but a two-fold rotation axis (C_2) is also observed for the compound, $[Cu(trisH_{-1})_2(H_2O)]$ (**2**), which is a *syn* conformer. Because of this internal symmetry, the deprotonation level of the ligands has to be identical, so both are either in a deprotonated or neutral form.

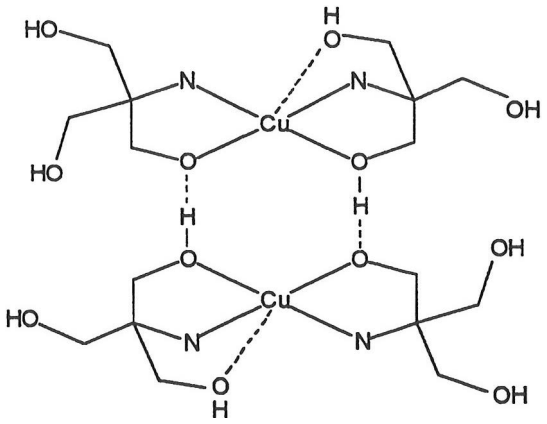

Fig. 3.6 Dimeric structure of *cis* copper–tris complex.

The structure of mononuclear *cis* complexes is less symmetrical, because one of the ligands is deprotonated and the other is neutral, hence the symmetry of the molecule is just the identity (*E*). Since there is a hydrogen atom in every other metal-bonded hydroxy group, the monomer is able to form hydrogen-bonded associates with another mononuclear unit via strong hydrogen bonds [O···O contacts in the range 2.459(3)–2.565(4) Å]. A step-like structure results, containing an eight-membered ring with two copper(II) ions (see Fig. 3.6). Masi *et al.*[41] were the first to write about these hydrogen-bonded copper–tris dimers in the literature, but the hydrogens in their dimer structure were calculated. Furthermore, their fitting program probably failed, because in all my dimeric structures the connecting hydrogens (located from the difference Fourier maps) are on the opposite side of the dimer ring (*i.e.* the hydrogen is on the tridentate side of the ligand). In addition, Mazus *et al.*[42] have written about the dimeric structure of *cis*-[Cu(trisH$_{-1}$)(tris)(H$_2$O)]Cl·H$_2$O (**11**), but they could not state unequivocally which of the coordinated OH groups had lost a proton. Similar dimeric structures have been reported by Muhonen,[53] when using 2-amino-2-methyl-1-propanol as a ligand.

Normally, the mononuclear complex is hydrogen bonded to its optical isomer, and as a result the eight-membered ring contains an inversion center. The only exceptions are isomorphic compounds **11** and **12**, where complex molecule 1 is hydrogen bonded to the enantiomer of molecule 2 (and *vice versa*). Since the mononuclear units are different, the structures of compounds **11** and **12** consist of optically active dimers and their dimeric enantiomers. The dimeric structures of mononuclear *cis* copper–tris complexes are presented in Fig. 3.9 in Figure Appendix I, and the corresponding Cu···Cu separations are given in Table 3.2. The illustrations show that these dimeric structures also possess

Table 3.2 Copper—copper separation of the dimers and polynuclear structures.

Compound		Cu···Cu' [Å]
Dimers:		
4 *cis*-[Cu(trisH$_{-1}$)(tris)(NO_3)]		4.9618(4)
5 *cis*-[Cu(trisH$_{-1}$)(tris)]Na(ClO_4)$_2$		4.7410(5)
6 *cis*-[Cu(trisH$_{-1}$)(tris)(H_2O)]$_2SO_4$		4.9866(7)
7 *cis*-[Cu(trisH$_{-1}$)(tris)(H_2O)]$_2CrO_4$	(Cu100···Cu100')	4.9012(6)
	(Cu200···Cu200')	4.9031(6)
11 *cis*-[Cu(trisH$_{-1}$)(tris)(H_2O)]Cl·H_2O	(Cu100···Cu200')	4.9181(5)
12 *cis*-[Cu(trisH$_{-1}$)(tris)(H_2O)]Br·H_2O	(Cu100···Cu200')	4.8870(6)
13 *cis*-[Cu(trisH$_{-1}$)(tris)(H_2O)]I·H_2O		4.8706(6)
15 *cis*-[Cu(trisH$_{-1}$)(tris)]F		4.9596(8)
16 *cis*-[Cu(trisH$_{-1}$)(tris)(H_2O)]$_2$\{SiF_6\}		5.0596(3)
Chain structures:		
14 *trans*-\{[Cu(tris)$_2$]F_2\}$_n$		5.9027(0)#
18 *cis*-[Cu(tris)$_2$(SO_4)]$_n$		5.1934(4)¤ , 7.2116(4)#
22 *cis*-\{[Cu(trisH$_{-1}$)(tris)]Br\}$_n$ (Masi *et al.*)[41]		5.044*, 7.229#
Polynuclear structures:		
19 [Cu$_8$(trisH$_{-2}$)$_4$(trisH$_{-1}$)$_2$(tris)$_2$]Br_6·6H_2O·EtOH		2.933(2)—3.263(1)
20 [Cu$_8$(trisH$_{-2}$)$_4$(trisH$_{-1}$)$_2$(tris)$_2$](ClO_4)$_6$·6H_2O·EtOH		2.925(1)—3.257(1)
23 [Cu(trisH$_{-1}$)Cl]$_4$ (Masi *et al.*)[41]		2.841(1), 3.233(2)

' Generated by inversion. # Along the chain. ¤ To the adjacent chain. * Dimer.

a kind of *syn—anti* isomerism regarding whether the coordinated groups are facing each other or pointing outside the dimer.

3.5 Polynuclear complexes

The chain structures and polynuclear complexes shown in Figs. 3.10 and 3.11 illustrate the diversity of copper—tris complexes, and the corresponding Cu···Cu separations of neighboring copper atoms are given in Table 3.2. More detailed descriptions of the structures are given in the corresponding publications or will be published later, but some general notions are given below.

Two of the chain structures presented in Fig. 3.10 consist of cationic molecules joined together by terminal hydroxymethyl groups, and the third structure contains a bridging sulfate unit in between the complex molecules. The *trans* fluoride compound $\{[Cu(tris)_2]F_2\}_n$ **(14)**[44] is the first structure, where the axial hydroxymethyl groups is coordinated to the neighboring complex (and *vice versa*), resulting in a very symmetric chain structure with an extra ring between copper(II) ions. The structure of *cis*-$\{[Cu(trisH_{-1})(tris)]Br\}_n$ **(22)**[41] is dimeric as well as a chain, so the figure shows only one half of the actual chain, and the other half is related by inversion. In this structure coordination to the adjacent dimer happens via equatorial hydroxymethyl groups, and the chain has a two-fold screw symmetry. Note also that the corresponding fluoride analogue, *cis*-$[Cu(trisH_{-1})(tris)]F$ **(15)**, does not exhibit this chain behavior. The last chain structure with bridging sulfate ligands, $[Cu(tris)_2(SO_4)]$ **(18)**,[44] is typical for the sulfate anion, and similar structures have been published for $[Cu(en)(H_2O)_2(SO_4)]$,[60] $[Cu(bipy)(H_2O)_2(SO_4)]$,[61] and $[Cu(phen)(H_2O)_2(SO_4)]$.[62]* In compound **18** the chain is bonded to another similar chain by lateral hydrogen bonds between coordinated hydroxy groups and coordinated oxygens of the sulfate ligand.

Polynuclear copper complexes with alkoxo-bridged structures are also formed with tris, and thus far, tetranuclear and octanuclear species are known (Fig. 3.11). Both complexes have a step-like structure with an inversion center in the middle, and they both contain triply bridging alkoxo oxygens in the Cu_nO_n rings (n = 2, 3). In these polynuclear complexes, halides are also coordinated to copper, which was not observed with the mononuclear species. In the tetranuclear $[Cu(trisH_{-1})Cl]_4$ complex, published by Masi *et al.*,[41] chlorides are located in the basal coordination plane of copper, and the Cu–Cl bond lengths [2.253(2) and 2.260(2) Å] are comparable to other basal coordination bonds [1.939(5)–2.020(6) Å], whereas the apical Cu–O bond is 2.407(6) Å. The folded structure is quite unusual for tetramers, since the cubane-type molecules with a Cu_4O_4 core are much more common for tetranuclear complexes, and also observed with aminoalcoholic ligands.[63–65] Octanuclear complexes are obtained when bromide or perchlorate are used as anions.[44] The actual structure of the complex is more complicated than shown in Fig 3.11, because the anions and crystalline water are coordinated to copper(II) [Cu–Br 2.764(2)–3.068(1) Å, Cu–O(ClO_4) 2.667(7)–3.17(3) Å]. Similar folded structures for polynuclear complexes have been reported by Watson and Holley,[66] and Olejnik *et al.*[67] The basal and apical coordination bond lengths of halides are typical for polynuclear copper complexes.[68,69]

---

* en = ethylenediamine
biby = 2,2'-bipyridine
phen = 1,10-phenantroline

3.6 Discussion

When the structures shown in Figure Appendix I are compared with the structure proposals deduced from the results of the solution studies (see Introduction, pages 20 and 21), the suggestions given by Bai and Martell[4] are in good agreement with the results obtained in the solid-state. Only the *cis* structure and its hydrogen-bonded dimer are missing, even though the presence of the semi-protonated $[Cu(trisH_{-1})(tris)]^+$ species was already concluded by titrations. Further, the dinuclear complex they have proposed is very likely a starting point for tetra- and octanuclear species, although it has never been isolated in solid form. On the other hand, the structure proposals given by Boyd *et al.*,[30] are less probable. In the dimer structure especially, where the coordination occurs via two hydroxymethyl groups, they have completely ignored the presence of the strongly coordinating amino group. However, they have quite successfully estimated the copper–copper separations of the dimeric and polynuclear species by ESR.

Crystal structures of *trans*-$[Cu(trisH_{-1})_2(H_2O)]$ (**2**),[29] *trans*-$[Cu(trisH_{-1})_2]\cdot 5H_2O$ (**3**),[43] and *cis*-$[Cu(trisH_{-1})(tris)(H_2O)]Cl\cdot H_2O$ (**11**)[42] are also published elsewhere, and in essence, they are identical with the structures determined in this work. The monohydrate structure presented by Colombo *et al.*[29] agrees well with the structure given in paper I, even though the number of reflections used in their refinement (938 refls.) is only half of the value used in our work (1841 refls.). On the other hand, the quality of the articles by Mazus *et al.*[42,43] is not the best. They were not able to refine the hydrogens in compound **11**, and the final R value, 0.090,[42] is quite poor for these types of complexes. Furthermore, there are several inconsistencies in the structural data of $[Cu(trisH_{-1})_2]\cdot 5H_2O$[43] (some of them indicated by the Editor of the translation). For example, the bond lengths given in the tables do not match those shown in the illustrations. In addition, they have stated that the apical coordination bond (Cu–O2 2.887 Å) is an intramolecular bond even though it is an intermolecular bond (the corresponding intramolecular distances between copper and terminal hydroxymethyl oxygens are more than 4 Å). If the longer apical bonds are taken into account, the structure would be a chain structure. However, because of the violet color of this compound, the square-planar *trans* arrangement is more probable, since the corresponding five- and six-coordinated species are normally blue.

The anions used in the synthesis of these copper–tris complexes have a great influence on the final molecular structure, even though they seldom enter the coordination sphere of

copper. Nitrate is the only anion coordinated to copper in mononuclear species, and both mono- and bisnitrate forms have been obtained in this work. This monodentate behavior of nitrate is common, and several mono-[70,71] and bisnitrate[72,73] copper complexes are reported earlier. On the other hand, a water molecule is a very favored ligand, because of its small size and high polarity. As a result, almost half of the mononuclear compounds consist of monohydrate complexes. In polynuclear species the coordination tendency of anions is more pronounced, and they all contain at least weakly coordinated anions. The tetranuclear behavior of the chloride complex, $[Cu(trisH_{-1})Cl]_4$, is exceptional in this series and can be explained by the strong coordination tendency of chloride, since it readily coordinates to copper and completes the square plane of the coordination sphere. With anions whose coordination tendency is not that strong, the polynuclear unit can grow further, yielding an octanuclear species.

The transformation of *cis–trans* isomers depends very much on concentration. In dilute solutions, where the complex molecule is surrounded by solvent molecules, the interactions between complexes are weak, hence the more symmetric *trans* isomer is energetically more favored than the *cis* isomer. But, when the solution is heavily concentrated (and the anion concentration is increased at the same time), the ionic interactions become more significant and the dimeric *cis* structure, where the negative hydroxy groups are hidden inside, is more favored. Further, when the dimers are stacked one on top of the other, the electrostatic repulsions are minimized between complexes and anions. The crystal structures of these complexes typically exhibit this stacking behavior (see Chapter 4). In the main, the *cis* and *trans* isomers represent an equilibrium process, which can be affected by concentration in a reversible manner.

How these *cis* and *trans* isomers transform from one form to the other, is another question. Because of the stabilizing effect of the five-membered chelate ring, transformations involving a bond rupture are not much favored. However, since the coordination sphere of copper is not rigid, these mononuclear complexes are potential fluxional complexes,[74] which can undergo deformational rearrangements in the solvated form without bond rupture. Hence, the square-planar complexes can be excited to a tetrahedral form by rearrangement of the coordination sphere, and then return to a square-planar form, but with a different orientation of ligands. Correspondingly, the rearrangement of a five-coordinated square-pyramidal species happens via trigonal-bipyramid geometry. Octahedral complexes are generally not fluxional, and the

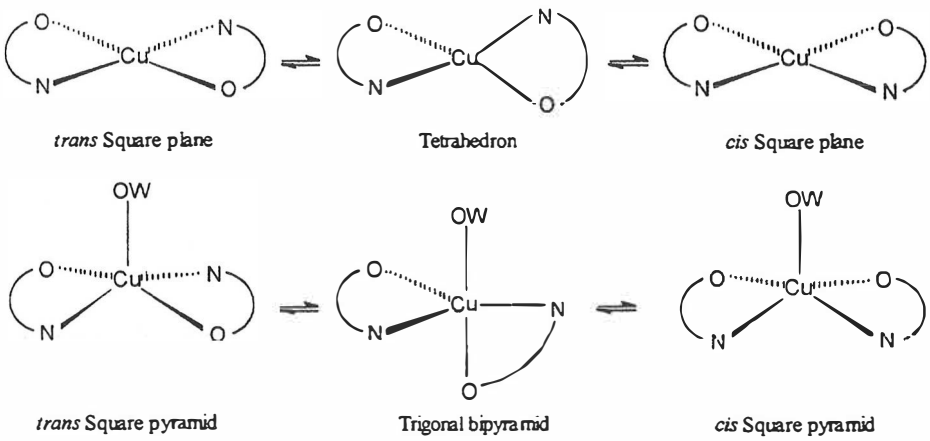

Fig. 3.7 Suggested fluxional behavior of square-planar and square-pyramidal copper–tris complexes.

interconverison of an octahedral species normally involves one bond rupture and the formation of a fluxional five-coordinated species. The suggested interconversion mechanisms for *cis* and *trans* isomers of square-planar and square-pyramidal copper–tris complexes are shown in Fig. 3.7. The same process also leads to the fluctuation of the optical isomers, when the procedure is repeated several times.

In water solution, a polynuclear species rarely forms because of the high polarity and dielectric constant of water. As a consequence of these properties, water forms strong hydrates with copper and copper–tris complexes, and acts as an insulator preventing further coordination with other copper–tris complexes. From this hydrate layer, one water molecule is readily withdrawn into the actual coordination sphere of copper, leading to these mononuclear monohydrated species mentioned above. In the ethanol synthesis, copper–tris complexes are also solvated, but this time the hydroxymethyl groups of tris can replace the solvated ethanol molecules more easily, because their bonding properties are quite similar. In ethanol solution, the polynuclear form is dominant, coloring the whole solution green, whereas the color of the corresponding water synthesis is medium blue, indicating the presence of the mononuclear species. Furthermore, in alcoholic solutions, the ligand can choose its deprotonation level in the complex more freely. All compounds containing only neutral ligands (compounds **14**, **17**, and **18**) are synthesized in alcohol solutions (50–100% EtOH or MeOH). In octanuclear complexes, the ligand is found at three different protonation levels (tris, $trisH_{-1}$, and $trisH_{-2}$), depending on the location of tris in the complex.

FIGURE APPENDIX I

a)

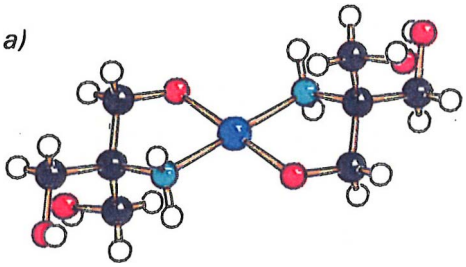

trans-anti-[Cu(trisH$_{-1}$)$_2$]
in [Cu(trisH$_{-1}$)$_2$] (**1**)^{I}

b)

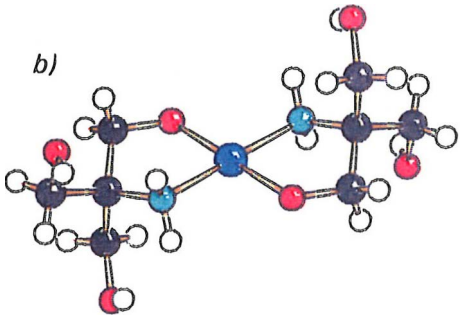

trans-anti-[Cu(trisH$_{-1}$)$_2$]
in [Cu(trisH$_{-1}$)$_2$]·5H$_2$O (**3**)^{I}

c)

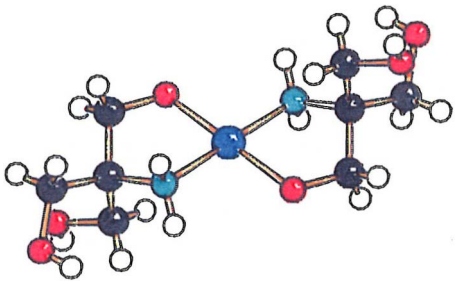

trans-anti-[Cu(trisH$_{-1}$)$_2$]
in [Cu(trisH$_{-1}$)$_2$]KF·3H$_2$O (**8**)^{IV}
and [Cu(trisH$_{-1}$)$_2$]KBr·2H$_2$O (**9**)^{IV}

d)

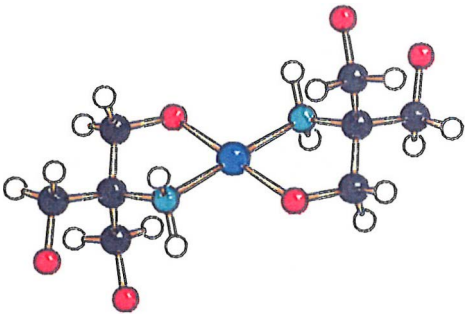

trans-anti-[Cu(trisH$_{-1}$)$_2$]
in [Cu(trisH$_{-1}$)$_2$]NaClO$_4$·H$_2$O (**21**)^{40}
(Ivarsson)

Fig. 3.8 Mononuclear copper–tris complexes (the first line shows the complex molecule, and the second line indicates the compound).

e)

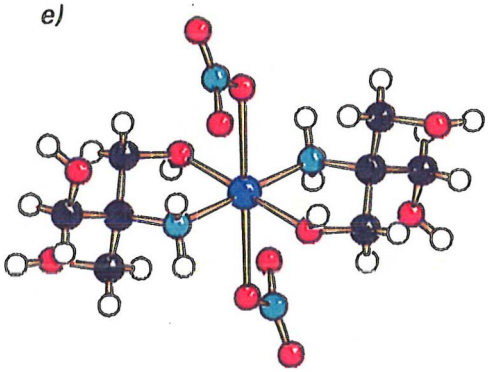

Molecule A (50%)

f)

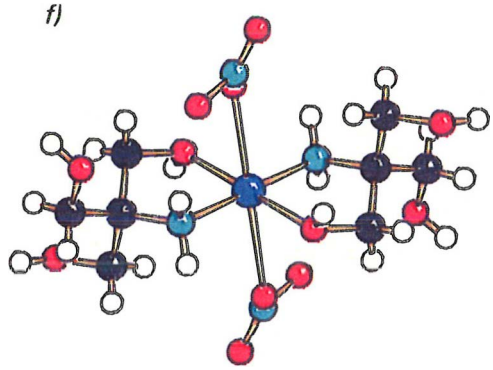

Molecule B (50%)

trans-anti-[Cu(tris)$_2$(NO$_3$)$_2$]
in [Cu(tris)$_2$(NO$_3$)$_2$] (**17**)[44]

g)

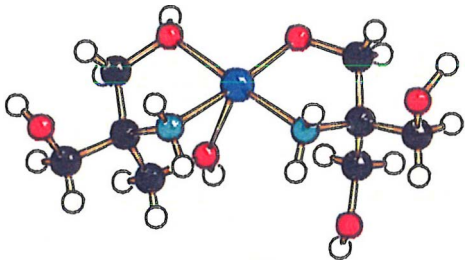

cis-syn-[Cu(trisH$_{-1}$)(tris)]$^+$
in [Cu(trisH$_{-1}$)(tris)]F (**15**)[44]

h)

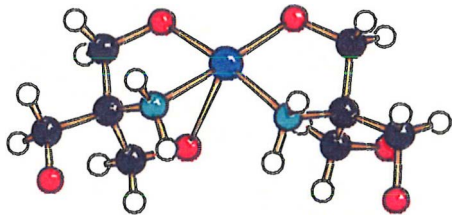

cis-syn-[Cu(trisH$_{-1}$)(tris)]$^+$
in {[Cu(trisH$_{-1}$)(tris)]Br}$_n$ (**22**)[41] (Masi *et al.*)
(see also Fig. 3.10, *c*)

Fig. 3.8 (continued)

i)

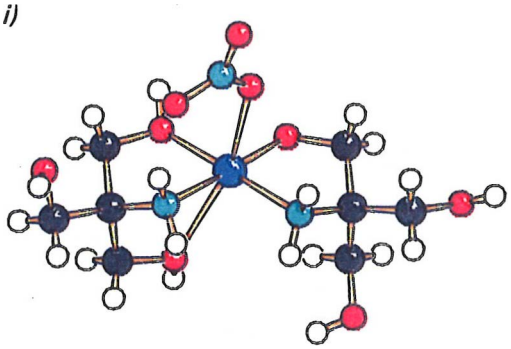

cis-syn-[Cu(trisH$_{-1}$)(tris)(NO$_3$)]
in [Cu(trisH$_{-1}$)(tris)(NO$_3$)] (**4**)^{II}

j)

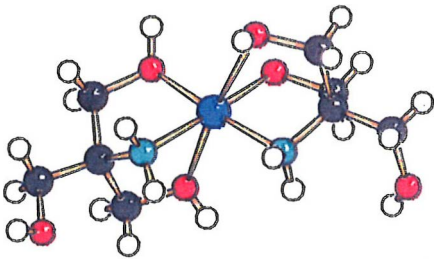

cis-anti-[Cu(trisH$_{-1}$)(tris)]$^+$
in [Cu(trisH$_{-1}$)(tris)]Na(ClO$_4$)$_2$ (**5**)^{II}

k)

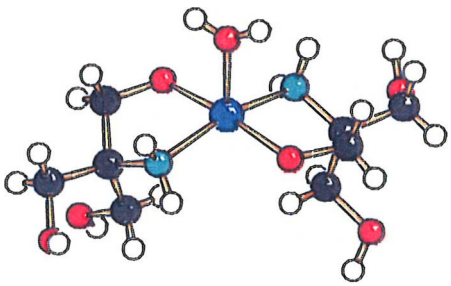

trans-syn-[Cu(trisH$_{-1}$)$_2$(H$_2$O)]
in [Cu(trisH$_{-1}$)$_2$(H$_2$O)] (**2**)^{I}

l)

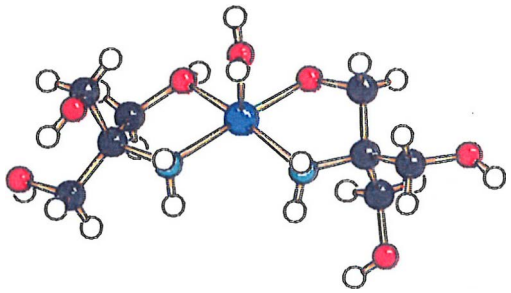

cis-anti-[Cu(trisH$_{-1}$)(tris)(H$_2$O)]$^+$
in [Cu(trisH$_{-1}$)(tris)(H$_2$O)]$_2${SiF$_6$} (**16**)^{44}

Fig. 3.8 (continued)

m) *n)*

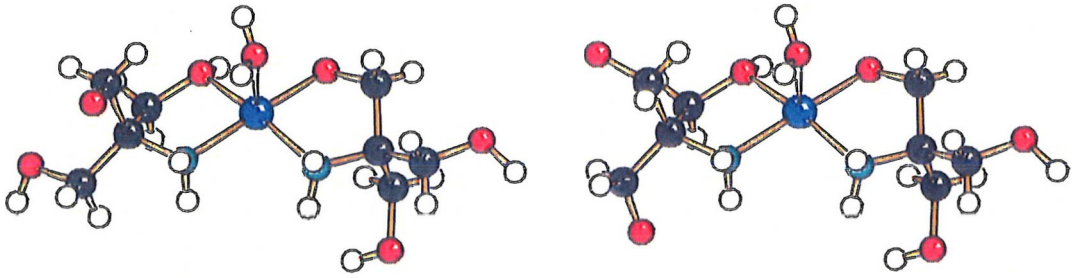

Molecule A (72%) Molecule B (28%)

cis-anti-[Cu(trisH$_{-1}$)(tris)(H$_2$O)]$^+$

in [Cu(trisH$_{-1}$)(tris)(H$_2$O)]$_2$SO$_4$ (**6**)^{III}

o) *p)*

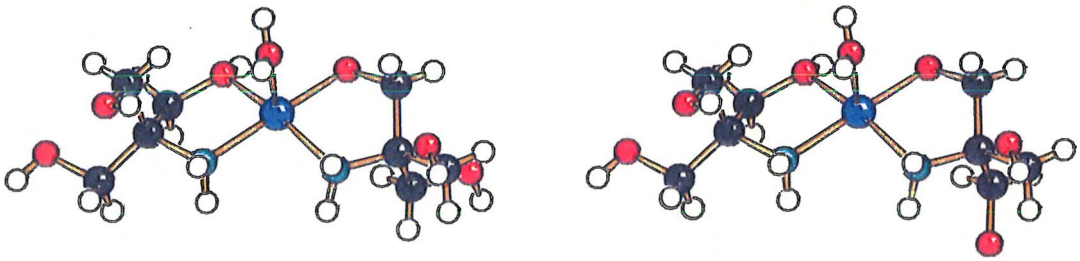

Molecule 1A (84%) Molecule 1B (16%)

cis-anti-[Cu(trisH$_{-1}$)(tris)(H$_2$O)]$^+$

in [Cu(trisH$_{-1}$)(tris)(H$_2$O)]$_2$CrO$_4$ (**7**)^{III}

(compound **7** contains two molecules in the asymmetric unit, and molecules 2A and 2B are almost identical to the structures of 1A and 1B)

Fig. 3.8 (continued)

q)

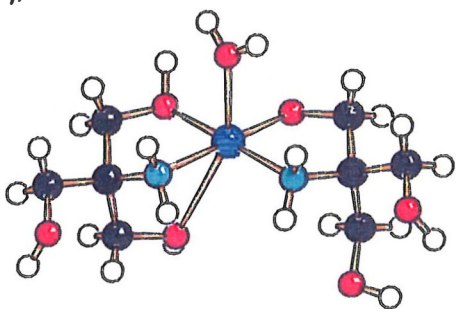

Molecule 1

r)

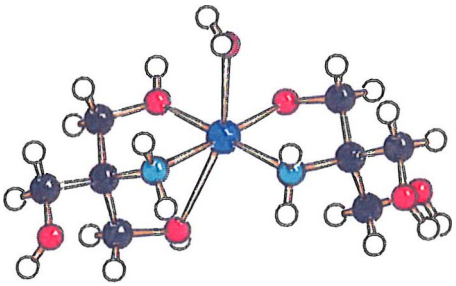

Molecule 2

cis-syn-[Cu(trisH$_{-1}$)(tris)(H$_2$O)]$^+$

in [Cu(trisH$_{-1}$)(tris)(H$_2$O)]Cl·H$_2$O (**11**)^V and [Cu(trisH$_{-1}$)(tris)(H$_2$O)]Br·H$_2$O (**12**)^V

s)

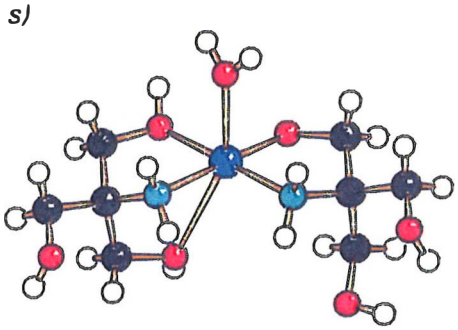

Molecule 1A (87%)

t)

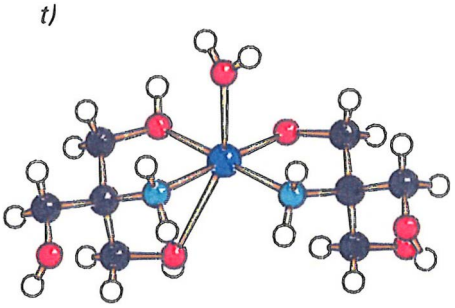

Molecule 1B (13%)

cis-syn-[Cu(trisH$_{-1}$)(tris)(H$_2$O)]$^+$

in [Cu(trisH$_{-1}$)(tris)(H$_2$O)]I·H$_2$O (**13**)^V

Fig. 3.8 (continued)

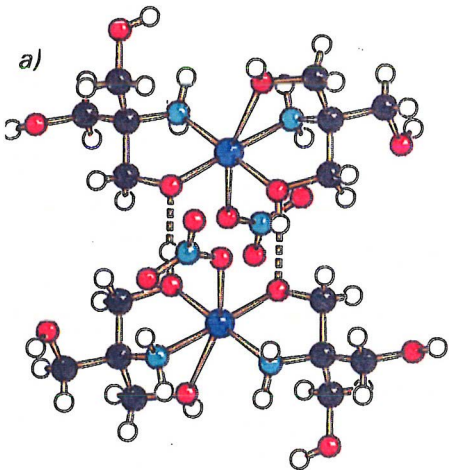

a)

$[Cu(trisH_{-1})(tris)(NO_3)]_2$

in $[Cu(trisH_{-1})(tris)(NO_3)]$ (**4**)[II]

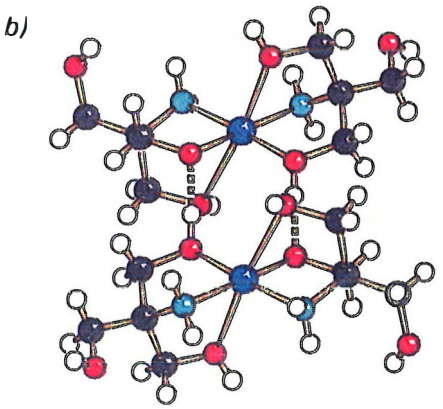

b)

$[Cu(trisH_{-1})(tris)]_2^{2+}$

in $[Cu(trisH_{-1})(tris)]Na(ClO_4)_2$ (**5**)[II]

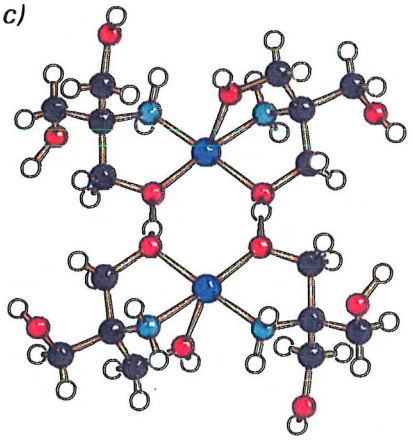

c)

$[Cu(trisH_{-1})(tris)]_2^{2+}$

in $[Cu(trisH_{-1})(tris)]F$ (**15**)[44]

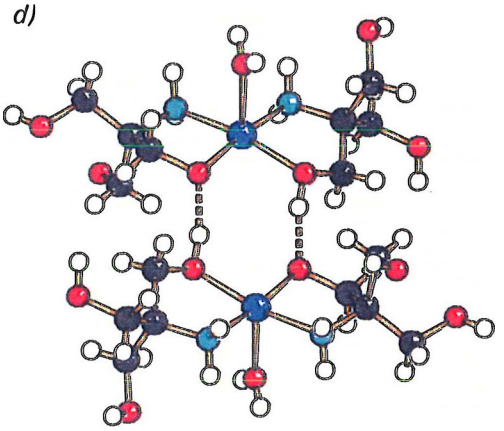

d)

$[Cu(trisH_{-1})(tris)(H_2O)]_2^{2+}$

in $[Cu(trisH_{-1})(tris)(H_2O)]_2\{SiF_6\}$ (**16**)[44]

Fig. 3.9 Hydrogen-bonded dimer structures of mononuclear *cis* complexes. The dimeric structures *a*, *g* and *h* are *syn* isomers and *d*–*f* are *anti* isomers with respect to the orientation of the coordinated water molecule or nitrate in the dimer.

e)

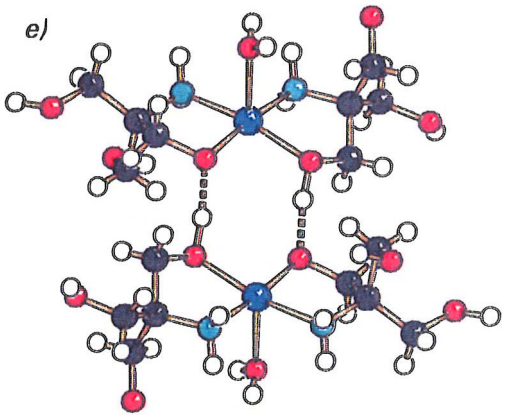

$[Cu(trisH_{-1})(tris)(H_2O)]_2^{2+}$ (72%)
in $[Cu(trisH_{-1})(tris)(H_2O)]_2SO_4$ (**6**)[III]

f)

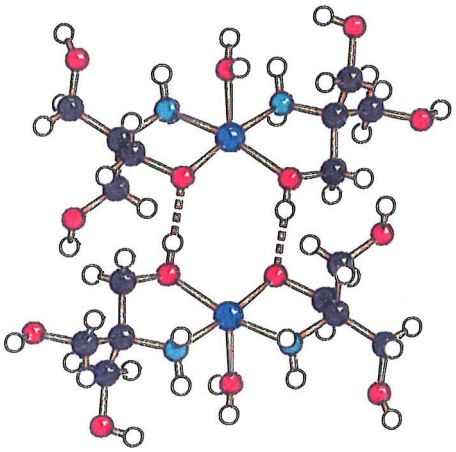

$[Cu(trisH_{-1})(tris)(H_2O)]_2^{2+}$ (84%)
in $[Cu(trisH_{-1})(tris)(H_2O)]_2CrO_4$ (**7**)[III]

g)

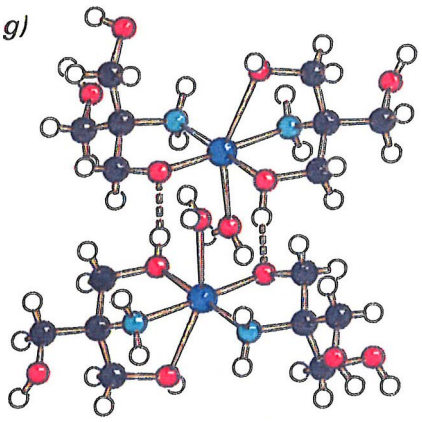

$[Cu(trisH_{-1})(tris)(H_2O)]_2^{2+}$
in $[Cu(trisH_{-1})(tris)(H_2O)]Cl{\cdot}H_2O$ (**11**)[V]
and $[Cu(trisH_{-1})(tris)(H_2O)]Br{\cdot}H_2O$ (**12**)[V]

h)

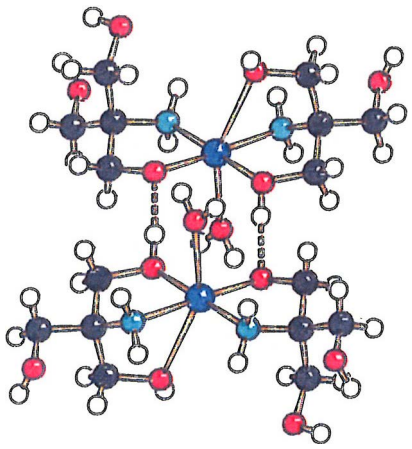

$[Cu(trisH_{-1})(tris)(H_2O)]_2^{2+}$ (87%)
in $[Cu(trisH_{-1})(tris)(H_2O)]I{\cdot}H_2O$ (**13**)[V]

Fig. 3.9 (continued)

a) *b)*

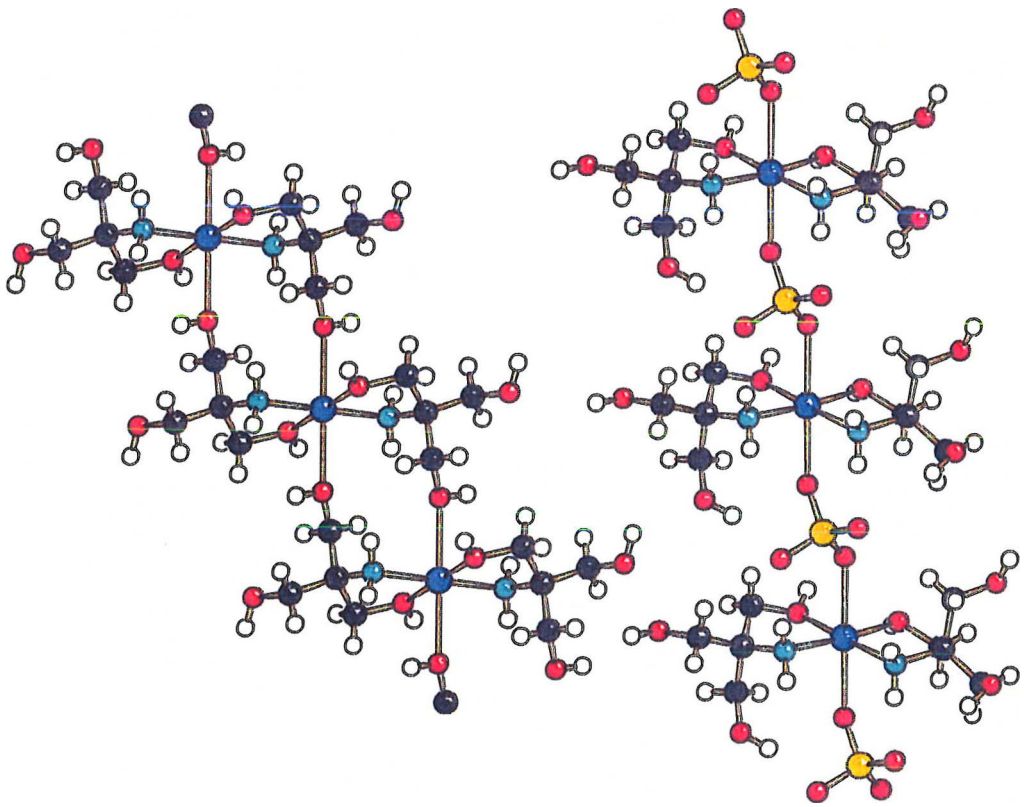

trans-{[Cu(tris)$_2$]F$_2$}$_n$ (**14**)[44] *cis*-[Cu(tris)$_2$(SO$_4$)]$_n$ (**18**)[44]

Fig. 3.10 Continuous chain structures of the copper–tris complexes.

c)

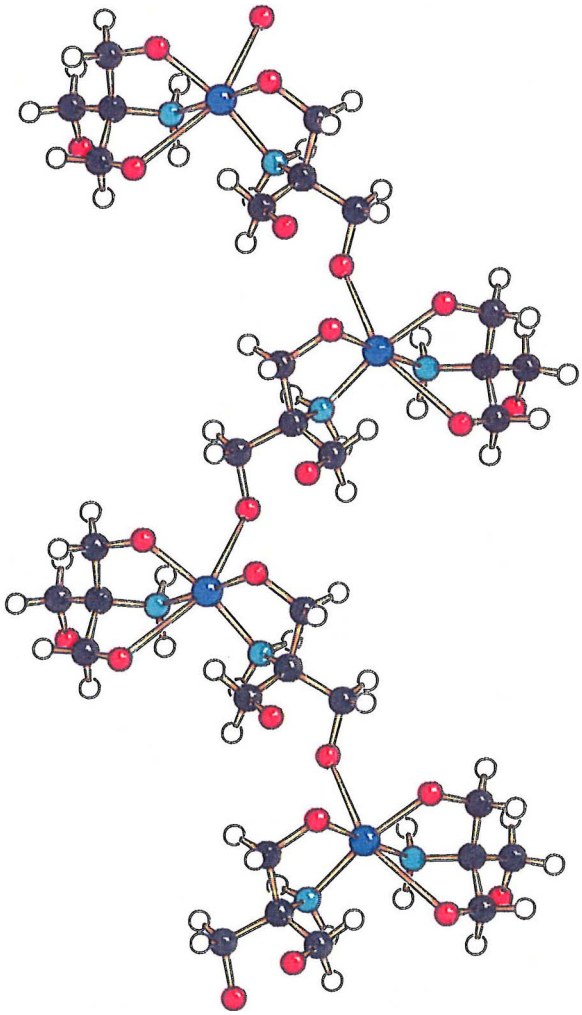

cis-{[Cu(trisH$_{-1}$)(tris)]Br}$_n$ (**22**)[41] (Masi *et al.*)

Fig. 3.10 (continued)

a)

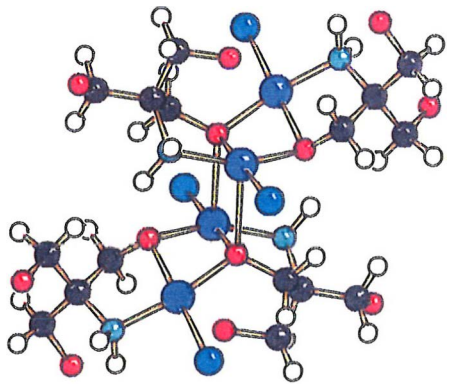

Tetranuclear $[Cu(trisH_{-1})Cl]_4$
in $[Cu(trisH_{-1})Cl]_4$ (**23**)[41] (Masi *et al.*)

b)

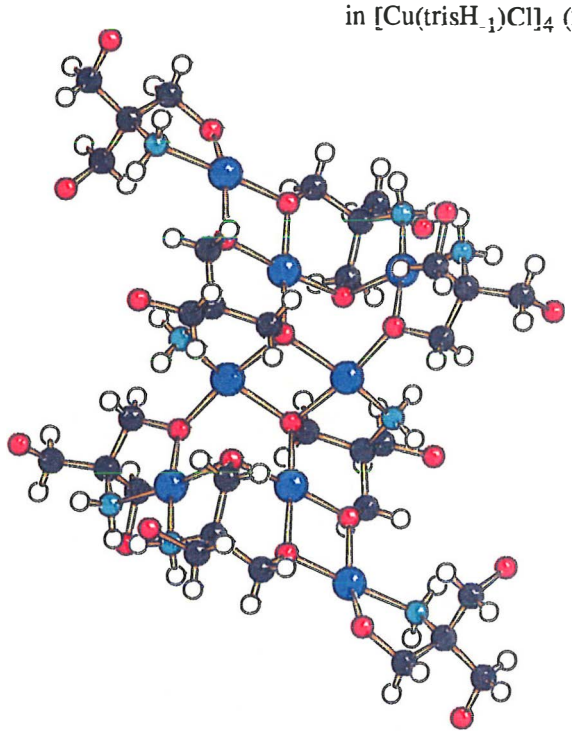

Octanuclear $[Cu_8(trisH_{-2})_4(trisH_{-1})_2(tris)_2]^{6+}$
in $[Cu_8(trisH_{-2})_4(trisH_{-1})_2(tris)_2]Br_6 \cdot 6H_2O \cdot CH_3CH_2OH$ (**19**)[44]
and $[Cu_8(trisH_{-2})_4(trisH_{-1})_2(tris)_2](ClO_4)_6 \cdot 6H_2O \cdot CH_3CH_2OH$ (**20**)[44]

Fig. 3.11 Polynuclear copper–tris complexes.

4. CRYSTAL STRUCTURES

4.1 General

Stereoscopic projections of the crystal structures (including the hydrogen bonding network) of compounds **1–13** are given in references I–V, and packing diagrams of all copper–tris structures are shown in Figure Appendix II at the end of this chapter. Space groups and unit cell parameters of the compounds are given in Appendix V.

The crystal structures of these compounds possess little symmetry, since the most common space group is triclinic $P\bar{1}$ (in Appendix V, 13 compounds out 23 are triclinic). Nevertheless, primitive and *C*-centered monoclinic cells have been observed for eight compounds (five are *trans* isomers), and even orthorhombic symmetry (*Pcca*) has been found for two compounds, *trans*-[Cu(trisH$_{-1}$)$_2$]KF·3H$_2$O (**8**) and *trans*-[Cu(trisH$_{-1}$)$_2$]-KBr·2H$_2$O (**9**). All space groups observed for these compounds are centrosymmetric, which is also a more likely choice for a racemic compound.

4.2 Crystal-packing types

The crystal packing of the copper–tris complexes is a consequence of three main effects: hydrogen bonding, electrostatic interactions and weak van der Waals forces between $CH_2\cdots CH_2$ groups. All OH, NH_2 and H_2O hydrogens are involved in the hydrogen bonding network, where the acceptor atoms of these hydrogen bonds are typically oxygen atoms of hydroxymethyl groups, water molecules or oxoanions (NO_3^-, ClO_4^-, SO_4^{2-}, and CrO_4^{2-}), as well as fluorine as a free fluoride anion or hexafluorosilicate. Electrostatically, the structures can be divided into two groups: structures containing only neutral complex molecules (**1–4**, **17**, and **23**) or chains (**18**), and structures consisting of cations and anions. Normally, the positively charged species are the cationic dimers, but in compounds **8**, **9**, and **21**, the molecule itself is neutral and an alkali metal ion (Na^+ or K^+) is acting as a cation. Combining these properties, the packing of the structures can be divided into seven subgroups given below, and one structure can possess characteristics of several subgroups.

- structures with a three-dimensional hydrogen-bonding network
- layer structures
- structures, based on stacking of the dimers
- tunnel compounds
- chain structures
- structures containing alkali metal cations
- polynuclear packing

Structures, with a three-dimensional hydrogen-bonding network

Anhydrous and monohydrate forms of the neutral *trans* complex, $[Cu(trisH_{-1})_2]$ (**1**) and $[Cu(trisH_{-1})_2(H_2O)]$ (**2**), are typical examples of the first subgroup, where the hydrogen-bonding network is comparable in all three dimensions of the lattice. Since the monoclinic space groups possess greater symmetry, the orientation of the complex molecules changes and the molecules are located at two different levels at least, making the hydrogen-bonding network more uniform in all directions. Compound **15**, *cis*-$[Cu(trisH_{-1})(tris)]F$, also has some character of this subgroup, because fluoride participates in the hydrogen-bonding network.

Layer structures

Typical layer structures are *trans*-$[Cu(trisH_{-1})_2]\cdot 5H_2O$ (**3**) and *trans*-$[Cu(trisH_{-1})_2]$-$NaClO_4\cdot H_2O$ (**21**), but *cis*-$[Cu(trisH_{-1})(tris)]Na(ClO_4)_2$ (**5**) and *trans*-$[Cu(tris)_2(NO_3)_2]$ (**17**) also have some layer character. In the pentahydrate compound (**3**), layers of molecules are divided by layers of crystalline water parallel to the *ab*-plane, and as a result, direct intermolecular hydrogen bonding is hindered, and all hydrogen bonds are formed between complex molecules and water. Even the color of the pentahydrate crystals shows that the structure is anisotropic, because from two directions the crystal looks blue–violet and from the third direction the color is red–violet. The layer structure of the *trans* perchlorate compound (**21**) consists of layers of neutral molecules and sodium ions, which are divided by layers of perchlorates parallel to the *ab*-plane. In the structure, perchlorates are acting as bidentate bridging groups between sodium ions. Furthermore, in the anhydrous *cis* perchlorate compound (**5**), sodium(I) is located in the same *bc*-plane as copper(II), but the perchlorate layers are diagonal this time and approximately parallel to plane (110).

Structures, based on stacking of the dimers

Most of the dimeric *cis* structures (**4**, **6**, **7**, **10**–**13**, **15**, and **16**) belong to this third group, principally characterized by the stacking of the dimers. In these structures, the dimers are stacked along one of the main axes via hydrogen bonds, which normally involve metal-coordinated and axial hydroxymethyl groups and coordinated water (or nitrate). The bond strength of some of these hydrogen bonds is almost comparable to the dimeric hydrogen bonds. Some examples of this stacking behavior are shown in Fig. 4.1. In the plane perpendicular to this stacking axis, the dimers are linked together via hydrogen-bond bridges consisting of amino groups and corresponding anions (NO_3^-, SO_4^{2-}, CrO_4^{2-}, and SiF_6^{2-}) as well as weak hydrogen bonds involving equatorial hydroxymethyl groups. The crystal packing of SO_4^{2-}, CrO_4^{2-} and SiF_6^{2-} compounds is strikingly similar, but even though sulfate and chromate share the same charge and tetrahedral geometry, the sulfate and chromate compounds are not isomorphic, due to the differences in the ionic radii.[III] The hydrogen-bonding surroundings are also different for each oxygen of the anion, and hence, the tetrahedral structures of SO_4^{2-} and CrO_4^{2-} are somewhat distorted. Nevertheless, the geometry of hexafluorosilicate is regular, and the bond lengths [Si–F 1.669(1)–1.679(2) Å] are normal for this ion.[75] Some of the halide structures also consist of stacked dimers, but they are characterized in more detail with tunnel compounds.

Tunnel compounds

Most of the structures containing halides (**8**, **9**, **10**–**15**, and **22**) can be classified as tunnel compounds, where the complex molecules form a frame structure — which can consist of hydrogen-bonded monomers (**8**, **9**), dimers (**10**–**13**, **15**) or continuous chains (**14**, **22**) — and halides occupy the hydrophobic cavities formed in the structure. In some structures the tunnels are filled with halides as well as crystalline water. The halide-hydrogen distances obtained for these cavities are F–H 1.52–2.06 Å, Cl–H 2.22–2.76 Å, Br–H 2.34–2.84 Å, and I–H 2.69–3.02 Å, and they (or the corresponding *X*–O distances) are comparable with other fluoride,[54,76] chloride,[58,69,77] bromide,[78] and iodide[79] structures reported in the literature. Furthermore, this increase in the ionic radius, when going from fluoride to iodide, can lead to changes in the crystal packing. For example, in the analogous compound series, *cis*-[Cu(trisH$_{-1}$)(tris)(H_2O)]X·H_2O, where X = F^-, Cl^-, Br^-, I^- (**10**–**13**), the chloride and bromide compounds are isomorphic and fluoride is suspected to be isomorphous with them on the basis of XRD studies, but the iodide analogue

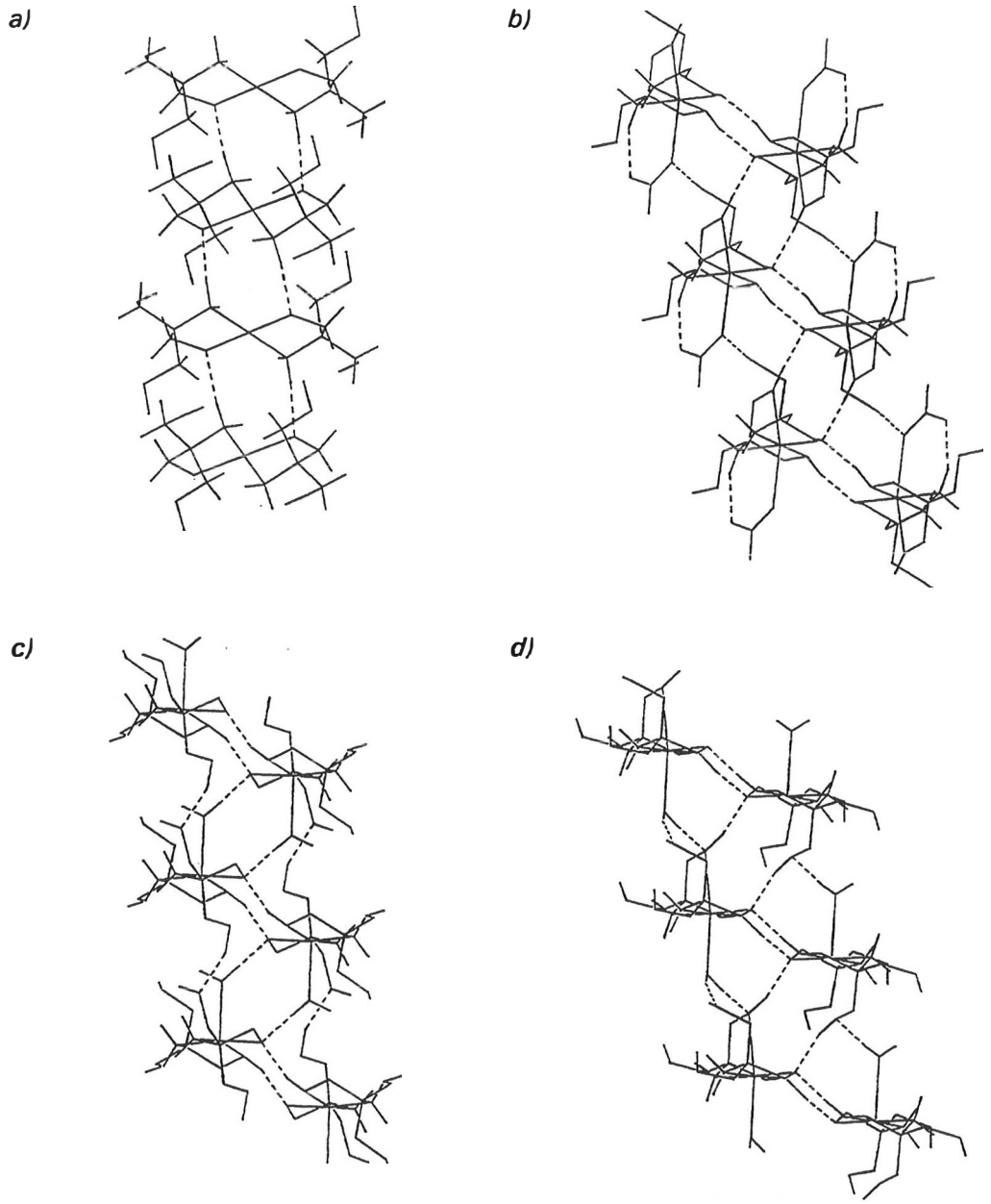

Fig. 4.1 Examples of stacking via hydrogen bonding: *a)* monomeric stacking in compound *trans*-[Cu(trisH$_{-1}$)$_2$]KBr·2H$_2$O (**9**);[IV] stacked dimers in *cis* compounds *b)* [Cu(trisH$_{-1}$)(tris)(NO$_3$)] (**4**),[II] *c)* [Cu(trisH$_{-1}$)(tris)(H$_2$O)]$_2$CrO$_4$ (**7**),[III] and *d)* [Cu(trisH$_{-1}$)(tris)(H$_2$O)]Cl·H$_2$O (**11**).[V]

crystallizes in a different unit cell.[V] The hydrogen-halide salts of tris ($trisH^+.X^-$, X = F, Cl, Br, I) published by Rudman *et al.*[35] behave in a corresponding manner; the first three compounds are isostructural with a rhombohedral space group, but the iodide salt crystallizes in a cubic space group with a higher symmetry. The crystal structures of *cis*-$[Cu(trisH_{-1})(tris)(H_2O)]Br\cdot H_2O$ (**12**)[V] and *trans*-$[Cu(trisH_{-1})_2]KBr\cdot 2H_2O$ (**9**)[IV] are shown in Figs. 4.8 and 4.9 to illustrate the tunnel structures of the halide compounds.

The behavior of fluoride compounds compared with other halides, is quite exceptional, most likely because of the small ionic size and excellent hydrogen-bonding properties of fluoride. The dihydrate compound (**10**) mentioned above is the only structure, in which the behavior of fluoride and other copper–tris halides is suspected to be identical. On the other hand, in most of the cases, fluoride behaves differently. For example, the molecular structure, crystal packing and unit cell parameters of *cis* compounds $[Cu(trisH_{-1})(tris)]F$ (**15**)[44] and $\{[Cu(trisH_{-1})(tris)]Br\}_n$ (**22**)[41] are quite different. Furthermore, in the isotypic compounds of *trans*-$[Cu(trisH_{-1})_2]KX\cdot nH_2O$, where $X = F^-$, Br^- (**8** and **9**),[IV] the fluoride anion withdraws an extra water molecule into the crystal structure and fills the tunnel with hydrogen-bonded F···H–O–H···F'···H'–O'–H' chains.[IV] Emsley *et al.*[54] have presented a similar structural case, where a hydrated fluoride ion, $[F(H_2O)_4]^-$, exists in the crystal structure. The hydrogen-bonding surroundings observed for fluoride in compounds **8**, **14**, and **15** are all tetrahedral.

Chain structures

The chain structures (**14**, **18**, and **22**) are comparable with the stacked dimer structures, because the intermolecular interactions are more pronounced in one direction, (= the direction of apical coordination bonds in this case). The double-chain structure of *cis*-$[Cu(tris)_2(SO_4)]_n$ (**18**)[44] is especially intriguing, because it is the only *cis* compound not consisting of hydrogen-bonded dimers. In the structure, the chains are held together by lateral hydrogen bonds between metal-coordinated hydroxy groups and coordinated oxygens of the bridging sulfato group of the adjacent chain. This is further assisted by weaker hydrogen bonds formed between amino groups and non-coordinated oxygens of sulfate on the opposite side of the chain. The effect of the hydroxy–sulfate hydrogen bonds can be seen as the lengthening of the coordinated S–O bonds in the sulfate species [1.480(2) and 1.492(2) Å] compared with non-coordinated S–O distances [1.473(2) and 1.456(2) Å]. Similar bridging systems have been reported for $[Cu(en)(H_2O)_2(SO_4)]$,[60]

$[Cu(bipy)(H_2O)_2(SO_4)]$,[61] and $[Cu(phen)(H_2O)_2(SO_4)]$,[62] but the interlinking hydrogen bonds involve water and non-coordinated oxygens of sulfate, hence the order of the noncoordinated and coordinated S—O bonds are reversed in these structures.*

Structures containing alkali metal cations

Sodium and potassium ions have a crucial linking effect in compounds **5**, **8**, **9**, and **21**, because these alkali metals form also coordination spheres, where the ligands are oxygen atoms of hydroxymethyl groups, water molecules and perchlorates (if present). The coordination sphere of sodium is octahedral and the Na—O distances are in the range 2.30—2.62 Å, whereas the coordination sphere of potassium is a square-antiprism with eight oxygen ligands, where the K—O distances are 2.78—2.99 Å. The structure of *trans*-$[Cu(trisH_{-1})_2]KBr{\cdot}2H_2O$ (**9**),[IV] showing the coordination sphere of potassium is presented in Fig. 4.9. Similar coordination spheres for alkali metals have been reported by Pangborn *et al.* (Na, K),[80] Calestani *et al.* (K),[81] and Dubourg *et al.* (K).[82] Due to the differences in coordination number and geometry, as well as to the different space requirements, the sodium and potassium ions are not interchangeable in these structures. For example, the sodium analogue of compound *trans*-$[Cu(trisH_{-1})_2]KBr{\cdot}2H_2O$ would be electrostatically possible, but the experimental work showed that it does not form.[IV] Typical examples of molecules that form coordination compounds with sodium and potassium are the crown-ethers,[83] coronands,[84] and spherands.[85]

Polynuclear packing

In the polynuclear packing (**19**, **20**, and **23**) the distances between the complex molecules are typically wider (especially in octanuclear compounds), and only a few hydrogen bonds are formed between molecules. Because of this space in the structure, an empty hole inbetween the octanuclear complexes results, which is filled with crystalline water and disordered ethanol. Anions and water are weakly coordinated to one or more copper ions at the same time. For example, the perchlorate anions in compound **20** are disordered, and one is acting as a tripod ligand connecting three copper(II) ions. This tridentate behavior of perchlorate is rather unusual, and it has been observed earlier by McKee and Tandon[86] in a similar octanuclear complex also containing methanol.

* en = ethylenediamine
biby = 2,2'-bipyridine
phen = 1,10-phenantroline

FIGURE APPENDIX II

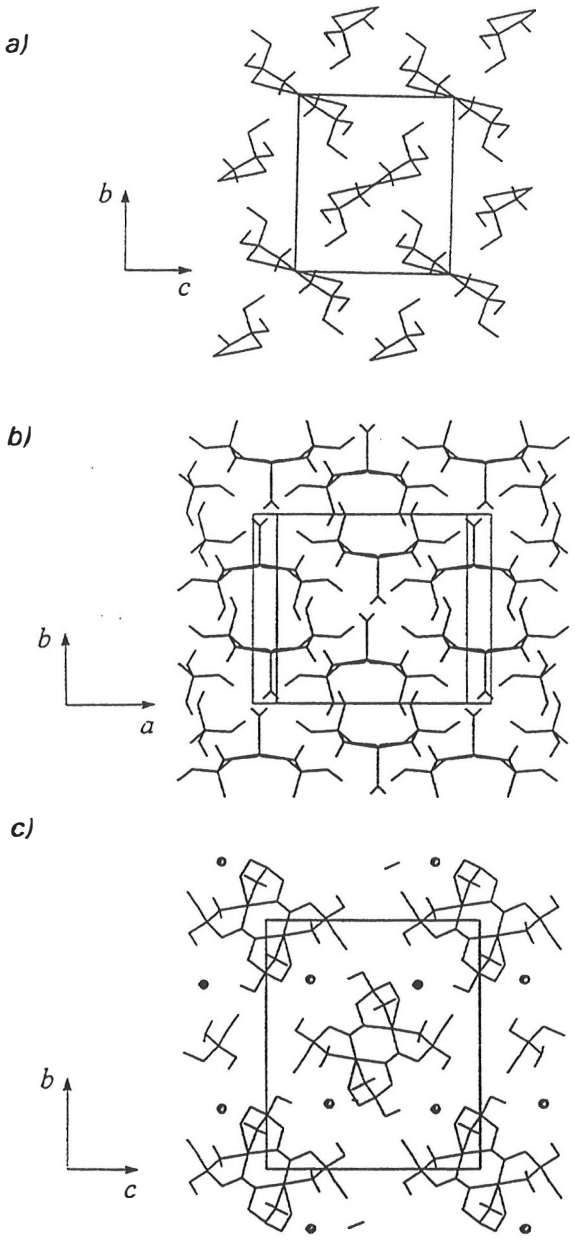

Fig. 4.2 Packing diagrams of structures, with a three-dimensional hydrogen-bonding network: *a) trans*-[Cu(trisH$_{-1}$)$_2$] (**1**),[I] *b) trans*-[Cu(trisH$_{-1}$)$_2$(H$_2$O)] (**2**),[I] and *c) cis*-[Cu(trisH$_{-1}$)(tris)]F (**15**).[44]

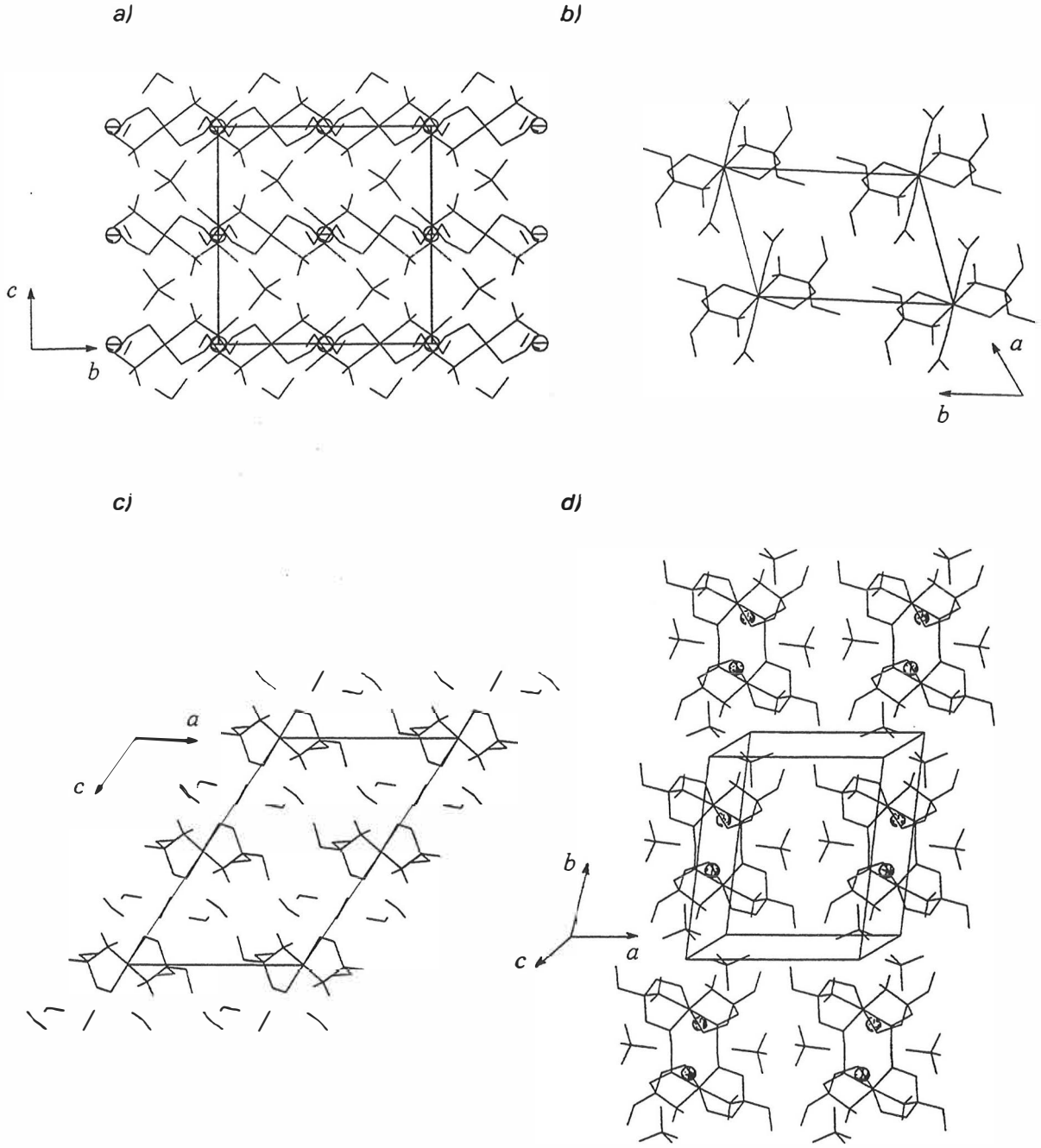

Fig. 4.3 Packing diagrams of layer structures: *a) trans*-[Cu(trisH$_{-1}$)$_2$]NaClO$_4$·H$_2$O (**21**),[40] *b) trans*-[Cu(tris)$_2$(NO$_3$)$_2$] (**17**),[44] *c) trans*-[Cu(trisH$_{-1}$)$_2$]·5H$_2$O (**3**),[I] and *d) cis*-[Cu(trisH$_{-1}$)(tris)]Na(ClO$_4$)$_2$ (**5**).[II]

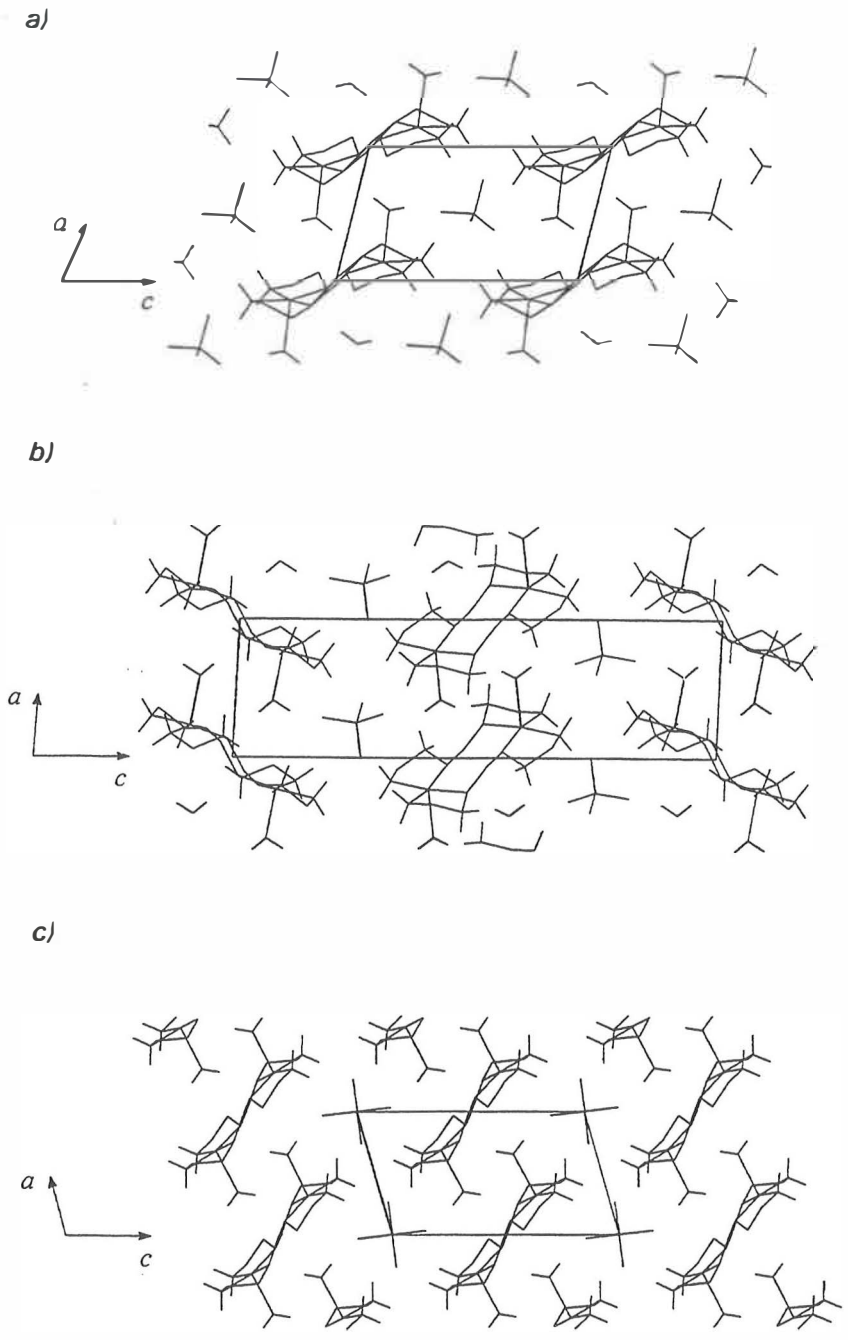

Fig. 4.4 Packing diagrams of structures based on stacking of the dimers: *a) cis*-$[Cu(trisH_{-1})(tris)(H_2O)]_2SO_4$ (**6**),[III] *b) cis*-$[Cu(trisH_{-1})(tris)(H_2O)]_2CrO_4$ (**7**),[III] and *c) cis*-$[Cu(trisH_{-1})(tris)(H_2O)]_2\{SiF_6\}$(**16**).[44]

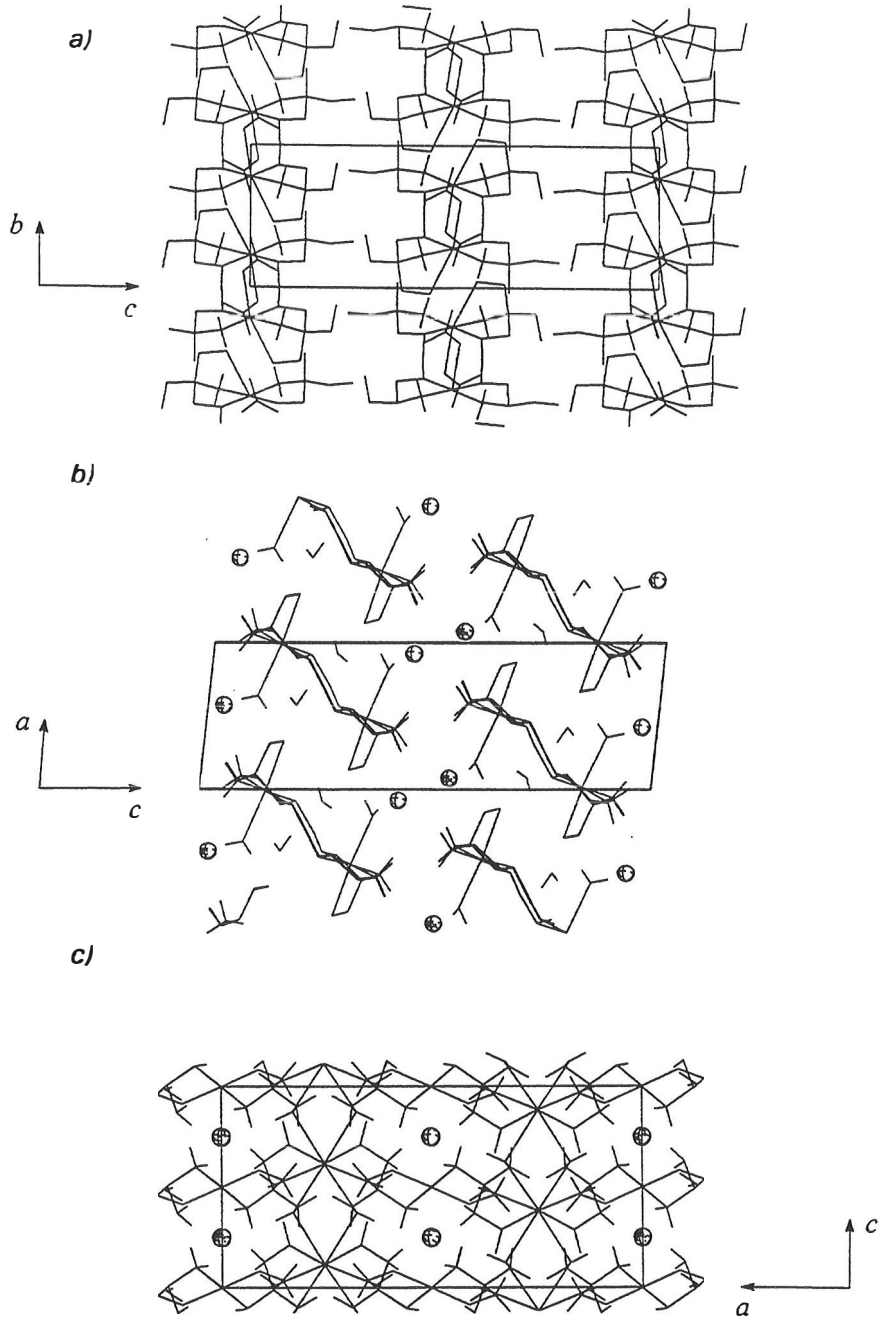

Fig. 4.5 Packing diagrams of stacked dimers (*a*, *b*) and tunnel compounds (*b*, *c*): *a) cis*-[Cu(trisH$_{-1}$)(tris)(NO_3)] (**4**),[II] *b) cis*-[Cu(trisH$_{-1}$)(tris)(H_2O)]Cl·H_2O (**11**),[V] and *c) trans*-[Cu(trisH$_{-1}$)$_2$]KBr·$2H_2O$ (**9**).[IV]

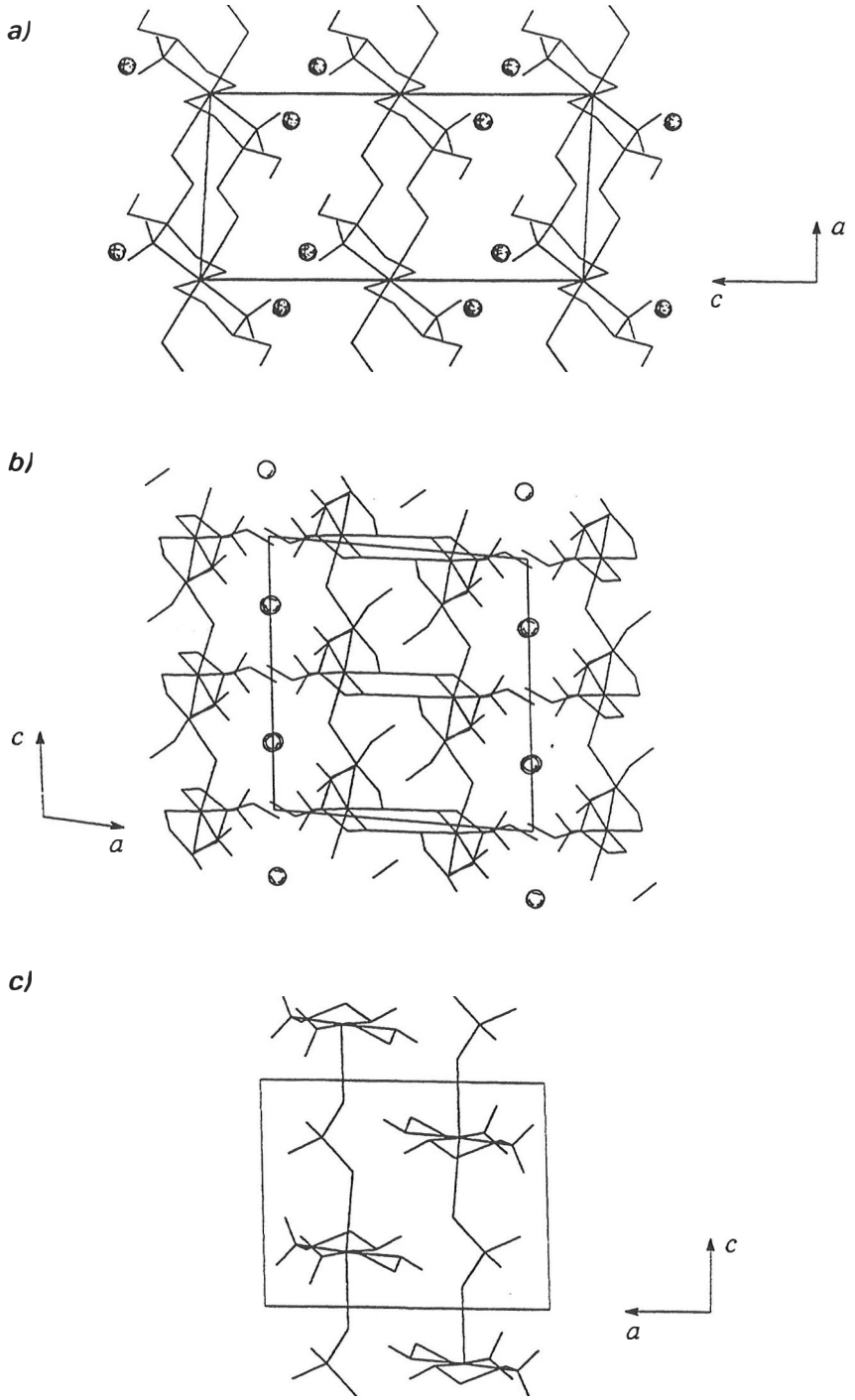

Fig. 4.6 Packing diagrams of chain structures: *a) trans*-$\{[Cu(tris)_2]F_2\}_n$ (**14**),[44] *b) cis*-$\{[Cu(trisH_{-1})(tris)]Br\}_n$ (**22**),[41] and *c) cis*-$[Cu(tris)_2(SO_4)]_n$ (**18**).[44]

a)

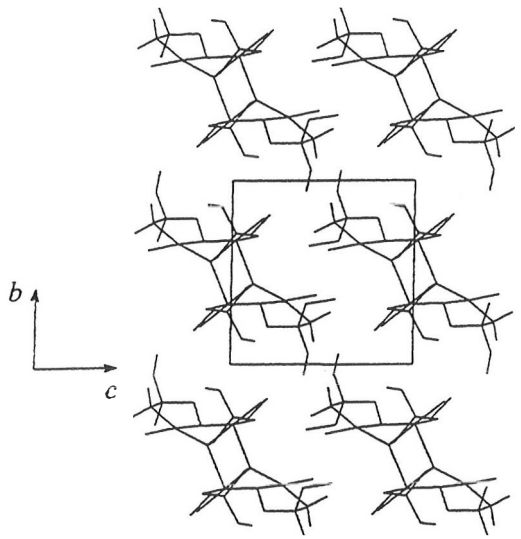

b)

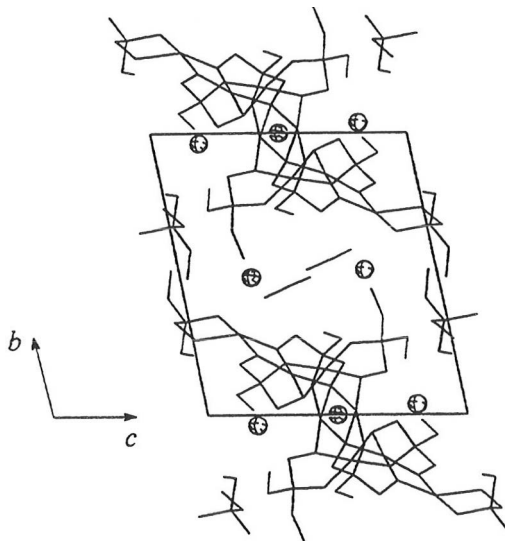

Fig. 4.7 Packing diagrams of polynuclear compounds: *a)* $[Cu(trisH_{-1})Cl]_4$ (**23**),[41] and *b)* $[Cu_8(trisH_{-2})_4(trisH_{-1})_2(tris)_2]Br_6 \cdot 6H_2O \cdot CH_3CH_2OH$ (**19**).[44]

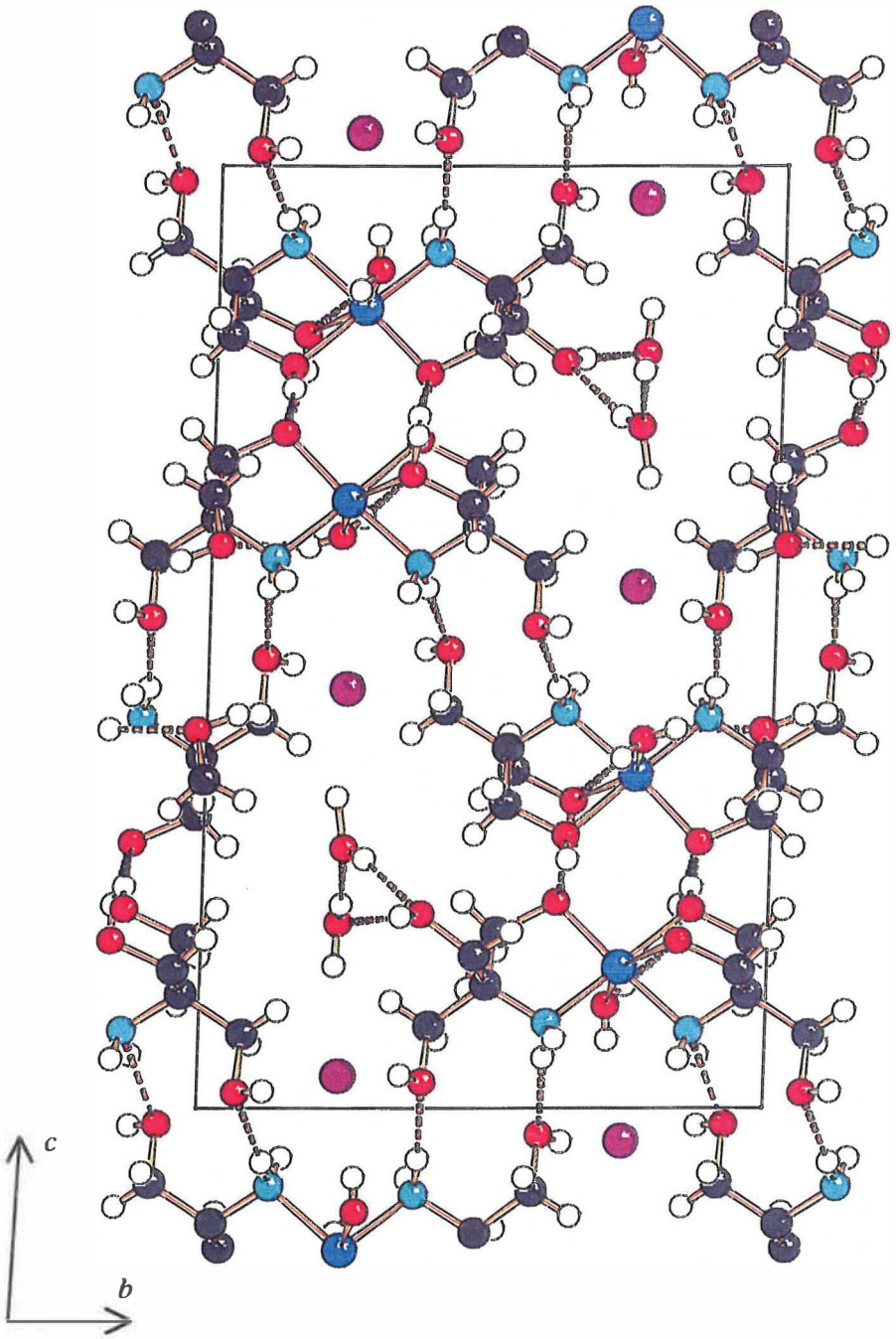

Fig. 4.8 Crystal structure of *cis*-[Cu(trisH$_{-1}$)(tris)(H_2O)]Br·H_2O (**12**).[V]

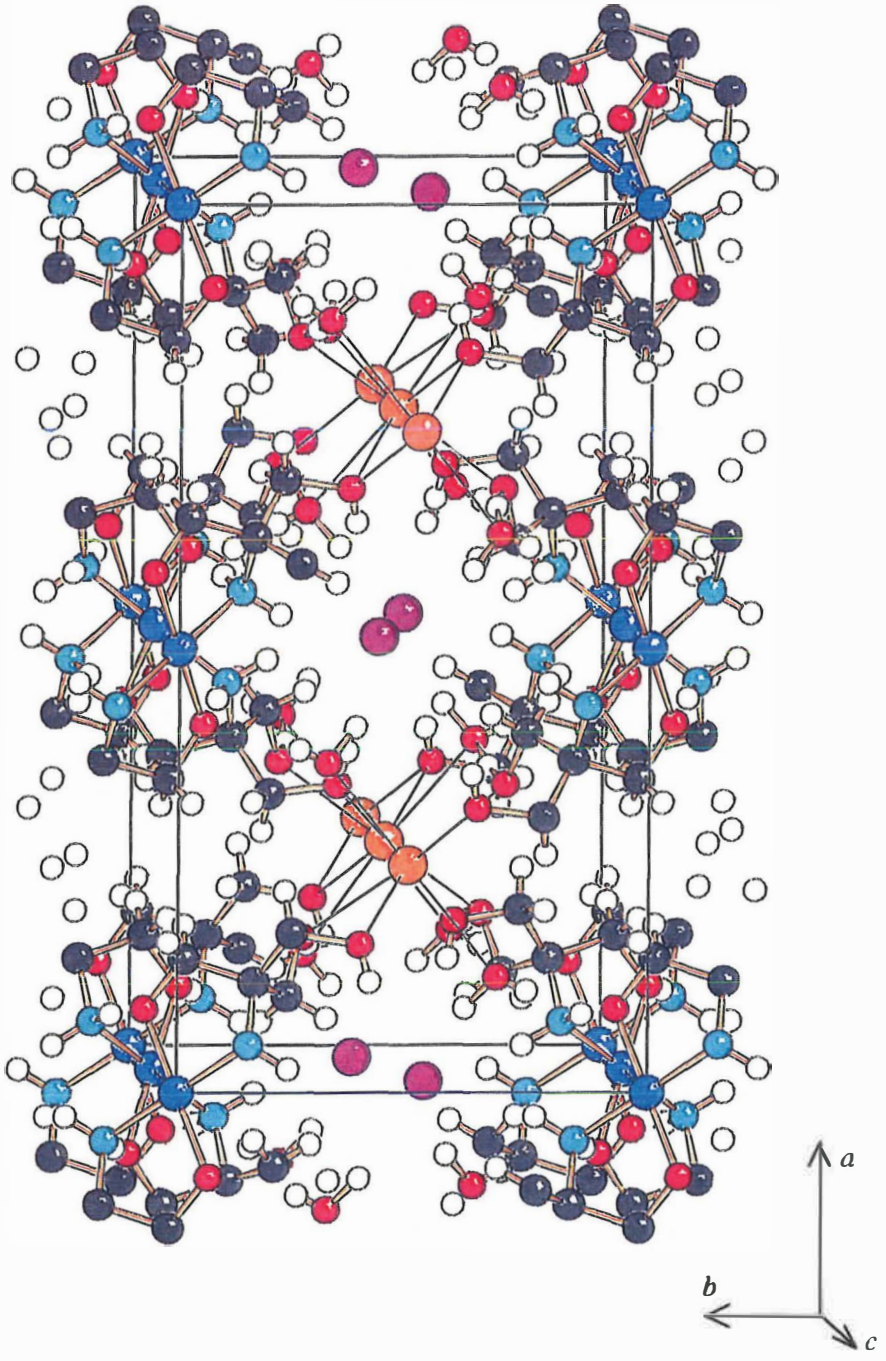

Fig. 4.9 Crystal structure of *trans*-[Cu(trisH$_{-1}$)$_2$]KBr·2H$_2$O (**9**).[IV]

5. MASS SPECTROMETRY

5.1 General

Mass spectrometry gives information about the molecular weight of the compound, elemental and isotopic composition, chemical stability and fragmentation mechanism of the molecule, as well as the structure and the stability of the fragments formed during ionization. Ionic and often radical species are involved in mass spectral fragmentation reactions. During electron bombardment, molecular ions ($M^{+\cdot}$) with a wide range of internal energies are formed. Those ions that are sufficiently 'cool' (low in energy) will not decompose before collection at the detector, and they will appear as a molecular peak in the mass spectrum. If sufficiently excited, the molecular ions can decompose by a variety of energy-dependent reactions, each resulting in the formation of an ion and a neutral species. These primary ions, formed from molecular ions, may have suffient energy to decompose further yielding secondary ions. Hence, the abundance of the primary ions observed in the final mass spectrum will depend on the average rates of their formation and decomposition, whereas the abundance of the secondary ions will depend on the relative rates of several competitive and consecutive reactions. In general, the most abundant fragment-ion peaks in the mass spectrum correspond to reactions that form the most stable ionic and neutral products. Such ion-decomposition reactions observed in mass spectrometry can be regarded as another field of chemistry, but there are also many close similarities to pyrolytic, photolytic, radiolytic, and other energetic reactions (*e.g.* thermogravimetry).[87]

5.2 Results and discussion

The electron-ionization (EI) mass spectra of tris, NH_2-C(-$CH_2OH)_3$, and deuterated tris, ND_2-C(-$CH_2OD)_3$, are shown in Figs. 5.1 and 5.2. Corresponding mass spectral fragmentation schemes are deduced according to McLafferty,[87] and the main fragmentation reactions, which explain the mass spectra of tris and deuterated tris, are given in Figs. 5.3 and 5.4. Mass spectra of the solid copper–tris compounds were also measured, but peaks with *m/z* values characteristic of tris were solely observed. In addition, the area from which the representative mass spectrum was taken from had a

greater influence on the ion-abundant variation than the compound from the sample was taken.

In the tris ligand two different types of functional groups (alcohol and amino groups), can act as an initiating site in ion fragmentations. When the fragmentation mechanisms of aliphatic alcohols and amines are applied to tris, one can notice that the whole fragmentation pattern can be explained by the reactions induced by the amino group, hence the amino group is a more powerful initiation site for ion framentation in tris than the hydroxy group. For example, the characteristic peak for hydroxy groups, $(M-H_2O)^{+\cdot}$, is completely missing in tris's mass spectrum at the *m/z* value of 103.

In the mass spectrum of tris, no observable molecular peak, $M^{+\cdot}$ (*m/z* 121), appers because of the ease of decomposition through reactions initiated by the ionized amino and hydroxy groups. Fortunately, aliphatic amines and alcohols have a strong tendency to undergo protonation to yield the characteristic, pressure-dependent $(M+H)^+$ peak, which in tris's mass spectrum appears at *m/z* 122. The base peak in the mass spectrum at *m/z* 90 results from the amino-induced alpha cleavage of the hydroxymethyl radical, $\cdot CH_2OH$, yielding an even-electron (EE^+) ion, which is stabilized by electron sharing with a tertiary carbon atom (Fig 5.3, reaction 5.1). All other important peaks in the mass spectrum can be derived from this significant even-electron ion by charge-site initiated reactions forming another EE^+ species and a neutral fragment. Fragmentation reactions 5.2 and 5.3 in Fig. 5.3 are charge-site initiated cleavages, and reaction path 5.4 contains a rearrangement of a hydrogen followed by an inductive cleavage of the amino group; most of the ionic species in these reactions can be stabilized via electron sharing, which involves a carbon atom and a nonbonding orbital of a heteroatom (N,O). The neutral losses in these secondary fragmentation reactions are water, formaldehyde, and ammonia. Note also that most of the important peaks in the mass spectrum have an even mass number, which means according to 'the nitrogen rule' for even-electron species, they will contain an odd number of nitrogen atoms (in this case one nitrogen). The remaining small peaks in the mass spectrum are due to the natural abundance of the heavier isotopes, like ^{13}C, ^{15}N, and ^{18}O, or gaseous impurities from the sample probe (*e.g.* *m/z* 44 refers to CO_2).

In a deuterated tris sample, the hydrogen atoms in the amino and hydroxy groups are replaced by deuterium isotopes. The fragmentation mechanism is identical to that of

normal tris, but the corresponding *m/z* values are higher because of the isotope substitution (Fig. 5.4). As a result of the incomplete deuteration, there is no single peak for each ion, but a set of peaks, where *m/z* values differ by one mass unit. These isotope patterns correspond to tris molecules with a varying number of deuterium atoms. Hence, the *m/z* peak 126 is more likely to belong to the isotope pattern of the $(M+D)^+$ peak (*m/z* 128) than being the real molecule peak $M^{+\cdot}$. However, some differences can be observed in the mass spectrum of the deuterated sample; there is a small peak group in the area *m/z* 108, which belongs to the alcoholic fragmentation ions, $(M-D_2O)^{+\cdot}$ and $(M-DHO)^{+\cdot}$. This indicates that deuteration may affect the driving force of alcoholic groups to initiate fragmentation reactions, and more complicated patterns result. In general, the majority of the ionic fragments of deuterated tris agree well with the fragmentation observed for tris.

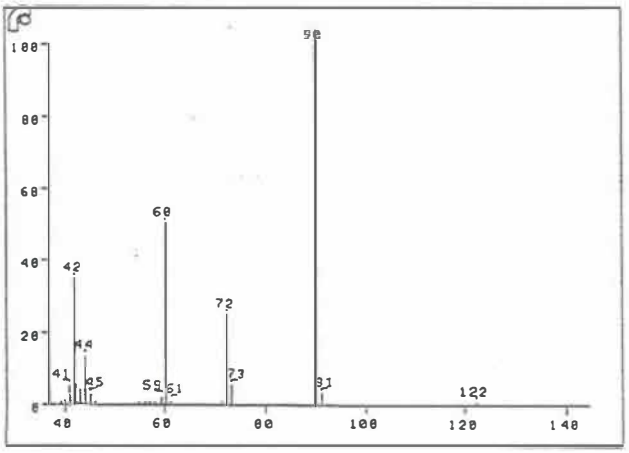

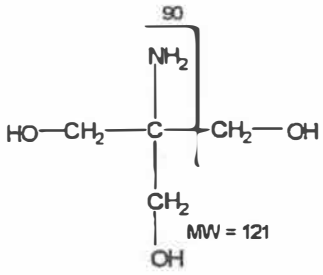

Fig 5.1 EI mass spectrum of tris (70 eV).

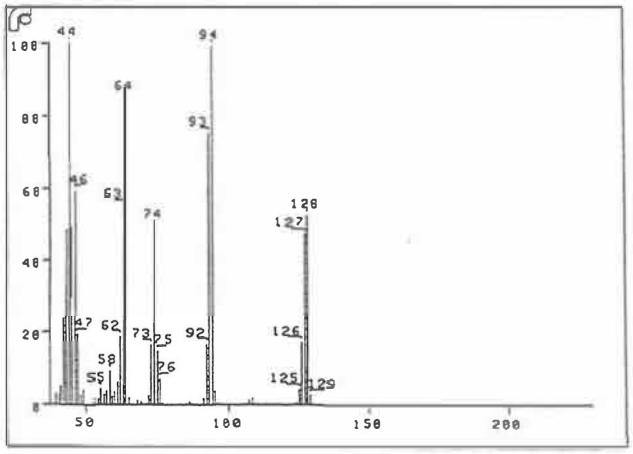

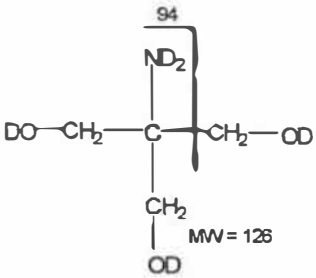

Fig 5.2 EI mass spectrum of deuterated tris (70 eV).

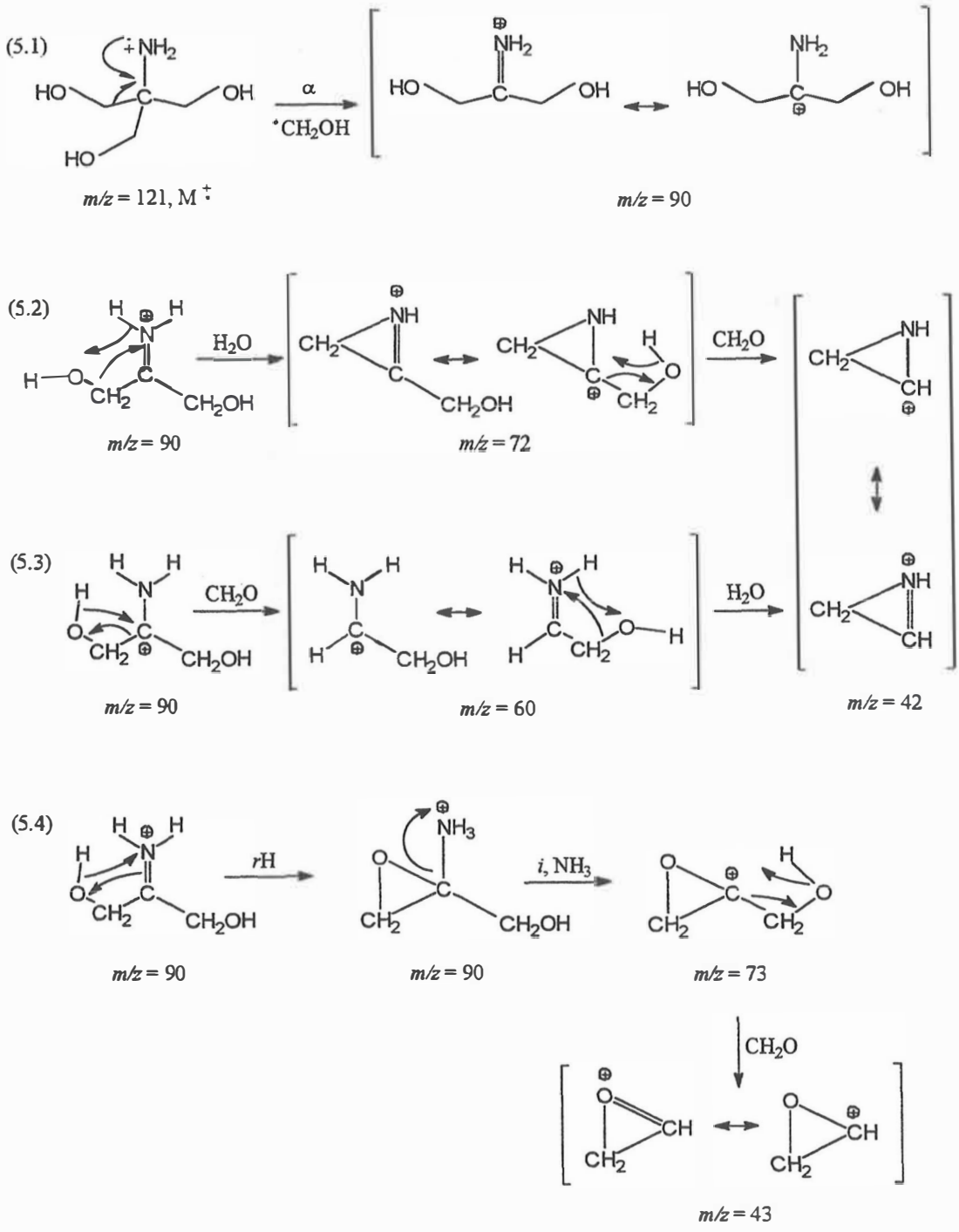

Fig 5.3 Mass-spectral fragmentation reactions of tris.

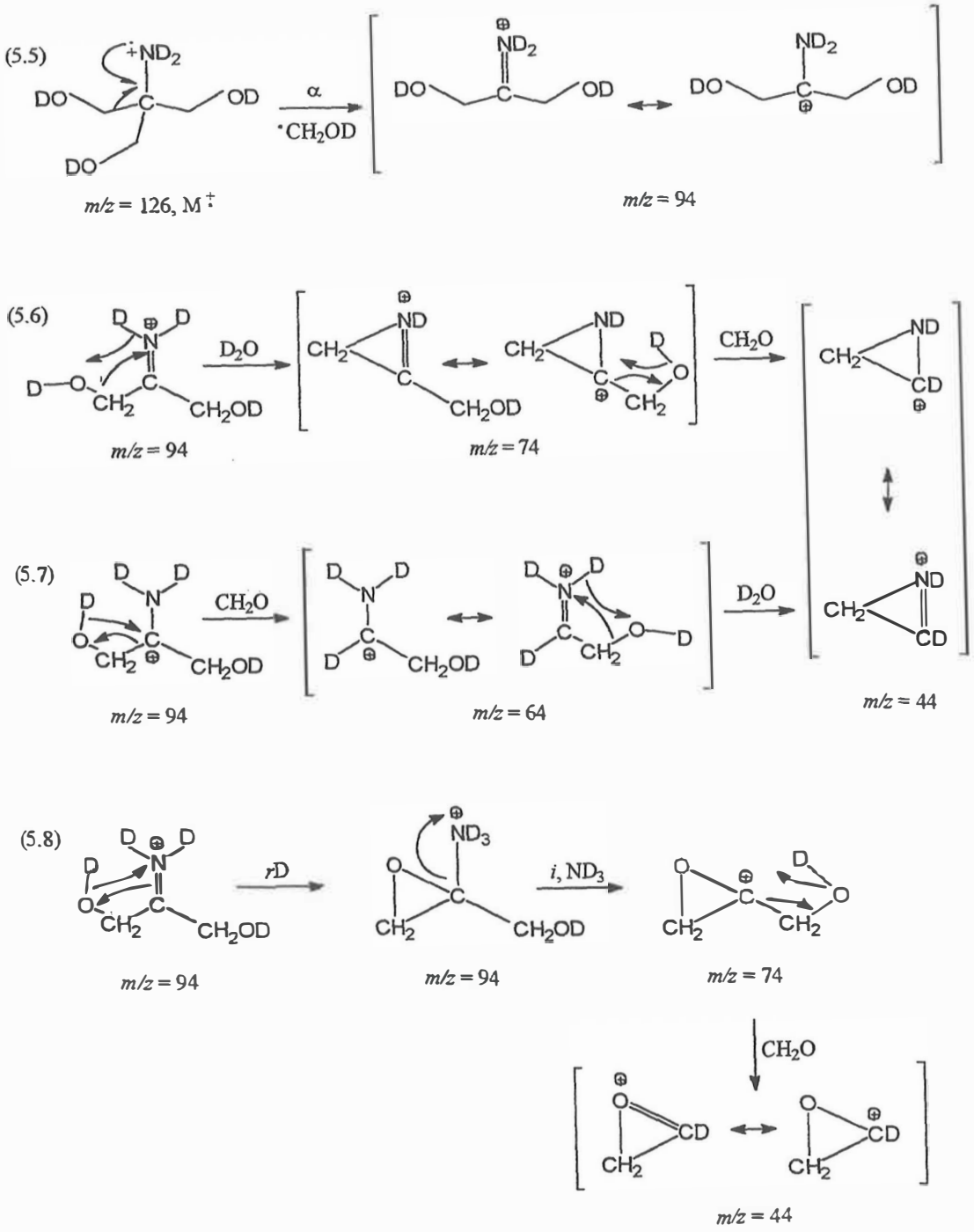

Fig 5.4 Mass-spectral fragmentation reactions of deuterated tris.

6. THERMOGRAVIMETRY

6.1 General

Thermal behavior of the copper–tris complexes was studied in dynamic air and nitrogen atmospheres in the temperature area 25–950°C. Thermogravimetric curves and their derivatives (DTG) for compounds **1–13** in air and nitrogen atmospheres are shown in Appendix VI, and the corresponding weight losses are given in each article[I–V] in Table 1. Summary of the end products as well as the temperature areas, where the organic ligand and the anions decompose, is given in Table 6.1 at the end of this chapter.

The purpose of these thermogravimetric (TG) measurements was to confirm the stoichiometric composition of the sample, and to gain some information about the thermal stability of the compounds. Thermal decomposition of the complexes was mainly concluded from the observed weight losses using the structural information obtained from single-crystal determinations; no further analyses were done to verify the products formed during the thermal decomposition. Nevertheless, in some cases thermogravimetric results also proved to be very useful for structure determination. For example, the third water molecule in the compound $[Cu(trisH_{-1})_2]KF{\cdot}3H_2O$ (**8**)[IV] was identified from TG analysis, and thereafter included in the structure refinement.

In the following TG interpretations the main interest has been focused on locating the temperature areas where dehydration and decomposition of the organic group and anions occur; the stable intermediates and the final products were also a matter of interest. Useful information has been obtained from literature references concerning thermal analysis of copper complexes of organic amino compounds with different anions. In addition, various inorganic alkali metal and copper compounds were used as thermogravimetric reference materials under the same conditions.

A detailed decomposition pattern of the tris ligand remained unanswered, because of the lack of methodology to investigate the gaseous products. However, the mass spectral fragmentation studies in Chapter 5 will give some guidelines for possible gaseous decomposition products of tris. Methanol (CH_3OH), formaldehyde (CH_2O), water (H_2O), and ammonia (NH_3) were the gaseous losses observed in mass spectrometry. In addition

to these products, different nitrogen and carbon compounds (NO, N_2O, HONO, HCN, HNCO, CO, CO_2) and carbohydrates (CH_4, C_2H_4) have also been mentioned in the literature as decomposition gases for copper–amine complexes.[88,89] In the last section, the effects of *cis–trans* isomerism, the length and number of the coordination bonds, the distortion of the coordination polyhedra of copper, along with the molecular structure (monomer, dimer, polymer) were discussed so that the thermal stability of the organic group in different copper–tris complexes could be compared.

6.2 Decomposition of copper–tris compounds

In general, the thermal decomposition of copper–tris complexes begins with dehydration of crystalline water, which is normally completed before the degradation of the organic part begins. The decomposition of the organic ligand is a complex process involving at least three stages, which do not correspond to any simple stoichiometry. The anions decompose either simultaneously with the organic group or afterwards at a higher temperature. The final residue in an air atmosphere is generally CuO, and correspondingly elemental copper in a nitrogen atmosphere.

Crystalline water

Crystalline water is rather loosely bonded to most of the structures, and the difference between lattice water and coordinated water is not very clear. Generally, lattice water dehydrates in the temperature range of 25–100°C, which is quite normal for copper complexes.[90–92] Thermally, the most resistant lattice water has been found in the compound, $[Cu(trisH_{-1})_2]KBr{\cdot}2H_2O$ (**9**), which structurally, has one water molecule involved in the coordination sphere of potassium and the other water molecule, hydrogen bonded to the deprotonated oxygen of the ligand, explaining this phenomen. In the fluoride analogue, $[Cu(trisH_{-1})_2]KF{\cdot}3H_2O$ (**8**), where the third water molecule is located in the tunnel with fluoride, water is thermally almost as stable as in the bromide compound **9**.[IV]

The coordinated water is thermally unstable in these complexes, because in most of the compounds, it is already dehydrated in the same temperature range as the lattice water. In addition, in the compounds that contain both lattice and coordinated water, the dehydration is generally a one-step procedure. The most stable coordinated water is found

in the *trans* monohydrate compound (2),[I] where the Cu—OW bond is the shortest [2.200(2) Å]. This water molecule is dehydrated in the temperature range 120—165°C (maximum in the derivative curve at 150—154°C) in both atmospheres, indicating a moderate coordination strength. For comparison, temperatures of 160°C or higher for the DTG maximum are common for coordinated water molecules in amino complexes of copper.[58,92–94] Further, coordinated water molecules that are stable up to 250°C have been reported for complexes, where water is bound to the inner coordination sphere of copper.[95]

Thermal decomposition of the organic ligand

General information on the thermal behavior of the ligand is obtained from the TG measurements of the free ligand and its three basic *trans* complexes (**1—3**).[I] The thermal decomposition of pure tris in air begins slowly at 120°C, and 79% of the compound is lost by 246°C; the rest of the compounds degrade in two phases at 246—330°C (7%) and 330—450°C (14%). In a nitrogen atmosphere the first decomposition stage (130—280°C) contains 93% of the sample, but the elimination of tris is partly due to the concurrent sublimation of the ligand.

In copper—tris complexes, the ligand a little more resistant to heat than in the free form, but the decomposition patterns and temperatures are similar to those observed for free tris. Reaction 6.1 shows the average mass losses observed for the organic group of different $[Cu(trisH_{-1})_2]$ complexes in air (the oxygen atom in CuO represents 7% of organic matter). In nitrogen atmosphere the decomposition of the organic group takes place at an elevated temperature, and the first decomposition stage is more pronounced than in air. Above 280°C, the decomposition of the remaining organic matter is very slow and the DTG curve is quite featureless. At 900°C, there is still 6—7% of the organic matter left, along with elemental copper. Formation of carbon in an inert atmosphere has also been observed by Angoso *et al.*[96]

$$\text{air: } \left[Cu(trisH_{-1})_2\right]\cdot nH_2O \xrightarrow[\text{org. I (67 - 70\%)}]{160-240^\circ C} \xrightarrow[\text{org. II (8\%)}]{240-320^\circ C} \xrightarrow[\text{org. III (15 - 18\%)}]{320-450^\circ C} CuO \qquad (6.1)$$

$$N_2\text{: } \left[Cu(trisH_{-1})_2\right]\cdot nH_2O \xrightarrow[\text{org. I (80 - 83\%)}]{170-280^\circ C} \xrightarrow[\text{org. II (7 - 9\%)}]{280-450^\circ C} \xrightarrow[\text{org. III (4\%)}]{450-900^\circ C} Cu + C \qquad (6.2)$$

Nitrate and perchlorate[II]

Because of their self-oxidative decomposition, relatively few thermal studies on the amine complexes containing nitrate or perchlorate anions exist. Thermal decomposition of such compounds can be very explosive, since it often involves the concurrent deamination and oxidation of the liberated amine (or ammonia) by the decomposition gases of nitrate or perchlorate anions. Explosives, such as NH_4NO_3 and NH_4ClO_4, typify these types of compounds.[89]

For nitrate two decomposition types have been observed depending on the number of nitrates in the coordination sphere of copper. In the *cis*-[Cu(trisH$_{-1}$)(tris)(NO_3)] dimer (**4**),[II] decomposition starts with the degradation of the organic ligand in three overlapping stages. Nitrate decomposes simultaneously with the last stage of the organic group (345–420°C) yielding CuO at 420°C. In nitrogen atmosphere, 97% of the organic part is decomposed by 290°C, leading to $CuNO_3$ and some additional carbon, which decompose very slowly to give metallic copper at 970°C. The *trans* bisnitrate compound, [Cu(tris)$_2$(NO_3)$_2$] (**17**),[44] exhibits a more explosive-type of behavior, where the first decomposition of the organic part is accompanied by a simultaneous decomposition of one nitrate, producing a sharp peak in the DTG curve in both atmospheres. In air, the second nitrogen is decomposed with the organic residue around 350°C, leading to CuO at 400°C. In nitrogen atmosphere, the first violent reaction of the organic group and nitrogen is followed by a slow decomposition of $CuNO_3$ and the remaining organic residue. The reduction of copper is still incomplete at 950°C (obs. 21.77%, theor. 14.78%). Mathew *et al.*,[97] Prabhumirashi *et al.*,[98] and Donia[99] have studied the thermal behavior of similar CuL_2(NO_3)$_2$ complexes, where *L* is an organic amine ligand, and they have obtained corresponding results for the decomposition pattern and temperature ranges.

Compound **5**, *cis*-[Cu(trisH$_{-1}$)(tris)]Na(ClO_4)$_2$,[II] contains two types of perchlorates; those which decompose in a manner similar to copper(II) perchlorate producing CuO as the final residue in air (or metallic copper in a nitrogen atmosphere); and those which behave like $NaClO_4$, giving NaCl as a stable intermediate in both atmospheres. Thermally, the formula [Cu(trisH$_{-1}$)(tris)]ClO_4·$NaClO_4$ would better describe the decomposition of this compound. The decomposition process is violent in air showing sharp DTG-peaks, where oxygen is liberated from perchlorates. A mixture of CuO and NaCl is produced as a stable intermediate at 500°C, and the last decomposition process at 800°C is due to the

sublimation of NaCl, leading to CuO as the final residue at 900°C (obs. 26.54%, theor. 26.20%). In nitrogen atmosphere, the reactions overlapp more, because of the decomposition of perchlorates occurs at a lower temperature than in air. The intermediate stage at 450°C is not so clear either, because the decomposition of the organic residue and the reduction of copper ($CuO \rightarrow Cu_2O \rightarrow Cu$) are still occurring when NaCl begins to sublimate at ~700°C. Formation of NaCl and KCl as stable decomposition products of $NaClO_4 \cdot H_2O$ and $KClO_4$ was also observed by Shimada[100] and Oyumi *et al.*[101]

Sulfate and chromate[III]

Generally, organic copper complexes containing sulfate as an anion decompose in an air atmosphere yielding $CuSO_4$, which is stable up to 600°C and then decomposes further to CuO[102–105] or Cu_2O.[106] For the copper complex of aminothiazole CuS was also observed as an intermediate product (350–600°C), which was degradated to CuO in the temperature range 600–805°C.[107]

However, the molar ratio of copper and sulphate is 1:2 in $[Cu(trisH_{-1})(tris)(H_2O)]_2SO_4$ (**6**), so the decomposition pattern suggested by Langfelderova *et al.*[102] is more likely. The organic group in compound **6** degradates in three successive stages, leading to an intermediate phase at 470°C, whose mass corresponds to $CuO \cdot CuSO_4$ (the observed mass 28.80%, when compared to the theoretical value 32.24%, indicates that some sulfate has already decomposed). At 600°C, the sulfate group decomposes further leading to another intermediate phase at 700°C, namely CuO·CuS (obs. 24.68%, theor. 23.62%). In some TG runs there is evidence that CuS begins to decompose to CuO above 800°C, but the process is not completed at 900°C. In nitrogen atomosphere, 87% of the organic group is decomposed in the temperature range 170–500°C, resulting in a mixture of CuO, $CuSO_4$ and an organic residue. Between 500–900°C the process corresponds to the incomplete reduction of copper and the decomposition of the organic residue.

The organic group of the chromate compound, $[Cu(trisH_{-1})(tris)(H_2O)]_2CrO_4$ (**7**), shows quite exceptional thermal behavior, since the degradation of the ligand already begins at 110°C, but the major portion of it does not decompose until chromate decomposes, liberating oxygen and producing an explosive type of reaction at 270°C. Hence, chromate belongs to the same category of oxidative anions as nitrate and perchlorate. The final products at 320°C are copper(II) and chromium(III) oxides (mass obs. 31.26%, theor.

30.87%). In a nitrogen atmosphere, the organic group has almost completely decomposed before chromate is decomposed at 800°C. The final residue is a mixture of elemental copper and chromium (mass obs. 25.97%, theor. 23.51%).

Halides[IV,V]

Many studies on the thermal behavior of copper–amino complexes containing chloride[107–113] as an anion have been published, and some on bromide[107,113] and iodide[113] compounds as well, but thermal studies on amino complexes containing fluoride were not found in the literature. The decomposition pathways observed for these compounds can be divided into two main categories. First, the reactions where the compounds decompose with the simultaneous loss of the organic ligand and halide to give CuO as the end product.[108,109,113] The other type involves separate stages for the decomposition of the organic group and halide, resulting in formation of copper(II) halide as an intermediate compound, which undergoes a further degradation above 600°C leading to CuO.[111,112]

The isotypic series of *cis*-[Cu(trisH$_{-1}$)(tris)(H_2O)]$X\cdot H_2O$, where X = F^-, Cl^-, Br^-, I^- (**10–13**),[V] contain copper and halide in an equal molar ratio, hence the formation of copper(II) halide is not very likely. In air, the organic group of these compounds decomposes in three, partly overlapping stages, where the last one is accompanied by a simultaneous loss of halide, leading to CuO. With fluoride and chloride compounds the final observed mass was much less than what was expected for CuO (F: obs. 9.19%, theor. 22.11%; Cl: obs. 9.03%, theor. 21.14%), and the results were explained by the formation of a covalent copper(I) halide, which was sublimated during the last stage. For both compounds, 58% of copper was sublimated as CuF or CuCl and 42% remained as CuO. Earlier, Tummavuori and Suontamo[114] have mentioned the formation of these volatile copper(I) halides in the literature. Similar behavior was also observed with copper(II) fluorides and chlorides when used as a reference material in the same conditions. Covalent halide formation is highly dependent on the copper–tris complex in question, because no such behavior was observed for other complexes containing fluoride in this study [*e.g.* *trans*-{[Cu(tris)$_2$]F_2}$_n$ (**14**) and *cis*-[Cu(trisH$_{-1}$)(tris)]F (**15**)].[44] For the bromide and iodide analogues the final weights correspond to CuO within the experimental error. In nitrogen atmosphere, the organic part is almost completely decomposed when 420°C is reached, resulting in copper(I) halide and an organic residue. CuF and CuCl

were stable up to 950°C, but CuBr and CuI decomposed further leading to metallic copper (the decomposition CuBr is still incomplete at 950°C).

Halide compounds containing alkali metals, *trans*-[Cu(trisH$_{-1}$)$_2$]KF·3H$_2$O (**8**) and *trans*-[Cu(trisH$_{-1}$)$_2$]KBr·2H$_2$O (**9**),[IV] can form thermally stable ionic intermediates, such as KF and KBr. These inorganic salts sublimate further giving a characteristic mass loss in the temperature range 700–900°C. In an air atmosphere, the intermediate phase of copper(II) oxide and potassium halide is observed at ~500°C, but in a nitrogen atmosphere, it is not so clear, because of the concurrent reduction of CuO to elemental copper in the same temperature range.

6.3 Comparison of thermal stability of the organic group

Copper–tris complexes exhibit a very characteristic thermal behavior, which depends very much on the anion in question. The DTG curve, especially, can be used to identify the compounds. However, there are some compounds with apparently similar behavior. For example, the organic group of the *trans* family (compounds **1**, **2**, **3**, **8**, **9**, **14**, and **17**) shows similar thermal behavior. The first decomposition reaction of the organic group in these *trans* compounds causes the highest peak in the derivative curve, which normally contains only one maximum and has a very symmetric shape. In an air atmosphere, this peak shows up in the temperature range 150–240°C, representing 65–75% of the organic matter. On the other hand, the decomposition of the dimeric *cis* complexes is a multi-step procedure, where the derivative curve contains several maxima and shoulders, indicating that many competing decomposition processes are going on at the same time. The only exception is *cis*-[Cu(trisH$_{-1}$)(tris)]F (**15**),[44] whose thermal behavior closely resembles the behavior of the *trans* family.

The thermal stability of the organic ligand may be correlated to a variety of properties, such as chelate-ring size, *cis–trans* isomerism, molecular structure (monomer, dimer, polymer), structure of the coordination polyhedra (the number and strength of the coordination bonds and the degree of distortion of the coordination sphere) and also the effectiveness of the hydrogen-bonding structure and other intermolecular interactions.

The chelate structure in copper–tris complexes is ideal, because five-membered chelate rings are normally more stable than the corresponding six-membered rings.[115] Further, if similar *cis* and *trans* isomers are compared, usually, the *trans* isomer is thermally more stable than the *cis* form.[102] However, Table 6.1 shows that the DTG maxima observed for the organic group are similar or somewhat higher for *cis* compounds, indicating that the dimeric structure of *cis* complexes is a more dominant factor in the thermal resistance than *cis–trans* isomerism. The thermal stability of the copper(II) complexes can also be increased by the formation of chains.[116] This behavior is also observed with the polymeric chain structures, since *trans*-$\{[Cu(tris)_2]F_2\}_n$ (**14**)[44] shows higher derivative values for the organic group than dimeric structures. On the other hand, the octanuclear complexes do not exhibit high thermal stability, probably because of the intramolecular angular strain, electrostatic repulsion between the copper(II) nuclei (Cu···Cu ~3Å), and lack of intermolecular hydrogen bonding.

When thermal stability is considered in terms of coordination polyhedra, the number of coordination bonds (especially with the ligand) as well as the bond length and degree of distortion are the most crucial parameters.[116,117] The most advantageous structure for copper–tris complexes is found in compounds with an octahedral coordination sphere, where all six coordination bonds are formed with tris, as in compounds **5** and **14**. The DTG maxima of the organic part for these compounds are the highest of all in Table 6.1. The octahedral coordination sphere of *trans*-$\{[Cu(tris)_2]F_2\}_n$ (**14**)[44] is more regular, because the apical coordination bonds are formed with the axial hydroxymethyl groups of the adjacent monomer units, resulting in a polymeric chain structure. In the perchlorate compound, *cis*-$[Cu(trisH_{-1})(tris)]Na(ClO_4)_2$ (**5**),[II] copper acts as a mononuclear center forming three coordination bonds with both tris ligands, but due to the steric hindrance of tris, the coordination sphere is distorted, and the angles between the coordination plane and the apical bonds are 79.15(9) and 77.23(9)°. Nevertheless, the dimeric structure, ionic interactions and the additional coordination properties of sodium compensate for the distortion effect, so the overall stability of the organic group is almost the same as found for compound **14**. The third stable complex is the anhydrous fluoride dimer, *cis*-$[Cu(trisH_{-1})(tris)]F$ (**15**),[44] which contains five coordination bonds to the ligands with exceptionally short bond distances [in plane 1.911(3)–1.993(3) Å, and the apical bond 2.386(3) Å]. The other dimeric structures with octahedral coordination spheres, where five coordination bonds out of six are formed with the ligands, come next in this series.

The effect of the hydrogen-bonding network is also important, because it levels off some of the differences in thermal stability. Hence, the monomeric structure of the *trans* complexes is quite effectively compensated by an extensive three-dimensional network of hydrogen bonds, whereas in dimeric *cis* complexes, there is always one direction where the intermolecular interactions are weak (mainly van der Waals forces or relatively long hydrogen-bond contacts). Thermally, the least stable compound is the chromate compound, *cis*-[Cu(trisH$_{-1}$)(tris)(H$_2$O)]$_2$CrO$_4$ (**7**),[III] which is completely decomposed to metal oxides by 320°C in air. The strong oxidative nature of chromate, as well as the large ionic radius of the chromate anion, which forces the complex molecules further away from each other and weakens the intermolecular hydrogen bonding, probably accounts for this low thermal stability. The same weakening effect of the large ion radius is observed with the halide series, *cis*-[Cu(trisH$_{-1}$)(tris)(H$_2$O)]*X*·H$_2$O (**10–13**),[V] where the iodide compound has already decomposed in air at 450°C and the other analogues at 560°C.

Table 6.1 Thermal decomposition of copper–tris complexes (DTG maximum temperatures in °C for the reaction).

Compound	Crystalline water		Organic ligand#		Anion		End product		Ref.
	Air	Nitrogen	Air	Nitrogen	Air	Nitrogen	Air	Nitrogen	
1 *trans*-[Cu(trisH$_{-1}$)$_2$]	–	–	194	218	–	–	CuO	Cu+C	I
2 *trans*-[Cu(trisH$_{-1}$)$_2$(H_2O)]	154	150	194	208	–	–	CuO	Cu+C	I
3 *trans*-[Cu(trisH$_{-1}$)$_2$]·5H_2O	84	87	197	208	–	–	CuO	Cu+C	I
4 *cis*-[Cu(trisH$_{-1}$)(tris)(NO_3)]	–	–	204	206,236	385	700–800	CuO	Cu+C	II
5 *cis*-[Cu(trisH$_{-1}$)(tris)]Na(ClO_4)$_2$	–	–	216	232	271,430,461	243,367,429	CuO	Cu	II
6 *cis*-[Cu(trisH$_{-1}$)(tris)(H_2O)]$_2$$SO_4$	99	92	184	208,250	863	–	CuO+CuS	CuO+$CuSO_4$	III
7 *cis*-[Cu(trisH$_{-1}$)(tris)(H_2O)]$_2$$CrO_4$	72	73	135	134	278	903	CuO+Cr_2O_3	Cu+Cr+C	III
8 *trans*-[Cu(trisH$_{-1}$)$_2$]KF·3H_2O	109	109	170,473	164,181	872	823	CuO	Cu	IV
9 *trans*-[Cu(trisH$_{-1}$)$_2$]KBr·2H_2O	128	121	192	182	775	763	CuO	Cu	IV
10 *cis*-[Cu(trisH$_{-1}$)(tris)(H_2O)]F·H_2O	53	42	204	189,256	453	–	CuO (42%)	CuF+C	V
11 *cis*-[Cu(trisH$_{-1}$)(tris)(H_2O)]Cl·H_2O	68	64	204	190,259	436,466	–	CuO (42%)	CuCl	V
12 *cis*-[Cu(trisH$_{-1}$)(tris)(H_2O)]Br·H_2O	62	58,83	217	191,245	456	470	CuO	Cu	V
13 *cis*-[Cu(trisH$_{-1}$)(tris)(H_2O)]I·H_2O	71	68,118	199,216	240	419	575	CuO	Cu+C	V
14 *trans*-{[Cu(tris)$_2$]F_2}$_n$	–	–	221	232	380	290–900	CuO	Cu+C	44
15 *cis*-[Cu(trisH$_{-1}$)(tris)]F	–	–	214	222	365	290–900	CuO	Cu	44
16 *cis*-[Cu(trisH$_{-1}$)(tris)(H_2O)]$_2${SiF_6}	60	59	*	*	390	243	CuO+Si	Cu+Si	44
17 *trans*-[Cu(tris)$_2$(NO_3)$_2$]	–	–	201	204	223,369	230	CuO	Cu+$CuNO_3$	44
19 [Cu8(trisH$_{-2}$)$_4$(trisH$_{-1}$)$_2$(tris)$_2$]Br_6·6H_2O·EtOH	42	50	175	174	465	300-700	CuO	Cu	44

The DTG maximum for the first (and normally also the dominant) decomposition reaction is given. If two values are shown, the second temperature represents the dominant reaction. * Undefined.

7. CONCLUSIONS

The twenty copper–tris complexes determined in this study very well show the versatility of this aminoalcohol ligand. Tris can act as a bidentate or tridentate ligand forming mononuclear chelate complexes, which can further produce hydrogen-bonded dimers or polymeric chain structures. In alcoholic solutions, even polynuclear species are obtained. The molecular structures also show great diversity in isomerism, typical for these compounds. Mononuclear complexes possess *cis–trans* isomerism of the nitrogen and oxygen atoms in the coordination plane, and the *cis* isomers are also closely related to the dimer formation. The orientation of the five-membered chelate rings (upwards or downwards) gives rise to *syn–anti* isomerism. Furthermore, the dimeric structures possess a similar *syn–anti* isomerism, depending on whether the coordinated groups in monomers are facing each other or ponting outside the dimer. In addition, some complexes exhibit coordination isomerism and distortion isomerism, in which the complexes have the same stoichiometric structure, but the number of coordination bonds or the degree of distortion in the coordination polyhedra differs. In addition, all five and six-coordinate species that do not contain an inversion center are optically active complexes with two possible enantiomers. Nevertheless, the product is a racemic mixture containing equal amounts of both optical isomers, because the syntheses are not stereoselective.

The formation of the complexes takes place through a complicated equilibrium process, which depends on many properties, such as solvent (water, methanol, ethanol, or their mixtures), metal–ligand–anion ratio, pH (addition of hydroxides), concentration, and temperature. Mononuclear *trans* complexes, $[Cu(trisH_{-1})_2]$, are formed in dilute or alkaline solutions with an excess of tris (metal–ligand ratio 1:4), whereas the dimeric *cis* structures are obtained from the concentrated aqueous solutions with the same metal–ligand ratio. Coordination of water as the apical ligand is favored, because of its small size and high polarity. Formation of polynuclear complexes more likely caused by ethanol as a solvent and a low metal–ligand ratio (1:1 or 1:2) rather than by alkaline addition, as stated earlier. In alcoholic solutions, the protolytic equilibrium of the amino group normally generates proper conditions, where the ligand can choose the deprotonation level of hydroxymethyl groups. For example, in the octanuclear species the deprotonation level of the ligand varies from 2 ($trisH_{-2}$) to zero (tris). Excessive use of hydroxides destroys this balance, and as a consequence, the octanuclear structure is broken and deprotonated

mononuclear complexes are obtained, instead. In general, the alcoholic solutions increase the coordination degree of tris, as well as formation of continuous chain structures.

Crystal structures of the copper–tris complexes show that only centrosymmetric space groups are observed for these compounds. Furthermore, isomorphism is not typical for these structures. Only two compounds out of 23 known copper–tris complexes have strictly isomorphic structures (the chloride and bromide analogues of *cis*-[Cu(trisH$_{-1}$)-(tris)(H_2O)]$X\cdot H_2O$), and the corresponding fluoride analogue is suspected to be isomorphous with them according to XRD and TG measurements. Two other halide compounds, *trans*-[Cu(trisH$_{-1}$)$_2$]$KF\cdot 3H_2O$ and *trans*-[Cu(trisH$_{-1}$)$_2$]$KBr\cdot 2H_2O$, can be classified as isotypic structures, containing a similar organic frame structure, but the locations of halides and the extra water molecule are different. Otherwise, even small changes in the anion radius can change the molecular packing and lead to a new type of a unit cell (*e.g.* sulfate *versus* chromate, iodide *versus* other halides). This behavior reflects the flexibility of tris as a ligand, and its ability to change the hydrogen-bonding network to produce the most effective bonding possible. Hydrogen bonding plays a very important role in most of the structures, and generally all OH, NH_2, and H_2O hydrogens are involved in these three-dimensional structures. The most characteristic hydrogen bonds are found in the dimer structures, and to my knowledge, this is the first time the structures of these hydrogen-bonded copper–tris dimers have been fully characterized.

The mass spectral fragmentation schemes deduced for tris and deuterated tris indicated that the amino group is the main driving force of the fragmentation reactions. The ion decomposition reactions in mass spectrometry are closely related to pyrolytic reactions, hence, the small gaseous products, which were obtained as neutral losses in fragmentation schemes, are also possible decomposition products in the thermal analysis of the organic group.

The thermal analysis showed that after dehydration, the organic part decomposes in several stages, which do not correspond to any simple stoichiometry. Normally, no stable intermediates were formed during decomposition, and the final residue in air was CuO and elemental copper in a nitrogen atmosphere. Compounds containing alkali metals and halides (or perchlorate) are exceptions, since they produce thermally stable ionic salts (NaCl, KF, KBr) as intermediates, which decompose further above 700°C. Crystalline water is quite loosely bonded to the structures.

For thermal stability of the organic group, the following trends could be observed. The thermal stability of the organic group increases in the order of: monomer < dimer < polymeric chain structure. The number and length of the coordination bonds between copper and tris, as well as the distortion of the coordination polyhedra affect the thermal stability of the ligand. The higher the number of coordination bonds, the shorter the bonds are, and the less distorted the coordination sphere, the more stable is the complex formed. These thermal observations also support the existence of the apical coordination bonds between copper and axial hydroxymethyl groups of tris, which were questioned in some of the earlier structural studies. Even though a straightforward thermal comparison between *cis* and *trans* complexes is not possible, because all *trans* complexes are monomers and *cis* complexes, correspondingly dimers, some observations can be made from the degradation pattern. The decomposition of the organic group is more symmetric in the monomeric *trans* compounds, reflecting the higher symmetry of the molecule, whereas the decomposition of the organic group in dimeric *cis* compounds is a complex multi-step process, producing very characteristic DTG curves. In the main, the temperature differences observed for the decomposition of the organic group were not very large, because thermal stability is the sum of many properties, which compensate each other.

8. REFERENCES

List of original publications by the author:

I Kotila, S. and Valkonen, J., Copper(II) Complexes of 2-Amino-2-hydroxymethyl-1,3-propanediol. Part 1. Synthesis, Structure and Thermal Behavior of Three *trans*-Bis[2-amino-2-hydroxymethyl-1,3-propanediolato-(1-)-*O,N*]copper(II) Complexes, $[Cu(C_4H_{10}NO_3)_2]$, $[Cu(C_4H_{10}NO_3)_2(H_2O)]$ and $[Cu(C_4H_{10}NO_3)_2]\cdot 5H_2O$. *Acta Chem. Scand. 47* (1993) 950–956.

II Kotila, S. and Valkonen, J., Copper(II) Complexes of 2-Amino-2-hydroxymethyl-1,3-propanediol. Part 2. Synthesis, Structure and Thermal Behavior of *cis*-[2-Amino-2-hydroxymethyl-1,3-propanediol(1,3-)-*O,O',N*][2-amino-2-hydroxymethyl-1,3-propanediolato(1-)-*O,N*]nitratocopper(II), $[Cu(C_4H_{10}NO_3)(C_4H_{11}NO_3)(NO_3)]$, and *cis*-[2-Amino-2-hydroxymethyl-1,3-propanediol(1,3-)-*O,O',N*][2-amino-2-hydroxymethyl-1,3-propanediolato(1,3-)-*O,O',N*]copper(II) Sodium Bis(perchlorate), $[Cu(C_4H_{10}NO_3)(C_4H_{11}NO_3)]Na(ClO_4)_2$. *Acta Chem. Scand. 47* (1993) 957–964.

III Kotila, S. and Valkonen, J., Copper(II) Complexes of 2-Amino-2-hydroxymethyl-1,3-propanediol. Part 3. Synthesis, Structure and Thermal Behavior of Bis-*cis*-[2-amino-2-hydroxymethyl-1,3-propanediol-*O,N*][2-amino-2-hydroxymethyl-1,3-propanediolato-*O,N*]aquacopper(II) Sulfate and Chromate, $[Cu(C_4H_{10}NO_3)(C_4H_{11}NO_3)(H_2O)]_2X$, where $X = SO_4^{2-}$, CrO_4^{2-}. *Acta Chem. Scand. 48* (1994) 200–208.

IV Kotila, S. and Valkonen, J., Copper(II) Complexes of 2-Amino-2-hydroxymethyl-1,3-propanediol. Part 4. Synthesis, Structure and Thermal Behavior of *trans*-Bis[2-amino-2-hydroxymethyl-1,3-propanediolato-*O,N*]copper(II) Potassium Fluoride and Bromide, $[Cu(C_4H_{10}NO_3)_2]KF\cdot 3H_2O$ and $[Cu(C_4H_{10}NO_3)_2]KBr\cdot 2H_2O$. *Acta Chem. Scand. 48* (1994) 312–318.

V Kotila, S., Copper(II) Complexes of 2-Amino-2-hydroxymethyl-1,3-propanediol. Part 5. Synthesis, Structure and Thermal Behavior of *cis*-[2-Amino-2-hydroxymethyl-1,3-propanediol-*O,O',N*][2-amino-2-hydroxymethyl-1,3-propanediolato-*O,N*]aquacopper(II) Halide Monohydrate, $[Cu(C_4H_{10}NO_3)(C_4H_{11}NO_3)(H_2O)]X\cdot H_2O$, where $X = F^-$, Cl^-, Br^-, I^-. *Acta Chem. Scand.* (1994) *In press*.

Literature references:

1. Sigma Technical Bulletin, No 106B, Sigma Chemical Co., St. Louis, MO.
2. Shakked, Z., Viswamitra, M. A. and Kennard, O. *Biochemistry 107* (1980) 455.
3. Ramette, R. W., Culberson, C. H. and Bates, R. G. *Anal. Chem. 49* (1977) 867.
4. Bai, K. S. and Martell, A. E. *J. Inorg. Nucl. Chem. 31* (1969) 1697.
5. Hall, J. L., Simmons, R. B., Morita, E., Joseph, E. and Gavlas, J. F. *Anal. Chem. 43* (1971) 634.
6. Sigel, H., Scheller, K. H. and Prijs, B. *Inorg. Chim. Acta 66* (1982) 147.
7. Fischer, B. E., Häring, U. K., Tribolet, R. and Sigel, H. *Eur. J. Biochem. 94* (1979) 523.
8. Fisher, J. F. and Hall, J. L. *Anal. Chem. 39* (1967) 1550.
9. Scheller, K. H., Abel, T. H. J., Polanyi, P. E., Wenk, P. K., Fischer, B. E. and Sigel, H. *Eur. J. Biochem. 107* (1980) 455.
10. Dotson, R. L. *Inorg. Nucl. Chem. Lett. 9* (1973) 215.
11. Bates, R. G. and Robinson, R. A. *Anal. Chem. 45* (1973) 420.
12. Hansen, L. D. and Lewis, E. A. *J. Chem. Thermodynamics 3* (1971) 35.
13. Mc Farland, W. and Norris, K. *Calif. Fish Game 44* (1958) 291.
14. Manfredi, F., Sieker, H., Spoto, A. and Saltzman, H. *J. Am. Med. Assoc. 173* (1960) 999.
15. Nahas, G. *Science 129* (1959) 782.
16. Crow, V. L. and Pritchard, G. G. *Biochim. Biophys. Acta 438* (1976) 90.
17. Guibault, G. G., Brignac, P., Jr. and Zimmer, M. *Anal. Chem. 40* (1968) 190.
18. Neumann, H., Kezdy, F., Hsu, J. and Rosenberg, I. H. *Biochim. Biophys. Acta 391* (1975) 292.
19. Allen, D. E., Baker, D. J. and Gillard, R. D. *Nature (London) 214* (1967) 906.
20. Benesch, R. E. and Benesch, R. *J. Am. Chem. Soc. 77* (1955) 2749.
21. Hall, J. L. and Swisher, J. A. *U.S. Department of Commerce, Office of Technical Services, Tecnical Report 5.*, 1959.
22. Hall, J. L., Swisher, J. A., Brannon, D. G. and Liden, T. M. *Inorg. Chem. 1* (1962) 409.
23. Hanlon, D. P., Watt, D. S. and Westhead, E. W. *Anal. Biochem. 16* (1966) 225.
24. Bologni, L., Sabatini, A. and Vacca, A. *Inorg. Chim. Acta 69* (1983) 71.
25. Forsling, W. *Acta Chem. Scand. A 32* (1978) 857.
26. Granberg, I., Forsling, W. and Sjöberg, S. *Acta Chem. Scand. A 36* (1982) 819.

27. Van der Linden, W. E. and Beers, C. *Talanta 22* (1975) 89.
28. Brignac, P. J. and Mo, C. *Anal. Chem. 47* (1975) 1465.
29. Colombo, M. F., Austrilino, L., Nascimento, O. R., Castellano, E. E. and Tabak, M. *Can. J. Chem. 65* (1987) 821.
30. Boyd, P. D. W., Pilbrow, J. R. and Smith, T. D. *Aust. J. Chem. 24* (1971) 59.
31. Bennet, C. R. *J. Inorg. Nucl. Chem. 43* (1981) 2555.
32. Irving, H. and Williams, R. J. P. *Nature (London) 162* (1948) 746.
33. Irving, H. and Williams, R. J. P. *J. Chem. Soc.* (1953) 3192.
34. Eilerman, D. and Rudman, R. *J. Chem. Phys. 72* (1980) 5656.
35. Rudman, R., Lippman, R., Sake Gowda, D. S. and Eilerman, D. *Acta Crystallogr., Sect. C 39* (1983) 1267.
36. Dotson, R. L. *J. Inorg. Nucl. Chem. 34* (1972) 3131.
37. Rochon, F. D., Kong, P. C. and Melanson, R. *Can. J. Chem. 62* (1984) 2657.
38. Dotson, R. D. *Inorg. Nucl. Chem. Lett. 8* (1972) 353.
39. Ivarsson, G. J. M. *Acta Crystallogr., Sect. B 38* (1982) 1828.
40. Ivarsson, G. J. M. *Acta Crystallogr., Sect. C 40* (1984) 67.
41. Masi, D., Mealli, C., Sabat, M., Sabatini, A., Vacca, A. and Zanobini, F. *Helv. Chim. Acta 67* (1984) 1818.
42. Mazus, M. D., Kovalenko, A. L., Polyakov, V. N., Simonov, Y. A. and Malinovskii, T. I. *Zh. Neorg. Khim. 31* (1986) 2023 {or *Russ. J. Inorg. Chem. 31* (1986) 1165}.
43. Mazus, M. D., Kovalenko, A. L., Simonov, Y. A. and Polyakov, V. N. *Zh. Neorg. Khim. 32* (1987) 2212 {or *Russ. J. Inorg. Chem. 32* (1987) 1295}.
44. Kotila, S. *Unpublished material.*
45. Polyakov, V. N., Kovalenko, A. L., Shafranskii, V. N., Zelentsov, V. V., Murashko, S. V. and Kryukov, V. V. *Zh. Neorg. Khim. 34* (1989) 1500 {or *Russ. J. Inorg. Chem. 34* (1989) 847}.
46. Brannon, D. G., Morrison, R. H., Hall, J. L., Humphrey, L. and Zimmerman, D. N. *J. Inorg. Nucl. Chem. 33* (1971) 981.
47. Walker, N. and Stuart, D. *Acta Crystallogr., Sect. A 39* (1983) 158.
48. Sheldrick, G. M. In: Sheldrick, G. M., Krüger,C. and Goddard, R., Eds., *Crystallographic Computing 3*, Oxford University Press., Oxford 1985, pp.175—189.
49. *MolEN, an Interactive Structure Solution Procedure*, Enraf—Nonius, Delft, The Netherlands 1990.

50. *International Tables for X-ray Crystallography*, Kynoch Press, Birmingham 1974, Vol. 4.

51. Keller, E. *SCHAKAL, a FORTRAN Program for the Graphic Representation of Molecular and Crystallographic Models*, University of Freiburg, Freiburg 1987.

52. Keller, E. *SCHAKAL92, a FORTRAN Program for the Graphic Representation of Molecular and Crystallographic Models*, University of Freiburg, Freiburg 1992.

53. Muhonen, H. *Inorg. Chem. 25* (1986) 4692.

54. Emsley, J., Arif, M., Bates, P. A. and Hursthouse, M. B. *J. Chem. Soc., Chem. Commun.* (1988) 1387.

55. Jameson, G. B., Seferiadis, N. and Oswald, H. R. *Acta Crystallogr., Sect. C 42* (1986) 984.

56. *CRC Handbook of Chemistry and Physics*, Weast, R. C., Ed., 70th Edition, CRC Press, Boca Raton, FL 1989, pp. F-188 and F-189.

57. Gazo, J., Bersuker, I. B., Garaj, J., Kabesova, M., Kohout, J., Langfelderova, H., Melnik, M., Serator, M. and Valach, F. *Coord. Chem. Rev. 19* (1976) 253.

58. Yukawa, Y. *J. Chem. Soc., Dalton Trans.* (1992) 3217.

59. Gazo, J. *Pure Appl. Chem. 38* (1974) 279.

60. Healy, P. C., Kennard, C. H. L, Smith, G. and White, A. H. *Cryst. Struct. Commun. 7* (1978) 563.

61. Tedenac, J. C., Nguyen Dinh Phung, Avinens, C. and Maurin, M. *J. Inorg. Nucl. Chem. 38* (1976) 85.

62. Healy, P. C., Patrick, J. M. and White, A. H. *Aust. J. Chem. 37* (1984) 1111.

63. Mergehenn, R. Haase, W. and Allmann, R. *Acta Crystallogr., Sect. B 31* (1975) 1847.

64. Schwabe, L. and Haase, W. *Acta Crystallogr., Sect. C 42* (1986) 667.

65. Muhonen, H. *Acta Chem. Scand. A 34* (1980) 79.

66. Watson, W. H. and Holley, W. W. *Croatica Chem. Acta 57* (1984) 467.

67. Olejnik, Z., Jezowska-Trzebiatowska, B. and Lis, T. *J. Chem. Soc., Dalton Trans.* (1986) 97.

68. Thompson, L. K., Mandal, S. K., Gabe, E. J., Lee, F. L. and Addison, A. W. *Inorg. Chem. 26* (1987) 657.

69. Ghedini, M., De Munno, G., Denti, G., Manotti Lanfredi, A. M. and Tiripicchio, A. *Inorg. Chim. Acta 57* (1982) 87.

70. Lee, T. J., Lu, T. H., Liu, S. H., Chung, C. S. and Lee, T. Y. *Acta Crystallogr., Sect. C 40* (1984) 1131.

71. Sillanpää, R. and Rissanen, K. *Acta Chem. Scand. 44* (1990) 1013.
72. Sletten, E. and Erevik, G. *Acta Crystallogr., Sect. B 33* (1977) 1633.
73. Xinmin, G., Ning, T., Xin, W., Yin, Z. and Minyu, T. *Polyhedron 8* (1989) 933.
74. Cotton, F. A. and Wilkinson, G., *Advanced Inorganic Chemistry*, 5th Edition, John Wiley & Sons, New York 1988.
75. Spek, A. L., Duisenberg, A. J. M., Bouwman, E., Driessen, W. L. and Reedijk, J. *Acta Crystallogr., Sect. C 44* (1988) 1569.
76. Vreugdenhil, W., Birker, P. J. M. W. L., ten Hoedt, R. W. M., Verschoor, G. C. and Reedijk, J. *J. Chem. Soc., Dalton Trans.* (1984) 429.
77. Sletten, E. and Ruud, M. *Acta Crystallogr., Sect. B 31* (1975) 982.
78. Mithell, T. P. and Bernard, W. H. and Wasson, J. R. *Acta Crystallogr., Sect. B 26* (1970) 2096.
79. Nieminen, K. and Näsäkkälä, M. *Acta Chem. Scand. A 34* (1980) 375.
80. Pangborn, W., Duax, W. and Langs, D. *J. Am. Chem. Soc. 109* (1987) 2163.
81. Calestani, G., Ugozzoli, F., Arduini, A., Ghidini, E. and Ungaro, R. *J. Chem. Soc., Chem. Commun.* (1987) 344.
82. Dubourg, A., Fabregue, E., Maury, L. and Declercq, J.-P. *Acta Crystallogr., Sect. C 46* (1990) 1394.
83. Veya, P., Floriani, C., Chiesi-Villa, A. and Guastini, C. *J. Chem. Soc., Chem. Commun.* (1991) 991.
84. Ward, D. L., Huang, R. H. and Dye, J. L. *Acta Crystallogr., Sect. C 46* (1990) 1833.
85. Weber, E. and Czugler, M. *Inorg. Chim. Acta 61* (1982) 33.
86. McKee, V. and Tandon, S. S. *J. Chem. Soc., Dalton Trans.* (1991) 221.
87. McLafferty, F. W. In: Turro, N. J., Ed., *Interpretation of Mass Spectra (Organic Chemistry Series)*, 3rd Edition, University Science Books, Mill Valley 1980.
88. Palopoli, S. F. and Brill, T. B. *Inorg. Chem. 27* (1988) 2971.
89. Stoner, C. E., Jr., Rheingold, A. L. and Brill, T. B. *Inorg. Chem. 30* (1991) 360.
90. Gili, P., Palacios, M. S., Martin-Reyes, M. G., Martin-Zarza, P., Ruiz-Perez, C., Rodrigues-Romero, F. V. and Lahoz, F. V. *Polyhedron 11* (1992) 2171.
91. Narain, G., Shakya, A. K. and Shukla, P. R. *Thermochim. Acta 64* (1983) 373.
92. Narain, G., Shakya, A. K. and Shukla, P. R. *Thermochim. Acta 67* (1983) 377.
93. Allan, J. R. and Dalrymple, J. *Thermochim. Acta 221* (1993) 199.
94. Allan, J. R., Carson, B. R., Gerrard, D. L. and Hoey, S. *Thermochim. Acta 153* (1989) 173.

95. Srivastava, P. C., Singh, B. N., Adhya, S. D. and Banerji, K. C. *J. Therm. Anal. 27* (1983) 263.

96. Angoso, A., Martin-Llorente, J. M., Manzano, J. L., Martin, M., Martin, R., Rodriguez, E. and Soria, J. *Inorg. Chim. Acta 195* (1992) 45.

97. Mathew, S., Nair, C. G. R. and Ninan, K. N. *Bull. Chem. Soc. Jpn. 64* (1991) 3207.

98. Prabhumirashi, L. S., Natu, G. N. and Khoje, J. K. *J. Therm. Anal. 35* (1989) 1097.

99. Donia, A. M. *J. Therm. Anal. 39* (1993) 323.

100. Shimada, S. *J. Therm. Anal. 40* (1993) 1063.

101. Oyumi, Y. and Brill, T. B., Rheingold, A. L. and Lowe-Ma, C. *J. Phys. Chem. 89* (1985) 2309.

102. Langfelderova, H., Jorik, V. and Cervena, J. *J. Therm. Anal. 39* (1993) 489.

103. Aleksovska, S. and Jordanovska, V. *Thermochim. Acta 228* (1993) 103.

104. Gutierrez, M. D., Romero, M. A., Lopez, R., Nogueras, M. and Sanchez, A. *Thermochim. Acta 168* (1990) 197.

105. Jordanovska, V. and Trojko, R. *Thermochim. Acta 228* (1993) 231.

106. Singh, N. B. and Singh, J. *J. Therm. Anal. 14* (1978) 229.

107. Jordan, B. M., Raper, E. S. and Creighton, J. R. *Thermochim. Acta 62* (1983) 21.

108. Allan, J. R., Beaumont, P. C., Macindole, L., Milburn, G. H. W. and Werninck, A. R. *Thermochim. Acta 131* (1988) 29.

109. Allan, J. R., Milburn, G. H. W., Richmond, F., Gerrard, D. L., Birnie, J. and Wilson, A. S. *Thermochim. Acta 177* (1991) 213.

110. Allan, J. R., Gardner, A. R., McCloy, B. and Smith, W. E. *Thermochim. Acta 208* (1992) 115.

111. Allan, J. R., Gardner, A. R., McCloy, B. and Smith, W. E. *Thermochim. Acta 208* (1992) 125.

112. Allan, J. R., Beaumont, P. C., Milburn, G. H. W. and Wood, I. *Thermochim. Acta 214* (1993) 243.

113. Allan, J. R., Baillie, G. M., Middlemist, N. S. and Pendlowski, M. J. *J. Therm. Anal. 22* (1981) 3.

114. Tummavuori, J. and Suontamo, R. *Finn. Chem. Lett.* (1979) 176.

115. Donia, A. M., Gouda, M. M., Ayad, M. I. and El-Boraey, H. A. *Thermochim. Acta 194* (1992) 155.

116. Langfelderova, H. *J. Therm. Anal. 12* (1977) 413.

117. Langfelderova, H., Foret, F., Ambrovic, P. and Gazo, J. *J. Therm. Anal. 19* (1980) 357.

APPENDIX I Bond lengths of the coordination sphere of copper in mononuclear complexes.

Compound		Basal coordination bonds [Å]				Apical coordination bonds [Å]	
		Cu100–O111	Cu100–O121	Cu100–N111	Cu100–N121	Cu100–O(up)	Cu100–O(down)
1 *trans*-[Cu(trisH_1)$_2$]		1.941(1)	–	1.991(1)	–	–	–
2 *trans*-[Cu(trisH_1)$_2$(H$_2$O)]		1.950(1)	–	2.032(1)	–	2.200(2)	–
3 *trans*-[Cu(trisH_1)$_2$]·5H$_2$O		1.929(2)	–	1.985(2)	–	–	–
4 *cis*-[Cu(trisH_1)(tris)(NO$_3$)]		1.987(1)	1.925(2)	1.997(2)	2.002(2)	2.553(2)	2.596(2)
5 *cis*-[Cu(trisH_1)(tris)]Na(ClO$_4$)$_2$		1.966(2)	1.968(2)	1.997(3)	2.000(2)	2.518(3)	2.431(3)
6 *cis*-[Cu(trisH_1)(tris)(H$_2$O)]$_2$SO$_4$		1.983(2)	1.924(3)	1.990(3)	2.009(2)	2.317(3)	–
7 *cis*-[Cu(trisH_1)(tris)(H$_2$O)]$_2$CrO$_4$	(Molecule 1)	1.975(3)	1.930(2)	1.997(3)	2.016(3)	2.301(3)	–
	(Molecule 2)	1.983(2)	1.928(2)	1.997(3)	2.017(3)	2.297(3)	–
8 *trans*-[Cu(trisH_1)$_2$]KF·3H$_2$O		1.901(3)	–	1.980(4)	–	–	–
9 *trans*-[Cu(trisH_1)$_2$]KBr·2H$_2$O		1.915(4)	–	1.988(4)	–	–	–
11 *cis*-[Cu(trisH_1)(tris)(H$_2$O)]Cl·H$_2$O	(Molecule 1)	1.997(2)	1.936(2)	1.994(3)	1.999(3)	2.355(3)	2.752(3)
	(Molecule 2)	1.999(2)	1.922(2)	1.991(3)	2.006(3)	2.486(3)	2.638(3)
12 *cis*-[Cu(trisH_1)(tris)(H$_2$O)]Br·H$_2$O	(Molecule 1)	1.993(3)	1.935(3)	1.992(3)	1.991(3)	2.366(3)	2.768(3)
	(Molecule 2)	1.997(3)	1.921(3)	1.984(3)	2.006(3)	2.482(4)	2.674(3)
13 *cis*-[Cu(trisH_1)(tris)(H$_2$O)]I·H$_2$O		2.008(2)	1.936(2)	1.995(2)	2.006(2)	2.397(2)	2.717(2)
14 *trans*-{[Cu(tris)$_2$]F$_2$}$_n$		1.964(2)	–	2.016(3)	–	2.479(2)	2.479(2)*
15 *cis*-[Cu(trisH_1)(tris)]F		1.973(3)	1.911(3)	1.993(3)	1.991(4)	–	2.386(3)
16 *cis*-[Cu(trisH_1)(tris)(H$_2$O)]$_2${SiF$_6$}		1.986(1)	1.928(1)	2.004(2)	2.014(1)	2.280(2)	–
17 *trans*-[Cu(tris)$_2$(NO$_3$)$_2$]	(Molecule A)	1.975(2)	–	1.979(2)	–	2.532(5)	2.532(5)*
	(Molecule B)	1.975(2)	–	1.979(2)	–	2.559(5)	2.559(5)*
18 *cis*-[Cu(tris)$_2$(SO$_4$)]$_n$		1.993(1)	1.971(2)	1.978(2)	2.006(2)	2.461(2)	2.527(2)
21 *trans*-[Cu(trisH_1)$_2$]NaClO$_4$·H$_2$O (Ivarsson)[40]		1.908(2)	–	1.999(2)	–	–	–
22 *cis*-{[Cu(trisH_1)(tris)]Br}$_n$ (Masi *et al.*)[41]		2.018(1)	1.943(1)	1.995(1)	1.993(1)	2.551	2.778

* Related by inversion with respect to the copper atom.

APPENDIX II Bond angles of the coordination sphere of copper in mononuclear complexes (definition of angles in Fig. 3.1, p. 33).

Compound		Basal coordination angles [°]				Apical coordination angles [°]	
		1	2	3	4	5	6
1 *trans*-[Cu(trisH$_{-1}$)$_2$]		85.67(4)	85.67(4)*	94.33(4)	94.33(4)*	–	–
2 *trans*-[Cu(trisH$_{-1}$)$_2$(H_2O)]		84.40(5)	84.40(5)*	94.32(5)	94.32(5)*	94.23(4)	–
3 *trans*-[Cu(trisH$_{-1}$)$_2$]·5H_2O		85.39(7)	85.39(7)*	94.61(7)	94.61(7)*	–	–
4 *cis*-[Cu(trisH$_{-1}$)(tris)(NO_3)]		84.22(7)	86.74(7)	92.04(7)	96.96(8)	96.52(6)	76.19(6)
5 *cis*-[Cu(trisH$_{-1}$)(tris)]Na(ClO_4)$_2$		84.43(9)	86.4(1)	87.67(9)	101.4(1)	79.15(9)#	77.23(9)
6 *cis*-[Cu(trisH$_{-1}$)(tris)(H_2O)]$_2SO_4$		83.3(1)	86.3(1)	92.6(1)	96.4(1)	106.0(1)	–
7 *cis*-[Cu(trisH$_{-1}$)(tris)(H_2O)]$_2CrO_4$	(Molecule 1)	83.1(1)	86.5(1)	92.6(1)	96.1(1)	104.1(1)	–
	(Molecule 2)	83.1(1)	86.4(1)	92.56(9)	96.3(1)	104.1(1)	–
8 *trans*-[Cu(trisH$_{-1}$)$_2$]KF·3H_2O		85.6(1)	85.6(1)*	94.4(1)	94.4(1)*	–	–
9 *trans*-[Cu(trisH$_{-1}$)$_2$]KBr·2H_2O		85.3(2)	85.3(2)*	94.7(2)	94.7(2)*	–	–
11 *cis*-[Cu(trisH$_{-1}$)(tris)(H_2O)]Cl·H_2O	(Molecule 1)	84.2(1)	86.2(1)	91.44(9)	97.9(1)	93.1(1)	71.96(8)
	(Molecule 2)	83.8(1)	85.7(1)	92.64(9)	97.8(1)	93.0(1)	74.58(9)
12 *cis*-[Cu(trisH$_{-1}$)(tris)(H_2O)]Br·H_2O	(Molecule 1)	83.8(1)	86.2(1)	92.0(1)	97.9(1)	92.8(1)	72.2(1)
	(Molecule 2)	83.5(1)	85.5(1)	92.9(1)	98.0(1)	92.9(1)	74.0(1)
13 *cis*-[Cu(trisH$_{-1}$)(tris)(H_2O)]I·H_2O		83.9(1)	86.4(1)	92.16(9)	97.5(1)	92.01(9)	73.70(8)
14 *trans*-{[Cu(tris)$_2$]F_2}$_n$		82.8(1)	82.8(1)*	97.2(1)	97.2(1)*	92.41(9)	87.59(9)
15 *cis*-[Cu(trisH$_{-1}$)(tris)]F		81.3(1)	84.9(1)	95.3(1)	98.1(1)	–	84.0(1)
16 *cis*-[Cu(trisH$_{-1}$)(tris)(H_2O)]$_2$\{SiF_6\}		83.38(6)	86.18(6)	92.42(5)	96.49(6)	103.69(6)	–
17 *trans*-[Cu(tris)$_2$(NO_3)$_2$]	(Molecule A)	83.92(9)	83.92(9)*	96.08(9)	96.08(9)*	79.5(1)	100.6(1)
	(Molecule B)	83.92(9)	83.92(9)*	96.08(9)	96.08(9)*	74.0(1)	106.1(1)
18 *cis*-[Cu(tris)$_2$(SO_4)]$_n$		83.19(7)	83.42(7)	90.91(6)	102.54(7)	86.03(6)	89.37(6)
21 *trans*-[Cu(trisH$_{-1}$)$_2$]$NaClO_4$·H_2O (Ivarsson)[40]		85.9(1)	85.9(1)*	94.1(1)	94.1(1)*	–	–
22 *cis*-{[Cu(trisH$_{-1}$)(tris)]Br}$_n$ (Masi *et al.*)[41]		82.3(5)	85.2(5)	96.5(4)	96.4(6)	87.8 ¤	73.4 ¤

* Related by inversion (or 2-fold rotation for **2**). # Calculated with respect to O121. ¤ Calculated with the SCHAKAL92 program.

APPENDIX III Planarity of the coordination plane.*

Compound		Coordination number	Deviation from the coordination plane				
			O111	N111	O121	N121	Cu100
2 *trans*-[Cu(trisH$_{-1}$)$_2$(H$_2$O)]		5	0.089(1)	−0.089(1)	—	—	0.2256(3)
4 *cis*-[Cu(trisH$_{-1}$)(tris)(NO$_3$)]		6	−0.007(2)	0.007(2)	0.007(2)	−0.007(2)	0.0249(3)
5 *cis*-[Cu(trisH$_{-1}$)(tris)]Na(ClO$_4$)$_2$		6	0.046(2)	−0.040(3)	−0.045(2)	0.040(3)	0.0594(4)
6 *cis*-[Cu(trisH$_{-1}$)(tris)(H$_2$O)]$_2$SO$_4$		5	−0.064(3)	0.060(4)	0.062(3)	−0.059(3)	0.1694(5)
7 *cis*-[Cu(trisH$_{-1}$)(tris)(H$_2$O)]$_2$CrO$_4$	(Molecule 1)	5	−0.085(3)	0.081(3)	0.083(2)	−0.079(3)	0.1898(4)
	(Molecule 2)	5	−0.087(3)	0.082(3)	0.085(2)	−0.080(3)	0.1873(4)
11 *cis*-[Cu(trisH$_{-1}$)(tris)(H$_2$O)]Cl·H$_2$O	(Molecule 1)	6	0.018(2)	−0.018(3)	−0.019(2)	0.018(3)	0.0602(4)
	(Molecule 2)	6	−0.010(2)	0.009(3)	0.010(2)	−0.009(3)	0.0190(4)
12 *cis*-[Cu(trisH$_{-1}$)(tris)(H$_2$O)]Br·H$_2$O	(Molecule 1)	6	0.027(3)	−0.025(3)	−0.026(3)	0.025(4)	0.0613(5)
	(Molecule 2)	6	0.002(3)	−0.002(3)	−0.002(2)	0.002(4)	0.0303(5)
13 *cis*-[Cu(trisH$_{-1}$)(tris)(H$_2$O)]I·H$_2$O		6	0.034(2)	−0.032(3)	−0.034(2)	0.032(3)	0.0538(4)
15 *cis*-[Cu(trisH$_{-1}$)(tris)]F		5	−0.011(3)	0.010(4)	0.011(3)	−0.010(3)	0.0708(5)
16 *cis*-[Cu(trisH$_{-1}$)(tris)(H$_2$O)]$_2${SiF$_6$}		5	−0.056(2)	0.053(2)	0.055(1)	−0.052(2)	0.1706(2)
18 *cis*-[Cu(tris)$_2$(SO$_4$)]$_n$		6	−0.034(2)	0.031(2)	0.034(2)	−0.031(2)	0.0032(3)

* Least-squares coordination plane is defined by atoms O111, N111, O121 and N121 in molecule 1 (or O211, N211, O221 and N221 in molecule 2).
NOTE: All other *trans* complexes are planar due to symmetry reasons.

APPENDIX IV Torsion angles (in °) of the terminal hydroxymethyl groups (see Fig. 3.3, p. 36).

Compound		C111–C112–C113–O112	C111–C112–C114–O113	C121–C122–C123–O122	C121–C122–C124–O123
1 *trans*-[Cu(trisH$_{-1}$)$_2$]		−69.1	−178.2	–	–
2 *trans*-[Cu(trisH$_{-1}$)$_2$(H$_2$O)]		−66.8	−177.4	–	–
3 *trans*-[Cu(trisH$_{-1}$)$_2$]·5H$_2$O		168.4	−67.6	–	–
4 *cis*-[Cu(trisH$_{-1}$)(tris)(NO$_3$)]		69.5	−56.2	−178.8	−60.8
5 *cis*-[Cu(trisH$_{-1}$)(tris)]Na(ClO$_4$)$_2$		60.8	−166.7	77.3	−61.5
6 *cis*-[Cu(trisH$_{-1}$)(tris)(H$_2$O)]$_2$SO$_4$		−176.5 (A) / 68.8 (B)	−53.3 (A) / 80.7 (B)	−174.6	−56.0
7 *cis*-[Cu(trisH$_{-1}$)(tris)(H$_2$O)]$_2$CrO$_4$	(Molecule 1)	177.2	−64.2	64.1 (A) / −178.5 (B)	66.4
	(Molecule 2)	177.7	−63.8	64.8 (A) / −177.3 (B)	66.7
8 *trans*-[Cu(trisH$_{-1}$)$_2$]KF·3H$_2$O		−73.5	170.6	–	–
9 *trans*-[Cu(trisH$_{-1}$)$_2$]KBr·2H$_2$O		−73.3	169.2	–	–
11 *cis*-[Cu(trisH$_{-1}$)(tris)(H$_2$O)]Cl·H$_2$O	(Molecule 1)	66.9	−169.6	−168.5	169.1
	(Molecule 2)	68.9	−168.9	58.4	171.2
12 *cis*-[Cu(trisH$_{-1}$)(tris)(H$_2$O)]Br·H$_2$O	(Molecule 1)	67.4	−169.0	−167.8	168.2
	(Molecule 2)	68.9	−168.0	57.9	170.3
13 *cis*-[Cu(trisH$_{-1}$)(tris)(H$_2$O)]I·H$_2$O		68.9	−169.9	−167.5 (A) / 64.7 (B)	169.4
14 *trans*-{[Cu(tris)$_2$]F$_2$}$_n$		167.3	64.3	–	–
15 *cis*-[Cu(trisH$_{-1}$)(tris)]F		59.6	−64.1	−170.8	65.9
16 *cis*-[Cu(trisH$_{-1}$)(tris)(H$_2$O)]$_2${SiF$_6$}		−172.5	−53.9	176.6	−68.2
17 *trans*-[Cu(tris)$_2$(NO$_3$)$_2$]		−64.6	−64.5	–	–
18 *cis*-[Cu(tris)$_2$(SO$_4$)]$_n$		163.5	59.7	−59.3	174.7
21 *trans*-[Cu(trisH$_{-1}$)$_2$]NaClO$_4$·H$_2$O (Ivarsson)[40]		167.6	173.6	–	–
22 *cis*-{[Cu(trisH$_{-1}$)(tris)]Br}$_n$ (Masi *et al.*)[41]		58.2	−167.5	70.3	−174.1

NOTE: Angles equal to ±180° represent an *anti* conformation and angles equal to ±60° represent a *gauche* conformation of terminal hydroxymethyl groups in relation to carbons in the chelate ring.

APPENDIX V Space groups and unit-cell parameters of the copper–tris complexes (T = 21±1°C).

Compound	Space group (no.)	a [Å]	b [Å]	c [Å]	α [°]	β [°]	γ [°]	V [Å^3]	R
1 *trans*-[Cu(trisH$_{-1}$)$_2$]	$P\,2_1/c$ (14)	6.261(1)	10.109(1)	10.028(1)	90.00	116.86(1)	90.00	566.3(1)	0.023
2 *trans*-[Cu(trisH$_{-1}$)$_2$(H$_2$O)]	$C\,2/c$ (15)	12.928(3)	10.783(1)	10.066(5)	90.00	116.59(2)	90.00	1254.8(7)	0.026
– " – (Colombo *et al.*)[29]	$C\,2/c$ (15)	12.955(2)	10.793(1)	10.091(2)	90.00	116.62(1)	90.00	1261.4(6)	0.034#
3 *trans*-[Cu(trisH$_{-1}$)$_2$]·5H$_2$O	$P\,2/c$ (13)	10.087(2)	6.340(3)	15.557(1)	90.00	124.36(1)	90.00	821.2(5)	0.026
– " – (Mazus *et al.*)[43]	$P\,2/n$ (*)	12.926(7)	10.116(3)	6.368(3)	90.00	95.8(4)	90.00	–	0.051¤
4 *cis*-[Cu(trisH$_{-1}$)(tris)(NO$_3$)]	$P\,2_1/c$ (14)	10.246(2)	6.950(1)	21.313(3)	90.00	110.54(1)	90.00	1421.2(4)	0.032
5 *cis*-[Cu(trisH$_{-1}$)(tris)]Na(ClO$_4$)$_2$	$P\,\bar{1}$ (2)	9.946(1)	11.793(2)	8.853(2)	109.39(1)	112.72(1)	82.02(1)	903.4(2)	0.043
6 *cis*-[Cu(trisH$_{-1}$)(tris)(H$_2$O)]$_2$SO$_4$	$P\,\bar{1}$ (2)	6.213(2)	11.009(4)	11.248(1)	70.88(1)	72.87(2)	79.67(2)	691.8(3)	0.032
7 *cis*-[Cu(trisH$_{-1}$)(tris)(H$_2$O)]$_2$CrO$_4$	$P\,\bar{1}$ (2)	6.424(1)	10.735(1)	21.578(2)	98.60(1)	89.97(1)	72.63(1)	1402.5(3)	0.033
8 *trans*-[Cu(trisH$_{-1}$)$_2$]KF·3H$_2$O	*Pcca* (54)	18.814(2)	9.623(1)	8.678(2)	90.00	90.00	90.00	1571.2(4)	0.040
9 *trans*-[Cu(trisH$_{-1}$)$_2$]KBr·2H$_2$O	*Pcca* (54)	18.482(2)	9.805(1)	8.776(3)	90.00	90.00	90.00	1590.4(5)	0.036
10 *cis*-[Cu(trisH$_{-1}$)(tris)(H$_2$O)]F·H$_2$O$	$P\,\bar{1}$ (2)	6.498(9)	11.857(13)	19.50(3)	88.6(2)	83.3(2)	90.7(1)	1491.7	–
11 *cis*-[Cu(trisH$_{-1}$)(tris)(H$_2$O)]Cl·H$_2$O	$P\,\bar{1}$ (2)	6.482(2)	11.805(1)	19.767(3)	88.22(1)	83.67(2)	90.30(2)	1502.6(6)	0.035
– " – (Mazus *et al.*)[42]	$P\,\bar{1}$ (2)	19.785(0)	11.798(6)	6.489(3)	90.13(5)	96.39(5)	91.84(5)	1502	0.090¤
12 *cis*-[Cu(trisH$_{-1}$)(tris)(H$_2$O)]Br·H$_2$O	$P\,\bar{1}$ (2)	6.574(1)	11.929(2)	19.792(2)	88.09(1)	83.43(1)	89.72(1)	1541.1(4)	0.039
13 *cis*-[Cu(trisH$_{-1}$)(tris)(H$_2$O)]I·H$_2$O	$P\,\bar{1}$ (2)	6.677(1)	11.582(1)	11.838(3)	63.02(2)	100.09(2)	100.92(1)	796.9(3)	0.030
14 *trans*-{[Cu(tris)$_2$]F$_2$}$_n$	$P\,2_1/c$ (14)	5.903(1)	8.875(1)	12.148(1)	90.00	93.02(1)	90.00	635.5(1)	0.033
15 *cis*-[Cu(trisH$_{-1}$)(tris)]F	$P\,2_1/c$ (14)	5.830(1)	15.886(2)	13.884(1)	90.00	101.56(1)	90.00	1259.8(3)	0.038
16 *cis*-[Cu(trisH$_{-1}$)(tris)(H$_2$O)]$_2${SiF$_6$}	$P\,\bar{1}$ (2)	6.271(1)	10.799(1)	11.448(2)	104.38(1)	104.08(1)	94.04(1)	721.4(2)	0.028
17 *trans*-[Cu(tris)$_2$(NO$_3$)$_2$]	$P\,\bar{1}$ (2)	6.721(1)	9.673(1)	6.252(1)	90.86(1)	95.22(1)	72.79(1)	386.6(2)	0.042
18 *cis*-[Cu(tris)$_2$(SO$_4$)]$_n$	$P\,\bar{1}$ (2)	9.527(1)	11.414(1)	7.212(3)	95.81(2)	90.33(2)	70.85(1)	736.6(3)	0.028
19 [Cu$_8$(trisH$_{-2}$)$_4$(trisH$_{-1}$)$_2$(tris)$_2$]Br$_6$·6H$_2$O·EtOH	$P\,\bar{1}$ (2)	11.596(3)	12.835(3)	11.262(1)	100.95(1)	92.00(1)	85.85(2)	1641.0(6)	0.048
20 [Cu$_8$(trisH$_{-2}$)$_4$(trisH$_{-1}$)$_2$(tris)$_2$](ClO$_4$)$_6$·6H$_2$O·EtOH	$P\,\bar{1}$ (2)	13.285(1)	14.217(6)	10.930(1)	102.58(2)	97.98(1)	72.08(1)	1911.2(8)	0.053
21 *trans*-[Cu(trisH$_{-1}$)$_2$]NaClO$_4$·H$_2$O (Ivarsson)[40]	$C\,2/c$ (15)	14.2872(6)	10.9454(4)	11.1921(5)	90.00	96.290(3)	90.00	1739.6(6)	0.044
22 *cis*-{[Cu(trisH$_{-1}$)(tris)]Br}$_n$ (Masi *et al.*)[41]	$P\,2_1/c$ (14)	11.394(2)	10.049(2)	12.149(2)	90.00	95.83(2)	90.00	1383.8	0.062¤
23 [Cu(trisH$_{-1}$)Cl]$_4$ (Masi *et al.*)[41]	$P\,\bar{1}$ (2)	9.182(1)	9.120(2)	8.817(1)	88.95(1)	87.01(1)	84.13(1)	733.4	0.041¤

* Non-standard space group. # T = 23°C. ¤ Temperature unknown. $ Determined by X-ray powder diffraction.

APPENDIX VI TG (—) and DTG (---) curves of copper–tris complexes.[I–V]

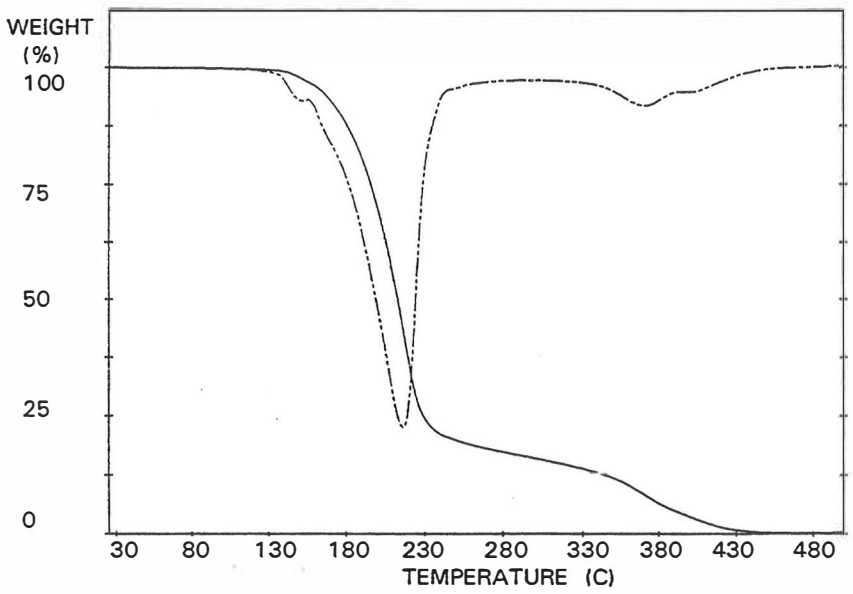

TG and DTG curves of tris in an air atmosphere.[I]

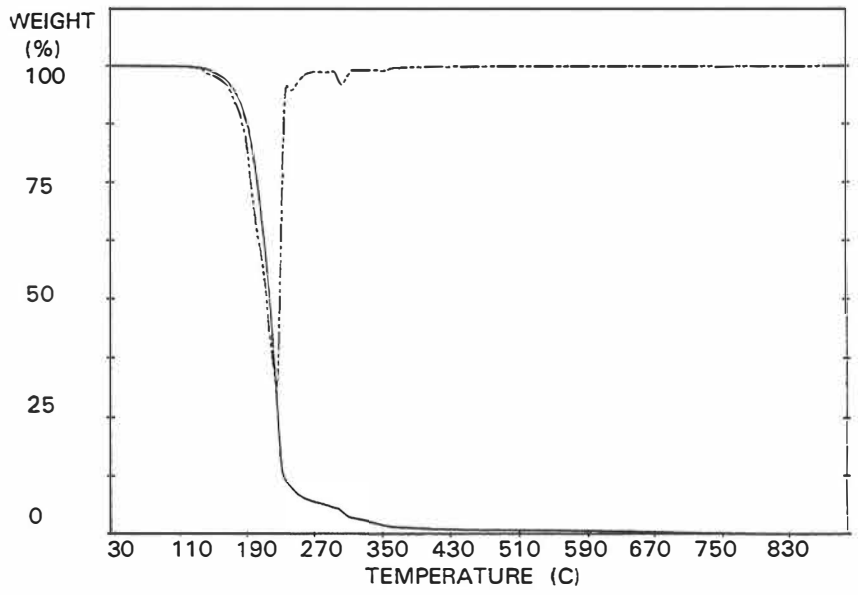

TG and DTG curves of tris in a nitrogen atmosphere.[I]

APPENDIX VI (continued)

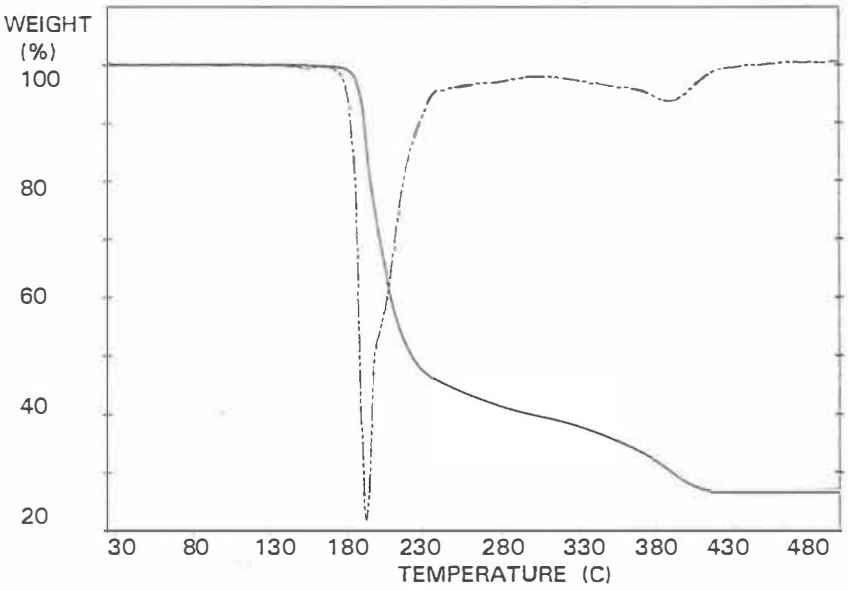

Fig. 1A TG and DTG curves of [Cu(trisH$_{-1}$)$_2$] (**1**) in an air atmosphere.[I]

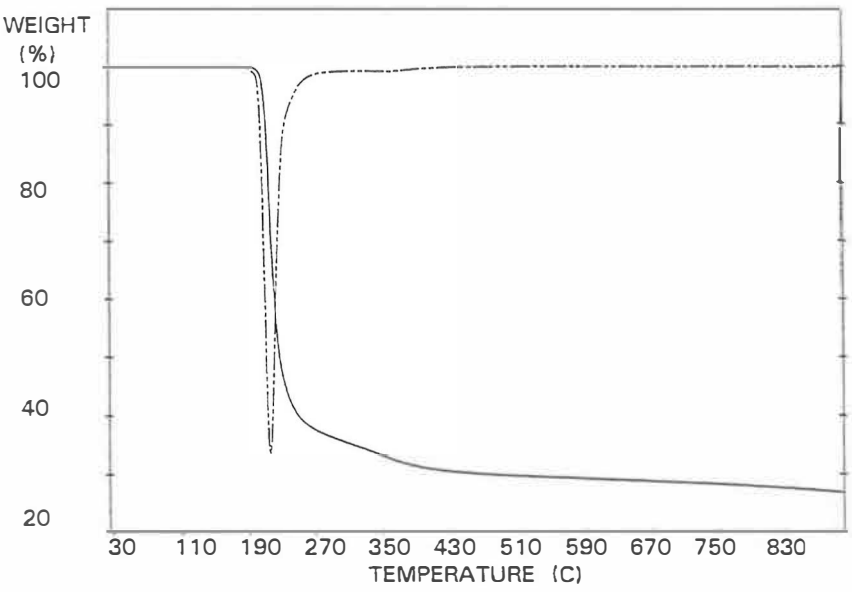

Fig. 1B TG and DTG curves of [Cu(trisH$_{-1}$)$_2$] (**1**) in a nitrogen atmosphere.[I]

APPENDIX VI (continued)

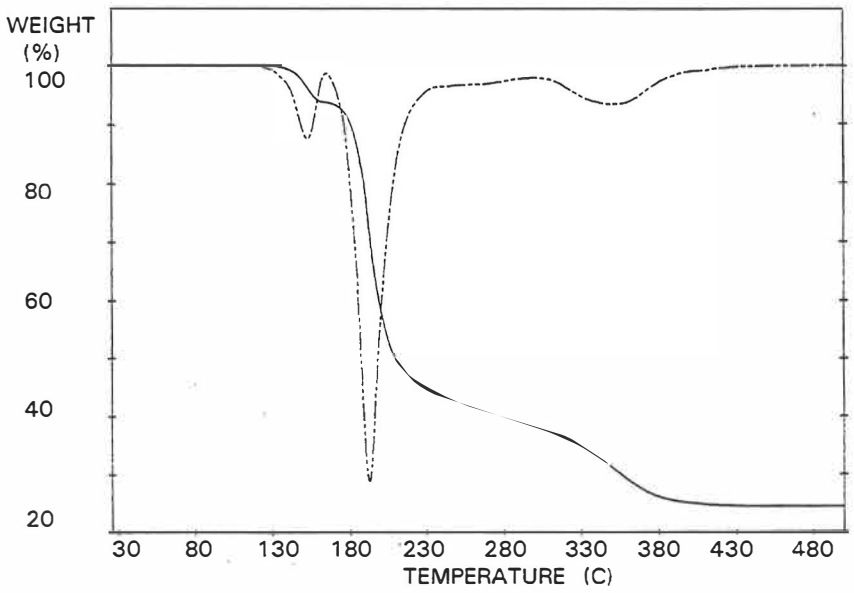

Fig. 2A TG and DTG curves of [Cu(trisH$_{-1}$)$_2$(H$_2$O)] (**2**) in an air atmosphere.[I]

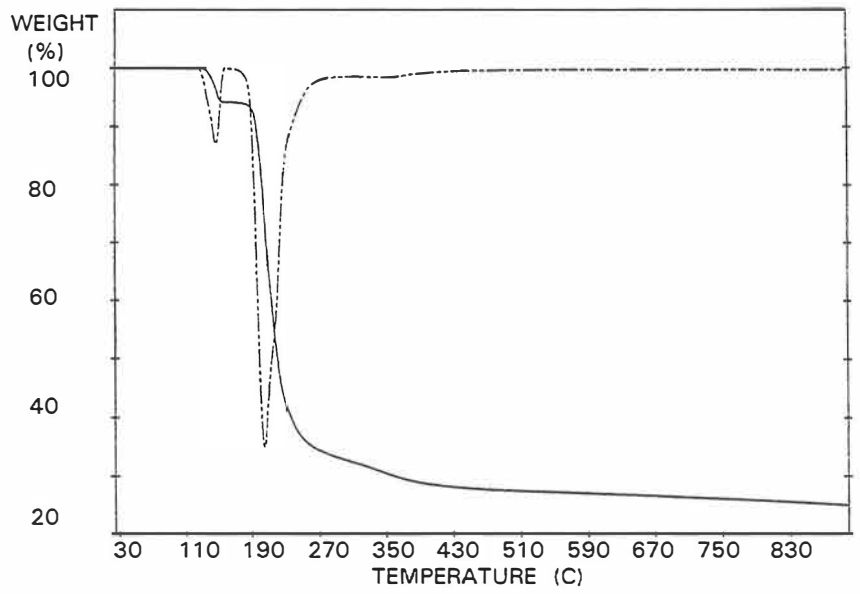

Fig. 2B TG and DTG curves of [Cu(trisH$_{-1}$)$_2$(H$_2$O)] (**2**) in a nitrogen atmosphere.[I]

APPENDIX VI (continued)

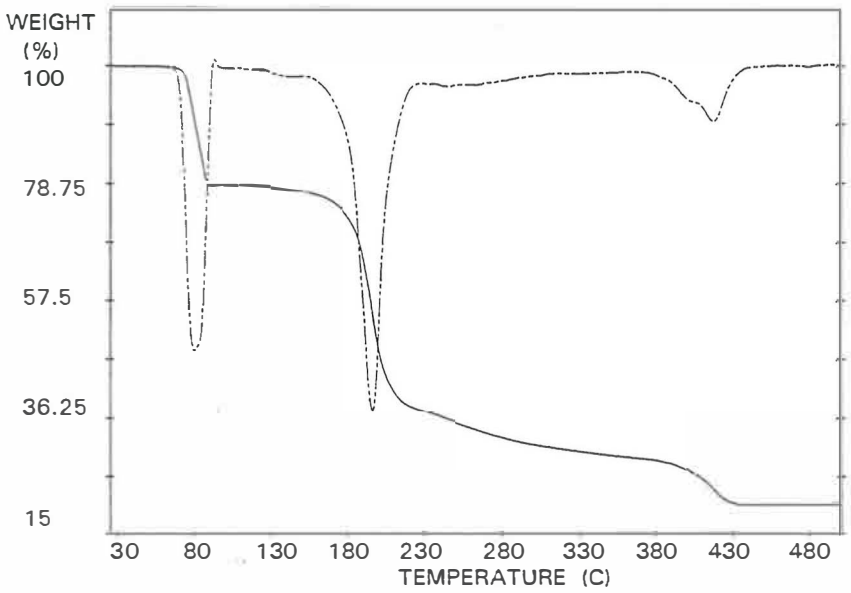

Fig. 3A TG and DTG curves of $[Cu(trisH_{-1})_2]\cdot 5H_2O$ (**3**) in an air atmosphere.[I]

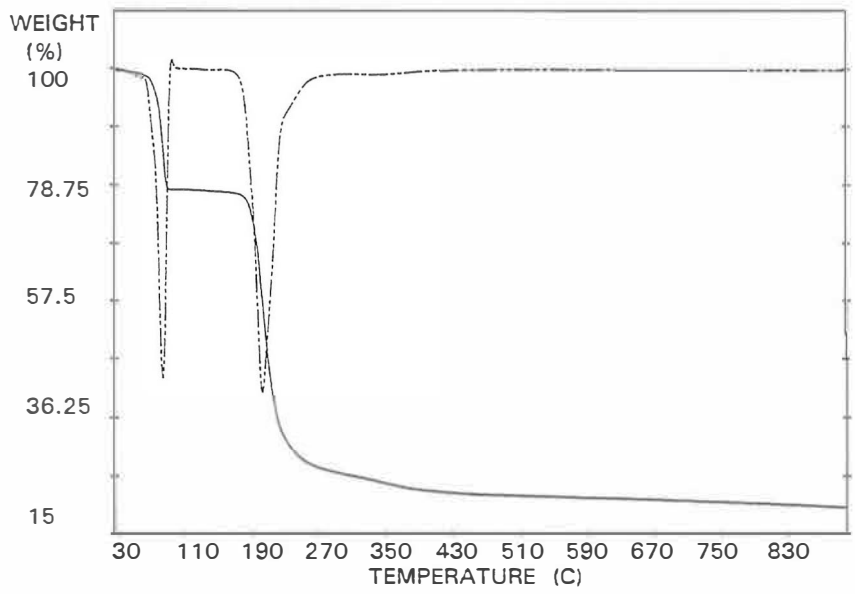

Fig. 3B TG and DTG curves of $[Cu(trisH_{-1})_2]\cdot 5H_2O$ (**3**) in a nitrogen atmosphere.[I]

APPENDIX VI (continued)

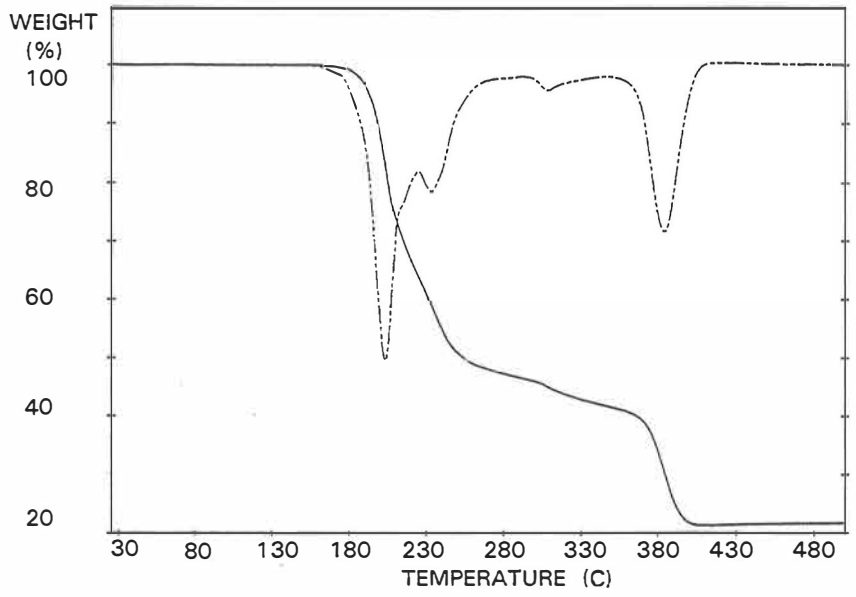

Fig. 4A TG and DTG curves of [Cu(trisH$_{-1}$)(tris)(NO_3)] (**4**) in an air atmosphere.[II]

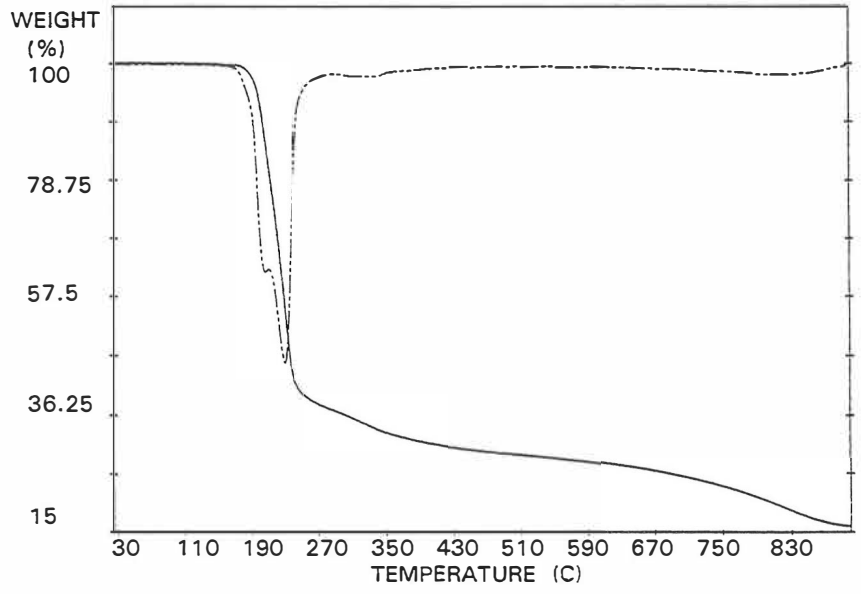

Fig. 4B TG and DTG curves of [Cu(trisH$_{-1}$)(tris)(NO_3)] (**4**) in a nitrogen atmosphere.[II]

APPENDIX VI (continued)

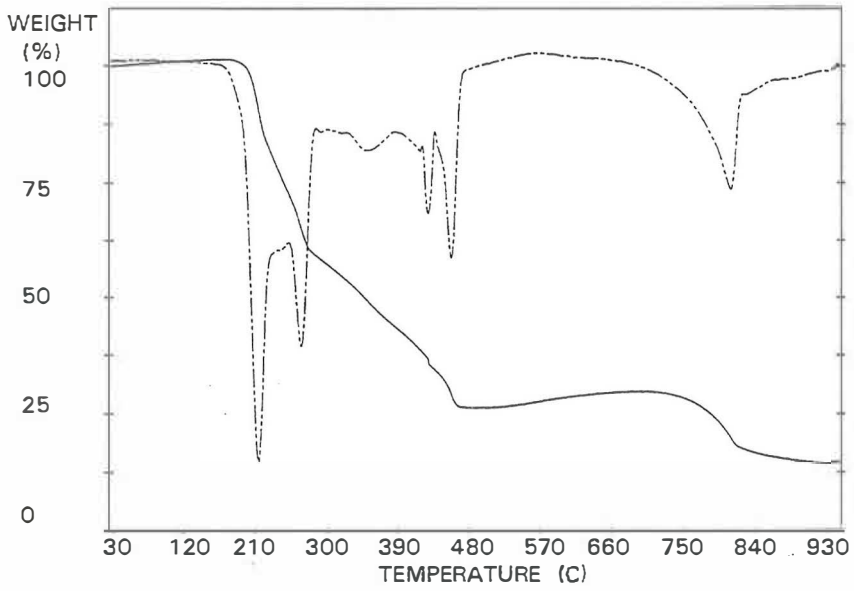

Fig. 5A TG and DTG curves of $[Cu(trisH_{-1})(tris)]Na(ClO_4)_2$ (5) in air.[II]

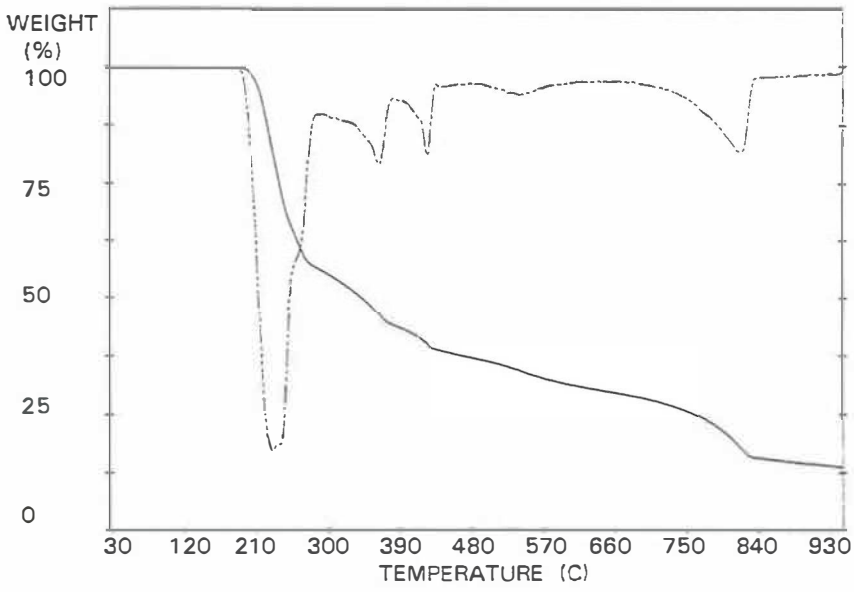

Fig. 5B TG and DTG curves of $[Cu(trisH_{-1})(tris)]Na(ClO_4)_2$ (5) in nitrogen.[II]

APPENDIX VI (continued)

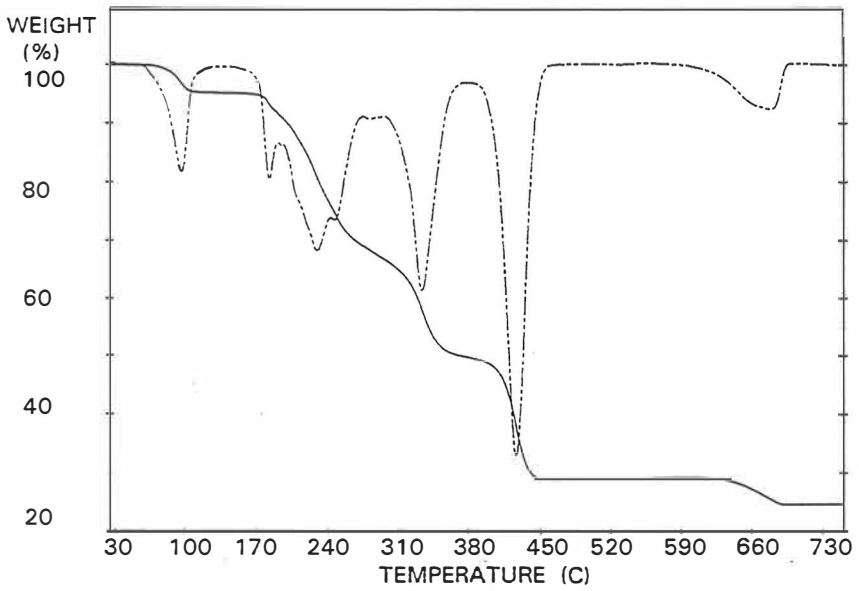

Fig. 6A TG and DTG curves of $[Cu(trisH_{-1})(tris)(H_2O)]_2SO_4$ (6) in air.[III]

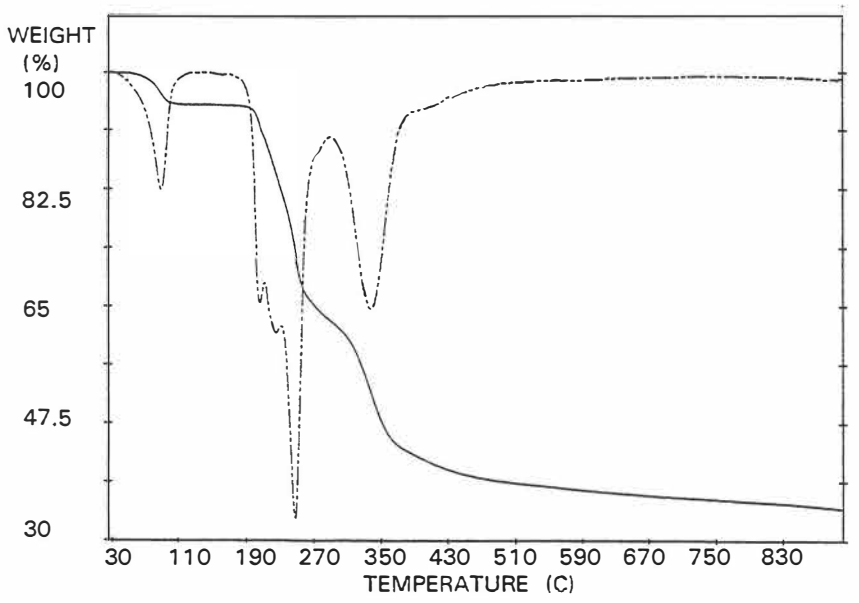

Fig. 6B TG and DTG curves of $[Cu(trisH_{-1})(tris)(H_2O)]_2SO_4$ (6) in nitrogen.[III]

APPENDIX VI (continued)

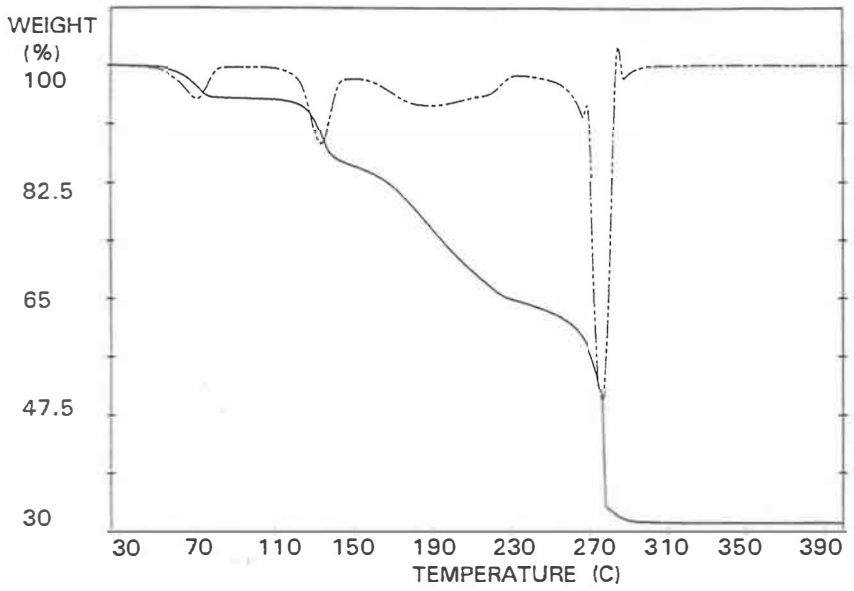

Fig. 7A TG and DTG curves of $[Cu(trisH_{-1})(tris)(H_2O)]_2CrO_4$ (7) in air.[III]

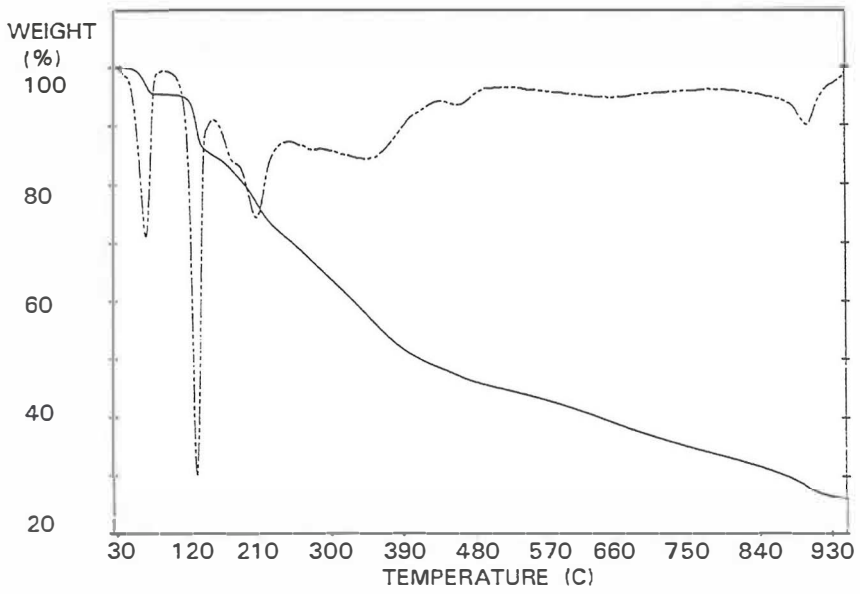

Fig. 7B TG and DTG curves of $[Cu(trisH_{-1})(tris)(H_2O)]_2CrO_4$ (7) in nitrogen.[III]

APPENDIX VI (continued)

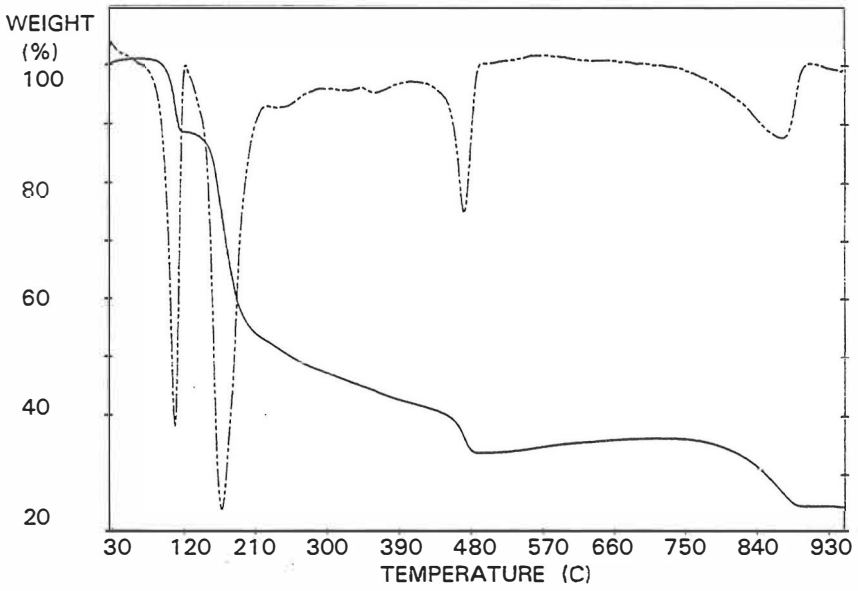

Fig. 8A TG and DTG curves of $[Cu(trisH_{-1})_2]KF{\cdot}3H_2O$ (**8**) in air.[IV]

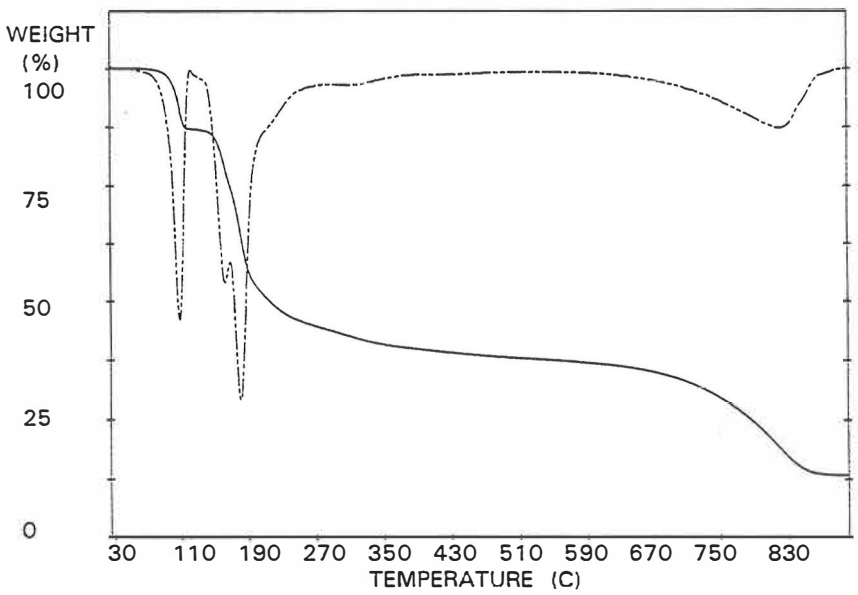

Fig. 8B TG and DTG curves of $[Cu(trisH_{-1})_2]KF{\cdot}3H_2O$ (**8**) in nitrogen.[IV]

APPENDIX VI (continued)

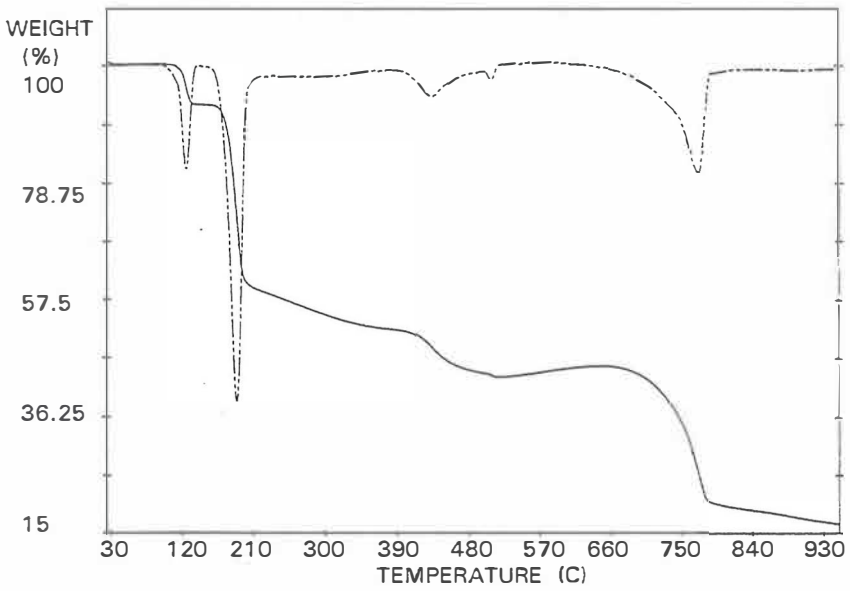

Fig. 9A TG and DTG curves of $[Cu(trisH_{-1})_2]KBr{\cdot}2H_2O$ (9) in air.[IV]

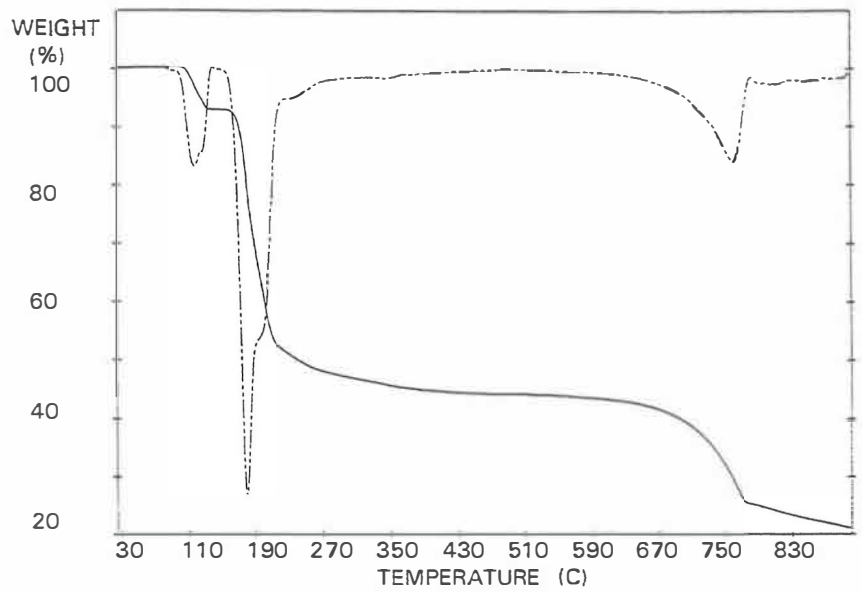

Fig. 9B TG and DTG curves of $[Cu(trisH_{-1})_2]KBr{\cdot}2H_2O$ (9) in nitrogen.[IV]

APPENDIX VI (continued)

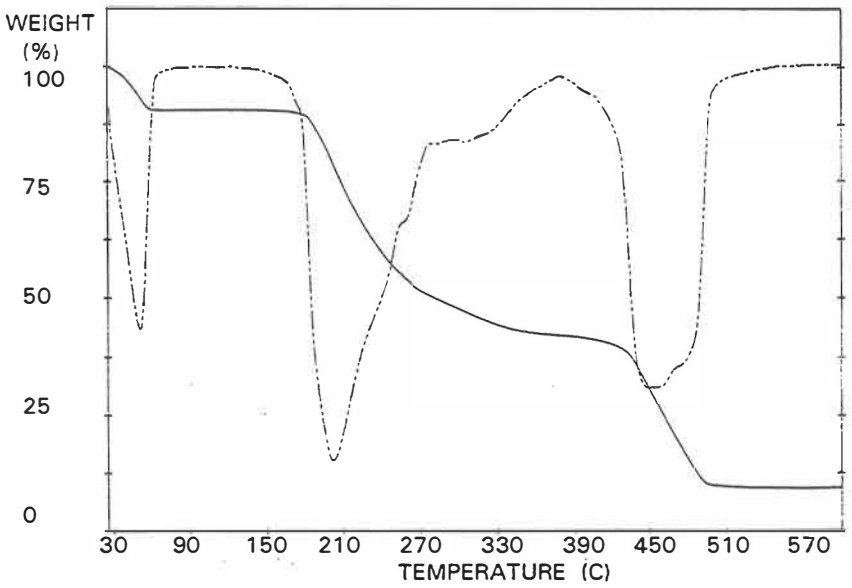

Fig. 10A TG and DTG curves of [Cu(trisH$_{-1}$)(tris)(H$_2$O)]F·H$_2$O (**10**) in air.[V]

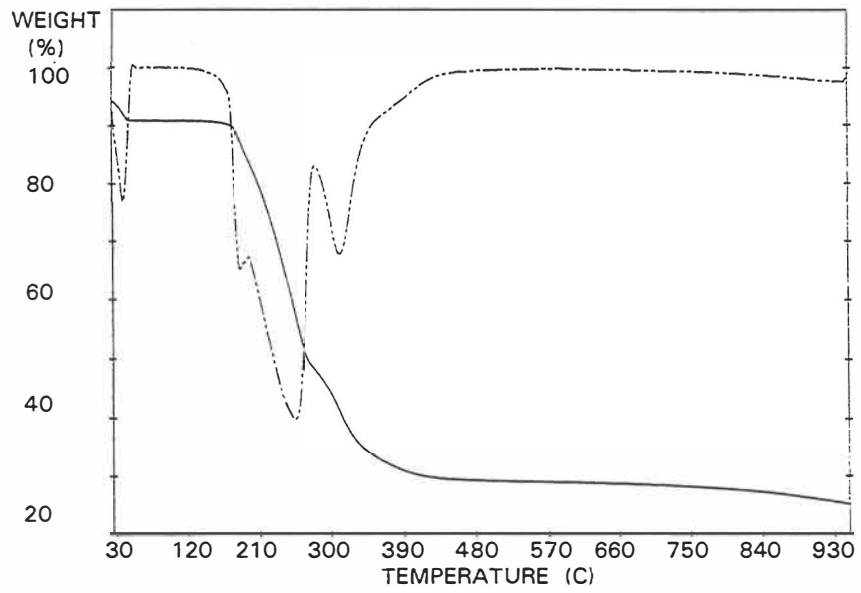

Fig. 10B TG and DTG curves of [Cu(trisH$_{-1}$)(tris)(H$_2$O)]F·H$_2$O (**10**) in nitrogen.[V]

APPENDIX VI (continued)

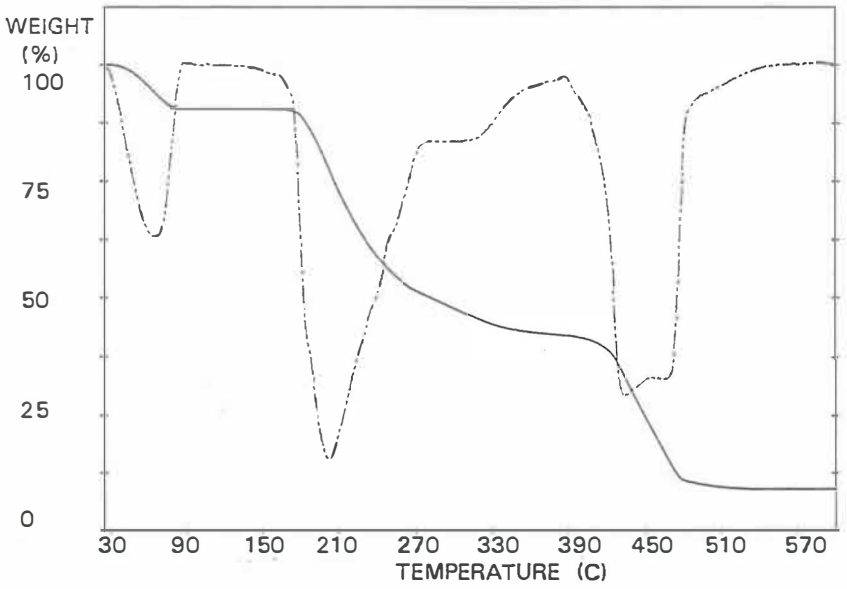

Fig. 11A TG and DTG curves of [Cu(trisH$_{-1}$)(tris)(H$_2$O)]Cl·H$_2$O (**11**) in air.[V]

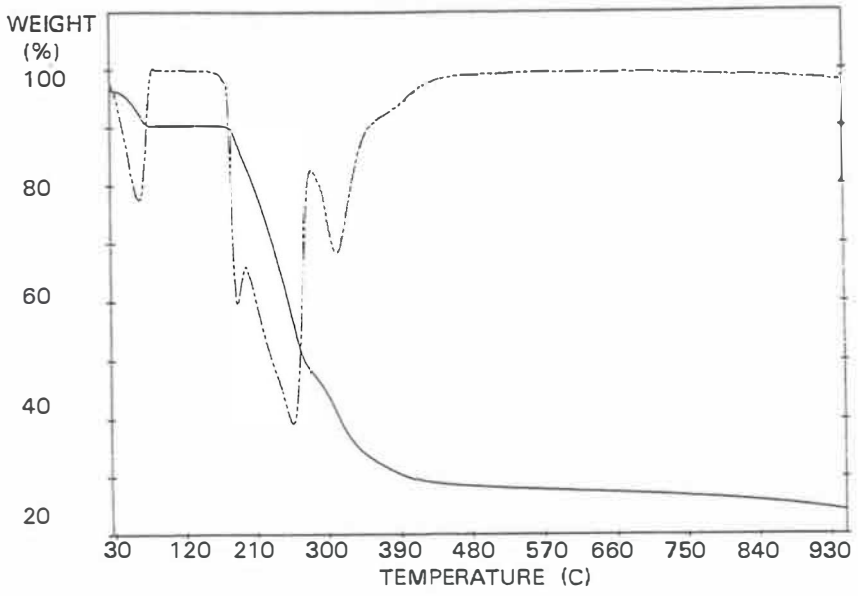

Fig. 11B TG and DTG curves of [Cu(trisH$_{-1}$)(tris)(H$_2$O)]Cl·H$_2$O (**11**) in nitrogen.[V]

APPENDIX VI (continued)

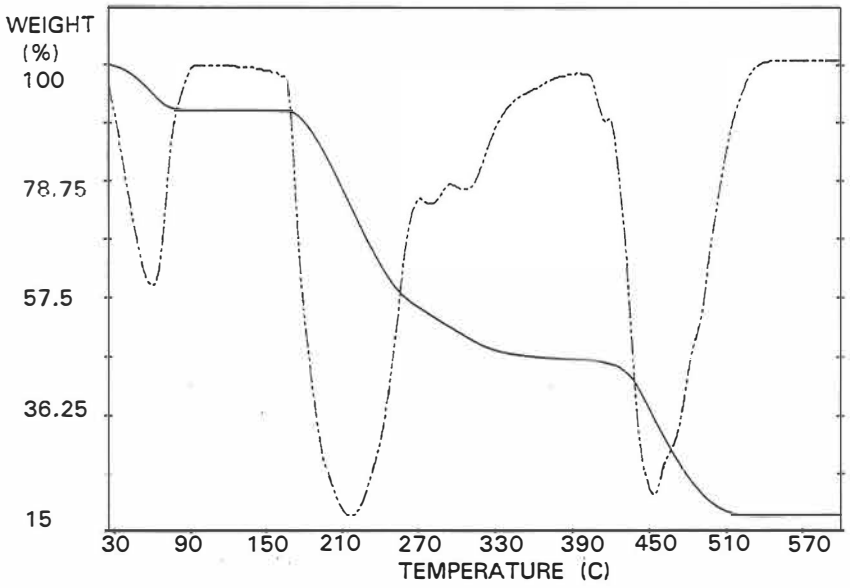

Fig. 12A TG and DTG curves of [Cu(trisH$_{-1}$)(tris)(H$_2$O)]Br·H$_2$O (**12**) in air.[V]

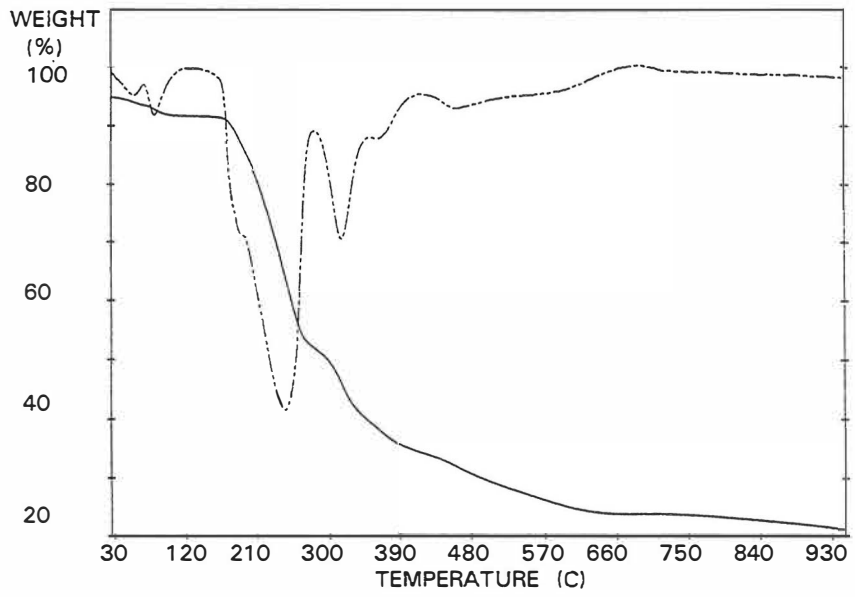

Fig. 12B TG and DTG curves of [Cu(trisH$_{-1}$)(tris)(H$_2$O)]Br·H$_2$O (**12**) in nitrogen.[V]

APPENDIX VI (continued)

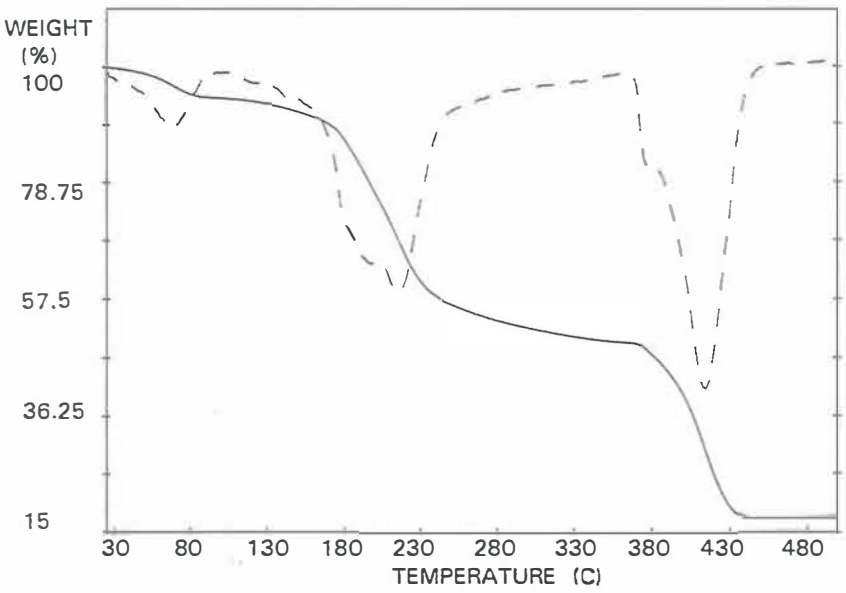

Fig. 13A TG and DTG curves of $[Cu(trisH_{-1})(tris)(H_2O)]I \cdot H_2O$ **(13)** in air.[V]

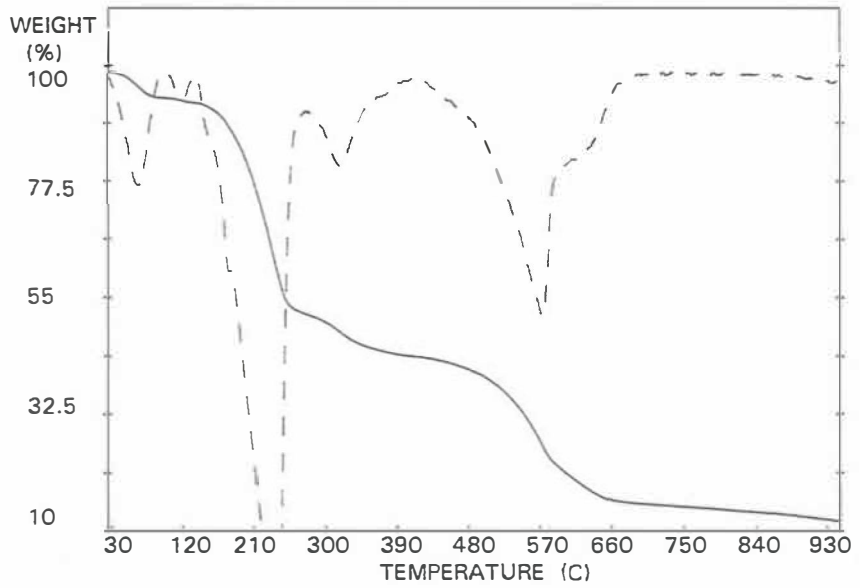

Fig. 13B TG and DTG curves of $[Cu(trisH_{-1})(tris)(H_2O)]I \cdot H_2O$ **(13)** in nitrogen.[V]

Erratum

Paper I

Page	line	is:	should be:
956	Reference 3.	*J. Inorg. Nucl. Chem. Lett.*	*Inorg. Nucl. Chem. Lett.*

Paper II

Page	line	is:	should be:
964	17	crystallographic ($\bar{1}01$) plane	crystallographic (110) plane
964	Reference 2.	*J. Inorg. Nucl. Chem. Lett.*	*Inorg. Nucl. Chem. Lett.*

Paper III

Page	line	is:	should be:
200	Abstract, line 6	$V =$ 691.76(3) Å^3	$V =$ 691.8(3) Å^3
202	Table 2, line 15 (V/Å^3)	691.76(3)	691.8(3)
202	Table 2, line 24 (Scan method)	ω/θ	$\omega/2\theta$
203	Table 3, x-coordinate of C121	0.279(6)	0.2779(6)
208	Reference 3.	*J. Inorg. Nucl. Chem. Lett.*	*Inorg. Nucl. Chem. Lett.*

Paper IV

Page	line	is:	should be:
312	Title, line 4	Fuoride	Fluoride
315	Table 4, heading	equivalant	equivalent

Paper V (proof)

Page	line	is:	should be:
3	Table 1, heading	[Cu(trisH$_{-1}$)(H$_2$O)]I·H$_2$O	[Cu(trisH$_{-1}$)(tris)(H$_2$O)]I·H$_2$O
5	Table 3, heading	[Cu(trisH$_{-1}$)(tris)(H$_2$O]Br·H$_2$O	[Cu(trisH$_{-1}$)(tris)(H$_2$O)]Br·H$_2$O
5	Table 3, line 19	cm$_{-1}$	cm^{-1}
6	Table 4, footnote	$B_{eq} = \frac{4}{3}\Sigma_{ij}\Sigma_j\beta_{ij}\mathbf{a}_i\cdot\mathbf{a}_j$	$B_{eq} = \frac{4}{3}\Sigma_i\Sigma_j\beta_{ij}\mathbf{a}_i\cdot\mathbf{a}_j$
8	Table 7, heading	[Cu(trisH$_{-1}$)(tris)(H$_2$O)](Cl·H$_2$O	[Cu(trisH$_{-1}$)(tris)(H$_2$O)]Cl·H$_2$O

PAPER I

(Reprinted by the permission of *Acta Chemica Scandinavica*)

https://eurekamag.com/research/074/612/074612489.php

Acta Chemica Scandinavica, 1993: 47: 950–956
Printed in Belgium – all rights reserved

ACTA
CHEMICA SCANDINAVICA
ISSN 0904–213X

Copper(II) Complexes of 2-Amino-2-hydroxymethyl-1,3-propanediol. Part 1. Synthesis, Structure and Thermal Behavior of Three *trans*-Bis[2-amino-2-hydroxymethyl-1,3-propanediolato-(1-)-*O*,*N*]copper(II) Complexes, $[Cu(C_4H_{10}NO_3)_2]$, $[Cu(C_4H_{10}NO_3)_2(H_2O)]$ and $[Cu(C_4H_{10}NO_3)_2]\cdot 5H_2O$

Sirpa Kotila* and Jussi Valkonen

Department of Chemistry, University of Jyväskylä, SF-40500 Jyväskylä, Finland

Kotila, S. and Valkonen, J., 1993. Copper(II) Complexes of 2-Amino-2-hydroxymethyl-1,3-propanediol. Part 1. Synthesis, Structure and Thermal Behavior of Three *trans*-Bis[2-amino-2-hydroxymethyl-1,3-propanediolato-(1-)-*O*,*N*]-copper(II) Complexes, $[Cu(C_4H_{10}NO_3)_2]$, $[Cu(C_4H_{10}NO_3)_2(H_2O)]$ and $[Cu(C_4H_{10}NO_3)_2]\cdot 5H_2O$. – Acta Chem. Scand. 47: 950–956.

The crystal and molecular structures of non-hydrate, monohydrate and pentahydrate of copper(II) complexes with 2-amino-2-hydroxymethyl-1,3-propanediol (=tris, deprotonated form abbreviated $trisH_{-1}$) as ligand have been determined from single-crystal X-ray data to the final *R*-values 0.023, 0.026 and 0.026 for the non-hydrate, monohydrate and pentahydrate compounds, respectively.

All three compounds are monoclinic. The non-hydrous violet compound crystallizes in the space group $P2_1/c$ with two molecules in a cell of dimensions $a = 6.261(1)$, $b = 10.109(1)$, $c = 10.028(1)$ Å, $\beta = 116.86(1)°$, $V = 566.3(1)$ Å^3. The space group and cell dimensions of the blue monohydrate are $C2/c$, $a = 12.928(3)$, $b = 10.783(1)$, $c = 10.066(5)$ Å, $\beta = 116.59(2)°$, $V = 1254.8(7)$ Å^3, $Z = 4$. The pentahydrate forms violet crystals with the space group $P2/c$ and the cell dimensions of $a = 10.087(2)$, $b = 6.340(3)$, $c = 15.557(1)$ Å, $\beta = 124.36(1)°$, $V = 821.2(5)$ Å^3, $Z = 2$.

The complexes are mononuclear with two tris ligands coordinated via amino and deprotonated hydroxy groups. The non-hydrate and pentahydrate molecules are centrosymmetric and have a square-planar four-coordination sphere, whereas the monohydrate has a square-pyramidal structure with oxygen from the water molecule as the fifth ligand. All the complexes have a *trans* coordination of oxygen and nitrogen around the copper(II) ion. The structures consist of neutral complexes linked together by extensive hydrogen bonding.

Thermal behavior of the complexes has been studied with TG in air and nitrogen atmospheres.

2-Amino-2-hydroxymethyl-1,3-propanediol (=tris) is a widely used buffer in biochemical or seawater studies, because its pH region 7–9 covers the physiological pH range.[1] Tris is also known as tris(hydroxymethyl)aminomethane (=tham) or Trizma.

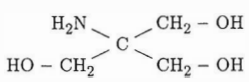

Tris contains a basic amino group and three hydroxy groups, which are all potential binding sites to form chelates with metal ions. As a ligand, tris forms complexes with transition metals primarily via the amino group and one of the hydroxymethyl OH groups.

In addition to the normal coordination bond of the OH group, it is known that hydroxy groups may lose a proton and form covalent bonds with metallic ions.[2,3] All three compounds in this paper contain the latter type of hydroxy bond and these deprotonated species are abbreviated $trisH_{-1}$.

In spite of the fact that the solution chemistry of tris is quite well known,[4–8] only few structural determinations of metal–tris complexes have been published. The crystal structure of the ligand itself has been determined at several temperatures and it has been found to have an orientationally disordered (plastic) crystalline phase just below the melting point.[9] The known struc-

* To whom correspondence should be addressed.

tures of metal–tris complexes involving copper(II) are $[Cu(trisH_{-1})_2]NaClO_4 \cdot H_2O$,[10] $[Cu(trisH_{-1})Cl]_4$,[11] $[Cu(trisH_{-1})(tris)]_2Br_2$,[11] and $[Cu(trisH_{-1})_2(H_2O)]$.[12] Thermoanalytical studies were not considered in any of these articles.

Experimental

Reagents. All the starting materials were Merck analytical grade reagents (unless otherwise indicated) and they were used without further purification.

Preparation of $[Cu(trisH_{-1})_2]$. 0.015 mol of tris was dissolved in 50 cm^3 of ethanol by refluxing. 0.0075 mol of $CuBr_2$ (B. D. H. Ltd., minimum 98%) was dissolved in 40 cm^3 of ethanol and added to the hot tris solution. The mixture was refluxed for 15 min, allowed to cool down to room temperature, and then an ethanolic solution of KOH (0.015 mol per 40 cm^3 EtOH) was added. The color of the solution turned blue, and blue precipitation appeared. The solution was filtered, precipitation discarded and the clear solution was allowed to stand at room temperature overnight. The dark violet crystals were filtered, washed with ethanol and dried in air.

Preparation of $[Cu(trisH_{-1})_2(H_2O)]$. Single crystals of the monohydrate could best be obtained from a water synthesis of tris and $CuCl_2 \cdot 2H_2O$. 0.04 mol of tris and 0.01 mol of $CuCl_2 \cdot 2H_2O$ were dissolved in a minimum amount of water in separate beakers. The solutions were combined, heated for 15–30 min and then filtered. The blue prismatic crystals were formed by slow evaporation at room temperature. The crystallization of the complex may take a few weeks.

Preparation of $[Cu(trisH_{-1})_2] \cdot 5H_2O$. The best results were obtained when $CuSO_4$ or $Cu(CH_3COOH)_2$ was used as starting materials. 0.04 mol of tris and 0.01 mol of $CuSO_4 \cdot 5H_2O$ were dissolved in a minimum amount of water in separate beakers. The solutions were combined and filtered. Crystallization usually takes place within half an hour, but if the solution needs a longer period of time to crystallize, it is preferable to store it at the temperature of 15–20°C. The pentahydrate crystals are plate-shaped and their violet color is anisotropic; the crystal looks blue–violet from two directions and from the third direction the color is more reddish.

Thermal analysis. The thermal behavior of the complexes was determined with a Perkin-Elmer TGA7 thermobalance in air and nitrogen atmospheres. Sample size varied between 7.0 ± 0.5 mg, heating rate was 2°C min^{-1} and gas flow was 50 cm^3 min^{-1}. The temperature range in air was from 25 to 500°C, and in a nitrogen atmosphere the samples were heated up to 900°C. When analyzing the samples in a nitrogen atmosphere, the oven was flushed with nitrogen for 30–45 min before the run was started to remove oxygen from the equipment. The observed weight losses were calculated for each compound in both atmospheres. The results are reported in Table 1.

X-Ray structure measurements. The single-crystal X-ray measurements were done with an Enraf-Nonius CAD-4 diffractometer using Mo K_α radiation. A summary of X-ray data collection parameters and structural refinement is given in Table 2. For all three cases the unit-cell dimensions and the orientation matrix were obtained from a least-squares fitting of 25 centered reflections. During data collection, an intensity check was made every 60 min with two reflections; the orientation matrix was also controlled after every 400–500 reflections. No significant decay in intensity was observed during data collection. The intensities were corrected for Lorentz and polarization effects.

The diffraction data of the pentahydrate were collected using a unit cell with the space group $P2/n$ [$a = 10.087(2)$, $b = 6.340(3)$, $c = 12.907(2)$ Å, $\beta = 95.80(1)°$] but, since the standard choice of the glide direction is c, the unit cell was changed before refinement.

Table 1. Thermal decomposition of tris, $[Cu(trisH_{-1})_2]$ (**1**), $[Cu(trisH_{-1})_2(H_2O)]$ (**2**) and $[Cu(trisH_{-1})_2] \cdot 5H_2O$ (**3**).

		Air atmosphere			Nitrogen atmosphere		
			Weight loss/%			Weight loss/%	
Compound	Lost in reaction	T/°C	Δ Obs.	Δ Theor.	T/°C	Δ Obs.	Δ Theor.
tris	tris	25–450	99.7	100.0	25–900	100.0	100.0
1	2 $trisH_{-1}$	168–450	73.5	73.8	178–450	69.8	79.1
	Total reaction	25–450	73.7	73.8	25–900	73.2	79.1
2	H_2O	120–165	6.4	5.6	123–163	5.9	5.6
	2 $trisH_{-1}$	165–430	69.3	69.7	168–450	66.2	74.7
	Total reaction	25–430	75.6	75.3	25–900	75.1	80.3
3	5 H_2O	63–99	21.3	22.9	37–110	21.8	22.9
	2 $trisH_{-1}$	117–450	58.2	56.9	162–450	55.1	61.0
	Total reaction	25–450	79.7	79.8	25–900	79.8	83.9

Table 2. Crystallographic experimental data for [Cu(trisH$_{-1}$)$_2$] (**1**), [Cu(trisH$_{-1}$)$_2$(H$_2$O)] (**2**) and [Cu(trisH$_{-1}$)$_2$]·5H$_2$O (**3**).

Compound	**1**	**2**	**3**
Unit cell determination:			
Formula	$CuO_6N_2C_8H_{20}$	$CuO_7N_2C_8H_{22}$	$CuO_{11}N_2C_8H_{30}$
Formula weight/g mol^{-1}	303.80	321.81	393.88
Color	Violet	Blue	Violet
Crystal size/mm	0.40 × 0.20 × 0.20	0.20 × 0.20 × 0.15	0.15 × 0.15 × 0.15
T/°C	21 ± 1	21 ± 1	21 ± 1
Reflections for lattice measurement	25	25	25
θ-Range for lattice measurement/°	6–13	7–14	7–14
a/Å	6.261(1)	12.928(3)	10.087(2)
b/Å	10.109(1)	10.783(1)	6.340(3)
c/Å	10.028(1)	10.066(5)	15.557(1)
β/°	116.86(1)	116.59(2)	124.36(1)
V/Å^3	566.3(1)	1254.8(7)	821.2(5)
Z	2	4	2
d_{calc}/g cm^{-3}	1.78	1.70	1.59
λ(Mo K_α)/Å	0.710 73	0.710 73	0.710 73
μ(Mo K_α)/cm^{-1}	19.51	17.71	13.84
F(000)	318	676	418
Space group	$P2_1/c$	$C2/c$	$P2/c$
Data collection and refinement:			
θ range for data collection/°	2–35	2–35	2–30
Scan method	ω/2θ	ω/2θ	ω/2θ
Scan speed in ω/° min^{-1}	0.87–5.50	0.79–16.50	0.79–16.50
Scan width in ω/°	0.80 + 0.34 tan θ	0.50 + 0.34 tan θ	0.50 + 0.34 tan θ
No. of measured refls.	2601	2880	2588
Reflections used in refinement, $I > 3\sigma(I)$	2029	1841	1759
Absorption correction (min./max.)	0.85/1.09	0.90/1.07	0.92/1.12
Max. shift/error	0.00	0.00	0.00
Max. in final Δp/e Å^{-3}	0.39	0.43	0.28
No. of parameters refined	79	83	102
R	0.023	0.026	0.026
R_w[a]	0.027	0.029	0.032
$S = [\Sigma w(F_o - F_c)^2/(n-m)]^{1/2}$	0.502	1.156	0.713

[a] $w = 1/\sigma^2(F_o)$.

The initial position of the copper atom was solved by direct methods (SHELXS-86),[13] and the remaining non-hydrogen atoms were found by alternating the least-squares full-matrix cycles of refinement and difference syntheses. The model was first refined with isotropic temperature factors to convergence, then the calculated hydrogens were placed in the model and refined as riding atoms with fixed isotropic parameters (B = 5.00 Å^2). After the absorption correction with the DIFABS program[14] the model was refined again with isotropic thermal parameters. Finally, after the anisotropic refinement, the missing hydrogens were located from a difference

Table 3. Atomic positional parameters and equivalent isotropic temperature factors[a] with e.s.d.s in parentheses for [Cu(trisH$_{-1}$)$_2$] (**1**).

Atom	x	y	z	B_{eq}/Å^2
Cu100	0.000	0.000	0.000	1.192(3)
O111	−0.0047(2)	−0.0376(1)	0.1885(1)	1.44(2)
O112	0.2967(2)	−0.3555(1)	0.3106(1)	1.62(2)
O113	0.7657(2)	−0.2241(1)	0.2843(1)	2.55(2)
N111	0.3350(2)	−0.0673(1)	0.0988(1)	1.21(2)
C111	0.2318(2)	−0.0616(1)	0.3009(1)	1.35(2)
C112	0.3694(2)	−0.1412(1)	0.2352(1)	1.03(2)
C113	0.2585(2)	−0.2777(1)	0.1841(1)	1.31(2)
C114	0.6351(2)	−0.1537(2)	0.3460(2)	1.53(2)

[a] $B_{eq} = \frac{4}{3}\Sigma_i\Sigma_j\beta_{ij}\mathbf{a}_i\cdot\mathbf{a}_j$.

Table 4. Atomic positional parameters and equivalent isotropic temperature factors[a] with e.s.d.s in parentheses for [Cu(trisH$_{-1}$)$_2$(H$_2$O)] (**2**).

Atom	x	y	z	B_{eq}/Å^2
Cu100	0.000	0.26885(3)	0.250	1.211(4)
OW100	0.000	0.0649(2)	0.250	3.27(4)
O111	0.00643(9)	0.2822(1)	0.4468(1)	1.50(2)
O112	−0.1696(1)	0.5617(1)	0.4090(1)	2.24(2)
O113	−0.3919(1)	0.4054(1)	0.1391(1)	2.14(3)
N111	−0.1724(1)	0.2974(1)	0.1760(1)	1.37(2)
C111	−0.1051(1)	0.2923(2)	0.4398(2)	1.58(3)
C112	−0.1880(1)	0.3589(2)	0.2976(2)	1.26(2)
C113	−0.1545(1)	0.4947(2)	0.2976(2)	1.69(3)
C114	−0.3128(1)	0.3487(2)	0.2743(2)	1.67(3)

[a] See Table 3.

Table 5. Atomic positional parameters and equivalent isotropic temperature factors[a] with e.s.d.s in parentheses for $[Cu(trisH_{-1})_2]\cdot 5H_2O$ (**3**).

Atom	*x*	*y*	*z*	B_{eq}/Å²
Cu100	0.000	0.000	0.000	1.651(6)
OW1	0.000	−0.8208(4)	−0.250	2.56(5)
OW2	−0.2862(2)	−0.6467(3)	−0.3073(1)	3.72(5)
OW3	−0.3052(2)	−0.2437(3)	−0.2490(1)	2.90(4)
O111	0.0119(1)	0.0935(3)	0.12221(9)	1.83(3)
O112	−0.4792(2)	0.0778(3)	−0.1265(1)	3.23(4)
O113	−0.2035(2)	0.6389(3)	−0.0480(1)	2.86(4)
N111	−0.1781(2)	0.2063(3)	−0.0764(1)	2.10(4)
C111	−0.0827(2)	0.2746(4)	0.1023(1)	1.93(4)
C112	−0.2323(2)	0.2760(3)	−0.0102(1)	1.55(4)
C113	−0.3533(2)	0.1168(4)	−0.0207(2)	2.35(5)
C114	−0.3067(2)	0.4958(4)	−0.0417(1)	2.18(4)

[a] See Table 3.

Table 6. Bond distances (Å) with e.s.d.s in parentheses for $[Cu(trisH_{-1})_2]$ (**1**), $[Cu(trisH_{-1})_2(H_2O)]$ (**2**) and $[Cu(trisH_{-1})_2]\cdot 5H_2O$ (**3**).

Bond distance/Å	1	2	3
Cu100–O111	1.941(1)	1.950(1)	1.929(2)
Cu100–OW100	—	2.200(2)	—
Cu100–N111	1.991(1)	2.032(1)	1.985(2)
O111–C111	1.419(1)	1.416(2)	1.411(3)
O112–C113	1.417(2)	1.419(2)	1.423(2)
O113–C114	1.420(2)	1.423(2)	1.425(3)
N111–C112	1.486(2)	1.483(2)	1.480(3)
C111–C112	1.529(2)	1.530(2)	1.536(2)
C112–C113	1.526(2)	1.527(2)	1.520(3)
C112–C114	1.532(1)	1.527(2)	1.527(3)

Table 7. Bond angles (°) with e.s.d.s in parentheses for $[Cu(trisH_{-1})_2]$ (**1**), $[Cu(trisH_{-1})_2(H_2O)]$ (**2**) and $[Cu(trisH_{-1})_2]\cdot 5H_2O$ (**3**).

Angle/°	1	2	3
O111–Cu100–O111[a]	180.0(0)	171.54(6)	180.0(0)
O111–Cu100–OW100	—	94.23(4)	—
O111–Cu100–N111	85.67(4)	84.40(5)	85.39(7)
O111–Cu100–N111[a]	94.33(4)	94.32(5)	94.61(7)
N111–Cu100–OW100	—	98.70(4)	—
N111–Cu100–N111[a]	180.0(0)	162.60(6)	180.0(0)
Cu100–O111–C111	109.73(9)	112.09(8)	112.1(1)
Cu100–N111–C112	108.17(9)	107.30(8)	110.2(1)
O111–C111–C112	109.7(1)	110.7(1)	111.3(2)
O112–C113–C112	109.51(9)	110.4(2)	112.2(2)
O113–C114–C112	112.1(1)	111.9(2)	110.9(2)
N111–C112–C111	104.9(1)	105.4(1)	106.3(2)
N111–C112–C113	106.90(9)	106.6(1)	108.4(2)
N111–C112–C114	111.6(1)	111.5(1)	110.9(2)
C111–C112–C113	111.2(1)	111.7(1)	109.4(2)
C111–C112–C114	111.7(1)	111.1(1)	111.1(2)
C113–C112–C114	110.4(1)	110.4(1)	110.6(2)

[a] Symmetry operation applied is $-x, -y, -z$ for **1** and **3**, and $-x, y, \frac{1}{2}-z$ for **2**.

Fourier map and refined isotropically with fixed thermal parameters. The final R (R_w) values for the non-hydrate, monohydrate and pentahydrate were 0.023 (0.027), 0.026 (0.029) and 0.026 (0.032), respectively.

The calculations were all performed on a MicroVAX 3100 computer using the MolEN[15] structure determination program. The scattering factors and real and imaginary dispersion corrections for atomic scattering factors were taken from Ref. 16. The figures were drawn using the SCHAKAL[17] program. The final positional parameters for the structures are given in Tables 3–5, and the selected bond distances and angles are listed in Tables 6 and 7. Tables of anisotropic thermal parameters, coordinates of hydrogen atoms and listings of observed and calculated structure factors are available from the authors on request.

Results and discussion

Syntheses. The syntheses given in the Experimental section are only examples of possible reactions, because the title compound crystallizes with varying amount of crystalline water from a number of synthesis having different copper(II) or copper(I) salts and tris as starting materials. In an ethanolic solution, tris was observed to react even with metallic copper powder, giving the non-hydrous $[Cu(trisH_{-1})_2]$ as the product.

The degree of crystalline water depends mainly on the solvent, the reaction temperature and the crystallization temperature. The non-hydrous complex crystallizes from various methanolic or ethanolic syntheses containing different Cu(II) salts and tris as starting materials. The product is very often a mixture of non-hydrate and monohydrate compounds, especially when the reaction mixture is refluxed for a long period of time.

In the water syntheses, the formation of monohydrate versus pentahydrate depends again on the temperature and the choice of the anion. Heating up the reaction mixture promotes the coordination of water to the copper ion, leading to the monohydrate structure. On the other hand, one can affect the final product with the choice of the anion. Anions which do not participate in protolytic reactions (Cl^-, Br^-) lead more often to the monohydrate structure, while anions which affect the pH of the solution by making it more alkaline (SO_4^{2-}, Ac^-) usually give the pentahydrate form. The crystallization of the complex below room temperature (15–20°C) also promotes the formation of the pentahydrate structure.

Thermal analysis. The thermal decomposition of the $Cu(trisH_{-1})_2\cdot nH_2O$ complexes took place in two basic stages; the dehydration of crystalline water was followed by the degradation of the organic part in two or three overlapping reactions leading to CuO in an air atmosphere and metallic copper in a nitrogen atmosphere.

The temperature of dehydration depends clearly on the coordination of water; in the pentahydrate structure, where the water molecules are not coordinated to copper

but are bonded to the structure by hydrogen bonding, the cleavage of water happens in one step between 63–99°C, whereas the coordinated water in the monohydrate structure lasts until 120–165°C. The thermal behavior of the ligand and the complexes is summarized in Table 1.

Molecular structures. The basic structure in all three cases is a mononuclear neutral complex with two deprotonated tris molecules covalently bonded to the copper atom in a *trans* configuration (Fig. 1).

The non-hydrate and pentahydrate complexes are almost identical, with square-planar structures, differing mainly in orientation of the terminal hydroxy groups. The four-coordination around copper is planar owing to symmetry reasons and the metal–ligand distances range from 1.929(2) Å (Cu–O) to 1.991(1) Å (Cu–N). The five-membered chelate rings are also nearly planar; the ring is in an *envelope* conformation with Cu100, O111, N111 and C111 defining the plane, and C112 is the atom which is bent out of the plane. The deviations of C112 from this least-squares plane are −0.582(1) Å for the non-hydrate and −0.491(2) Å for the pentahydrate molecule. Furthermore, the terminal hydroxymethyl groups can take an axial or an equatorial position in relation to this chelate plane. The corresponding C113 and C114 distances from the plane are −2.094(1) and −0.255(2) Å for the non-hydrate and −2.010(3) and 0.022(2) Å for the pentahydrate.

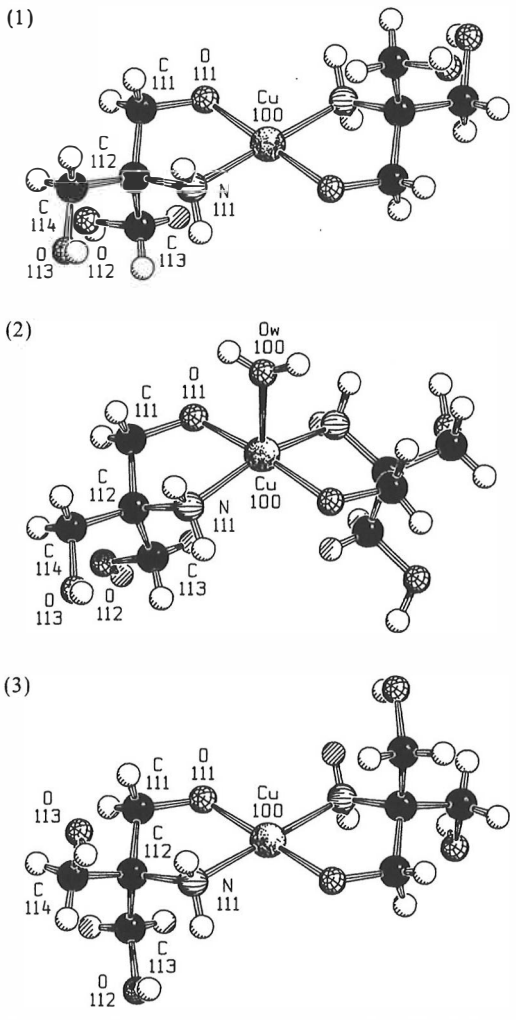

Fig. 1. SCHAKAL projections of the molecules $[Cu(trisH_{-1})_2]$ (**1**), $[Cu(trisH_{-1})_2(H_2O)]$ (**2**) and $[Cu(trisH_{-1})_2]\cdot 5H_2O$ (**3**). The other half of the molecule is generated by inversion with respect to the copper atom in the case of **1** and **3**, and by two-fold rotation around the Cu100–OW100 bond (two-fold axis) in the case of **2**.

In the monohydrate complex the copper atom has a square-pyramidal five-coordination with tris molecules in the basal plane and the oxygen atom of the water molecule occupies the apical position. The deviations of O111, N111, O111′ and N111′ atoms from the least-squares plane range from 0.074(1) to 0.089(1) Å, and the copper atom is displaced 0.226(1) Å from this plane toward the apex of the pyramid. The metal–ligand distances in the equatorial plane of the coordination sphere range from 1.950(1) Å (Cu–O) to 2.032(1) Å (Cu–N), while the apical bond length is a little longer, Cu–OW = 2.200(2) Å. The chelate rings in the monohydrate molecule are nearly planar, with C112 deviating −0.602(2) Å from the Cu100–O111–N111–C111 least-squares plane. The corresponding axial and equatorial C113 and C114 distances are −2.109(2) Å and −0.296(2) Å. The dihedral angle between the two-fold symmetry related Cu100–O111–N111–C111 planes is 161.30(3)°. The monohydrate molecule is an optically active complex with two possible enantiomers, which are mirror images of each other, but because the synthesis is not stereoselective and the product is a racemic mixture, the compound crystallizes in a centrosymmetric space group where both enantiomers are present.

All the bond lengths and angles summarized in Tables 6 and 7 are consistent with the previously reported structures of tris-containing copper complexes.[10–12]

Crystal structures. The projections of the crystal structures and hydrogen bonding of $Cu(trisH_{-1})_2$ complexes are presented in Fig. 2.

In the $[Cu(trisH_{-1})_2]$ structure the copper atom is located at the inversion center and surrounded by two symmetry-related tris ligands. The molecule forms 14 hydrogen bonds with six surrounding complex units via all OH and NH_2 hydrogens. Two short hydrogen bond distances (O···O = 2.60–2.79 Å) are found from the deprotonated metal-bonded hydroxy group (O111) to the adjacent terminal hydroxymethyl groups. The amino-hydrogen contacts (N···O = 2.90–2.97 Å) to the neighboring hydroxymethyl are also shorter than in the monohydrate structure (in the pentahydrate structure,

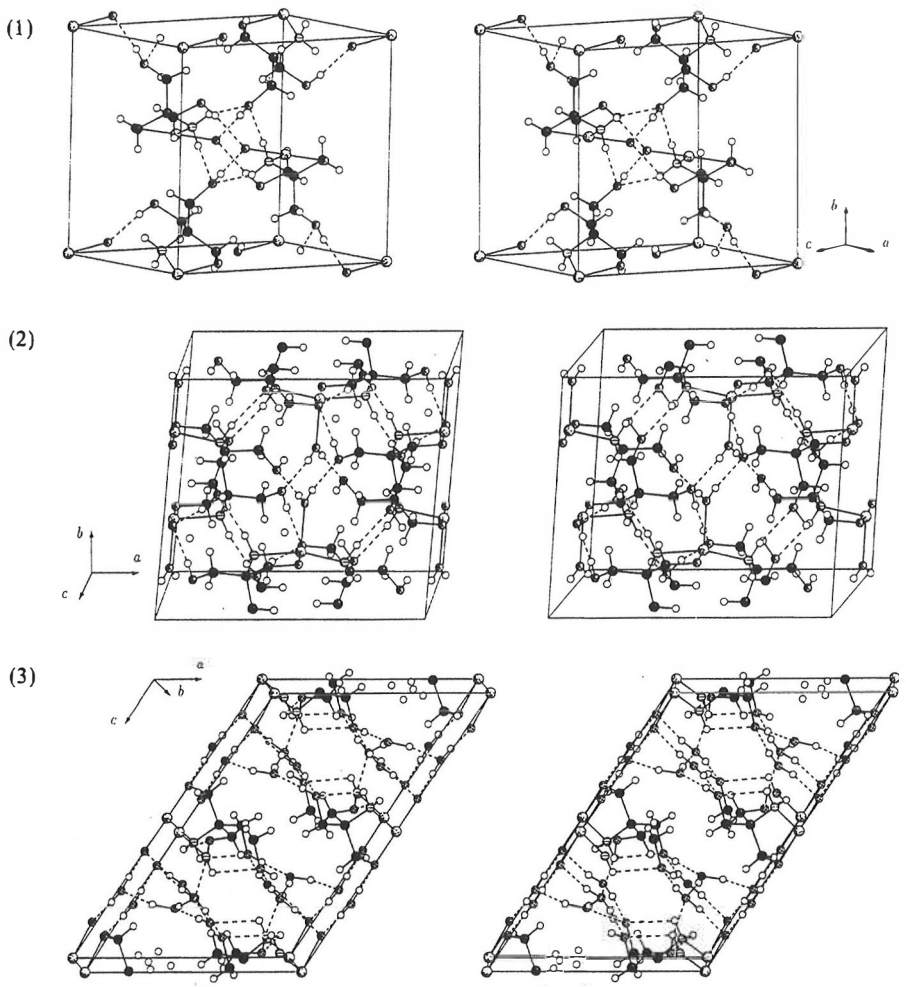

Fig. 2. Stereoscopic representations of hydrogen bonding for $[Cu(trisH_{-1})_2]$ (**1**), $[Cu(trisH_{-1})_2(H_2O)]$ (**2**) and $[Cu(trisH_{-1})_2]\cdot 5H_2O$ (**3**). Hydrogen bonds are indicated by dashed lines.

the NH_2 hydrogen bonds are even shorter, but they are intramolecular bonds).

The monohydrate, $[Cu(trisH_{-1})_2(H_2O)]$, has a doubly primitive C-centered lattice with four molecules in a unit cell. The asymmetric unit is half of the molecule and the other half is generated by two-fold rotation along the Cu100–OW100 bond (the copper atom and the coordinated water are located at the two-fold rotation axis). There is, again, an extensive framework of hydrogen bonds; one molecule forms 14 hydrogen bonds with seven adjacent complexes, utilizing all OH, NH_2 and H_2O hydrogens in bonding. The most distinctive bonding modes are the Cu100···O111···O113···OW100···O113···O111′–Cu100···O111··· chains which lie in the direction of the *c*-axis.

In the crystal structure of the pentahydrate, the copper atom is positioned in the center of symmetry which also lies in the *c*-glide plane. In addition, the two-fold axis passes through the OW1 atom (crystalline water) in the *b*-direction. The general structure of the pentahydrate consists of layers of molecules divided by layers of crystalline water parallel to the *ab*-plane. Because of this layer-like structure, direct intermolecular hydrogen bonding between molecules is hindered and all the hydrogen bonds formed are between molecules and crystalline water. In addition, in this structure, the NH_2 hydrogen bonds have only an intramolecular effect on the orientation of the terminal hydroxymethyl groups. In the framework, the most characteristic hydrogen bond chain is Cu100–O111···OW1···O111′–Cu100–O111···,

which also includes the strongly bonding O111 hydroxy group. The other interactions within the molecule layers are weak van der Waals type $CH_2 \cdots CH_2$ contacts. The layer structure of the pentahydrate explains the anisotropicity observed in the crystal color (see Experimental).

References

1. Ramette, R. W., Culberson, C. H. and Bates, R. G. *Anal. Chem. 49* (1977) 867.
2. Dotson, R. L. *J. Inorg. Nucl. Chem. 34* (1972) 3131.
3. Dotson, R. L. *J. Inorg. Nucl. Chem. Lett. 9* (1973) 215.
4. Hall, J. L., Simmons, R. B., Morita, E., Joseph, E. and Gavlas, J. F. *Anal. Chem. 43* (1971) 634.
5. Bai, K. S. and Martell, A. E. *J. Inorg. Nucl. Chem. 31* (1969) 1697.
6. Boyd, P. D., Pilbrow, J. R. and Smith, T. D. *Aust. J. Chem. 24* (1971) 59.
7. Brignac, P. J. and Mo, C. *Anal. Chem. 47* (1975) 1465.
8. Bologni, L., Sabatini, A. and Vacca, A. *Inorg. Chim. Acta 69* (1983) 71.
9. Eilerman, D. and Rudman, R. *J. Chem. Phys. 72* (1980) 5656.
10. Ivarsson, G. J. M. *Acta Crystallogr., Sect. C 40* (1984) 67.
11. Masi, D., Mealli, C., Sabat, M., Sabatini, A., Vacca, A. and Zanobini, F. *Helv. Chim. Acta 67* (1984) 1818.
12. Colombo, M. F., Austrilino, L., Nascimento, O. R., Castellano, E. E. and Tabak, M. *Can. J. Chem. 65* (1987) 821.
13. Sheldrick, G. M. In: Sheldrick, G. M., Krüger, C. and Goddard, R., Eds., *Crystallographic Computing 3*, Oxford University Press, Oxford 1985, pp. 175–189.
14. Walker, N. and Stuart, D. *Acta Crystallogr., Sect. A 39* (1983) 158.
15. *MolEN, An Interactive Structure Solution Procedure*, Enraf-Nonius, Delft, The Netherlands 1990.
16. *International Tables for X-Ray Crystallography*, Kynoch Press, Birmingham 1974. Vol. 4.
17. Keller, E., *SCHAKAL, a FORTRAN Program for the Graphic Representation of Molecular and Crystallographic Models*, University of Freiburg, Freiburg 1987.

Received February 5, 1993.

PAPER II

(Reprinted by the permission of *Acta Chemica Scandinavica*)

https://eurekamag.com/research/074/612/074612490.php

Acta Chemica Scandinavica, 1993: 47: 957–964
Printed in Belgium – all rights reserved

ACTA
CHEMICA SCANDINAVICA
ISSN 0904–213X

Copper(II) Complexes of 2-Amino-2-hydroxymethyl-1,3-propanediol. Part 2. Synthesis, Structure and Thermal Behavior of *cis*-[2-Amino-2-hydroxymethyl-1,3-propanediol(1,3-)-*O*,*O*′,*N*][2-amino-2-hydroxymethyl-1,3-propanediolato(1-)-*O*,*N*]nitratocopper(II), $[Cu(C_4H_{10}NO_3)(C_4H_{11}NO_3)(NO_3)]$, and *cis*-[2-Amino-2-hydroxymethyl-1,3-propanediol(1,3-)-*O*,*O*′,*N*][2-amino-2-hydroxymethyl-1,3-propanediolato(1,3-)-*O*,*O*′,*N*]copper(II) Sodium Bis(perchlorate), $[Cu(C_4H_{10}NO_3)(C_4H_{11}NO_3)]Na(ClO_4)_2$

Sirpa Kotila* and Jussi Valkonen

Department of Chemistry, University of Jyväskylä, SF-40500 Jyväskylä, Finland

Kotila, S. and Valkonen, J., 1993. Copper(II) Complexes of 2-Amino-2-hydroxymethyl-1,3-propanediol. Part 2. Synthesis, Structure and Thermal Behavior of *cis*-[2-Amino-2-hydroxymethyl-1,3-propanediol(1,3-)-*O*,*O*′,*N*][2-amino-2-hydroxymethyl-1,3-propanediolato(1-)-*O*,*N*]nitratocopper(II), $[Cu(C_4H_{10}NO_3)(C_4H_{11}NO_3)(NO_3)]$, and *cis*-[2-Amino-2-hydroxymethyl-1,3-propanediol(1,3-)-*O*,*O*′,*N*][2-amino-2-hydroxymethyl-1,3-propanediolato(1,3-)-*O*,*O*′,*N*]copper(II) Sodium Bis(perchlorate), $[Cu(C_4H_{10}NO_3)(C_4H_{11}NO_3)]Na(ClO_4)_2$. – Acta Chem. Scand. 47: 957–964.

The crystal structures of two copper(II) complexes with 2-amino-2-hydroxymethyl-1,3-propanediol (=tris, deprotonated form abbreviated $trisH_{-1}$) as ligand were determined by the conventional single-crystal X-ray diffraction technique. The blue crystals of $[Cu(trisH_{-1})(tris)(NO_3)]$ were refined to the final *R*-value of 0.032 for 3418 reflections. The compound crystallizes in monoclinic space group $P2_1/c$ with four molecules in a cell of dimensions $a = 10.246(2)$, $b = 6.950(1)$, $c = 21.313(3)$ Å, $\beta = 110.54(1)°$, $V = 1421.2(4)$ Å^3. The crystal structure of the blue perchlorate complex, $[Cu(trisH_{-1})(tris)]Na(ClO_4)_2$, is triclinic with the following crystal data: space group $P\bar{1}$, $a = 9.946(1)$, $b = 11.793(2)$, $c = 8.853(2)$ Å, $\alpha = 109.39(1)°$, $\beta = 112.72(1)°$, $\gamma = 82.02(1)°$, $V = 903.4(2)$ Å^3, $Z = 2$, $R = 0.043$ for 4646 reflections.

Both complexes are mononuclear with two tris ligands coordinated to the metal ion via amino and hydroxymethyl groups in a *cis* arrangement. In the nitrate compound, the copper atom has an octahedral sphere of coordination with two pairs of oxygen and nitrogen atoms in the square plane and two weaker apical interactions with nitrate oxygen and a terminal hydroxymethyl oxygen (4 + 2). The perchlorate molecule has a similar, tetragonally distorted octahedral structure (4 + 2), but this time the apical bonds are formed with two terminal hydroxymethyl groups. The molecules form hydrogen-bonded dimers in both structures.

The thermal behavior of the complexes was studied by TG in air and nitrogen atmospheres.

The complex formation of tris (deprotonated form abbreviated $trisH_{-1}$) with various transition metals in aqueous and non-aqueous solutions has been widely studied.[1–6]

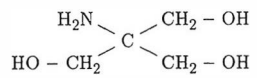

The early studies in solution already predicted the displacement of an alcoholic proton, as well as formation of different types of bridges involving deprotonated hydroxy groups.[1–4] The solid-state chemistry of tris is less well known. So far, the following crystal structures of tris–metal complexes have been published: $[Ni(tris)_2](ClO_4)_2$,[7] $[Cu(trisH_{-1})_2]NaClO_4 \cdot H_2O$,[8] $[Cu(trisH_{-1})Cl]_4$,[9] $[Cu(trisH_{-1})(tris)]_2Br_2$[9] and $[Cu(trisH_{-1})_2(H_2O)]$.[10]

* To whom correspondence should be addressed.

The aim of the present study was to obtain information about copper(II)–tris complexes containing different types of anions. Our previous article discussed the structures and thermal behavior of the basic *trans* complexes with three stages of crystalline water, $[Cu(trisH_{-1})_2]$, $[Cu(trisH_{-1})_2(H_2O)]$ and $[Cu(trisH_{-1})_2]\cdot 5H_2O$.[11] In this article we report molecular and crystal structures and the thermal behavior of two new copper(II)–tris complexes, $[Cu(trisH_{-1})(tris)(NO_3)]$ and $[Cu(trisH_{-1})(tris)]Na(ClO_4)_2$.

Experimental

Reagents. All the reagents were Merck 'pro analyse' grade (unless otherwise indicated) and were used as obtained without further purification.

Preparation of $[Cu(trisH_{-1})(tris)(NO_3)]$. The blue crystals of the nitrate complex were crystallized from water solution with a metal–ligand–anion stoichiometric ratio of 1 : 4 : 8. 0.01 mol of $Cu(NO_3)_2\cdot 3H_2O$, 0.04 mol of tris and 0.06 mol of $NaNO_3$ were dissolved in a minimum amount of distilled water in separate beakers with moderate heating. The complex was formed by adding copper solution to the tris solution and finally pouring the $NaNO_3$ solution into the blue complex mixture. The solution was warmed for 15 min to promote the coordination of nitrate oxygen to the complex, and then the solution was concentrated with a rotavapor to a volume of 10–15 cm^3. Blue, rod-shaped crystals were formed within a few days at room temperature. Crystals were filtered, washed with a small amount of cold water, and dried in air.

Preparation of $[Cu(trisH_{-1})(tris)]Na(ClO_4)_2$. The light blue crystals of $[Cu(trisH_{-1})(tris)]Na(ClO_4)_2$ were crystallized from solution with a metal–ligand–anion stoichiometric ratio 1 : 4 : 8. 0.01 mol of $Cu(ClO_4)_2\cdot 6H_2O$ (Frederic Smith Chemical Co.) 0.04 mol of tris, and 0.06 mol of $NaClO_4\cdot H_2O$ (B.D.H. Ltd., laboratory reagent, 'low in chloride' grade) were dissolved in a minimum amount of distilled water in separate beakers. First, Cu(II) perchlorate solution was added to the tris solution, and then the sodium perchlorate solution was added to the complex solution. Excessive water was removed with a rotavapor until the final volume was ~10 cm^3. The complex was crystallized by adding 40 cm^3 of methanol that had been saturated with anhydrous $NaClO_4$. Crystallization time may vary from a few days to weeks (at room temperature), but the process can be speeded up by a further addition of saturated $NaClO_4$–MeOH solution after a few days. Clear blue prismatic crystals were filtered, washed with water–methanol solution, and dried in air.

Table 1. Thermal decomposition of $[Cu(trisH_{-1})(tris)(NO_3)]$ (**1**) and $[Cu(trisH_{-1})(tris)]Na(ClO_4)_2$ (**2**).

Compound	Lost in reaction	T/°C	Weight loss/% Δ Obs.	Δ Theor.
Air atmosphere:				
1	Org.	150–292	53.1	—
	Org.	292–345	4.2	—
	Org. + NO_3	345–420	21.2	—
	Total reaction → CuO	25–420	78.6	78.3
2	Org. + ClO_4	157–289	42.6	—
	Org.	289–408	18.2	—
	$O_2(NaClO_4)$	408–440	6.5	6.1
	$O_2(NaClO_4)$	440–474	7.6	6.1
	Total reaction → CuO + NaCl	157–474	74.9	73.8
	NaCl	720–820	11.6	11.2
	Total reaction → CuO	25–900	84.9	84.9
Nitrogen atmosphere				
1	Org.	164–290	63.9	—
	Org.	290–390	4.5	—
	Org. total	164–390	68.4	65.8
	NO_3	390–970	14.5	16.9
	Total reaction → Cu	25–970	83.1	82.7
2	Org. + ClO_4	185–290	43.4	—
	Org.	290–333	4.8	—
	$O_2(NaClO_4)$ (+org.)	333–384	7.4	6.1
	$O_2(NaClO_4)$	384–446	5.6	6.1
	Org.	446–720	10.7	—
	NaCl	720–840	11.9	11.2
	Total reaction → Cu	25–950	86.4	87.9

Thermal analysis. Thermal behavior of the complexes in air and nitrogen atmospheres was determined with a Perkin-Elmer thermogravimetric analyzer TGA7. The sample size of the nitrate compound was 7.00 ± 0.50 mg; the amount of the perchlorate compound was smaller (3.20–3.30 mg) because of the risk of explosion. The crystalline samples were analyzed with heating rate 2°C min^{-1} and gas flow 50 cm^3 min^{-1}. The temperature range with the nitrate complex was 25–500°C in air and 25–970°C in a nitrogen atmosphere. Both perchlorate curves were run from 25 to 950°C. When a nitrogen atmosphere was used, the equipment was flushed for 30–45 min with nitrogen before the start of the temperature program to remove oxygen from the oven. Observed and theoretical weight losses are reported in Table 1.

X-Ray structure measurements. Single-crystal X-ray measurements were carried out with an Enraf-Nonius CAD-4 diffractometer using Mo K_α radiation. Crystals were mounted on a glass fiber and measured in an air atmosphere. All relevant crystallographic information is given in Table 2. Accurate unit-cell parameters were obtained by a least-squares analysis of 25 centered reflections. The calculations were done on a MicroVAX 3100 computer using the MolEN[12] program supplied by Enraf-Nonius. Intensity data on each compound were collected by a $\omega/2\theta$ scanning method, with two (NO_3^-) or three (ClO_4^-) standard reflections recorded for an intensity check every 60 min. Similarly, the orientation matrix was confirmed at an interval of 500 reflections. The data were corrected for linear decay, since a decay of 2.3% (72.8 h) was observed for the nitrate compound, and there was a total gain in intensity of 10.0% (91.3 h) during data collection for the perchlorate complex. In addition, Lorentz and polarization effects were taken into account, and absorption correction was done by the DIFABS[13] program.

The positions of the heavy atoms (Cu, Na, Cl) were solved by direct methods with the SHELXS-86[14]

Table 2. Crystallographic experimental data for [Cu(trisH$_{-1}$)(tris)(NO_3)] (**1**) and [Cu(trisH$_{-1}$)(tris)]Na(ClO_4)$_2$ (**2**).

Compound	**1**	**2**
Unit cell determination:		
Formula	$CuO_9N_3C_8H_{21}$	$CuCl_2NaO_{14}N_2C_8H_{21}$
Formula weight/g mol^{-1}	366.81	526.70
Color	Blue	Blue
Crystal size/mm	$0.18 \times 0.15 \times 0.08$	$0.30 \times 0.18 \times 0.13$
T/°C	21 ± 1	21 ± 1
Reflections for lattice measurement	25	25
θ-Range for lattice measurement/°	8–13	9–13
a/Å	10.246(2)	9.946(1)
b/Å	6.950(1)	11.793(2)
c/Å	21.313(3)	8.853(2)
α/°	90.00	109.39(1)
β/°	110.54(1)	112.72(1)
γ/°	90.00	82.02(1)
V/Å^3	1421.2(4)	903.4(2)
Z	4	2
d_{calc}/g cm^{-3}	1.71	1.94
λ(Mo K_α)/Å	0.71073	0.71073
μ(Mo K_α)/cm^{-1}	15.86	16.05
F(000)	764	538
Space group	$P2_1/c$	$P\bar{1}$
Data collection and refinement:		
θ-Range for data collection/°	2–32.5	2–30
Scan method	$\omega/2\theta$	$\omega/2\theta$
Scan speed in ω/° min^{-1}	0.92–5.50	0.59–5.50
Scan width in ω/°	$0.60 + 0.34 \tan\theta$	$0.50 + 0.34 \tan\theta$
No. of measured refls.	5502	5254
Reflections used in refinement $I > 3\sigma(I)$	3418	4646
Absorption correction (min./max.)	0.77/1.18	0.85/1.26
Max. shift/error	0.00	0.00
Max. in final Δρ/e Å^{-3}	0.39	0.97
No. of parameters refined	190	253
R	0.032	0.043
R_w[a]	0.035	0.055
$S = [\Sigma w(F_o - F_c)^2/(n-m)]^{1/2}$	1.103	1.326

[a] $w = 1/\sigma^2(F_o)$.

Table 3. Atomic positional parameters and equivalent isotropic temperature factors[a] with e.s.d.s in parentheses for [Cu(trisH$_{-1}$)(tris)(NO_3)] (**1**).

Atom	*x*	*y*	*z*	B_{eq}/Å^2
Cu100	0.31081(3)	0.72289(4)	0.49991(1)	1.389(4)
O111	0.4874(2)	0.6421(3)	0.57072(8)	1.77(3)
O112	0.4171(2)	1.0431(3)	0.55832(9)	2.37(4)
O113	0.3046(2)	0.6283(3)	0.71379(9)	3.13(4)
O121	0.3852(2)	0.6746(2)	0.43011(7)	1.48(3)
O122	0.1324(2)	1.1818(3)	0.36446(9)	2.35(4)
O123	0.0672(2)	0.8215(3)	0.24460(8)	2.66(4)
N111	0.2467(2)	0.7720(3)	0.57679(8)	1.52(3)
N121	0.1371(2)	0.8118(3)	0.42740(9)	1.55(3)
C111	0.4808(2)	0.6652(4)	0.6364(1)	1.81(4)
C112	0.3726(2)	0.8195(3)	0.6347(1)	1.48(4)
C113	0.4163(2)	1.0231(4)	0.6245(1)	2.02(4)
C114	0.3467(3)	0.8145(4)	0.7012(1)	2.41(5)
C121	0.2760(2)	0.6790(3)	0.3666(1)	1.55(4)
C122	0.1676(2)	0.8345(3)	0.3647(1)	1.33(3)
C123	0.2292(2)	1.0342(3)	0.3648(1)	1.63(4)
C124	0.0348(2)	0.8061(4)	0.3040(1)	1.81(4)
Nitrate:				
N1	0.1362(2)	0.3119(3)	0.5177(1)	2.12(4)
O1	0.1942(2)	0.3927(3)	0.48183(9)	2.85(4)
O2	0.1372(3)	0.3885(3)	0.5707(1)	4.33(5)
O3	0.0771(2)	0.1547(3)	0.5007(1)	3.00(4)

[a] $B_{eq} = \frac{4}{3}\Sigma_i\Sigma_j\beta_{ij}\mathbf{a}_i\cdot\mathbf{a}_j$.

Table 4. Atomic positional parameters and equivalent isotropic temperature factors[a] with e.s.d.s in parentheses for [Cu(trisH$_{-1}$)(tris)]Na(ClO_4)$_2$ (**2**).

Atom	*x*	*y*	*z*	B_{eq}/Å^2
Cu100	0.02923(4)	0.28996(3)	0.38352(4)	1.097(7)
O111	0.1647(2)	0.4168(2)	0.5588(3)	1.33(4)
O112	0.1438(3)	0.2059(2)	0.6207(3)	2.22(5)
O113	0.4811(3)	0.0849(3)	0.4105(4)	2.84(6)
O121	−0.1241(2)	0.3787(2)	0.4664(3)	1.10(4)
O122	−0.1192(3)	0.3732(2)	0.1398(3)	2.05(5)
O123	−0.4040(4)	0.0782(3)	0.1545(4)	4.04(8)
N111	0.2074(3)	0.2091(2)	0.3417(3)	1.34(5)
N121	−0.1239(3)	0.1693(2)	0.2160(3)	1.48(5)
C111	0.3142(3)	0.3785(3)	0.5921(4)	1.39(6)
C112	0.3220(3)	0.2413(3)	0.5173(4)	1.21(5)
C113	0.2887(4)	0.1758(3)	0.6210(4)	1.96(6)
C114	0.4749(3)	0.2061(3)	0.5128(4)	1.78(6)
C121	−0.2562(3)	0.3116(3)	0.3716(4)	1.37(6)
C122	−0.2610(3)	0.2420(3)	0.1891(4)	1.41(6)
C123	−0.2608(4)	0.3267(3)	0.0891(4)	2.03(7)
C124	−0.3965(4)	0.1658(4)	0.0831(5)	2.58(8)
Na1	0.0416(2)	0.4078(1)	0.7628(2)	2.27(3)
Perchlorates:				
Cl1	0.28655(9)	0.44034(8)	0.1443(1)	2.01(2)
Cl2	−0.0665(1)	0.12455(8)	0.7921(1)	2.70(2)
O1	0.1334(4)	0.4515(4)	0.1088(6)	4.8(1)
O2	0.3084(5)	0.4123(4)	−0.0136(4)	6.3(1)
O3	0.3477(5)	0.3458(4)	0.2158(5)	6.29(9)
O4	0.3498(5)	0.5509(5)	0.2563(8)	7.8(2)
O5	−0.0873(4)	0.2489(3)	0.8033(4)	3.75(7)
O6	−0.0358(4)	0.0539(3)	0.6456(4)	5.18(8)
O7	−0.1883(4)	0.0781(3)	0.7980(5)	5.36(8)
O8	0.0557(7)	0.1143(5)	0.9428(7)	8.2(2)

[a] See Table 3.

program, and the remaining non-hydrogen atoms were located by a difference Fourier method. The refinement was done using full-matrix least-squares techniques with anisotropic temperature factors for all non-hydrogen atoms and isotropic thermal parameters with fixed $B = 5.00$ Å^2 for all hydrogen atoms. The final R-values were $R = \Sigma\,||F_o| - |F_c||/\Sigma\,|F_o| = 0.032$ for the nitrate complex and $R = 0.043$ for the perchlorate complex. The corresponding weighted R_w-values (with unit weighting) were 0.035 for the nitrate and 0.055 for the perchlorate compound, respectively. All shift/error values were < 0.01 in the last refinement cycle.

Scattering factors and real and imaginary dispersion corrections for atomic scattering factors were taken from Ref. 15. The figures were drawn with the SCHAKAL[16] program. The final atomic positional parameters and equivalent isotropic temperature factors are given in Tables 3 and 4. The relevant molecular bond distances and angles for the complexes and anions are reported in Tables 5 and 6. Tables of anisotropic thermal parameters,

Table 5. Bond distances (Å) with e.s.d.s in parentheses for [Cu(trisH$_{-1}$)(tris)(NO_3)] (**1**) and [Cu(trisH$_{-1}$)(tris)]-Na(ClO_4)$_2$ (**2**).

Bond distance/Å	**1**	**2**
Cu100–O111	1.987(1)	1.966(2)
Cu100–O112	2.596(2)	2.431(3)
Cu100–O121	1.925(2)	1.968(2)
Cu100–O122	—	2.518(3)
Cu100–O1(NO_3)	2.553(2)	—
Cu100–N111	1.997(2)	1.997(3)
Cu100–N121	2.002(2)	2.000(2)
O111–C111	1.433(3)	1.437(4)
O112–C113	1.419(3)	1.434(5)
O113–C114	1.419(4)	1.423(4)
O121–C121	1.422(2)	1.433(4)
O122–C123	1.425(3)	1.431(5)
O123–C124	1.422(3)	1.402(7)
N111–C112	1.476(2)	1.490(3)
N121–C122	1.484(3)	1.487(4)
C111–C112	1.534(3)	1.535(4)
C112–C113	1.523(3)	1.525(6)
C112–C114	1.532(4)	1.532(5)
C121–C122	1.540(3)	1.536(4)
C122–C123	1.525(3)	1.539(6)
C122–C124	1.526(3)	1.518(5)
Nitrate:		
N1–O1	1.254(3)	—
N1–O2	1.246(3)	—
N1–O3	1.240(3)	—
Perchlorates:		
Cl1–O1	—	1.427(4)
Cl1–O2	—	1.421(5)
Cl1–O3	—	1.413(4)
Cl1–O4	—	1.402(5)
Cl2–O5	—	1.428(3)
Cl2–O6	—	1.409(4)
Cl2–O7	—	1.422(5)
Cl2–O8	—	1.444(5)

Table 6. Bond angles (in °) with e.s.d.s in parentheses for $[Cu(trisH_{-1})(tris)(NO_3)]$ (1) and $[Cu(trisH_{-1})(tris)]$-$Na(ClO_4)_2$ (**2**).

Angle/°	1	2
O111–Cu100–O112	76.19(6)	77.23(9)
O111–Cu100–O121	92.04(7)	87.67(9)
O111–Cu100–O1(NO_3)	96.52(6)	—
O111–Cu100–O122	—	106.67(9)
O111–Cu100–N111	84.22(7)	84.43(9)
O111–Cu100–N121	177.81(8)	174.1(1)
O112–Cu100–O1(NO_3)	159.79(7)	—
O112–Cu100–O122	—	172.9(1)
N111–Cu100–N121	96.96(8)	101.4(1)
Cu100–O111–C111	111.6(1)	111.9(2)
Cu100–O121–C121	109.8(1)	108.6(2)
Cu100–O1–N1(NO_3)	127.4(2)	—
Cu100–N111–C112	106.3(1)	102.9(2)
Cu100–N121–C122	108.5(1)	103.4(2)
O111–C111–C112	109.7(2)	109.7(2)
O112–C113–C112	109.8(2)	109.8(3)
O113–C114–C112	111.0(2)	111.7(3)
O121–C121–C122	111.1(2)	109.5(3)
O122–C123–C122	111.6(2)	112.5(3)
O123–C124–C122	109.1(2)	112.3(3)
N111–C112–C111	106.0(2)	106.4(2)
N111–C112–C113	107.6(2)	107.8(3)
N111–C112–C114	112.6(2)	111.9(3)
N121–C122–C121	106.2(2)	104.3(2)
N121–C122–C123	108.2(2)	108.9(3)
N121–C122–C124	110.0(2)	112.9(3)
C111–C112–C113	114.0(2)	112.4(3)
C111–C112–C114	108.7(2)	108.6(3)
C113–C112–C114	108.0(2)	109.8(3)
C121–C122–C123	110.2(2)	111.9(3)
C121–C122–C124	110.6(2)	112.2(3)
C123–C122–C124	111.4(2)	106.7(3)
Nitrate:		
O1–N1–O2	120.5(2)	—
O1–N1–O3	120.3(2)	—
Perchlorates:		
O1–Cl1–O2	—	108.1(3)
O1–Cl1–O3	—	111.0(3)
O1–Cl1–O4	—	107.8(3)
O5–Cl2–O6	—	112.9(2)
O5–Cl2–O7	—	111.2(2)
O5–Cl2–O8	—	107.8(3)

coordinates of hydrogen atoms, and listings of observed and calculated structure factors are available from the authors on request.

Results and discussion

Thermal analysis. The thermal behavior of the complexes under study is summarized in Table 1. The thermal decomposition of $[Cu(trisH_{-1})(tris)(NO_3)]$ in an air atmosphere begins at 150°C with the decomposition of the organic part. The major degradation reaction occurring between 150 and 292°C consists of two unresolved processes with peaks in the DTG curve at 204 and 230°C. The small intermediate step (292–345°C) is due to the organic ligand, and the final step (345–420°C) involves the simultaneous decomposition of the remaining organic residue and nitrate group. The final product in an air atmosphere is CuO.

In a nitrogen atmosphere the overall decomposition processes of the nitrate compound takes place at elevated temperature. The major degradation reactions of the organic part are poorly resolved, and the following step (290–390°C) is very broad and flat. The decomposition of the nitrate group is a slow and broad process which starts around 400°C and has a maximum in the DTG curve at ~800°C. The final residue in a nitrogen atmosphere is metallic copper.

The perchlorate compound contains two types of perchlorate groups after the organic part begins to decompose: those attracted to the copper cation, which decompose in a similar manner as in copper(II) perchlorate, with the production of CuO in air and metallic copper in nitrogen atmosphere, respectively, and those that behave like $NaClO_4$, giving NaCl as a stable intermediate product in both atmospheres. The formula $[Cu(trisH_{-1})(tris)]ClO_4 \cdot NaClO_4$ would better describe the thermal behavior of the perchlorate compound.

In the decomposition of the perchlorate compound in an air atmosphere, the main decomposition process (157–289°C) appears as two distinctive peaks in the DTG curve at 216 and 271°C. The first peak is due to the organic ligand and the second to the perchlorate groups associated with the copper ion. The following slow process (289–408°C) is due to the decomposition of the organic part; the subsequent sharp peaks indicate the decomposition of $NaClO_4$, which leads to a mixture of CuO and NaCl as a stable intermediate product. The last phase in the TG curve at 720–820°C is the sublimation of NaCl leading to CuO as the final product at 900°C.

The decomposition reactions of the perchlorate compound in a nitrogen atmosphere are basically the same as in air. The major differences are that the organic part decomposes at a higher temperature, and the degradation of perchlorate groups is less fierce and occurs at a lower temperature than in an air atmosphere. As a result the TG curve is less resolved, and the $NaClO_4$ peaks and the broad organic peak have changed position. The intermediate phase is not so clear this time because copper(II) is reduced to metallic copper in several successive reactions ($CuO \rightarrow Cu_2O \rightarrow Cu$), which are still occuring when NaCl begins to decompose. The end product in a nitrogen atmosphere is metallic copper.

The interpretation above is based on our earlier study of thermal behavior of three copper(II)–tris complexes[11] and on the TG runs of various alkali metal and copper(II) perchlorates in air and nitrogen atmospheres.

A comparison of the present thermogravimetric results with those published earlier[11] reveals certain differences. All the compounds discussed previously, $[Cu(trisH_{-1})_2]$, $[Cu(trisH_{-1})_2(H_2O)]$, and $[Cu(trisH_{-1})_2] \cdot 5H_2O$, are mononuclear *trans* isomers with two deprotonated

ligands in square-planar or square-pyramidal coordination. In the TG curves of these *trans* complexes the main derivative peak (due to the decomposition of the organic part) is more symmetric, with the peak at 194–198°C in air and 209–217°C in a nitrogen atmosphere. With the present *cis* complexes, $[Cu(trisH_{-1})(tris)(NO_3)]$ and $[Cu(trisH_{-1})(tris)]Na(ClO_4)_2$, the degradation of the organic part is more complex, resulting in a derivative peak with at least two observable maxima. The reason for this behavior may be the unequal coordination of deprotonated and nonprotonated ligands. Moreover, the coordination number is higher in the nitrate and perchlorate complexes, since the terminal hydroxymethyl groups participate in coordination (and are more strongly bonded to the structure). The existence of a hydrogen in the metal-coordinated hydroxy group also allows dimeric structure (see section on Crystal Structure), which may affect the thermal behavior of the nitrate and perchlorate compounds.

Molecular structures. The molecular structures of the nitrate and perchlorate complexes are presented in Fig. 1, and the representative bond lengths and angles are listed in Tables 5 and 6.

The $[Cu(trisH_{-1})(tris)(NO_3)]$ molecule is a mononuclear uncharged complex with two tris ligands (of which one is deprotonated) and one coordinated nitrate group. The nonprotonated tris unit is coordinated to the copper ion via one amino and two hydroxymethyl groups, whereas the negatively charged $trisH_{-1}$ ligand has coordination bonds to copper only by amino nitrogen and deprotonated hydroxy oxygen. The coordination sphere is a tetragonally distorted octahedron with four shorter bonds in a square plane and two longer bonds perpendicular to this plane. In the basal plane there are two pairs of Cu–O and Cu–N bonds (in a *cis* arrangement), all of which lie in the range 1.92–2.01 Å. The two apical bonds involve coordinated nitrate oxygen and one terminal hydroxymethyl group from the nonprotonated side of the molecule. These apical bond lengths are 2.553(2) and 2.596(2) Å.

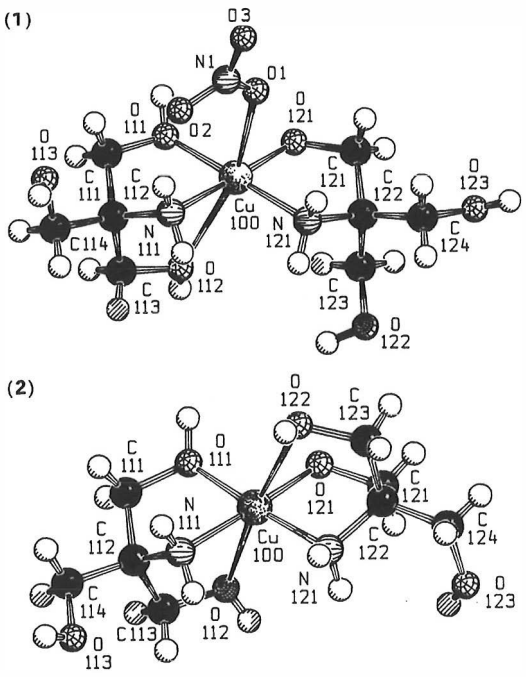

Fig. 1. SCHAKAL projections of the $[Cu(trisH_{-1})(tris)(NO_3)]$ molecule (**1**) and the cation complex of $[Cu(trisH_{-1})(tris)]Na(ClO_4)_2$ (**2**).

The five-membered chelate rings are almost planar, with C112 deviating from the Cu100–O111–N111–C111 plane by −0.649(2) Å and C122 from the Cu100–O121–N121–C121 plane by −0.511(2) Å. The corresponding distances between the equatorial and axial hydroxymethyl carbons and these planes are −2.146(3) Å (C113) and −0.424(3) Å (C114) from the Cu100–O111–N111–C111 plane and −2.034(2) Å (C123) and −0.008(3) Å (C124) from the Cu100–O121–N121–C121 plane. The dihedral angle between the two planes is 175.9(5)°. The N–O bond lengths of the nitrate ion [N1–O1 1.254(3) Å, N1–O2 1.246(3) Å and N1–O3 1.240(3) Å] are very similar, indicating that the nitrate ion is only weakly bonded to the copper(II) ion.[17] The observed bond lengths and angles are consistent with the copper-tris structures[7–11] published earlier, as well as with the nitrate complexes of the same type of amino alcohols.[17,18]

The perchlorate molecule is the same type of complex as the nitrate molecule described above, except that it has a unit charge +1 and the deprotonated tris ligand, like the nonprotonated ligand, forms three coordination bonds with copper. In the $[Cu(trisH_{-1})(tris)]^+$ molecule the coordination sphere is a tetragonally distorted octahedron with Cu–O and Cu–N bonds in the plane ranging from 1.96 to 2.00 Å. The apical interactions are caused by two axial hydroxymethyl groups which are bent toward the copper(II) ion from the opposite sides of the plane. The bond distances in apical direction are 2.431(3) Å (Cu100–O112) and 2.518(3) Å (Cu100–O122). The five-membered chelate rings are *envelope* conformers with C112 deviating from the Cu100–O111–N111–C111 plane by −0.690(3) Å. The corresponding deviation of C122 on the other side is 0.712(3) Å. The distances of equatorial and axial hydroxymethyl carbons from the chelate planes are −2.164(4) Å (C113), −0.529(4) Å (C114), 2.193(4) Å (C123) and 0.686(4) Å (C124). All the bond lengths and angles summarized in Tables 5 and 6 are in good agreement with the previously reported structures of perchlorate-containing metal–tris complexes.[7,8]

Both complex molecules have two optical isomers that are mirror images of each other. Since the syntheses are not stereoselective, both isomers are found in equal proportions in the crystal structures, and the compounds are not optically active.

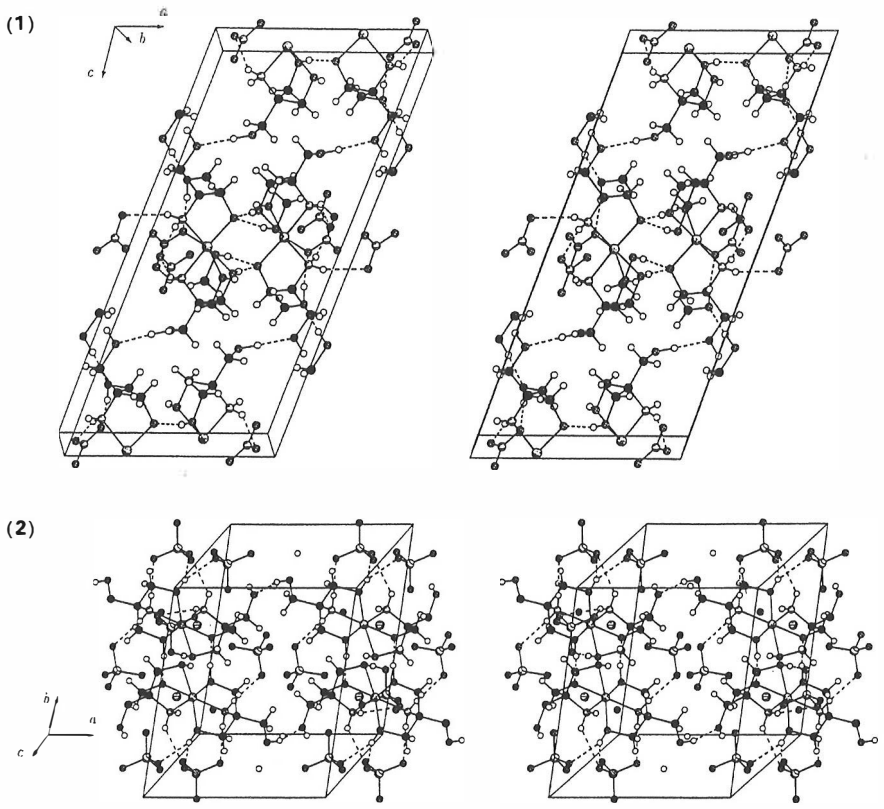

Fig. 2. Stereoscopic representations of hydrogen bonding for $[Cu(trisH_{-1})(tris)(NO_3)]$ (**1**) and $[Cu(trisH_{-1})(tris)]Na(ClO_4)_2$ (**2**). Hydrogen bonds are indicated by dashed lines.

Crystal structures. Stereoscopic projections of the crystal structures and the hydrogen-bonding framework for both compounds are presented in Fig. 2.

Common to both of these structures is the formation of hydrogen-bonded dimers. Because of the *cis* arrangement and the existence of a hydrogen in every other metal-bonded hydroxymethyl group, the monomer is able to form hydrogen-bonded associates with another mononuclear unit. The dimer is not coplanar; on the contrary, when one looks towards the dimer from one end the monomer units appear to form a step-like structure with an inversion center in the middle of the eight-membered ring. The hydrogen bonds in the dimer structure are strong, with donor–acceptor distances of 2.46–2.56 Å for the O111 ··· O121 contacts.

In the dimer structure of the nitrate compound the nitrate groups are oriented towards one of the monomer units, while the apical bonds with hydroxymethyl groups are directed outwards. The corresponding situation in the perchlorate complex dimer is that the apical bonds of the deprotonated ligands are facing one of the monomers, while the apical bonds of normal tris point outside the dimer. The simplified scheme of the dimer structure is shown below.

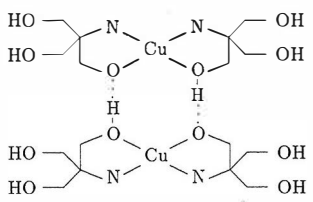

The occurrence of H-bonded polynuclear complexes of this kind has earlier been reported by Masi *et al.*[9]

The crystal structure of the nitrate compound is built up from uncharged molecules which are connected into a three-dimensional framework by extensive hydrogen bonding by OH, NH_2, and coordinated nitrate groups. The dimers are polymerized along the *b*-axis by hydrogen bonds between metal-coordinated deprotonated oxygen and apical hydroxymethyl groups of the adjacent

dimer. Coordinated nitrate groups interact mainly with amino hydrogens; first, nitrate forms an intramolecular hydrogen bond with amino hydrogen of the same molecule; then the nitrate groups connect the dimers along the *a*- and *b*-axes by hydrogen bonds with amino hydrogens of the neighboring dimers. The other interactions are hydrogen bonds between noncoordinated terminal hydroxymethyl groups or weak van der Waals forces between $CH_2 \cdots CH_2$ groups.

The crystal structure of the perchlorate compound consists of charged units of $[Cu(trisH_{-1})(tris)]^+$, Na^+ and ClO_4^-, so that the interactions are more electrostatic in nature. The hydrogen bonding in this structure occurs primarily between perchlorate oxygens and OH or NH_2 hydrogens of the molecules, because the interactions between molecules are prevented by perchlorate layers along the crystallographic ($\bar{1}01$) plane. In addition to the hydrogen bond involved in dimerization there is only one other intermolecular hydrogen bond joining the adjacent dimers by noncoordinated terminal hydroxymethyl groups O113 $\cdots$ O123′. Correspondingly, all perchlorate anions are bonded by at least one hydrogen bond to the neighboring dimer. The Na^+ ions are located in the same *bc*-plane as copper(II) and form a parallelepiped where two copper atoms and two sodium atoms are at the corners. The interatomic distances between these metal ions are 3.138(2) and 4.067(2) Å (Na–Cu), 4.7410(5) Å (Cu–Cu) and 5.505(3) Å (Na–Na), respectively. Otherwise the sodium ions are octahedrally surrounded by three perchlorate oxygens and three oxygens of dimeric hydroxymethyl groups, with distances falling in the range 2.56–2.62 Å.

References

1. Dotson, R. L. *J. Inorg. Nucl. Chem. 34* (1972) 3131.
2. Dotson, R. L. *J. Inorg. Nucl. Chem. Lett. 9* (1973) 215.
3. Bai, K. S. and Martell, A. E. *J. Inorg. Nucl. Chem. 31* (1969) 1697.
4. Boyd, P. D., Pilbrow, J. R. and Smith, T. D. *Aust. J. Chem. 24* (1971) 59.
5. Brignac, P. J. and Mo, C. *Anal. Chem. 47* (1975) 1465.
6. Bologni, L., Sabatini, A. and Vacca, A. *Inorg. Chim. Acta 69* (1983) 71.
7. Ivarsson, G. J. M. *Acta Crystallogr., Sect. B 38* (1982) 1828.
8. Ivarsson, G. J. M. *Acta Crystallogr., Sect. C 40* (1984) 67.
9. Masi, D., Mealli, C., Sabat, M., Sabatini, A., Vacca, A. and Zanobini, F. *Helv. Chim. Acta 67* (1984) 1818.
10. Colombo, M. F., Austrilino, L., Nascimento, O. R., Castellano, E. E. and Tabak, M. *Can. J. Chem. 65* (1987) 821.
11. Kotila, S. and Valkonen, J. *Acta Chem. Scand. 47* (1993) 000.
12. *MolEN*, An Interactive Structure Solution Procedure, Enraf-Nonius, Delft. The Netherlands, 1990.
13. Walker, N. and Stuart, D. *Acta Crystallogr., Sect. A 39* (1983) 158.
14. Sheldrick, G. M. In: Sheldrick, G. M., Krüger, C. and Goddard, R., Eds., *Crystallographic Computing 3*, Oxford University Press, Oxford 1985, pp. 175-189.
15. *International Tables for X-Ray Crystallography*, Kynoch Press, Birmingham 1974, Vol. 4.
16. Keller, E. *SCHAKAL, a FORTRAN Program for the Graphic Representation of Molecular and Crystallographic Models*, University of Freiburg, Freiburg 1987.
17. Sillanpää, R. and Rissanen, K. *Acta Chem. Scand. 44* (1990) 1013.
18. Lindgren, R., Sillanpää, R., Rissanen, K., Thompson, L. K., O'Connor, C. J., van Albada, G. A. and Reedijk, J. *Inorg. Chim. Acta 171* (1990) 95.

Received February 5, 1993.

PAPER III

(Reprinted by the permission of *Acta Chemica Scandinavica*)

https://eurekamag.com/research/074/612/074612491.php

Acta Chemica Scandinavica. 1994: 48: 200–208
Printed in Belgium – all rights reserved

ACTA
CHEMICA SCANDINAVICA
ISSN 0904–213X

Copper(II) Complexes of 2-Amino-2-hydroxymethyl-1,3-propanediol. Part 3. Synthesis, Structure and Thermal Behavior of Bis-*cis*[2-amino-2-hydroxymethyl-1,3-propanediol-*O,N*][2-amino-2-hydroxymethyl-1,3-propanediolato-*O,N*]aquacopper(II) Sulfate and Chromate, $[Cu(C_4H_{10}NO_3)(C_4H_{11}NO_3)(H_2O)]_2X$, where $X = SO_4^{2-}$, CrO_4^{2-}

Sirpa Kotila* and Jussi Valkonen

Department of Chemistry, University of Jyväskylä, FIN-40500 Jyväskylä, Finland

Kotila, S. and Valkonen, J., 1994. Copper(II) Complexes of 2-Amino-2-hydroxymethyl-1,3-propanediol. Part 3. Synthesis, Structure and Thermal Behavior of Bis-*cis*[2-amino-2-hydroxymethyl-1,3-propanediol-*O,N*][2-amino-2-hydroxymethyl-1,3-propanediolato-*O,N*]aquacopper(II) Sulfate and Chromate, $[Cu(C_4H_{10}NO_3)(C_4H_{11}NO_3)(H_2O)]_2X$, where $X = SO_4^{2-}$, CrO_4^{2-}. – Acta Chem. Scand. 48: 200–208 © Acta Chemica Scandinavica 1994.

Crystal structures of the title compounds with 2-amino-2-hydroxymethyl-1,3-propanediol (= tris, deprotonated form abbreviated $trisH_{-1}$) as ligand have been determined from single-crystal X-ray data. The blue $[Cu(trisH_{-1})(tris)(H_2O)]_2SO_4$ compound crystallizes in the triclinic space group $P\bar{1}$ with two complexes in a cell of dimensions $a = 6.213(2)$, $b = 11.009(4)$, $c = 11.248(1)$ Å, $\alpha = 70.88(1)$, $\beta = 72.87(2)$, $\gamma = 79.67(2)°$, $V = 691.76(3)$ Å^3, $R = 0.032$ (2169 reflections). The space group of the green $[Cu(trisH_{-1})(tris)(H_2O)]_2CrO_4$ compound is also $P\bar{1}$, but the unit cell is twice as large, containing four complexes, and the dimensions are $a = 6.424(1)$, $b = 10.735(1)$, $c = 21.578(2)$ Å, $\alpha = 98.60(1)$, $\beta = 89.97(1)$, $\gamma = 72.63(1)°$, $V = 1402.5(3)$ Å^3, $R = 0.033$ (4698 reflections).

Both complexes are mononuclear and have a square-pyramidal coordination sphere with two amino and two hydroxymethyl groups in the basal plane and a water molecule as the apical ligand. The complexes form dimers with their optical enantiomorphs via strong hydrogen bonds, which involve the deprotonated hydroxymethyl groups [O···O distances 2.509(3)–2.525(4) Å]. The disorder of the terminal hydroxymethyl groups and the anions has been determined, and the three-dimensional network of hydrogen bonding is discussed. Thermal behavior was characterized by TG in air and nitrogen atmospheres.

2-Amino-2-hydroxymethyl-1,3-propanediol (tris) is a common buffering agent in biochemical and sea-water[1] studies, because its buffering range lies in the physiological pH area 7–9. The ligand also has various other names, such as tris(hydroxymethyl)aminomethane (tham), Trizma Base or less often used Tromethamine and Trometamol.[2]

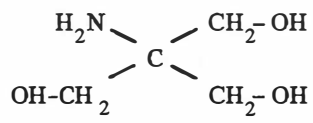

Tris forms chelates with metallic cations mainly via the amino group and one or two of the hydroxymethyl groups. Alcoholic ligands also have two distinctly different bond types with metal cations. One type involves a normal metal–oxygen coordination bond, whereas the second type includes a covalent coordination bond with the alkoxy oxygen.[3] These deprotonated species are abbreviated $trisH_{-1}$.

Our special interest is the solid-state chemistry of tris compounds and the aim of this study is to reveal the variety of copper(II)–tris compounds containing different anions. In our earlier articles we reported the structures and thermal behavior of three *trans* complexes, $[Cu(trisH_{-1})_2]$, $[Cu(trisH_{-1})_2(H_2O)]$ and $[Cu(trisH_{-1})_2]\cdot 5H_2O$[4] as well as two *cis*-complexes, $[Cu(trisH_{-1})(tris)$-

* To whom correspondence should be addressed.

$(NO_3)]$ and $[Cu(trisH_{-1})(tris)]Na(ClO_4)_2$.[5] In this paper we concentrate on two new copper(II)–tris complexes, $[Cu(trisH_{-1})(tris)(H_2O)]_2SO_4$ and $[Cu(trisH_{-1})(tris)(H_2O)]_2CrO_4$.

Experimental

Reagents. All the reagents were used without further purification.

Preparation of $[Cu(trisH_{-1})(tris)(H_2O)]_2SO_4$. 0.03 mol of $CuSO_4 \cdot 5H_2O$ (J.T. Baker, minimum 99.0%) was placed into a 250 cm^3 round-bottomed flask with a reflux condenser and was dissolved in 15 cm^3 of distilled water. Then 0.09 mol of tris (Sigma, 99–99.5%) was added and the mixture was gently refluxed for 5 h. The complex solution was cooled to room temperature, poured into a beaker, and three 15 cm^3 portions of methanol added, whereupon a thick syrupy solution formed on the bottom of the beaker. After the cloudy methanol solution on the top had been discarded, the syrupy complex solution was dissolved in a minimum volume of water–methanol (1:1 v/v) solution by heating. The solution was filtered, and the compound crystallized within a few days. The bright blue rod-shaped crystals were filtered, washed with a cold water–methanol (1:1) solution and dried in air.

Preparation of $[Cu(trisH_{-1})(tris)(H_2O)]_2CrO_4$. The chromate compound was crystallized from a water solution with a metal–ligand–anion stoichiometric ratio of 1:4:2. The following compounds, 0.04 mol of tris (Sigma, 99–99.5%), 0.01 mol of $CuCl_2 \cdot 2H_2O$ (Merck, p.a.), and 0.02 mol of Na_2CrO_4 (Merck, puriss.), were dissolved in a minimum amount of distilled water in separate beakers by moderate heating. The solutions were cooled to room temperature, and the complex was formed by adding the copper solution to the tris solution and finally pouring the sodium chromate solution into the blue complex mixture. The green solution was filtered and concentrated with a rotavapor to a volume of ~ 10 cm^3. The dark green needle-shaped crystals, formed within a week at room temperature, were separated with vacuum filtration (with no washing, because the compound is very soluble in water) and dried in air. If the complex solution is too dilute or has been heated during the procedure, some monohydrate, $[Cu(trisH_{-1})_2(H_2O)]$,[4] might result as a side-product.

Thermal analysis. The thermal behavior of the complexes in air and nitrogen atmospheres was determined with a Perkin-Elmer thermogravimetric analyzer TGA7. The sample size of the sulfate compound was 7.00 ± 0.50 mg; the amount of the chromate compound was smaller (4.00–4.30 mg), because the needle-shaped crystals took more space. The crystalline samples were analyzed with a heating rate of 2°C min^{-1} and a gas flow of 50 cm^3 min^{-1}. Temperature ranges with the sulfate and chromate compounds were 25–900 and 25–950°C, respectively, in both atmospheres. To remove oxygen from the oven when a nitrogen atmosphere was used, the equipment was flushed for 30–45 min with nitrogen before the

Table 1. Thermal decomposition of $[Cu(trisH_{-1})(tris)(H_2O)]_2SO_4$ (**1**) and $[Cu(trisH_{-1})(tris)(H_2O)]_2CrO_4$ (**2**).

Compound	Lost in reaction	T/°C	Weight loss (%) Δ Obs.	Δ Theor.
Air atmosphere				
1	$2\ H_2O$	52–128	4.9	4.9
	Org.	148–468	66.4	65.1
	$1\frac{1}{2}\ O_2\ (SO_4)$	575–715	4.6	6.5
	Total reaction $\rightarrow CuS + CuO$	25–800	75.4	76.4
2	$2\ H_2O$	38–87	4.9	4.7
	Org.	109–323	64.0	64.4
	Total reaction $\rightarrow 2\ CuO + \frac{1}{2}\ Cr_2O_3$	25–323	68.9	69.1
Nitrogen atmosphere				
1	$2\ H_2O$	25–123	4.9	4.9
	Org.	170–900	60.3	65.0
	Total reaction $\rightarrow Cu_2SO_4\ (+C)$	25–900	65.2	69.9
2	$2\ H_2O$	25–95	4.8	4.7
	Org.	95–780	61.3	63.4
	$2\ O_2\ (CrO_4)$	780–950	8.1	8.4
	Total reaction $\rightarrow 2\ Cu + Cr\ (+C)$	25–950	74.2	76.5

temperature program was initiated. Observed and theoretical weight losses are reported in Table 1.

X-Ray structure measurements. Diffracted intensities were measured with an Enraf-Nonius CAD-4 diffractometer and with monochromatized Mo$K\alpha$ radiation. Crystals were mounted on a glass fiber and measured in air. The lattice parameters were calculated by least-squares fitting of 25 centered reflections. Crystal data and experimental details are presented in Table 2.

During the data collection the decay of crystals was monitored with three reflections every 60 min, and the orientation of the crystal was checked every 500 reflections. The total gain in intensity was 10.5% in 27.7 h for the sulfate compound, and for the chromate compound the total loss in intensity was 12.5% in 136.4 h. In addition to the correction for the decay, Lorentz and polarization effects were also taken into account and the absorption correction was done by the DIFABS[6] program.

Positions of the heavy atoms (Cu, Cr) were determined by direct methods with the SHELXS-86 program;[7] the remaining non-hydrogen atoms were located from difference Fourier maps, and their coordinates were refined to convergence by the full-matrix least-squares method. Hydrogen atoms were placed in their calculated positions (CH_2, NH_2, $d = 0.95$ Å) after the isotropic refinement of the displacement parameters, and most of the OH and H_2O hydrogens were found from the residual electron density map after the anisotropic refinement of the displacement parameters. All hydrogens were refined as riding atoms with fixed isotropic displacement parameters $B = 5.00$ Å^2. After all atoms in the complex molecules had been determined, the R-values were still 0.054 (SO_4) and 0.037 (CrO_4), and the maxima in residual electron density maps were 2.89 e Å^{-3} (SO_4) and 1.42 e Å^{-3} (CrO_4). A closer analysis of the difference Fourier map showed that the terminal hydroxymethyi groups in both compounds were disordered, having two possible orientations. The multiplicities were found by presuming that the isotropic displacement parameters of both orientations would be equal in magnitude. In the sulfate com

Table 2. Crystallographic experimental data for $[Cu(trisH_{-1})(tris)(H_2O)]_2SO_4$ (**1**) and $[Cu(trisH_{-1})(tris)(H_2O)]_2CrO_4$ (**2**).

	1	**2**
Unit cell determination:		
Formula	$Cu_2SO_{18}N_4C_{16}H_{46}$	$Cu_2CrO_{18}N_4C_{16}H_{46}$
Formula weight	741.71	761.64
Color	Blue	Green
Crystal size/mm	0.18×0.15×0.13	0.23×0.15×0.05
T/°C	21±1	21±1
Reflections for lattice measurement	25	25
θ-Range for lattice measurement/°	5–12	8–13
a/Å	6.213(2)	6.424(1)
b/Å	11.009(4)	10.735(1)
c/Å	11.248(1)	21.578(2)
α/°	70.88(1)	98.60(1)
β/°	72.87(2)	89.97(1)
γ/°	79.67(2)	72.63(1)
V/Å^3	691.76(3)	1402.5(3)
Z	1	2
d_{calc}/g cm^{-3}	1.78	1.80
λ(Mo$K\alpha$)/Å	0.71073	0.71073
μ(Mo$K\alpha$)/cm^{-1}	16.98	19.62
F(000)	388	792
Space group	$P\bar{1}$	$P\bar{1}$
Data collection and refinement:		
θ-Range for data collection/°	2–25	2–30
Scan method	ω/2θ	ω/θ
Scan speed in ω/° min^{-1}	1.03–16.50	0.79–5.50
Scan width in ω/°	0.50+0.34 tan θ	0.70+0.34 tan θ
No. of measured reflections	2438	8131
Reflections used in refinement, $I > 3\sigma(I)$	2169	4698
Absorption correction (min./max.)	0.98/1.02	0.84/1.27
Max. shift/error	0.00	0.00
Max. in final Δρ/e Å^{-3}	0.68	0.45
No. of parameters refined	223	424
R	0.032	0.033
R_w [a]	0.040	0.035
$S=[\Sigma w(F_o-F_c)^2/(n-m)]^{1/2}$	1.018	1.332

[a] $w = 1/\sigma^2(F_o)$.

Table 3. Atomic positional parameters and equivalent isotropic displacement parameters[a] with e.s.d.s in parentheses for $[Cu(trisH_{-1})(tris)(H_2O)]_2SO_4$ (**1**).

Atom	*x*	*y*	*z*	B_{eq}/Å^2
Molecule				
Cu100	0.14192(7)	0.51101(4)	0.18142(4)	1.202(8)
OW100	0.5269(4)	0.5125(3)	0.1513(3)	2.77(7)
O111	0.0574(4)	0.6557(2)	0.0379(2)	1.61(5)
O112[b]	0.3640(8)	0.8352(5)	0.2093(5)	5.2(1)
O1128[c]	0.283(2)	0.9464(9)	0.049(1)	3.2(3)
O113[b]	−0.1993(8)	0.9808(4)	0.1866(4)	3.4(1)
O1138[c]	−0.288(2)	0.811(1)	0.351(1)	5.0(3)
O121	0.1839(4)	0.3879(2)	0.0866(2)	1.41(5)
O122	−0.2076(5)	0.1936(3)	0.4560(3)	3.03(7)
O123	0.3203(7)	0.0178(3)	0.3386(3)	4.37(9)
N111	0.0598(6)	0.6439(3)	0.2758(3)	1.85(7)
N121	0.1514(5)	0.3577(3)	0.3382(3)	1.48(6)
C111	−0.0690(6)	0.7618(3)	0.0836(3)	1.84(8)
C112	0.0310(6)	0.7751(3)	0.1872(3)	1.57(7)
C113	0.2615(7)	0.8278(4)	0.1240(4)	2.91(9)
C114	−0.1317(7)	0.8610(4)	0.2646(4)	2.53(9)
C121	0.279(6)	0.2692(3)	0.1567(3)	1.63(7)
C122	0.1572(6)	0.2384(3)	0.3026(3)	1.32(7)
C123	−0.0834(6)	0.2108(4)	0.3241(4)	2.14(8)
C124	0.2881(7)	0.1267(4)	0.3818(4)	2.29(9)
Sulfate				
S1	0.500	0.500	0.500	1.95(3)
O1[d]	0.487(1)	0.4062(7)	0.6332(6)	4.1(2)
O2[d]	0.2496(9)	0.5189(7)	0.4972(5)	3.3(1)
O3[d]	0.554(1)	0.6221(6)	0.5039(7)	4.3(2)
O4[d]	0.623(1)	0.4515(7)	0.3991(6)	5.2(2)

[a] $B_{eq}=\frac{4}{3}\Sigma_i\Sigma_j\beta_{ij}\boldsymbol{a}_i\cdot\boldsymbol{a}_j$. [b] pp=0.72. [c] pp=0.28. [d] pp=0.50.

pound the molecule has two disordered hydroxymethyl groups, and the multiplicities of these orientations are 72 and 28% for molecules A and B, respectively. In the chromate compound there is one disordered hydroxymethyl group in each molecule; in this case multiplicities of 84% (molecules 1A and 2A) and 16% (molecules 1B and 2B) were found. The hydrogens of these disordered hydroxy groups were not found from the difference Fourier map. When the disorder was included in the model, the major peaks in the final difference Fourier map were located close to the copper atoms and sulfate or chromate ions. The sulfate structure was also solved in the non-centrosymmetric space group *P*1 to confirm the disorder.

All calculations were done on a MicroVAX 3100 computer with the MolEN[8] structure-determination package. The atomic scattering factors and real and imaginary dispersion corrections for scattering factors were taken from Ref. 9. The figures were drawn with the SCHAKAL program.[10] The final atomic positional parameters and equivalent isotropic displacement parameters are given in Tables 3 and 4. The relevant molecular bond distances and angles for the complexes and anions are listed in Tables 5 and 6. Tables of anisotropic displacement parameters, coordinates of hydrogen atoms and listings of observed and calculated structure factors are available from the authors upon request.

Results and discussion

Thermal analysis. The thermal behavior of the compounds, determined in air and nitrogen atmospheres, is summarized in Table 1.

Molecular structures. The molecular structures of the complexes are presented in Figs. 1 and 2, and the bond lengths and angles characterizing the molecules are listed in Tables 5 and 6.

The complex molecules in both structures are mononuclear cation complexes with two tris ligands (one of them deprotonated) and one water molecule coordinated to the copper atom. The coordination sphere around copper is square-pyramidal five-coordination with tris molecules in the basal plane (*cis* configuration) and a water molecule occupying the apical position.

In the sulfate compound the metal–ligand distances in the equatorial plane range from 1.924(3) (Cu–O) to 2.009(2) Å (Cu–N), and the apical bond with water is a little longer 2.317(3) Å (Cu–OW). In the square pyramid the deviations of O111, N111, O121 and N121 from the least-squares plane differ by from 0.059(3) to 0.064(3) Å and the copper atom is displaced 0.1694(5) Å from this plane towards the apex of the pyramid. The five-membered chelate rings have an *envelope* conformation, where C112 and C122 are the atoms bent out of the planes.

Table 4. Atomic positional parameters and equivalent isotropic displacement parameters [a] with e.s.d.s in parentheses for $[Cu(trisH_{-1})(tris)(H_2O)]_2CrO_4$ (**2**).

Atom	*x*	*y*	*z*	B_{eq}/Å^2
Molecule 1				
Cu100	0.23135(6)	0.99737(4)	0.90917(2)	1.328(7)
OW100	0.5878(4)	0.9934(3)	0.9241(1)	2.75(6)
O111	0.2050(4)	0.8435(2)	0.9449(1)	1.72(4)
O112	0.7450(4)	0.6711(3)	0.8096(2)	3.15(6)
O113	0.3717(5)	0.5093(3)	0.7952(1)	3.13(6)
O121	0.1334(4)	1.1153(2)	0.9873(1)	1.50(4)
O122[b]	−0.3005(6)	1.4023(4)	0.9601(2)	3.37(8)
O122B[c]	−0.241(3)	1.322(2)	0.8557(9)	3.3(4)
O123	0.3264(5)	1.3817(3)	0.8929(2)	3.08(6)
N111	0.2988(5)	0.8685(3)	0.8295(1)	1.86(6)
N121	0.1716(5)	1.1610(3)	0.8685(1)	1.75(5)
C111	0.2066(6)	0.7338(3)	0.8981(2)	1.91(6)
C112	0.3556(5)	0.7303(3)	0.8421(1)	1.29(5)
C113	0.5929(6)	0.6837(4)	0.8598(2)	2.16(7)
C114	0.3156(6)	0.6415(3)	0.7841(2)	1.92(6)
C121	0.1512(5)	1.2421(3)	0.9791(2)	1.65(6)
C122	0.0597(5)	1.2769(3)	0.9164(2)	1.53(6)
C123	−0.1836(6)	1.2942(4)	0.9152(2)	2.46(8)
C124	0.1017(6)	1.4030(4)	0.9024(2)	2.16(7)
Molecule 2				
Cu200	0.22865(6)	1.00264(4)	0.59082(2)	1.334(7)
OW200	0.5803(4)	1.0069(3)	0.5760(1)	2.82(6)
O211	0.0482(4)	1.1571(2)	0.5549(1)	1.67(4)
O212	0.4153(4)	1.3287(3)	0.6904(2)	3.16(6)
O213	−0.1193(5)	1.4904(3)	0.7048(1)	3.19(7)
O221	0.2489(4)	0.8848(2)	0.5128(1)	1.50(4)
O222[b]	0.1022(6)	0.5981(4)	0.5399(2)	3.35(8)
O222B[c]	0.079(3)	0.681(2)	0.6431(9)	3.1(4)
O223	0.7085(5)	0.6184(3)	0.6073(2)	3.18(6)
N211	0.1680(5)	1.1316(3)	0.6704(1)	1.79(5)
N221	0.3327(5)	0.8387(3)	0.6314(1)	1.72(5)
C211	−0.0589(6)	1.2660(4)	0.6021(2)	1.91(7)
C212	0.0850(5)	1.2697(3)	0.6579(1)	1.35(5)
C213	0.2763(6)	1.3169(4)	0.6405(2)	2.20(7)
C214	−0.0426(6)	1.3584(4)	0.7158(2)	1.91(7)
C221	0.3927(6)	0.7585(3)	0.5209(2)	1.69(6)
C222	0.3369(5)	0.7225(3)	0.5836(2)	1.54(6)
C223	0.1095(6)	0.7063(4)	0.5849(2)	2.32(7)
C224	0.5043(6)	0.5967(4)	0.5972(2)	2.18(7)
Chromate				
Cr1	0.74858(9)	1.00001(7)	0.74999(3)	1.708(9)
O1[d]	0.684(1)	1.1016(6)	0.6945(3)	3.0(1)
O2[d]	1.006(1)	0.9217(9)	0.7370(3)	5.2(2)
O3[d]	0.710(1)	1.0815(8)	0.8190(3)	5.9(2)
O4[d]	0.603(1)	0.8984(6)	0.7404(3)	4.2(1)
O5[d]	0.785(1)	0.8988(6)	0.8050(3)	3.1(1)
O6[d]	0.500(1)	1.1019(8)	0.7592(3)	4.1(2)
O7[d]	0.790(2)	0.918(1)	0.6815(4)	6.3(2)
O8[d]	0.927(1)	1.0790(7)	0.7628(3)	5.3(1)

[a] See Table 3. [b] pp=0.84. [c] pp=0.16. [d] pp=0.50.

These carbons are located at the opposite sides of the coordination plane, leading to an *anti* conformer. Furthermore, the terminal hydroxymethyl groups can take an axial or an equatorial position in relation to this chelate plane. On the non-deprotonated side of the complex both terminal hydroxy groups are disordered, having two possible orientations with multiplicities of 0.72 and 0.28. The orientations refer to two different ways of forming hydrogen bonds with the neighboring groups. The angles between these different orientations are 96.8(8)° (O112–C113–O112B) and 112.7(7)° (O113–C114–O113B). The dihedral angle between the chelate planes is 13.5(3)°.

The asymmetric unit of the chromate compound contains two almost identical complex molecules (Fig. 2),

Table 5. Bond distances (in Å) with e.s.d.s in parentheses for $[Cu(trisH_{-1})(tris)(H_2O)]_2SO_4$ (**1**) and $[Cu(trisH_{-1})(tris)(H_2O)]_2CrO_4$ (**2**).

Bond distance	1	2	Bond distance	2
Cu100–OW100	2.317(3)	2.301(3)	Cu200–OW200	2.297(3)
Cu100–O111	1.983(2)	1.975(3)	Cu200–O211	1.983(2)
Cu100–O121	1.924(3)	1.930(2)	Cu200–O221	1.928(2)
Cu100–N111	1.990(3)	1.997(3)	Cu200–N211	1.997(3)
Cu100–N121	2.009(2)	2.016(3)	Cu200–N221	2.017(3)
O111–C111	1.439(4)	1.429(4)	O211–C211	1.428(4)
O112–C113	1.328(8)	1.421(5)	O212–C213	1.414(5)
O112B–C113	1.31(1)	–	–	–
O113–C114	1.394(5)	1.414(5)	O213–C214	1.412(5)
O113B–C114	1.22(1)	–	–	–
O121–C121	1.412(4)	1.435(4)	O221–C221	1.430(4)
O122–C123	1.423(5)	1.411(5)	O222–C223	1.411(5)
O122B–C123	–	1.39(2)	O222B–C223	1.35(2)
O123–C124	1.397(6)	1.402(5)	O223–C224	1.411(5)
N111–C112	1.477(4)	1.486(4)	N211–C212	1.485(4)
N121–C122	1.485(5)	1.488(4)	N221–C222	1.489(4)
C111–C112	1.529(6)	1.531(5)	C211–C212	1.522(5)
C112–C113	1.523(6)	1.523(5)	C212–C213	1.528(5)
C112–C114	1.533(5)	1.527(5)	C212–C214	1.523(4)
C121–C122	1.540(4)	1.529(5)	C221–C222	1.531(5)
C122–C123	1.512(6)	1.519(5)	C222–C223	1.522(5)
C122–C124	1.523(5)	1.528(6)	C222–C224	1.523(5)
Sulfate or chromate (X=S, Cr)				
X–O1	1.505(6)	1.707(6)		
X–O2	1.541(6)	1.621(6)		
X–O3	1.461(8)	1.589(7)		
X–O4	1.376(8)	1.626(8)		
X–O5	–	1.696(7)		
X–O6	–	1.635(6)		
X–O7	–	1.580(7)		
X–O8	–	1.620(8)		

both having one disordered hydroxy group (O122 and O222) on the deprotonated side of the complex, and the multiplicities of these two possible orientations are 0.84 (molecules 1A and 2A) and 0.16 (molecules 1B and 2B). In the five-coordination spheres of copper atoms the metal–ligand distances are in the range 1.93–2.02 Å, where the shortest bond length refers to the covalent coordination bond of the alkoxy group. The apical coordination bonds with water are 2.301(3) and 2.297(3) Å in molecules 1 (Cu100–OW100) and 2 (Cu200–OW200), respectively. In the square-pyramidal structure the deviations of the oxygen and nitrogen atoms from the least-squares plane range from 0.079(3) to 0.087(3) Å, and the corresponding distances of the copper atoms from that plane towards the apex of the pyramid are 0.1898(4) and 0.1873(4) Å for molecules 1 and 2, respectively. The conformation of the five-membered chelate rings is also *anti* as in the sulfate compound. The dihedral angle between the chelate planes is 13.7(2)° in both complex molecules, and the angles between the two orientations of the disordered hydroxy groups are 109.1(8)° (O122–C123–O122B) and 109.7(10)° (O222–C223–O222B).

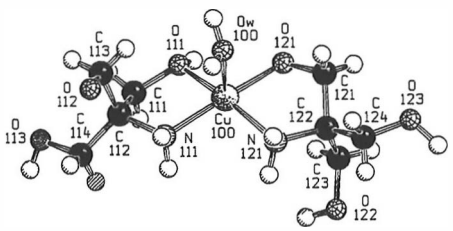

Fig. 1. SCHAKAL drawing of the cation complex A (72%) in $[Cu(trisH_{-1})(tris)(H_2O)]_2SO_4$ (**1**).

The complex molecules in the sulfate and chromate compounds are optically active with two possible enantiomers. Because the syntheses are not stereoselective, the product is a racemic mixture, and the compounds crystallize in centrosymmetric space groups where both enantiomers are present in equal amounts. The bond lengths and angles obtained for the molecules are consistent with the previously reported structures of copper–tris complexes.[4,5]

Crystal structures. Stereoscopic projections of the crystal structures and the hydrogen bonding framework for both compounds are presented in Figs. 3 and 4.

Very often sulfate and chromate compounds have isomorphic structures, because the anions share the same

Table 6. Bond angles (in °) with e.s.d.s in parentheses for $[Cu(trisH_{-1})(tris)(H_2O)]_2SO_4$ (**1**) and $[Cu(trisH_{-1})(tris)(H_2O)]_2CrO_4$ (**2**).

Angle	1	2	Angle	2
O111–Cu100–O121	92.6(1)	92.6(1)	O211–Cu200–O221	92.56(9)
O111–Cu100–OW100	106.0(1)	104.1(1)	O211–Cu200–OW200	104.1(1)
O111–Cu100–N111	83.3(1)	83.1(1)	O211–Cu200–N211	83.1(1)
O111–Cu100–N121	166.7(1)	164.3(1)	O211–Cu200–N221	164.4(1)
O121–Cu100–N111	172.8(1)	172.8(1)	O221–Cu200–N211	172.9(1)
O121–Cu100–N121	86.3(1)	86.5(1)	O221–Cu200–N221	86.4(1)
N111–Cu100–N121	96.4(1)	96.1(1)	N211–Cu200–N221	96.3(1)
Cu100–O111–C111	111.7(2)	113.1(2)	Cu200–O211–C211	112.6(2)
Cu100–O121–C121	108.5(2)	107.5(2)	Cu200–O221–C221	107.5(2)
Cu100–N111–C112	111.7(2)	111.2(2)	Cu200–N211–C212	111.3(2)
Cu100–N121–C122	108.8(2)	108.0(2)	Cu200–N221–C222	108.2(2)
O111–C111–C112	108.2(3)	109.2(3)	O211–C211–C212	109.7(2)
O112–C113–C112	113.3(4)	113.5(3)	O212–C213–C212	113.6(3)
O112B–C113–C112	121.8(6)	–	–	–
O113–C114–C112	113.6(3)	109.9(3)	O213–C214–C212	110.1(3)
O113B–C114–C112	117.0(7)	–	–	–
O121–C121–C122	110.4(3)	109.7(3)	O221–C221–C222	110.2(2)
O122–C123–C122	111.6(4)	110.7(3)	O222–C223–C222	109.9(3)
O122B–C123–C122	–	104.9(8)	O222B–C223–C222	105.0(8)
O123–C124–C122	111.1(4)	110.1(3)	O223–C224–C222	110.1(3)
N111–C112–C111	106.6(3)	105.8(2)	N211–C212–C211	106.0(3)
N111–C112–C113	109.0(3)	110.1(3)	N211–C212–C213	109.7(2)
N111–C112–C114	109.1(3)	109.3(3)	N211–C212–C214	109.5(3)
N121–C122–C121	105.7(3)	105.7(2)	N221–C222–C221	105.2(3)
N121–C122–C123	108.5(3)	107.6(3)	N221–C222–C223	107.1(3)
N121–C122–C124	110.1(3)	111.6(3)	N221–C222–C224	111.9(3)
C111–C112–C113	110.0(3)	109.2(3)	C211–C212–C213	109.4(3)
C111–C112–C114	110.4(3)	111.4(3)	C211–C212–C214	111.8(2)
C113–C112–C114	111.5(4)	110.9(2)	C213–C212–C214	110.4(3)
C121–C122–C123	109.8(3)	111.6(3)	C221–C222–C223	111.5(3)
C121–C122–C124	110.5(3)	111.0(3)	C221–C222–C224	111.3(3)
C123–C122–C124	112.0(3)	109.3(3)	C223–C222–C224	109.7(3)
Sulfate or chromate (X=S, Cr)				
O1–X–O2	100.7(3)	105.3(4)		
O1–X–O3	106.9(4)	111.6(3)		
O1–X–O4	114.5(4)	108.7(3)		
O5–X–O6	–	108.9(3)		
O5–X–O7	–	111.2(4)		
O5–X–O8	–	105.6(4)		

charge and tetrahedral geometry. In this case the sulfate and chromate compounds proved to be non-isomorphic, even though they possess many similarities in structure.

Both structures consist of anions and hydrogen-bonded cationic dimers, which contain the optically active complex and its enantiomer. The dimer has a step-like structure (in which there is an inversion center in the middle of the eight-membered ring) and the apical water ligands are pointing outwards. The hydrogen bonds in the dimer include the deprotonated hydroxy groups, so the donor–acceptor distances are short [O···O distances 2.525(4) Å (SO_4) and 2.509(3)–2.510(3) Å (CrO_4)]. The corresponding Cu···Cu distances in the dimers are 4.9866(7) Å (SO_4) as well as 4.9012(6) and 4.9031(6) Å (CrO_4).

In both structures the anions (SO_4^{2-} and CrO_4^{2-}) are disordered, having two centrosymmetrically related orientations, where the multiplicities for oxygen atoms are 0.50. The sulfate anion is in a special position, and the other

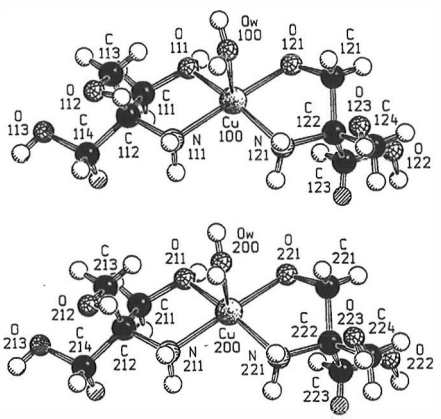

Fig. 2. SCHAKAL drawings of the cation complexes 1A and 2A (84%) in $[Cu(trisH_{-1})(tris)(H_2O)]_2CrO_4$ (**2**).

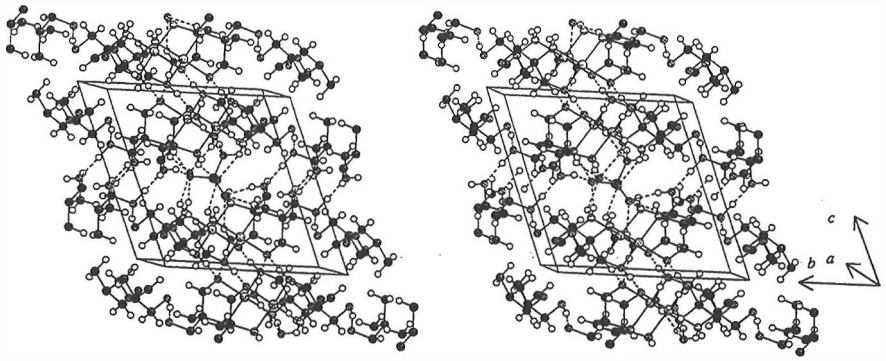

Fig. 3. Stereoscopic representation of hydrogen bonding for $[Cu(trisH_{-1})(tris)(H_2O)]_2SO_4$ (**1**) (molecule A, 72%). Hydrogen bonds are indicated by dashed lines, and sulfate is shown in one of the two centrosymmetric orientations.

set of oxygens is generated by symmetry, whereas the chromate anion is in a general position and has two sets of oxygens (O1–O4 and O5–O8). The geometry of both anion types is not regular, indicating that the hydrogen-bonding surroundings are different for each oxygen.[11,12] Nevertheless, the average bond lengths and angles (SO_4, 1.47 Å and 107°; CrO_4, 1.63 Å and 109°) are normal for these anions.[11–14]

The differences in the structures arise from the fact that the unit cell of the sulfate compound contains only one dimer, whereas the unit cell of the chromate compound contains two dimers,of which one is tilted around to form almost a mirror image of the other (see packing diagrams in Figs. 5 and 6). The reason for this non-isomorphic packing lies in the difference of the anion size and therefore changes in the hydrogen-bonding network.

In both structures the dimers are stacked along the *a*-direction and polymerized by OW100–HW···O121′ (OW200–HW···O221′) and O122–H···O123′ (O222–H···O223′) hydrogen bonds. The dimers have their amino groups oriented towards the sulfate or chromate ions, and the anions connect the dimers with N–H···O(SO_4 or CrO_4) hydrogen bonds in the *a*- and *c*-directions. The coordinated water molecule also forms hydrogen-bonded chains with the sulfate or chromate ions in the *c*-direction, like the OW100–HW···O1–S–

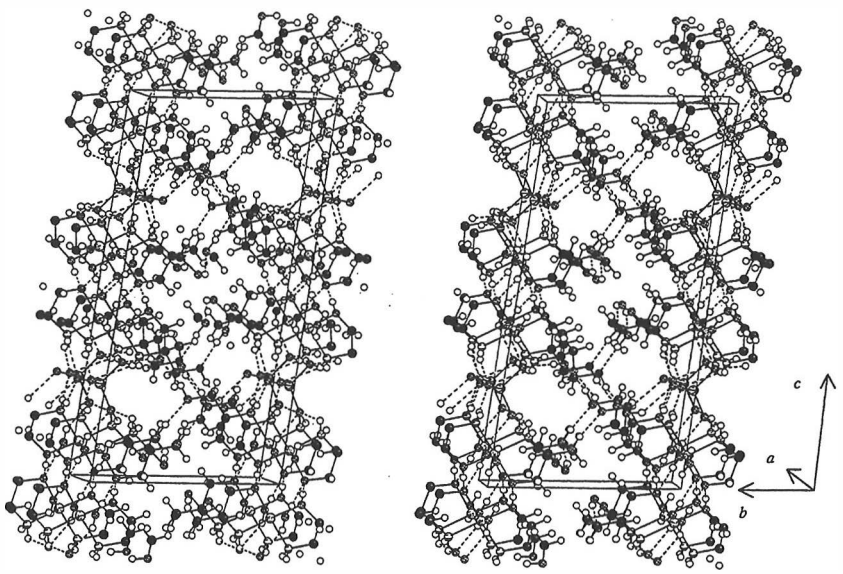

Fig. 4. Stereoscopic representation of hydrogen bonding for $[Cu(trisH_{-1})(tris)(H_2O)]_2CrO_4$ (**2**) (molecules 1A and 2A, 84%). Hydrogen bonds are indicated by dashed lines, and chromate is shown in one of the two centrosymmetric orientations.

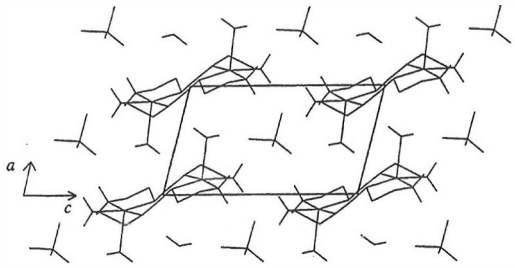

Fig. 5. Packing diagram of the dimers and anions in $[Cu(trisH_{-1})(tris)(H_2O)]_2SO_4$ (**1**). Terminal hydroxymethyl groups are omitted for clarity, and anions are shown in one orientation.

O4···HW′–OW100′ chain in the sulfate compound and OW100–HW···O3–Cr–O1···HW–OW200 and OW100–HW···O5–Cr–O7···HW–OW200 chains in the chromate compound. In the *bc*-plane the interactions are mainly hydrogen bonds between terminal hydroxymethyl groups or weak van der Waals forces between $CH_2\cdots CH_2$ groups. The hydrogen bonding of disordered hydroxy groups is not included because these hydrogens could not be located from the difference Fourier map, but otherwise all H_2O, OH and NH_2 hydrogens are involved in the hydrogen-bonding network.

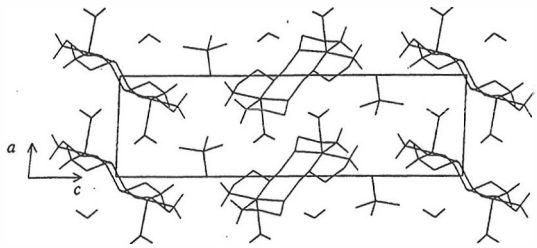

Fig. 6. Packing diagram of the dimers and anions in $[Cu(trisH_{-1})(tris)(H_2O)]_2CrO_4$ (**2**). Terminal hydroxymethyl groups are omitted for clarity, and anions are shown in one orientation.

References

1. Ramette, R. W., Culberson, C. H. and Bates, R. G. *Anal. Chem. 49* (1977) 867.
2. *Sigma Technical Bulletin, No 106B*, Sigma Chemical Co., St. Louis, MO.
3. Dotson, R. L. *J. Inorg. Nucl. Chem. Lett. 9* (1973) 215.
4. Kotila, S. and Valkonen, J. *Acta Chem. Scand. 47* (1993) 950.
5. Kotila, S. and Valkonen, J. *Acta Chem. Scand. 47* (1993) 957.
6. Walker, N. and Stuart, D. *Acta Crystallogr., Sect. A 39* (1983) 158.
7. Sheldrick, G. M. In: Sheldrick, G. M., Krüger, C. and Goddard, R., Eds., *Crystallographic Computing 3*, Oxford University Press., Oxford 1985, pp. 175–189.
8. *MolEN, An Interactive Structure Solution Procedure*, Enraf-Nonius, Delft, The Netherlands 1990.
9. *International Tables for X-Ray Crystallography*, Kynoch Press, Birmingham 1974, Vol. 4.
10. Keller, E. *SCHAKAL, a FORTRAN Program for the Graphic Representation of Molecular and Crystallographic Models*, University of Freiburg, Freiburg 1987.
11. Meester, P. and Skapski, A. C. *J. Chem. Soc., Dalton Trans* (1973) 1596.
12. Sletten, E. and Thorstensen, B. *Acta Crystallogr., Sect. B 30* (1974) 2438.
13. Brauer, C., Jannin, M., Puget, R. and Perret, R. *Acta Crystallogr., Sect. C 47* (1991) 2231.
14. Pressprich, M. R., Willett, R. D., Poshusta, R. D., Saunders, S. C., Davis, H. B. and Gard, G. L. *Inorg. Chem. 27* (1988) 260.

Received August 29, 1993.

PAPER IV

(Reprinted by the permission of *Acta Chemica Scandinavica*)

https://eurekamag.com/research/082/717/082717838.php

Acta Chemica Scandinavica, 1994: 48: 312–318
Printed in Belgium – all rights reserved

ACTA
CHEMICA SCANDINAVICA
ISSN 0904–213X

Copper(II) Complexes of 2-Amino-2-hydroxymethyl-1,3-propanediol. Part 4. Synthesis, Structure and Thermal Behavior of *trans*-Bis[2-amino-2-hydroxymethyl-1,3-propanediolato-*O,N*]copper(II) Potassium Fuoride and Bromide, $[Cu(C_4H_{10}NO_3)_2]KF \cdot 3H_2O$ and $[Cu(C_4H_{10}NO_3)_2]KBr \cdot 2H_2O$

Sirpa Kotila* and Jussi Valkonen

Department of Chemistry, University of Jyväskylä, FIN-40500 Jyväskylä, Finland

Kotila, S. and Valkonen, J., 1994. Copper(II) Complexes of 2-Amino-2-hydroxymethyl-1,3-propanediol. Part 4. Synthesis, Structure and Thermal Behavior of *trans*-Bis[2-amino-2-hydroxymethyl-1,3-propanediolato-*O,N*]copper(II) Potassium Fluoride and Bromide, $[Cu(C_4H_{10}NO_3)_2]KF \cdot 3H_2O$ and $[Cu(C_4H_{10}NO_3)_2]KBr \cdot 2H_2O$. – Acta Chem. Scand. 48: 312–318 © Acta Chemica Scandinavica 1994.

Crystal structures of two copper(II) potassium halides with 2-amino-2-hydroxymethyl-1,3-propanediol (= tris, deprotonated form abbreviated $trisH_{-1}$) as a ligand have been determined from single-crystal X-ray data and refined to the final *R* values of 0.040 (F^-) and 0.036 (Br^-). The compounds are almost isomorphic except that the fluoride compound has disordered fluoride ions and an extra disordered water molecule. The compounds crystallize in the orthorhombic space group *Pcca* (No. 54) with four molecules in a unit cell. Crystal data for $[Cu(trisH_{-1})_2]KF \cdot 3H_2O$ are as follows: $a = 18.814(2)$, $b = 9.623(1)$, $c = 8.678(2)$ Å, $V = 1571.2(4)$ Å^3; and for $[Cu(trisH_{-1})_2]KBr \cdot 2H_2O$: $a = 18.482(2)$, $b = 9.805(1)$, $c = 8.776(3)$ Å, $V = 1590.4(5)$ Å^3.

The structure is a tunnel compound with neutral copper–tris complexes (square-planar *trans* coordination of nitrogen and oxygen) polymerized by hydrogen bonding in the *c*-direction forming hydrophobic and hydrophilic cavities along the same axis. Potassium occupies the hydrophilic cavity and is surrounded by eight oxygens with K–O distances 2.776(5)–2.988(4) Å. Halogenides are located in the hydrophobic cavity. The three-dimensional network consists of hydrogen bonds and the coordination bonds of potassium linking the complex molecules together. Thermal behaviour is characterized by TG in air and nitrogen atmospheres.

2-Amino-2-hydroxymethyl-1,3-propanediol (tris) also known as tris(hydroxymethyl)aminomethane (tham) or commercially as Trizma Base, is a widely used buffering agent in biochemical studies[1] in the physiological pH range 7–9.

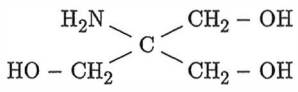

Tris chelates with transition metals are usually formed via amino and one or two hydroxymethyl groups. The reaction of aminoalcohols with metal cations also yields deprotonated complexes with coordinated alkoxy groups, and these deprotonated species are abbreviated $trisH_{-1}$.

We are especially interested in solid tris compounds with copper(II) as a metal cation. In our earlier articles we have reported the synthesis, structures and thermal behavior of three *trans* complexes, $[Cu(trisH_{-1})_2]$, $[Cu(trisH_{-1})_2(H_2O)]$ and $[Cu(trisH_{-1})_2] \cdot 5H_2O$,[2] and four *cis* compounds, $[Cu(trisH_{-1})(tris)(NO_3)]$,[3] $[Cu(trisH_{-1})(tris)]Na(ClO_4)_2$,[3] $[Cu(trisH_{-1})(tris)(H_2O)]_2SO_4$,[4] and $[Cu(trisH_{-1})(tris)(H_2O)]_2CrO_4$.[4] The structures of the following copper–tris complexes are also known, $[Cu(trisH_{-1})_2]NaClO_4 \cdot H_2O$,[5] $[Cu(trisH_{-1})Cl]_4$,[6] and $[Cu(trisH_{-1})(tris)]_2Br_2$.[6] In this paper we present two new tris compounds containing two metal cations and having a tunnel structure, namely $[Cu(trisH_{-1})_2]KF \cdot 3H_2O$ and $[Cu(trisH_{-1})_2]KBr \cdot 2H_2O$.

* To whom correspondence should be addressed.

Experimental

Preparation of $[Cu(trisH_{-1})_2]KX\cdot nH_2O$, where $X = F^-$ (n = 3), Br^- (n = 2). Both compounds were prepared by the same procedure using $CuF_2\cdot 2H_2O$ (Fluka, min. 97%) or $CuBr_2$ (B.D.H. Ltd., min. 98%) as starting materials. The reaction was also tested with copper(II) chloride, but under these conditions tris forms polynuclear complexes giving a green tetramer, $[Cu(trisH_{-1})Cl]_4$,[6] as a product. Attempts to prepare similar sodium compounds using NaOH in the reaction were not successful either.

A 250 cm^3 round-bottomed, two-neck flask was fitted with a refluxing condenser and a thermometer. Into the flask 0.015 mol of tris (Sigma, 99–99.5%) was placed and dissolved in 40 cm^3 of ethanol by refluxing. At the same time 0.0075 mol of copper(II) halide was dissolved separately in 30 cm^3 of ethanol by heating. The warm copper halide solution was added to the tris solution, the reaction temperature was raised to 70°C, and the mixture was maintained at this temperature for 5 min. The reaction was then cooled to 45°C, the clear solution was separated from the undissolved copper halide by decantation, and the solution was made alkaline with KOH (Riedel-de-Haën, 0.015 mol KOH in 30 cm^3 EtOH). The solution was filtered with a sintered glass crucible and allowed to crystallize at room temperature; needle-shaped brownish crystals were obtained as a product. The first crystal fraction appearing within 2 h is usually of poor quality and not suitable for a single-crystal determination. After 2 h the mother liquor was decanted to another Erlenmeyer flask, and a few drops of water were added to the solution. The second fraction, crystallizing overnight, yields crystals of a better size and quality for X-ray measurements. The compounds are not very stable; if they are ground into powder and kept in an air atmosphere, they slowly transform into the blue monohydrate complex, $[Cu(trisH_{-1})_2(H_2O)]$,[2] and potassium halide (confirmed by IR).

Possible side-products in the reaction are the anhydrous and monohydrate *trans* complexes, $[Cu(trisH_{-1})_2]$ and $[Cu(trisH_{-1})_2(H_2O)]$.[2] The formation of the monohydrate complex is favored especially if the reaction temperature is too high or prolonged heating takes place during the reaction.

Thermal analysis. Thermal behaviour of the complexes in air and nitrogen atmospheres was determined with a Perkin-Elmer thermogravimetric analyzer TGA7. The sample size varied between 3.0 ± 0.3 mg, and the crystalline samples were analyzed with a heating rate 2°C min^{-1} and gas flow 50 cm^3 min^{-1}. Temperature ranges in air and nitrogen atmospheres were 25–950 and 25–900°C, respectively. To remove oxygen from the oven when using nitrogen atmosphere, the equipment was flushed with nitrogen for 30–45 min before the temperature program was initiated. Observed ans theoretical weight losses are reported in Table 1.

Crystal structure determinations. Single-crystal X-ray measurements were made with an Enraf-Nonius CAD-4 diffractometer using MoK_α radiation. The fluoride compound was measured in a glass capillary containing a drop of mother liquor, whereas the crystal of the bromide compound was covered with epoxy glue and mounted on a glass fiber. Crystal data and experimental details are given in Table 2.

Accurate cell constants were obtained by a least-squares analysis of 25 centered reflections. Three reflec-

Table 1. Thermal decomposition of $[Cu(trisH_{-1})_2]KF\cdot 3H_2O$ (**1**) and $[Cu(trisH_{-1})_2]KBr\cdot 2H_2O$ (**2**).

Compound	Lost in reaction	T/°C	Weight loss (%) ΔObs.	ΔTheor.
Air atmosphere				
1	$3\ H_2O$	25–125	11.6	13.0
	Org. (→CuO+KF)	125–503	54.9	53.9
	KF	727–907	11.6	14.0
	Total reaction→CuO	25–950	75.7	80.9
2	$2\ H_2O$	97–145	7.3	7.9
	Org. (→CuO+KBr)	145–525	49.7	48.9
	KBr	625–797	24.9	25.9
	Total reaction→CuO	25–950	83.3	82.7
Nitrogen atmosphere				
1	$3\ H_2O$	25–123	13.0	13.0
	Org. (→CuO+KF)	123–618	50.6	53.9
	$KF+{}^1/_2O_2$	618–891	23.2	17.8
	Total reaction→Cu	25–900	86.8	84.7
2	$2\ H_2O$	84–136	7.9	7.9
	Org. (→Cu+KBr)	136–608	48.0	52.4
	KBr	608–830	25.4	25.9
	Total reaction→Cu	25–900	82.2	86.2

Table 2. Crystallographic experimental data for $[Cu(trisH_{-1})_2]KF\cdot 3H_2O$ (**1**) and $[Cu(trisH_{-1})_2]KBr\cdot 2H_2O$ (**2**).

Compound	**1**	**2**
Unit cell determination		
Formula	$CuKFO_9N_2C_8H_{26}$	$CuBrKO_8N_2C_8H_{24}$
Formula weight	415.94	458.84
Color	Light brown	Brown
Crystal size/mm	0.25×0.20×0.15	0.28×0.03×0.03
T/°C	21±1	21±1
Reflections for lattice measurement	25	25
θ-Range for lattice measurement/°	7–13	4–13
Crystal system	Orthorhombic	Orthorhombic
a/Å	18.814(2)	18.482(2)
b/Å	9.623(1)	9.805(1)
c/Å	8.678(2)	8.776(3)
V/Å^3	1571.2(4)	1590.4(5)
Z	4	4
d_{calc}/g cm^{-3}	1.76	1.92
λ(MoK_α)/Å	0.710 73	0.710 73
μ(MoK_α)/Å	17.11	41.62
F(000)	868	932
Space group	*Pcca*(No. 54)	*Pcca*(No. 54)
Data collection and refinement		
θ range for data collection/°	2–30	2–30
Scan method	ω/2θ	ω/2θ
Scan speed in ω/° min^{-1}	0.92–5.50	0.59–5.50
Scan width in ω/°	0.60+0.34 tan θ	0.50+0.34 tan θ
No. of measured reflections	2630	2662
Reflections used in refinement, $I > 3\sigma(I)$	1339	1132
Absorption correction (min./max.)	0.71/1.41	0.86/1.25
Max. shift/error	0.00	0.00
Max. in final $\Delta\rho$/e Å^{-3}	0.48	0.58
No. of parameters refined	102	98
R	0.040	0.036
R_w[a]	0.048	0.040
$S=[\Sigma w(F_o-F_c)^2/(n-m)]^{1/2}$	2.048	2.381

[a] $w = 1/\sigma^2(F_o)$.

tions were monitored every 60 min as an intensity check, and the crystal orientation was confirmed after every 500 reflections. The total losses in intensity during data collection were 1.0% in 29.8 h (F) and 2.1% in 36.6 h (Br). The data obtained were corrected for linear decay as well as Lorentz and polarization effects. Absorption corrections were made according to Walker and Stuart.[7]

Positions of the heavy atoms (Cu, Br) in the bromide compound were solved by direct methods (SHELXS-86).[8] The remaining non-hydrogen atoms were located by subsequent electron density calculations and refined by full-matrix least-squares methods with anisotropic thermal parameters. The hydrogens attached to carbons and nitrogens were included in their calculated positions after isotropic refinement (C–H, N–H = 0.95 Å), and the hydrogens in hydroxy groups and water molecules were located from a difference Fourier map, after anisotropic refinement. All hydrogens were refined as riding atoms with a fixed isotropic temperature parameter $B = 5.00$ Å^2.

The structure of the bromide compound was determined first because the results from the direct methods were clear. In the case of the fluoride compound, the disorder of fluorides and the smaller number of heavy atoms made it difficult to obtain a conclusive solution from the direct methods, so we took advantage of the fact that the two compounds are almost isomorphic and used the non-hydrogen atom coordinates of the bromide compound as a starting set in the refinement of the fluoride compound.

Table 3. Atomic positional parameters and equivalent isotropic temperature factors[a] with e.s.d.s in parentheses for $[Cu(trisH_{-1})_2]KF\cdot 3H_2O$ (**1**).

Atom	x	y	z	B_{eq}/Å^2
Cu100	0.500	0.000	0.000	1.51(1)
O111	0.4144(2)	−0.0660(3)	−0.0906(4)	1.97(6)
O112	0.3308(2)	0.2703(4)	−0.2336(4)	3.06(7)
O113	0.3237(2)	0.3780(4)	0.1028(4)	2.39(6)
N111	0.4403(2)	0.1493(4)	0.0889(4)	1.61(6)
C111	0.3539(2)	0.0132(5)	−0.0433(5)	1.96(7)
C112	0.3757(2)	0.1618(4)	−0.0058(6)	1.48(6)
C113	0.3947(3)	0.2402(5)	−0.1520(6)	2.06(9)
C114	0.3150(3)	0.2318(5)	0.0815(6)	2.09(8)
K1	0.250	0.500	−0.1407(2)	2.36(2)
F1[b]	0.4644(5)	0.4675(9)	0.097(1)	5.9(2)[c]
OW1	0.3704(2)	0.6733(4)	−0.0329(5)	3.41(8)
OW2[b]	0.4654(6)	0.447(1)	0.160(2)	6.2(3)[c]

[a] $B_{eq} = \frac{4}{3}\Sigma_i \Sigma_j \beta_{ij} \boldsymbol{a}_i \cdot \boldsymbol{a}_j$. [b] Disordered fluoride and water were refined one at a time while the other one was fixed. [c] pp = 0.50.

Table 4. Atomic positional parameters and equivalant isotropic temperature factors[a] with e.s.d.s in parentheses for $[Cu(trisH_{-1})_2]KBr\cdot 2H_2O$ (**2**).

Atom	x	y	z	$B_{eq}/Å^2$
Cu100	0.500	0.000	0.000	1.28(1)
O111	0.4101(2)	−0.0611(4)	−0.0842(5)	1.80(7)
O112	0.3354(2)	0.2836(5)	−0.2120(5)	2.68(9)
O113	0.3265(2)	0.3750(4)	0.1250(5)	2.08(7)
N111	0.4409(2)	0.1420(5)	0.1032(5)	1.48(8)
C111	0.3510(3)	0.0185(6)	−0.0376(6)	1.5(1)
C112	0.3748(3)	0.1615(5)	0.0094(6)	1.20(8)
C113	0.3977(3)	0.2455(6)	−0.1280(7)	1.9(1)
C114	0.3150(3)	0.2320(6)	0.0992(6)	1.6(1)
Br1	0.500	0.44931(8)	0.250	2.42(1)
K1	0.250	0.500	−0.1159(2)	2.05(3)
OW1	0.3704(2)	0.6812(4)	−0.0126(5)	2.50(8)

[a] See Table 3.

After the refinement of the fluoride disorder was complete, the *R*-value was still 0.051, and there was a maximum of 1.28 e Å^{-3} in the residual electron density map, which proved to be an extra disordered water molecule (TG analysis also confirmed the amount of water). The coordinates of these disordered fluorides and water are very close, so simultaneous anisotropic refinement of both atoms was impossible. In all other respects, the procedures for the fluoride and bromide structure determinations were identical.

All calculations were done on a MicroVAX 3100 computer using MolEN[9] software. The atomic scattering factors, including the contribution from anomalous dispersion, were taken from Ref. 10. The figures were drawn with the SCHAKAL[11] program. The final atomic positional parameters and equivalent isotropic temperature factors for non-hydrogen atoms are given in Tables 3 and 4. The molecular bond distances and angles for the complexes are reported in Tables 5 and 6 and the distances associated with the coordination sphere of potassium ion are shown in Table 7. Tables of anisotropic thermal parameters, coordinates of hydrogen atoms and listings of observed and calculated structure factors are available from the authors on request.

Table 5. Bond distances (in Å) with e.s.d.s. in parentheses for $[Cu(trisH_{-1})_2]KF\cdot 3H_2O$ (**1**) and $[Cu(trisH_{-1})_2]KBr\cdot 2H_2O$ (**2**).

Bond	1	2
Cu100–O111	1.901(3)	1.915(4)
Cu100–N111	1.980(4)	1.988(4)
O111–C111	1.429(5)	1.404(6)
O112–C113	1.425(6)	1.418(7)
O113–C114	1.429(6)	1.436(7)
N111–C112	1.472(6)	1.486(7)
C111–C112	1.523(6)	1.526(7)
C112–C113	1.520(7)	1.520(8)
C112–C114	1.526(6)	1.524(7)

Table 6. Bond angles (in °) with e.s.d.s in parentheses for $[Cu(trisH_{-1})_2]KF\cdot 3H_2O$ (**1**) and $[Cu(trisH_{-1})_2]KBr\cdot 2H_2O$ (**2**).

Angle	1	2
O111–Cu100–N111	85.6(1)	85.3(2)
O111–Cu100–N111[a]	94.4(1)	94.7(2)
Cu100–O111–C111	112.3(3)	112.9(3)
Cu100–N111–C112	108.1(3)	106.8(3)
O111–C111–C112	110.4(3)	111.4(4)
O112–C113–C112	108.5(4)	109.2(4)
O113–C114–C112	114.4(4)	114.7(4)
N111–C112–C111	105.3(3)	105.6(4)
N111–C112–C113	108.2(3)	106.3(4)
N111–C112–C114	112.1(4)	111.6(4)
C111–C112–C113	110.5(4)	111.3(4)
C111–C112–C114	108.7(3)	110.3(4)
C113–C112–C114	111.8(4)	111.5(4)

[a] Symmetry operation applied is $-x, -y, -z$.

Table 7. Bond distances (in Å) of potassium coordination sphere for $[Cu(trisH_{-1})_2]KF\cdot 3H_2O$ (**1**) and $[Cu(trisH_{-1})_2]KBr\cdot 2H_2O$ (**2**).

Bond	1	2
K–O112	2.801(4)	2.776(5)
K–O113	2.787(4)	2.822(4)
K–O113'[a]	2.873(4)	2.945(4)
K–OW1	2.965(4)	2.988(4)

[a] Symmetry operation applied is $x, 1-y, z-0.5$.

Results and discussion

Thermal analysis. The thermal behaviour of the complexes under study is summarized in Table 1. The decomposition process of both complexes was very similar in both atmospheres. The degradation happened in four basic steps; first, the crystalline water was dehydrated in one step, the organic part was then decomposed in two phases and finally potassium halide was sublimated at an elevated temperature (600–900 °C). The final product in an air atmosphere was CuO, and metallic copper in a nitrogen atmosphere.

In an air atmosphere the organic part decomposed in two separate steps; the main reaction happened at 125–221 °C (F) or 145–228 °C (Br) and the second, smaller

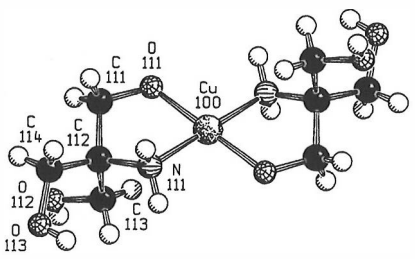

Fig. 1. SCHAKAL projection of the molecule in both structures (coordinates taken from **2**).

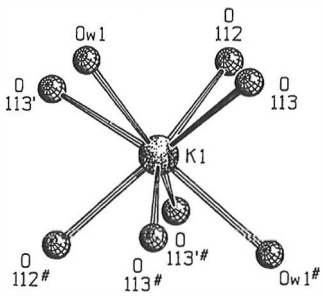

Fig. 2. Coordination sphere of potassium in both structures (coordinates taken from **2**). Symmetry operation applied for O113′ is $x, 1-y, z-0.5$, and the other half of the coordination sphere (marked with #) is generated by symmetry operation $0.5-x, 1-y, z$.

reaction took place at 400–500 °C. In a nitrogen atmosphere these reactions occurred in the same temperature area at 130–280 °C, the result being an overlapped DTG peak with two maxima for the organic ligand. At 280 °C 74.5% (F) or 86.3% (Br) of the organic part has decomposed, and above 280 °C the decomposition of the remaining organic residue was very slow. The sublimation temperature of potassium halide was not much affected by the atmosphere, but the corresponding DTG peaks were narrower in air. Furthermore, the temperature range in which alkaline halides start to sublimate was checked with KBr, NaCl and NaF under the same conditions.

TG analysis clearly shows that the water content of the fluoride compound is higher than in the bromide compound. On the other hand, the crystalline water in the fluoride compound is very easily dehydrated, so the samples must be analyzed immediately after they are removed from the mother liquor.

Molecular structures. The complex molecule of the bromide compound is presented in Fig. 1, and the representative bond lengths and angles for both compounds are listed in Tables 5 and 6. The basic molecular structure in both compounds is a mononuclear neutral complex with two tris ligands coordinated to the copper atom via amino and deprotonated hydroxy groups. The asymmetric unit is half of the molecule, and the other half is generated by inversion with respect to the copper atom. The coordination sphere is a square-planar *trans* coordination, and the metal–ligand distances range from 1.901(3) (Cu–O) to 1.980(4) Å (Cu–N) in the fluoride compound; the corresponding distances in the bromide compound are 1.915(4) and 1.988(4) Å, respectively. The five-membered chelate rings are *envelope* conformers, where Cu100, O111, N111, and C111 define the plane and C112 is bent out of the plane. The deviations of C112 from this plane are 0.583(5) Å for **1** and 0.594(5) Å for **2**, and the whole molecule is an *anti* isomer, where the chelate rings are bent in opposite directions from the coordination plane. The terminal hydroxymethyl groups can take an axial (ax) or an equatorial (eq) position in relation to this chelate plane. The corresponding distances for C113 (ax) and C114 (eq) atoms from the plane are 2.090(5) and 0.196(5) Å in the fluoride compound and 2.095(6) and 0.252(6) Å in the bromide compound.

The bond lengths and angles shown in Tables 5 and 6 coincide with the previously reported structures of copper–tris complexes.[2-6] The molecular structures

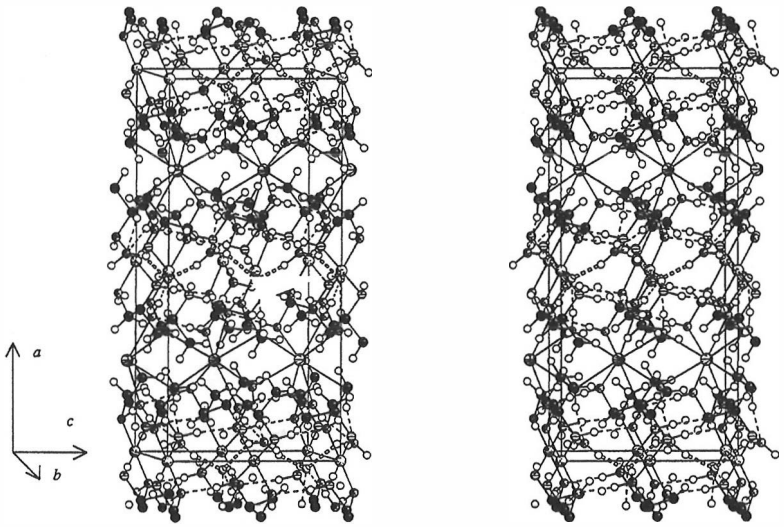

Fig. 3. A stereoscopic representation of $[Cu(trisH_{-1})_2]KF\cdot 3H_2O$ (**1**). Hydrogen bonds are indicated by dashed lines and only one orientation of disordered fluoride and OW2 is shown.

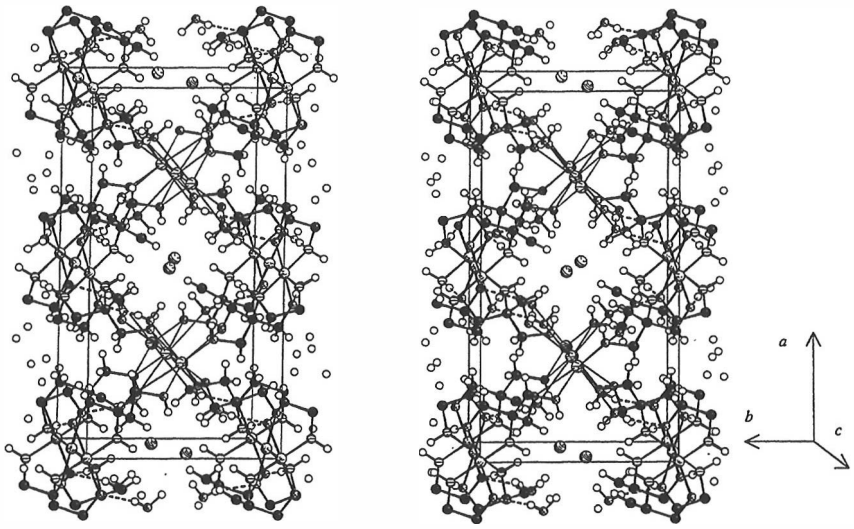

Fig. 4. A stereoscopic representation of $[Cu(trisH_{-1})_2]KBr \cdot 2H_2O$ (**2**). Hydrogen bonds are indicated by dashed lines.

of $[Cu(trisH_{-1})_2]$ and $[Cu(trisH_{-1})_2] \cdot 5H_2O$[2] in particular are almost identical with these complexes, differing mainly in the orientation of the terminal hydroxymethyl groups.

Crystal structures. The coordination sphere of the potassium ion is shown in Fig. 2, and stereoscopic projections of the crystal structures and hydrogen bonding are presented in Figs. 3 and 4.

Both compounds share the same basic structure in which the uncharged molecules are polymerized in the *c*-direction by N111–H···O111′ hydrogen bonds, forming a zigzag chain, and the potassium(I) and halogenide ions occupy the hydrophilic and hydrophobic cavities, formed as a consequence of the polymerization. The crystalline water OW1 also assists in joining the molecules together; with one strong hydrogen bond the water molecule is connected to the deprotonated hydroxy oxygen (OW1–HW···O111), and another hydrogen bond is formed between OW1 and the axial hydroxymethyl group of the adjacent complex molecule (OW1···H′–O112′). In the direction of the *a*-axis the interactions between molecules are weak van der Waals forces between CH_2 groups.

The potassium ion plays a major role in connecting the molecular chains in all three directions. Potassium is located in a special position with multiplicity 4 (the general position has multiplicity 8), and it is surrounded by six hydroxy oxygens and two water molecules. The coordination sphere of potassium can be described as a square-antiprism with K–O distances falling in the range 2.776(5)–2.988(4) Å (Table 7). With these K–O bonds each potassium is directly linking four molecules together, and indirectly two more molecules via hydrogen-bonded crystalline water. Similar K–O bond lengths and geometries have also been observed with other potassium complexes containing alkoxy, ether, carbonyl or amide oxygens and crystalline water.[12–15]

The differences in the structures arise from the halides: their ionic radii and ability to form hydrogen bonds are not the same. The halogenides are located in the hydrophobic cavity where hydrogens are pointing inside the cavity. The bromide ion is large enough to fill the cavity, so there is no disorder, and each bromide is surrounded by six hydrogens with Br–H distances in the range 2.43–2.64 Å. On the other hand, the fluoride anion is so small that there are two centrosymmetrically related positions for fluoride in each cavity with 50% occupational probability. Furthermore, each fluoride is accompanied by an extra water molecule (OW2), which has almost the same coordinates as fluoride. Structurally, this means that in the cavities, every other position is taken by fluoride and every other by water molecule, and the whole hydrophobic tunnel is filled with a hydrogen-bonded chain of fluorides and water molecules, ···F1···HW21–OW2–HW22···F1′···HW21′–OW2′–HW22′···. The chain has two orientations, in which the positions of fluoride and water oxygen are reversed, and the probability of each orientation is 50%. The F···O distances in the chain are 2.494 and 2.721 Å. In addition, this chain forms five hydrogen bonds per each F1 and OW2 pair with terminal hydroxy groups, amino hydrogens and OW1.

References

1. Ramette, R. W., Culberson, C. H. and Bates, R. G. *Anal. Chem. 49* (1977) 867.
2. Kotila, S. and Valkonen, J. *Acta Chem. Scand. 47* (1993) 950.

3. Kotila, S. and Valkonen, J. *Acta Chem. Scand. 47* (1993) 957.
4. Kotila, S. and Valkonen, J. *Acta Chem. Scand. In press.*
5. Ivarsson, G. J. M. *Acta Crystallogr., Sect. C 40* (1984) 67.
6. Masi, D., Mealli, C., Sabat, M., Sabatini, A., Vacca, A. and Zanobini, F. *Helv. Chim. Acta 67* (1984) 1818.
7. Walker, N. and Stuart, D. *Acta Crystallogr., Sect. A 39* (1983) 158.
8. Sheldrick, G. M. In: Sheldrick, G. M., Krüger, C. and Goddard, R., Eds., *Crystallographic Computing 3*, Oxford University Press., Oxford 1985, pp. 175–189.
9. *MolEN, An Interactive Structure Solution Procedure*, Enraf-Nonius, Delft, The Netherlands 1990.
10. *International Tables for X-Ray Crystallography*, Kynoch Press, Birmingham 1974, Vol. 4.
11. Keller, E. *SCHAKAL, a FORTRAN Program for the Graphic Representation of Molecular and Crystallographic Models*, University of Freiburg, Freiburg 1987.
12. Dubourg, A., Fabregue, E., Maury, L. and Declercq, J.-P. *Acta Crystallogr., Sect. C 46* (1990) 1394.
13. Brooker, S., Edelmann, F. T., Kottke, T., Roesky, H. W., Sheldrick, G. M., Stalke, D. and Whitmire, K. H. *J. Chem. Soc., Chem. Commun.* (1991) 144.
14. Calestani, G., Ugozzoli, F., Arduini, A., Ghidini, E. and Ungaro, R. *J. Chem. Soc., Chem. Commun.* (1987) 344.
15. Kaziro, R., Hambley, T. W., Binstead, R. A. and Beattie, J. K. *Inorg. Chim. Acta 164* (1989) 85.

Received 29 August, 1993.

PAPER V
(Proof)

(Reprinted by the permission of *Acta Chemica Scandinavica*)

https://eurekamag.com/research/082/717/082717839.php

Acta Chemica Scandinavica. 1994: 0: 1–11
Printed in Belgium – all rights reserved

ACTA
CHEMICA SCANDINAVICA
ISSN 0904–213X

Copper(II) Complexes of 2-Amino-2-hydroxymethyl-1,3-propanediol. Part 5. Synthesis, Structure and Thermal Behavior of *cis*-[2-Amino-2-hydroxymethyl-1,3-propanediol-*O,O',N*][2-amino-2-hydroxymethyl-1,3-propanediolato-*O,N*]aquacopper(II) Halide Monohydrate, $[Cu(C_4H_{10}NO_3)(C_4H_{11}NO_3)(H_2O)]X\cdot H_2O$, where $X=F^-$, Cl^-, Br^-, I^-

Sirpa Kotila

Department of Chemistry, University of Jyväskylä, FIN-40500 Jyväskylä, Finland

Kotila, S., 1994. Copper(II) Complexes of 2-Amino-2-hydroxymethyl-1,3-propanediol. Part 5. Synthesis, Structure and Thermal Behavior of *cis*-[2-Amino-2-hydroxymethyl-1,3-propanediol-*O,O',N*][2-amino-2-hydroxymethyl-1,3-propanediolato-*O,N*]aquacopper(II) Halide Monohydrate, $[Cu(C_4H_{10}NO_3)(C_4H_{11}NO_3)(H_2O)]X\cdot H_2O$, where $X=F^-$, Cl^-, Br^-, I^-. – Acta Chem. Scand. 0: 1–11 © Acta Chemica Scandinavica 1994.

The structures of the chloride, bromide and iodide compounds with 2-amino-2-hydroxymethyl-1,3-propanediol (= tris) as a ligand have been determined by single-crystal X-ray analysis. The chloride and bromide compounds are isomorphic, with the following crystal data: (Cl^-) triclinic space group $P\bar{1}$ with four complexes in a cell of dimensions $a=6.482(2)$, $b=11.805(1)$, $c=19.767(3)$ Å, $\alpha=88.22(1)$, $\beta=83.67(2)$, $\gamma=90.30(2)°$, $V=1502.6(6)$ Å^3, $R=0.035$ (6084 reflections); (Br^-) $a=6.574(1)$, $b=11.929(2)$, $c=19.792(2)$ Å, $\alpha=88.09(1)$, $\beta=83.43(1)$, $\gamma=89.72(1)°$, $V=1541.1(4)$ Å^3, $R=0.039$ (5519 reflections). With the iodide compound, the unit-cell volume is only half of what is observed with the chloride and bromide analogs, and the crystal data are as follows: space group $P\bar{1}$ with two complexes in a cell of dimensions $a=6.677(1)$, $b=11.582(1)$, $c=11.838(3)$ Å, $\alpha=63.02(2)$, $\beta=100.09(2)$, $\gamma=100.92(1)°$, $V=796.9(3)$ Å^3, $R=0.030$ (3735 reflections). The unit cell of the fluoride compound is determined by X-ray powder diffraction, and the results suggest that it is isomorphous with the chloride and bromide compounds [$a=6.498(9)$, $b=11.857(13)$, $c=19.50(3)$ Å, $\alpha=88.6(2)$, $\beta=83.3(2)$, $\gamma=90.7(1)°$, $V=1491.7$ Å^3].

The complexes are mononuclear with two tris ligands and one water coordinated to the copper ion in a distorted octahedral arrangement (4 + 2); two amino and two hydroxymethyl groups are in the basal plane, and a water molecule and one terminal hydroxymethyl oxygen are forming the longer apical bonds. The dimeric structure of the complexes, the hydrogen-bonding network, and the non-isomorphic behavior as well as the disorder of the iodide compound are also discussed. Thermal behavior is characterized by TG in air and nitrogen atmospheres.

The ligand 2-amino-2-hydroxymethyl-1,3-propanediol (= tris) is primarily used as a buffering medium in many biochemical applications, because its buffering region is in the physiological pH range. The inhibitory effect of tris relative to other buffers is also known, and the inhibitory mechanism often involves the metal binding capacity of tris. As a weak base, tris is also used as a primary standard for HCl, even though it has a fairly low molecular weight, 121.1. Various other names, such as tris(hydroxymethyl)aminomethane, THAM or Trizma Base, are also used for the ligand.[1,2]

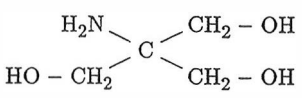

The tris-ligand, like amino alcohols, forms two distinctly different bond types with metal cations. One type of bonding involves a normal coordination bond between the metal and a lone-pair of oxygen or nitrogen atoms. The other type involves a classical coordinate–covalent bond with an alkoxy oxygen[3] (these deprotonated forms are abbreviated trisH$_{-1}$). Both coordination types are observed in the structures of the title compounds.

This article continues our previous study of the solid copper–tris compounds. The structures published earlier are the three basic *trans* complexes, [Cu(trisH$_{-1}$)$_2$], [Cu(trisH$_{-1}$)$_2$(H$_2$O)] and [Cu(trisH$_{-1}$)$_2$]·5H$_2$O,[4] four *cis* complexes, [Cu(trisH$_{-1}$)(tris)(NO$_3$)] and [Cu(trisH$_{-1}$)(tris)]Na(ClO$_4$)$_2$,[5] [Cu(trisH$_{-1}$)(tris)(H$_2$O)]$_2$SO$_4$ and [Cu(trisH$_{-1}$)(tris)(H$_2$O)]$_2$CrO$_4$,[6] as well as two *trans* compounds with potassium halide, [Cu(trisH$_{-1}$)$_2$]-KF·3H$_2$O and [Cu(trisH$_{-1}$)$_2$]KBr·2H$_2$O.[7] None of these compounds is related by isomorphism.

Experimental

Reagents. The reagents used were tris (Sigma, 99–99.5%), $CuF_2·2H_2O$ (Fluka, purum, ~97%), $CuCl_2·2H_2O$ (Merck, p.a.), $CuBr_2$ (B. D. H., >98%), CuI (Fluka, >98%) and NaI (J. T. Baker, 'Baker Analyzed'). CuCl (Merck, p.a.) and CuBr (Fluka, purum) were also used as reference materials in the TG analysis. All the reagents were used without further purification.

Preparation of [Cu(trisH$_{-1}$)(tris)(H$_2$O)]X·H$_2$O, where X = F, Cl, Br, I. General procedure. The following reagents, 0.04 mol of tris and 0.01 mol of copper halide, were dissolved in a minimum amount of distilled water in separate beakers, combined and heated for 15–30 min. The blue complex solution was filtered and concentrated with a rotavapor into a syrupy solution with a volume of 5–10 cm^3.

In the case of the fluoride compound (**1**), the synthesis needed an ethanol addition to crystallize the product (40 cm^3 of EtOH per concentrated reaction solution). The light-blue, needle-shaped crystals produced lost their clarity and started to crack when they were removed from the mother liquor. The crystal quality was also poor, and in spite of numerous attempts, it was not possible to prepare crystals suitable for single-crystal X-ray measurements. The existence of the fluoride compound is based on TG, IR and X-ray powder diffraction measurements.

The chloride (**2**) and bromide (**3**) compounds crystallized directly from the concentrated water solution overnight (if not, then the solution was concentrated more). Medium-blue, rod-shaped crystals were produced in both cases.

Since no copper(II) iodide was available, because of the reductive properties of iodide, problems arose with the iodide compound (**4**). When CuI was used as a starting material, copper was in the wrong oxidizing state, and the stoichiometric ratio of copper and iodide differed from the other reactions above. The best yield of the iodide compound was obtained according to the following procedure: 0.02 mol of tris was dissolved in 45 cm^3 of ethanol, 0.005 mol of CuI was wetted with 25 cm^3 of EtOH and this slurry was added to the tris solution. CuI was sparingly soluble in ethanol, but in the presence of tris, it was slowly oxidized to copper(II) by oxygen in the air. This was observed as a color change from colorless to blue and the disappearance of solid CuI, when the solution was kept in an open beaker. This oxidation step took a few days, but the reaction speed could be increased by stirring the mixture occasionally. When most of the copper iodide was dissolved and the blue color had become intense, the solution on top was separated from the unreacted CuI by decantation, then 0.005 mol of NaI was added in a small amount of ethanol, and the mixture was allowed to crystallize at room temperature. Similar ethanol reactions with a higher CuI content (0.01 mol), and without NaI addition also yielded compound **4** as a product.

A typical side product in the reactions was the *trans* monohydrate, [Cu(trisH$_{-1}$)$_2$(H$_2$O)],[4] especially if the concentrations were too dilute.

Thermal analysis. Thermal behavior of the complexes in air and nitrogen atmospheres was determined with a Perkin-Elmer thermogravimetric analyzer TGA7. The sample size was 7.00 ± 0.50 mg, and the crystalline samples were analyzed with a heating rate of 2 °C min^{-1} and a gas flow of 50 cm^3 min^{-1}. Temperature ranges were 25–800 and 25–950 °C in air and nitrogen, respectively. To obtain an oxygen-free nitrogen atmosphere, the equipment was flushed for 30 min with nitrogen before the temperature program was initiated. Thermogravimetric results are reported in Table 1.

X-Ray measurements

Powder diffraction. The X-ray powder diffraction pattern of **1** was recorded on a Philips PW 1840 powder diffractometer with β-filtered CuK_α radiation (λ = 1.54060 Å). The diffraction pattern was scanned from 5 to 80° (in 2θ) with a receiving slit of 0.1° and a step width of 0.002° per 1 s. The data were analyzed with Philips APD[8] software using K_{α_2} stripping, and the peak positions were calibrated with an internal silicon powder standard (20% of Standard Reference Material 640b).[9] ITO[10] and TREOR90[11] programs failed to find a unit cell with a comparable geometry, probably because the crystal quality (and therefore the data set) was not very good. However, when the unit-cell parameters of the chloride compound were used as initial values in the PIRUM[12] program, 68 out of 69 strongest lines (in the 2θ range 5–50) could be indexed, and the number of single indexed lines was 10. On the other hand, the calculated powder pattern of the chloride compound (produced by the CERIUS[13] program) showed that reflections (004), (200) and (040) have a moderate intensity, and they can be used to estimate the unit-cell edges *a*, *b* and *c*. When

Table 1. Thermal decomposition of $[Cu(trisH_{-1})(tris)(H_2O)]F \cdot H_2O$ (1), $[Cu(trisH_{-1})(tris)(H_2O)]Cl \cdot H_2O$ (2), $[Cu(trisH_{-1})(tris)(H_2O)]Br \cdot H_2O$ (3) and $[Cu(trisH_{-1})(H_2O)]I \cdot H_2O$ (4).

Compound	Lost in reaction	T/°C	Weight loss (%) Δ Obs.	Δ Theor.
Air atmosphere				
1	2 H_2O	25–85	9.5	10.0
	Org.	122–382	48.4	62.6 (Org.)
	Org. + F + 58.4% Cu (as CuF↑)	382–570	32.9	5.3 (F)
	Total reaction → CuO (41.6% of theor.)	25–570	90.8	77.9
2	2 H_2O	25–92	9.3	9.6
	Org.	122–388	48.8	59.9 (Org.)
	Org. + Cl + 57.7% Cu (as CuCl↑)	388–570	32.9	9.4 (Cl)
	Total reaction → CuO (42.3% of theor.)	25–570	91.0	78.9
3	2 H_2O	25–98	8.2	8.6
	Org.	123–398	45.3	53.5 (Org.)
	Org. + Br	398–560	28.5	19.0 (Br)
	Total reaction → CuO	25–560	82.0	81.1
4	2 H_2O	25–130	6.8	7.7
	Org.	130–364	43.5	48.2 (Org.)
	Org. + I	364–455	32.3	27.1 (I)
	Total reaction → CuO	25–455	82.5	83.0
Nitrogen atmosphere				
1	2 H_2O	25–58	9.2	10.0
	Org.	128–478	61.5	67.0
	Org. (incomplete)	478–950	4.0	
	Total reaction → CuF	25–950	74.7	77.0
2	2 H_2O	25–90	9.7	9.6
	Org.	151–474	61.8	64.1
	Org.	474–950	4.3	
	Total reaction → CuCl	25–950	75.8	73.7
3	2 H_2O	25–125	8.4	8.6
	Org.	135–420	57.5	57.3
	Br (incomplete)	420–950	12.9	19.0
	Total reaction → Cu	25–950	78.8	84.9
4	2 H_2O	25–139	7.5	7.7
	Org.	139–420	49.0	51.6
	I	420–700	28.4	27.1
	Total reaction → Cu	25–840	86.5	86.4

corresponding peaks in the fluoride pattern were assigned as above, better values were obtained for the unit-cell edges. After introducing these new values for the edges, along with the angles from the chloride structure, the PIRUM refinement was completed with all 69 peaks indexed, and 25 of them were single indexed lines. The possibility that the unit cell would be the small one (similar to the unit cell of **4**), was checked by PIRUM analysis using the small unit-cell parameters of the chloride compound; the results showed that four significant lines were unindexed, so the compatibility was better with the large unit cell. The final indexing pattern and the observed and calculated reflections are listed in Table 2.

Single-crystal measurements All of the data were collected on a computer-controlled Enraf–Nonius CAD-4 diffractometer equipped with a graphite monochromator and molybdenum X-ray tube. Crystals were mounted on a glass fiber and measured in an air atmosphere. Lattice parameters were determined by a least-squares fit of 25 centered reflections. Two standard reflections were monitored after every 60 min as an intensity check, and they showed that no decomposition occurred with compound **2** (0.2% gain in intensity in 152.1 h), but with compounds **3** and **4** the total loss in intensity was 8.5% in 149.4 h and 3.2% in 85.7 h, respectively. Crystal orientation was checked at an interval of 500 reflections with three standard reflections. Lorentz and polarization effects were taken into account, and the absorption correction was done by the DIFABS[14] program for compounds **2** and **3**; an empiric absorption correction (Ψ-scan) was done for compound **4**. A summary of the crystallographic parameters is presented in Table 3.

The structure solution and refinement procedure was identical to our previous studies on copper–tris complexes.[4–7] The programs used were SHELXS-86[15] (structure solution by direct methods), MolEN[16] (refinement) and SCHAKAL[17] (illustrations). Anisotropic thermal parameters were used for the non-hydrogen atoms, and hydrogens were refined as riding atoms with fixed isotropic thermal parameters, $B = 5.00$ Å^2. The largest peaks in the final difference Fourier maps were in the vicinity of copper or halide atoms (or disordered water in **4**).

Table 2. X-Ray powder diffraction data for [Cu(trisH$_{-1}$)(tris)(H$_2$O)]F · H$_2$O (1) [a=6.498(9), b=11.857(13), c=19.50(3) Å, α=88.6(2), β=83.3(2), γ=90.7(1)°, V=1491.7 Å^3].[a]

h	k	l	$2\theta_{obs}$/°	$2\theta_{calc}$/°	d_{obs}/Å	I/I_{max}
0	1	1	8.627	8.636	10.2415	100
0	−1	1	8.847	8.844	9.9873	24
1	0	−1	14.938	14.938	5.9282	5
1	1	2	17.202	17.279	5.1507	14
1	0	3	18.107	18.259	4.8925	19
0	0	4	18.192	18.312	4.8726	18
−1	1	2	18.672	18.735	4.7484	6
−1	−1	2	18.977	19.104	4.6727	6
0	1	4	19.512	19.608	4.5458	3
1	2	1	20.557	20.558	4.3170	3
−1	2	1	20.972	20.954	4.2325	4
−1	−2	1	21.397	21.441	4.1494	6
−1	−1	3	22.102	22.086	4.0186	2
−1	2	2	22.607	22.674	3.9300	8
0	0	5	22.912	22.945	3.8784	5
1	2	3	23.607	23.578	3.7657	9
1	−2	3	23.742	23.768	3.7446	9
0	3	2	24.062	24.084	3.6955	11
−1	2	3	25.047	25.146	3.5524	8
1	0	5	25.397	25.387	3.5042	8
−1	−2	3	25.852	25.848	3.4436	5
0	3	3	26.042	26.110	3.4189	8
1	1	5	26.387	26.380	3.3750	6
0	−3	3	26.752	26.748	3.3297	6
0	2	5	27.207	27.148	3.2751	10
−1	−3	1	27.412	27.404	3.2510	8
2	0	0	27.672	27.624	3.2211	9
2	1	2	29.137	29.155	3.0624	4
−2	−1	1	29.653	29.691	3.0102	7
1	−2	5	29.778	29.788	2.9979	7
0	4	0	30.248	30.248	2.9524	9
−2	1	2	30.984	30.953	2.8839	11
2	0	4	31.429	31.455	2.8441	13
−1	2	5	31.664	31.650	2.8235	9
2	−2	2	31.855	31.868	2.8070	12
0	0	7	32.335	32.337	2.7664	6
−2	−2	1	32.630	32.637	2.7421	8
0	1	7	33.011	33.029	2.7113	5
1	4	0	33.461	33.452	2.6759	5
1	0	7	33.656	33.706	2.6608	6
−2	−2	2	34.167	34.143	2.6222	6
1	−1	7	34.692	34.713	2.5837	10
2	2	4	34.952	34.967	2.5650	19
−2	2	3	35.503	35.503	2.5265	7
0	−4	4	35.953	35.926	2.4959	8
2	3	2	36.408	36.405	2.4657	12
1	3	6	37.073	37.036	2.4230	8
2	2	5	37.224	37.253	2.4135	8
2	3	3	37.429	37.414	2.4008	6
−2	1	5	38.909	38.859	2.3128	6
−1	2	7	39.444	39.467	2.2827	5
−1	−4	4	39.625	39.605	2.2727	5
0	5	3	40.150	40.145	2.2441	7
0	4	6	40.795	40.757	2.2101	9
−2	0	6	41.795	41.794	2.1595	10
−1	−4	5	42.401	42.382	2.1301	7
−2	−1	6	42.736	42.739	2.1141	9
2	4	4	44.106	44.084	2.0516	17
−3	−1	2	44.981	44.999	2.0137	17
1	−3	8	45.131	45.133	2.0074	16
0	−5	5	45.362	45.350	1.9977	14
−3	−2	1	45.872	45.860	1.9766	11
−1	−5	4	46.102	46.146	1.9673	13
−2	4	4	46.312	46.303	1.9589	11
3	2	4	46.773	46.776	1.9406	10
2	5	0	47.945	47.944	1.8959	9
3	−1	6	48.650	48.643	1.8701	9
1	−3	9	49.225	49.229	1.8496	8
2	−3	8	50.255	50.273	1.8140	8

[a] Input values for the least-squares program: a=6.442, b=11.809, c=19.490 Å, α=88.22, β=83.67, γ=90.30°.

The main problem in solving these structures was deciding which unit cell and space group were the correct ones. Both chloride and bromide compounds could also be solved in a unit cell with half of the volume (similar cell as with the iodide compound) with $P\bar{1}$ as a space group, but the convergence of the refinement and the e.s.d.s of the results were much poorer than in the large unit cell. The unit cell of the iodide compound had been consistently the small one, but originally the structure could be solved only in $P\bar{1}$ (R = 0.040). To confirm the unit cell, the iodide compound was also forced to the large unit cell ($a' = -a$, $b' = -b+c$, $c' = b+c$), but the structure was not refineable in the large unit cell. Furthermore, the total number of reflections fulfilling the $3\sigma(I)$ criterion did not increase when the large unit cell was introduced. The centrosymmetric choice of the space group was also supported by the fact that the compounds are racemic mixtures of optical enantiomers. Because of the larger crystal dimensions of the iodide compound, the data set is more biased by absorption. When the empirical absorption correction was introduced to the iodide compound, the structure was also solved in the centrosymmetric space group $P\bar{1}$. The rotation photographs of aligned crystals support the chosen unit-cell edges. A similar structural case, in which the iodide compound possesses higher symmetry than other halide analogs, is observed with tris–hydrogen-halide salts, trisH$^+ \cdot X^-$ (X = F, Cl, Br, I).[18]

The final atomic positional parameters and equivalent isotropic temperature factors are given in Tables 4–6. Tables of bond angles, anisotropic thermal parameters, least-squares planes, coordinates of hydrogen atoms, as well as listings of observed and calculated structure factors, are available from the author on request.

Results and discussion

Thermal analysis. The thermal behavior of the title compounds is summarized in Table 1. The thermal decomposition process of all complexes is quite similar. The fluoride and chloride compounds show identical behavior, and correspondingly, the heavier bromide and iodide analogs have similar decomposition patterns in both atmospheres.

Table 3. Crystallographic experimental data for [Cu(trisH$_{-1}$)(tris)(H$_2$O)]Cl·H$_2$O (**2**), [Cu(trisH$_{-1}$)(tris)(H$_2$O]Br·H$_2$O (**3**) and [Cu(trisH$_{-1}$)(tris)(H$_2$O)]I·H$_2$O (**4**).

Compound	**2**	**3**	**4**
Unit-cell determination			
Formula	$CuClO_8N_2C_8H_{25}$	$CuBrO_8N_2C_8H_{25}$	$CuIO_8N_2C_8H_{25}$
Formula weight	376.29	420.74	467.74
Color	Blue	Blue	Blue
Crystal size/mm	0.20×0.20×0.13	0.18×0.14×0.10	0.25×0.20×0.15
T/°C	21±1	21±1	21±1
Reflections for lattice measurements	25	25	25
θ-Range for lattice measurement/°	9–12	5–13	9–13
a/Å	6.482 (2)	6.574 (1)	6.677 (1)
b/Å	11.805 (1)	11.929 (2)	11.582 (1)
c/Å	19.767 (3)	19.792 (2)	11.838 (3)
α/°	88.22 (1)	88.09 (1)	63.02 (2)
β/°	83.67 (2)	83.43 (1)	100.09 (2)
γ/°	90.30 (2)	89.72 (1)	100.92 (1)
V/Å^3	1502.6 (6)	1541.1 (4)	796.9 (3)
Z	4	4	2
d_{calc}/g cm^{-3}	1.66	1.81	1.95
λ(MoK_α)/Å	0.71073	0.71073	0.71073
μ(MoK_α)/cm$_{-1}$	16.70	40.23	33.23
F(000)	788	860	466
Space group	$P\bar{1}$ (No. 2)	$P\bar{1}$ (No. 2)	$P\bar{1}$ (No. 2)
Data collection and refinement			
θ-Range for data collection/°	2–30	2–30	2–30
Scan method	ω/2θ	ω/2θ	ω/2θ
Scan speed in ω/° min^{-1}	0.87–5.50	1.03–5.50	0.92–5.50
Scan width in ω/°	0.80+0.34 tan θ	0.90+0.34 tan θ	0.80+0.34 tan θ
No. of measured reflections	8718	8962	4635
Reflections used in refinement, $I>3\sigma(I)$	6084	5519	3735
Absorption correction (min./max.)	0.85/1.17	0.84/1.11	0.88/1.00
Max. shift/error	0.00	0.00	0.00
Max. in final Δρ/e Å^{-3}	0.63	1.08	1.41
No. of parameters refined	361	361	197
R	0.035	0.039	0.030
R_w[a]	0.043	0.039	0.032
$S=[\Sigma w(F_o-F_c)^2/(n-m)]^{1/2}$	1.469	1.638	1.019

[a] $w=1/\sigma^2(F_o)$.

Thermal decomposition starts with the dehydration of water (normally in one step, but sometimes two steps are observed with compounds **3** and **4**). The dehydration temperatures show that water in the fluoride compound is most easily dehydrated, and the dehydration temperature rises, when the weight of the halide increases. In an air atmosphere, the organic ligand decomposes in two successive phases, and the latter is accompanied by the simultaneous degradation of halide. With the bromide and iodide compounds the last degradation step is clear, and the final product is CuO, but with the fluoride and chloride compounds, the final weight is much less than what is expected for CuO (see the theoretical values in Table 1). The most likely explanation is that covalent copper halides are formed during the decomposition process of the fluoride and chloride compounds,[19] and as a consequence, 58% of copper is sublimated as CuF or CuCl, and 42% of copper remains as CuO. Similar behavior was also observed with copper fluorides and chlorides, when samples of $CuF_2·2H_2O$, CuCl, $CuCl_2·2H_2O$, CuBr, $CuBr_2$ and CuI were each analyzed as a reference material in the same conditions.

In nitrogen atmosphere, most of the organic part is decomposed by 500°C, but the process produces some carbon, which may interfere with the interpretation above 500°C.[4,5] With the fluoride and chloride compounds the TG curve is quite featureless above 500°C, and the final product is copper(I) halide. The bromide and iodide compounds decompose further giving elemental copper as the final residue (with the bromide compound the last step is still incomplete at 950°C).

Molecular structures. The molecular structures of the complexes are shown in Figs. 1 and 2, and the bond lengths describing these molecules are listed in Table 7. The angles characterizing the distortion of the coordination sphere of copper are shown in Table 8.

The complex molecules in all structures are mononuclear cation complexes with two tris ligands (one of them is deprotonated) and one water molecule coordi-

Table 4. Atomic positional parameters and equivalent isotropic temperature factors[a] with e.s.d.s in parentheses for $[Cu(trisH_{-1})(tris)(H_2O)]Cl \cdot H_2O$ (**2**).

Atom	*x*	*y*	*z*	$B_{eq}/Å^2$
Molecule 1				
Cu100	−0.48621(6)	0.23944(3)	0.64546(2)	1.087(6)
OW100	−0.8181(4)	0.2284(2)	0.6081(2)	2.50(5)
O111	−0.5694(4)	0.3621(2)	0.7100(1)	1.51(4)
O112	−0.1316(4)	0.3498(2)	0.6732(1)	1.94(4)
O113	−0.2557(4)	0.5757(2)	0.5124(1)	2.19(5)
O121	−0.5383(3)	0.1243(2)	0.7173(1)	1.33(4)
O122	−0.0022(4)	0.0165(2)	0.5982(2)	2.66(5)
O123	−0.3179(4)	−0.1024(3)	0.5216(1)	2.65(5)
N111	−0.4164(4)	0.3675(2)	0.5785(1)	1.29(4)
N121	−0.3932(4)	0.1132(2)	0.5845(1)	1.36(4)
C111	−0.5451(5)	0.4709(3)	0.6772(2)	1.61(5)
C112	−0.3741(5)	0.4687(3)	0.6176(2)	1.17(5)
C113	−0.1580(5)	0.4575(3)	0.6406(2)	1.72(6)
C114	−0.3854(6)	0.5787(3)	0.5759(2)	1.85(6)
C121	−0.5445(5)	0.0154(3)	0.6883(2)	1.47(5)
C122	−0.3809(5)	0.0075(3)	0.6263(2)	1.24(5)
C123	−0.1681(5)	0.0021(3)	0.6511(2)	1.85(6)
C124	−0.4343(6)	−0.0963(3)	0.5869(2)	2.09(6)
Molecule 2				
Cu200	−0.01073(6)	0.73989(3)	0.15009(2)	1.168(6)
OW200	−0.3576(4)	0.7166(3)	0.1095(2)	3.07(6)
O211	−0.1072 (4)	0.8641(2)	0.2121(1)	1.68(4)
O212	0.3303(4)	0.8426(2)	0.1784(1)	2.01(4)
O213	0.2369(4)	1.0680(2)	0.0164(1)	2.21(5)
O221	−0.0813(3)	0.6244(2)	0.2196(1)	1.32(4)
O222	0.2525(5)	0.3853(3)	0.2066(2)	2.91(6)
O223	0.1651(5)	0.3961(3)	0.0278(1)	2.90(6)
N211	0.0586(4)	0.8667(2)	0.0825(1)	1.24(4)
N221	0.0917(4)	0.6123(2)	0.0909(1)	1.58(5)
C211	−0.0751(5)	0.9734(3)	0.1795(2)	1.67(6)
C212	0.1017(5)	0.9673(3)	0.1219(2)	1.18(5)
C213	0.3139(5)	0.9524(3)	0.1472(2)	1.87(6)
C214	0.1019(6)	1.0772(3)	0.0785(2)	1.85(6)
C221	−0.1043(5)	0.5197(3)	0.1874(2)	1.51(5)
C222	0.0749(5)	0.5034(3)	0.1314(2)	1.28(5)
C223	0.2755(5)	0.4823(3)	0.1623(2)	1.92(6)
C224	0.0209(6)	0.4059(3)	0.0872(2)	1.98(6)
Cl1	0.0767(1)	0.75424(9)	0.55432(5)	2.61(2)
Cl2	−0.5736(1)	0.75191(9)	−0.03443(5)	2.71(2)
OW1	0.5737(6)	0.2397(3)	0.1973(2)	4.29(8)
OW2	−0.0824(6)	0.2462(3)	0.2762(2)	4.97(9)

[a] $B_{eq} = \frac{4}{3}\sum_i\sum_j \beta_{ij} \mathbf{a}_i \cdot \mathbf{a}_j$.

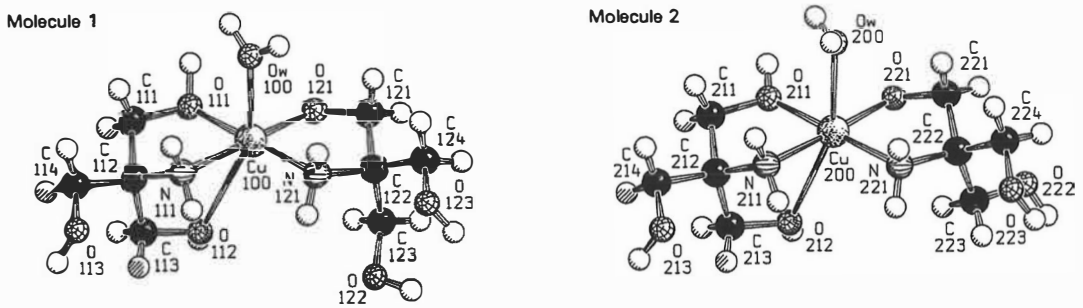

Fig. 1. SCHAKAL projections of cation complexes 1 and 2 in the chloride (**2**) and bromide (3) compounds (coordinates taken from **2**).

Table 5. Atomic positional parameters and equivalent isotropic temperature factors[a] with e.s.d.s in parentheses for $[Cu(trisH_{-1})(tris)(H_2O)]Br \cdot H_2O$ (**3**).

Atom	*x*	*y*	*z*	B_{eq}/Å^2
Molecule 1				
Cu100	−0.49163(7)	0.24051(4)	0.64586(2)	1.485(8)
OW100	−0.8201(5)	0.2315(3)	0.6081(2)	3.01(7)
O111	−0.5761(5)	0.3616(2)	0.7102(1)	1.97(5)
O112	−0.1408(5)	0.3485(3)	0.6741(2)	2.40(6)
O113	−0.2649(5)	0.5722(3)	0.5137(2)	2.58(6)
O121	−0.5413(4)	0.1254(2)	0.7171(1)	1.64(5)
O122	−0.0087(5)	0.0242(3)	0.5982(2)	3.02(7)
O123	−0.3145(5)	−0.0951(3)	0.5214(2)	2.88(6)
N111	−0.4220(5)	0.3680(3)	0.5798(2)	1.64(6)
N121	−0.3991(5)	0.1163(3)	0.5848(2)	1.68(6)
C111	−0.5504(7)	0.4706(3)	0.6778(2)	1.98(7)
C112	−0.3813(6)	0.4679(3)	0.6192(2)	1.48(6)
C113	−0.1682(6)	0.4556(4)	0.6422(2)	2.07(7)
C114	−0.3925(7)	0.5768(4)	0.5764(2)	2.13(8)
C121	−0.5443(6)	0.0182(3)	0.6874(2)	1.78(7)
C122	−0.3822(6)	0.0111(3)	0.6257(2)	1.45(6)
C123	−0.1703(7)	0.0078(4)	0.6505(2)	2.26(8)
C124	−0.4281(7)	−0.0914(4)	0.5864(2)	2.38(8)
Molecule 2				
Cu200	−0.01217(8)	0.74097(4)	0.15116(2)	1.593(8)
OW200	−0.3534(6)	0.7220(4)	0.1110(2)	3.78(8)
O211	−0.1065(5)	0.8637(2)	0.2136(1)	2.10(5)
O212	0.3267(5)	0.8433(3)	0.1800(2)	2.42(6)
O213	0.2243(5)	1.0664(3)	0.0182(2)	2.71(6)
O221	−0.0764(5)	0.6260(2)	0.2205(1)	1.80(5)
O222	0.2563(7)	0.3896(3)	0.2059(2)	4.03(8)
O223	0.1628(6)	0.4026(3)	0.0279(2)	3.47(7)
N211	0.0568(5)	0.8670(3)	0.0847(2)	1.57(6)
N221	0.0884(6)	0.6151(3)	0.0915(2)	2.03(6)
C211	−0.0769(7)	0.9724(4)	0.1810(2)	1.98(7)
C212	0.0966(6)	0.9669(3)	0.1238(2)	1.52(6)
C213	0.3059(7)	0.9518(4)	0.1488(2)	2.29(8)
C214	0.0944(7)	1.0750(4)	0.0800(2)	2.31(8)
C221	−0.0957(7)	0.5225(4)	0.1884(2)	2.21(8)
C222	0.0773(7)	0.5072(3)	0.1319(2)	1.83(7)
C223	0.2801(7)	0.4872(4)	0.1609(2)	2.63(9)
C224	0.0262(8)	0.4108(4)	0.0878(2)	2.65(9)
Br1	0.08263(7)	0.74961(4)	0.55804(3)	2.660(8)
Br2	−0.57674(8)	0.75367(5)	−0.03887(3)	3.11(1)
OW1	0.5762(8)	0.2466(4)	0.2062(2)	5.8(1)
OW2	−0.0582(8)	0.2417(4)	0.2690(2)	5.8(1)

[a] See Table 4.

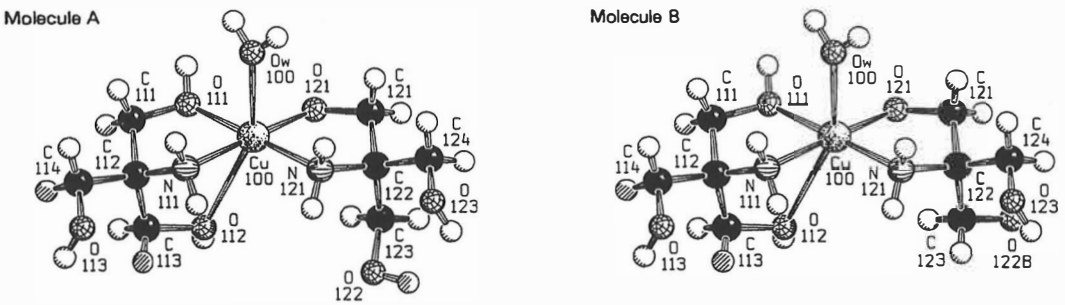

Fig. 2. SCHAKAL projection of the disordered cation complex in the iodide compound (**4**) (molecule A 87% and B 13%).

Table 6. Atomic positional parameters and equivalent isotropic temperature factors[a] with e.s.d.s in parentheses for $[Cu(trisH_{-1})(tris)(H_2O)]I \cdot H_2O$ (**4**).

Atom	*x*	*y*	*z*	$B_{eq}/Å^2$	
Molecule					
Cu100	0.85487(5)	0.59438(3)	0.60926(3)	1.434(6)	
OW100	1.2195(4)	0.6251(3)	0.6569(2)	3.21(6)	
O111	0.8807(3)	0.6474(2)	0.4252(2)	1.79(4)	
O112	0.4869(4)	0.6671(2)	0.4801(2)	2.25(5)	
O113	0.7565(4)	1.0486(2)	0.4180(2)	2.62(5)	
O121	0.8321(3)	0.4107(2)	0.6507(2)	1.55(4)	
O122	0.4215(4)	0.4373(3)	0.8674(3)	2.95(6)	pp=0.87
O1228	0.459(3)	0.233(2)	0.886(2)	3.0(4)	pp=0.13
O123	0.7884(4)	0.3947(2)	1.0638(2)	3.08(6)	
N111	0.8534(4)	0.7851(2)	0.5511(2)	1.58(4)	
N121	0.8225(4)	0.5365(2)	0.7932(2)	1.71(5)	
C111	0.8853(5)	0.7855(3)	0.3513(3)	2.01(6)	
C112	0.7743(4)	0.8408(2)	0.4144(2)	1.46(5)	
C113	0.5431(5)	0.8036(3)	0.4045(3)	2.16(6)	
C114	0.8246(5)	0.9902(3)	0.3508(3)	2.15(6)	
C121	0.8616(5)	0.3368(3)	0.7854(3)	1.79(5)	
C122	0.7619(4)	0.3928(3)	0.8537(2)	1.51(5)	
C123	0.5294(5)	0.3662(3)	0.8312(3)	2.21(6)	
C124	0.8420(5)	0.3327(3)	0.9947(3)	2.29(6)	
I1	0.65016(4)	0.82268(3)	0.81298(2)	3.233(5)	
OW1A	0.764(2)	0.942(1)	0.939(1)	6.8(3)[b]	pp=0.34
OW1B	0.888(4)	0.995(2)	1.012(2)	8.6(6)[b]	pp=0.22
OW1C	0.426(3)	1.001(3)	0.996(3)	9.1(7)[b]	pp=0.22
OW1D	0.732(5)	0.995(3)	1.014(3)	10.7(8)[b]	pp=0.22

[a] See Table 4.
[b] Refined isotropically.

nated to the copper atom. The coordination sphere around copper is a distorted octahedron with tris molecules coordinated via amino and hydroxymethyl groups in the basal plane (*cis* configuration), and the apical positions are occupied by water and one terminal hydroxymethyl oxygen from the non-protonated ligand. The basal plane of the O111, N111, O121 and N121 (or O211, N211, O221 and N221) atoms is almost planar, and the copper atom is displaced 0.019–0.060 Å towards the apical water molecule. Furthermore, the five-membered chelate rings are in an *envelope* conformation, where Cu100, O111, N111, C111 (or corresponding set) are the atoms

Table 7. Bond distances (in Å) with e.s.d.s in parentheses for $[Cu(trisH_{-1})(tris)(H_2O)](Cl \cdot H_2O$ (**2**), $[Cu(trisH_{-1})(tris)(H_2O)]Br \cdot H_2O$ (**3**) and $[Cu(trisH_{-1})(tris)(H_2O)]I \cdot H_2O$ (**4**).

Bond	**2**	**3**	**4**	Bond	**2**	**3**
Cu100–OW100	2.355(3)	2.366(3)	2.397(2)	Cu200–OW200	2.486(3)	2.482(4)
Cu100–O111	1.997(2)	1.993(3)	2.008(2)	Cu200–O211	1.999(2)	1.997(3)
Cu100–O112	2.752(3)	2.768(2)	2.717(2)	Cu200–O212	2.638(3)	2.674(3)
Cu100–O121	1.936(2)	1.935(3)	1.936(2)	Cu200–O221	1.922(2)	1.921(3)
Cu100–N111	1.994(3)	1.992(3)	1.995(2)	Cu200–N211	1.991(3)	1.984(3)
Cu100–N121	1.999(3)	1.991(3)	2.006(2)	Cu200–N221	2.006(3)	2.006(3)
O111–C111	1.422(4)	1.434(5)	1.431(3)	O211–C211	1.428(4)	1.433(5)
O112–C113	1.427(4)	1.427(5)	1.432(3)	O212–C213	1.428(4)	1.427(6)
O113–C114	1.432(4)	1.417(5)	1.424(5)	O213–C214	1.433(4)	1.416(5)
O121–C121	1.426(4)	1.426(5)	1.424(3)	O221–C221	1.422(4)	1.420(5)
O122–C123	1.420(4)	1.408(5)	1.426(6)	O222–C223	1.417(5)	1.440(6)
O122B–C123	–	–	1.40(2)	–	–	–
O123–C124	1.426(4)	1.413(5)	1.430(5)	O223–C224	1.426(4)	1.406(6)
N111–C112	1.482(4)	1.487(5)	1.483(3)	N211–C212	1.481(4)	1.483(5)
N121–C122	1.483(4)	1.484(5)	1.487(5)	N221–C222	1.490(4)	1.489(5)
C111–C112	1.527(4)	1.513(5)	1.525(5)	C211–C212	1.529(4)	1.515(5)
C112–C113	1.525(4)	1.526(6)	1.521(4)	C212–C213	1.524(5)	1.523(6)
C112–C114	1.524(5)	1.533(6)	1.536(4)	C212–C214	1.533(5)	1.530(6)
C121–C122	1.535(4)	1.530(5)	1.531(5)	C221–C222	1.530(4)	1.517(6)
C122–C123	1.514(5)	1.529(6)	1.525(4)	C222–C223	1.515(5)	1.525(7)
C122–C124	1.530(5)	1.518(6)	1.527(4)	C222–C224	1.528(5)	1.529(6)

Table 8. Bond angles (in °) of the coordination sphere of copper with e.s.d.s in parentheses for [Cu(trisH$_{-1}$)(tris)(H_2O)]Cl · H_2O (**2**), [Cu(trisH$_{-1}$)(tris)(H_2O)]Br · H_2O (**3**) and [Cu(trisH$_{-1}$)(tris)(H_2O)]I · H_2O (**4**).*

Angle	2	3	4	Angle	2	3
OW100–Cu100–O111	93.1(1)	92.8(1)	92.01(9)	OW200–Cu200–O211	93.0(1)	92.9(1)
OW100–Cu100–O112	154.61(9)	154.6(1)	155.03(7)	OW200–Cu200–O212	158.6(1)	158.0(1)
OW100–Cu100–O121	95.6(1)	95.9(1)	96.43(9)	OW200–Cu200–O221	89.9(1)	91.0(1)
OW100–Cu100–N111	89.1(1)	89.3(1)	88.7(1)	OW200–Cu200–N211	90.8(1)	91.0(1)
OW100–Cu100–N121	89.4(1)	89.4(1)	89.3(1)	OW200–Cu200–N221	88.6(1)	88.7(1)
O111–Cu100–O112	71.96(8)	72.2(1)	73.70(8)	O211–Cu200–O212	74.58(9)	74.0(1)
O111–Cu100–O121	91.44(9)	92.0(1)	92.16(9)	O211–Cu200–O221	92.64(9)	92.9(1)
O111–Cu100–N111	84.2(1)	83.8(1)	83.9(1)	O211–Cu200–N211	83.8(1)	83.5(1)
O121–Cu100–N121	86.5(1)	86.2(1)	86.4(1)	O221–Cu200–N221	85.7(1)	85.5(1)
N111–Cu100–O112	69.44(9)	69.2(1)	69.79(8)	N211–Cu200–O212	70.9(1)	70.3(1)
N111–Cu100–N121	97.7(1)	97.9(1)	97.5(1)	N211–Cu200–N221	97.8(1)	98.0(1)

* Other angles in the structures are normal to these copper–tris complexes.[4–7]

defining the plane, and C112 (or C122, C212, C222) are the atoms bent out of the plane. In each molecule, these five-membered rings are bent in the same direction, meaning that the complex is a *syn* conformer. Terminal hydroxymethyl groups can take an axial or an equatorial position in relation to these planes. The complex molecules are also optically active, with two possible enantiomers. The product contains both enantiomers in equal amounts.

In the isomorphic chloride and bromide structures, there are two molecules (molecules 1 and 2) in the asymmetric unit, which are structurally quite similar, differing mainly in the orientation of one axial hydroxymethyl group on the deprotonated side and in the positions of the hydrogens in the coordinated water molecule. A closer inspection of the bond lengths shows that there are distinctive differences in the apical bond lengths of the coordination spheres. In molecule 1, the coordination sphere is more distorted with a short Cu100–OW100 bond [2.355 Å (**2**)/2.366 Å (**3**)] and a long Cu100–O112 bond (2.752/2.768 Å), whereas the apical bond lengths in molecule 2 are closer to each other (Cu200–OW200 = 2.486/2.482 Å and Cu200–O212 = 2.638/2.674 Å). In the basal plane, the lengths of the coordination bonds do not vary that much. Furthermore, calculations of the least-squares planes show that the basal plane in molecule 1 is less planar than in molecule 2, and that the dihedral angle between the chelate planes is smaller in molecule 1 (3.7/3.3°) than in molecule 2 (9.0/7.8°).

In the iodide structure (**4**), there is only one molecule in the asymmetric unit, where the axial hydroxymethyl group on the non-protonated side is disordered, having two possible orientations with occupancies 87% (molecule A) and 13% (molecule B). Molecule A is structurally very close to molecule 1 in compounds **2** and **3**; the apical bond lengths, Cu100–OW100 (2.397 Å) and Cu100–O112 (2.717 Å), the planarity of the basal plane and the dihedral angle between the chelate planes (3.3°) are in good agreement with the values mentioned above. On the other hand, molecule B is quite like molecule 2 in compounds **2** and **3** (only the disorder of O122 and two calculated hydrogens riding on carbon C123 are refined, otherwise the structure is the same as in molecule A). It is very likely that the orientation of the O122 group also affects the geometry of the coordination sphere, and that the true structure of the iodide compound consists of two types of molecules, which are closer to molecules 1 and 2 in compounds **2** and **3**, and the statistical structure that is obtained in the refinement is more or less a weighted average of these two molecules, where the weights are given by occupancies.

Similar distorted octahedral coordination spheres have been observed earlier with copper–tris compounds containing nitrate and perchlorate as an anion,[5] [Cu(trisH$_{-1}$)(tris)(NO_3)] and [Cu(trisH$_{-1}$)(tris)]Na(ClO_4)$_2$.

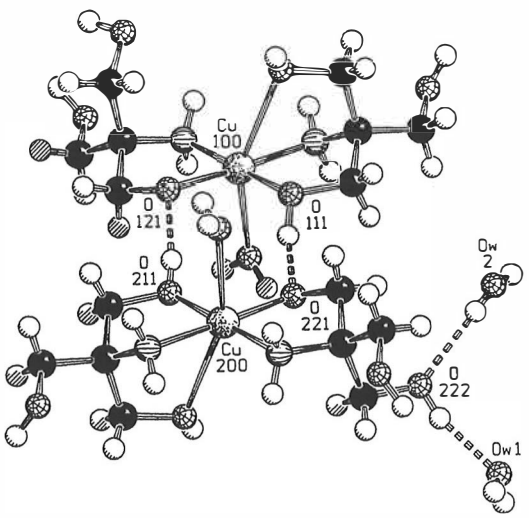

Fig. 3. Example of the dimer structure in the chloride and bromide compounds; cation complex 2 and the optical enantiomer of complex 1 form the hydrogen-bonded associate above, in which crystalline water molecules are attached to the terminal hydroxymethyl group O222 (enantiomer of complex 1 is generated by symmetry operation $-1-x$, $1-y$, $1-z$).

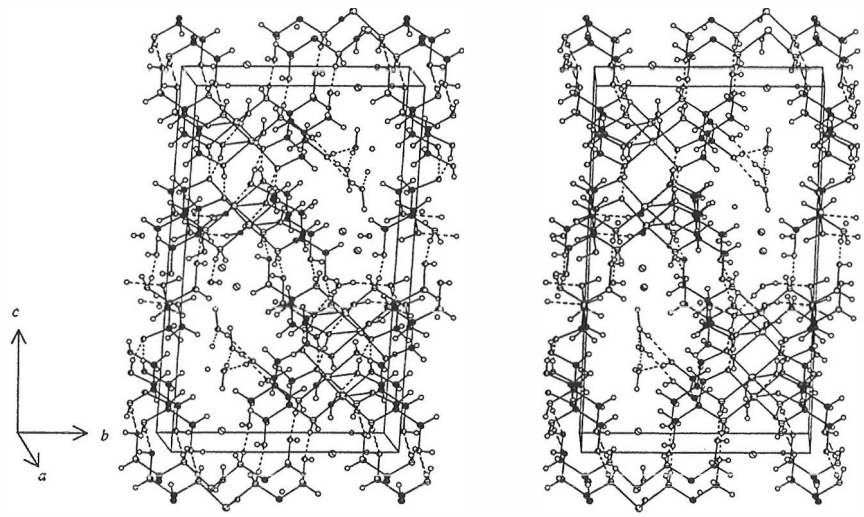

Fig. 4. Stereoscopic representation of hydrogen bonding for the chloride (**2**) and bromide (**3**) compounds (coordinates taken from **2**). Hydrogen bonds are indicated by dashed lines.

Crystal structures. A hydrogen-bonded dimer structure of the complexes is shown in Fig. 3, and stereoscopic projections of the crystal structures and the hydrogen-bonding framework for both compound types are presented in Figs. 4 and 5.

The chloride and bromide compounds are strictly isomorphic, and they consist of hydrogen-bonded cationic dimers, halides and crystalline water. The dimer structures are formed from complex molecule 1, which is hydrogen-bonded to the optical enantiomer of complex 2, or *vice versa* (Fig. 3). The hydrogen bonds in the dimers include the deprotonated hydroxymethyl groups, so the O···O distances are short [2.532(3)–2.560(3) Å]. The dimer forms a step-like structure, where the apical water ligands are pointing towards the other molecule in the dimer, and the Cu100···Cu200′ distances are 4.9181(5) Å (**2**) and 4.8870(6) Å (**3**). The dimers are stacked along the *a*-axis and polymerized by the hydro-

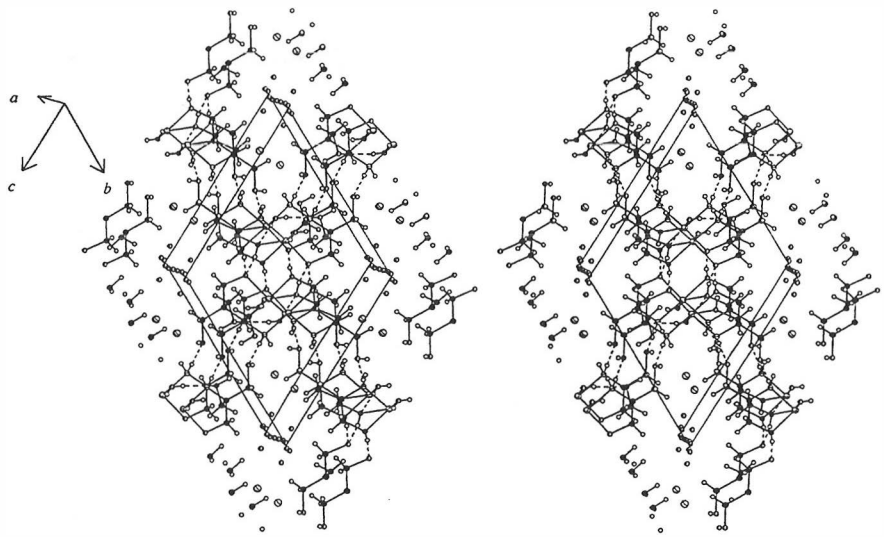

Fig. 5. Stereoscopic representation of hydrogen bonding for the iodide compound (**4**) (molecule A, 87%). Hydrogen bonds are indicated by dashed lines, and all the locations of the disordered water molecule OW1 are approximately along the *a*-axis.

gen bonds between the coordinated water and the coordinated hydroxymethyl groups of the adjacent dimers. The coordinated water OW100 also fixes the position of the free axial hydroxymethyl group O122 in the dimer on the top. In the *bc*-plane the dimers are linked to four neighboring dimers via hydrogen bonds between amino and equatorial hydroxymethyl groups (two N–H···O and N···H–O bonds for each pair). As a result, the compound forms a net-like structure with tunnels along the *a*-direction, and these tunnels are filled with crystalline water (OW1 and OW2) and halides. The halides are located in the hydrophobic cavities, with the hydrogens pointing towards the halide [each halide is surrounded by six hydrogens with Cl–H and Br–H distances in the range 2.22–2.76 Å (**2**) and 2.34–2.84 Å (**3**)]. Similar hydrophobic tunnels have been observed earlier with copper–tris halides containing potassium as a cation.[7] The axial hydroxymethyl group O222 from molecule 2 is turned into the tunnel, and it serves as an arm to which the crystalline water can attach and form a hydrogen-bonded zigzag chain of OW2–H···O222–H···OW1–H···OW2′–H′··· with fixed positions for crystalline water.

Even though the iodide compound is not isomorphic with compounds **2** and **3**, the structures are very similar, and they can be described as isotypic. In the iodide structure, the dimers are formed from the complex molecule and its optical isomer via strong hydrogen bonds [O111···O121′ = 2.565(4) Å]. The eight-membered ring in the dimer contains an inversion center, and the Cu100···Cu100′ separation is 4.8706(6) Å. The stacking of the dimers along the *a*-axis, as well as the net-like structure with tunnels along the *a*-axis and halide occupying the hydrophobic cavities (I–H distances in the range 2.69–3.02 Å) are common features for all these compounds. Nevertheless, since the ionic radius of iodide (2.16 Å) is larger than the radii of chloride (1.81 Å) or bromide (1.95 Å),[20] there is not enough space in the tunnel for the hydroxymethyl arm (O122) in compound **4**. Only 13% of O122 is oriented in a manner suitable for fixing the crystalline water. As a consequence, the crystalline water is disordered along the *a*-axis, having at least four possible locations with occupancies 0.34 or less.

Acknowledgements. Financial support from the Leo and Regina Wainstein Foundation is gratefully acknowledged.

References

1. Brignac, P. J. Jr. and Mo, C. *Anal. Chem. 47* (1975) 1465.
2. Allen, D. E., Baker, D. J. and Gillard, R. D. *Nature (London) 214* (1967) 906.
3. Dotson, R. L. *Inorg. Nucl. Chem. Lett. 9* (1973) 215.
4. Kotila, S. and Valkonen, J. *Acta Chem. Scand. 47* (1993) 950.
5. Kotila, S. and Valkonen, J. *Acta Chem. Scand. 47* (1993) 957.
6. Kotila, S. and Valkonen, J. *Acta Chem. Scand. 48* (1994) 200.
7. Kotila, S. and Valkonen, J. *Acta Chem. Scand. 48* (1994) 312.
8. *PC-APD Software for Automated Powder Diffraction PW1710*, Version 2.0. N.V. Philips Gloeilampenfabrieken, Eindhoven, The Netherlands 1989.
9. *Standard Reference Material 640b, Silicon Powder 2θ/d-Spacing Standard for X-Ray Diffraction*. National Bureau of Standards Certificate, Gaithersburg, MD 1987.
10. Visser, J. W. *J. Appl. Crystallogr. 2* (1969) 89.
11. Werner, P.-E., Eriksson, L. and Westdahl, M. *J. Appl. Crystallogr. 18* (1985) 367.
12. Werner, P.-E. *Arkiv Kemi 31* (1969) 513.
13. *CERIUS, a Molecular Modeling Environment for Material Research*, Cambridge Molecular Design, Cambridge, UK 1991.
14. Walker, N. and Stuart, D. *Acta Crystallogr., Sect. A 39* (1983) 158.
15. Sheldrick, G. M. In: Sheldrick, G. M., Krüger, C. and Goddard, R., Eds., *Crystallographic Computing 3*, Oxford University Press, Oxford 1985, pp. 175–189.
16. *MolEN, an Interactive Structure Solution Procedure*, Enraf–Nonius, Delft, The Netherlands 1990.
17. Keller, E. *SCHAKAL, a FORTRAN Program for the Graphic Representation of Molecular and Crystallographic Models*, University of Freiburg, Freiburg 1987.
18. Rudman, R., Lippman, R., Sake Gowda, D. S. and Eilerman, D. *Acta Crystallogr., Sect. C 39* (1983) 1267.
19. Tummavuori, J. and Suontamo, R. *Finn. Chem. Lett.* (1979) 176.
20. Holtzclaw, H. F. Jr, Robinson, W. R. and Odom, J. D. *General Chemistry*, 9th Edn, D. C. Heath and Co., Lexington, MA 1991.

Received February 28, 1994.